Analysis, Control and Synchronization of nonlinear systems and networks via Contraction Theory: theory and applications

by
Giovanni Russo

Thesis Supervisor:

Professor Mario di Bernardo

Thesis for the Degree of Doctor of Philosophy
Department of Systems and Computer Engineering
University of Naples Federico II
Napoli, Italy

Submitted to the Faculty of Engineering, University of Naples Federico II, in partial fulfillment of the requirements for the degree of Doctor of Philosophy.

Printed in Italy.
Napoli, November 2010.

UNIVERSITY OF NAPLES FEDERICO II
DEPARTMENT OF SYSTEM AND COMPUTER ENGINEERING

The undersigned hereby certify that they have read and recommend to the **Faculty of Engineering** for acceptance the Thesis entitled "**Analysis, Control and Synchronization of nonlinear systems and networks via Contraction Theory: theory and applications**" by **Giovanni Russo** in partial fulfillment of the requirements for the degree of **Doctor of Philosophy**.

Dated: November, 2010

External Examiner: ______________________________
Examiner

Research Supervisor: ______________________________
Mario di Bernardo

Examing Committee: ______________________________
First Reader

To my Family.

Acknowledgements

There are so many people that I need to thank…First of all, I would like to express my gratitude to my supervisor, Prof. Mario di Bernardo for his continuous support and patience, which made those three years of intense work an unforgivable creative experience (and also for giving me the opportunity - unexpected when I was an undergrad - of starting this fantastic adventure!). I felt completely free to explore any land of the beautiful world represented by nonlinear dynamics and learned how research should be done, even despite the difficulties of an external environment which is not always ”helpful”…thanks! Another very special thanks goes to Prof. Stefania Santini, Prof. Francesco Garofalo and all the people at the Sincro Group of the University of Naples Federico II. In particular, I wish to acknowledge all the guys with whom I split the ”legendary” room 2.22 at Department of Systems and Computer Engineering and all the guys that made lunch time a funny time.

Thanks to Dr. Diego di Bernardo and all his group at the Telethon Institute of Genetics and Medicine for hosting me lots of times and for all the invaluable discussions which were really helpful for my works in systems biology.

It is a pleasure for me to thank Prof. Jean-Jacques Slotine, who hosted me at his lab, the Nonlinear Systems Laboratory of the Massachusetts Institute of Technology. Working at the MIT was a dream that I had from my childhood, when I used to look to this unique University with admiration and infinite respect. Working with Prof. Slotine made my stay at MIT the best possible working experience. A very special thanks goes to Prof. Eduardo Sontag for all the always interesting-and-inspiring discussions: I really learned a lot…thanks!

I would like to thank my family (my mother, my father, my sister and my dog) for the never-ending support that they gave me through all my life which is a solid foundation for my strength. I also wish to thank my family in the US for all their warmth that made me feel like at home. I would like to thank Alessandra for her constant presence and for her understanding during all the lots of times when I was deeply (or - to be more precise - uniquely) focussed on my work.

Finally, I recognize that my work would not have been possible without financial assistance. I wish to acknowledge support from the European Union Project ”Engineering Complexity in Biological Systems (COBIOS)”, VI Framework program (Grant no. 043379). I also wish to acknowledge the University of Naples Federico

II and the Honors Center Of Italian Universities, H2CU, for the financial support during my stay at MIT.

Giovanni Russo.
November, 2010.

Contents

Chapter 1

Introduction

La Nature est un temple *où* de vivants piliers
Laissent parfois sortir de confuses paroles;
L'homme y passe *à* travers des forêts de symboles
Qui l'observent avec des regards familiers.

(Nature is a temple in which living pillars
Sometimes give voice to confused words;
Man passes there through forests of symbols
Which look at him with understanding eyes.)

C. Baudelaire - Correspondances

Complex networked systems abound in Nature and Technology. They consist of a multitude of interacting agents communicating over a web of connections (*correspondances*). The Internet, power grids, flocks of birds, are all examples of networked systems. The dynamics of such systems can be modeled in terms of three essential *ingredients*: (i) a mathematical description of the behavior of each isolated *agent* in the network; (ii) an interaction function, or coupling protocol, used by agents (or nodes) to communicate; (iii) a *graph* describing the network of interconnections between neighboring agents.

One of the most striking feature of networked systems is their ability to show some *emergent* behavior that cannot be explained in terms of the individual dynamics of each single agent. In this sense, an example is provided by the typical *patterns* formed by flocks of birds and schools of fishes, [36]. Another notable example of emerging behavior is synchronization, see e.g. [143, 178]. Many dynamical phenomena in biology involve some form of synchronization, like e.g. circadian rhythms in mammals, the cell cycle, spiking neurons, respiratory oscillations [205, 122, 84]. More generally, for networks of non-identical nodes, an interesting emerging behavior is the so-called cluster synchronization [142, 164, 163]. Cluster synchronization is the regime where nodes having the same dynamics (i.e. identical nodes) become synchronized with each other.

From the above discussion, it can be understood why over the past few years much research effort within both the Physics and Control Theoretic communities has been devoted to the study of networked and biochemical systems [4, 3, 25, 26, 117, 198, 132]. Indeed, understanding those systems may provide advances in many application areas, like e.g. synthetic and computational biology, distributed control and optimization, sensor networks, [126, 81, 61, 23, 187, 203, 131, 135, 83].

Typically, the analysis and control of networked systems can be recast as a stability problem of some invariant set of network dynamics. However, the systems that are considered here are characterized by the fact that they are often non-autonomous, affected by noise and uncertain [65, 100, 146, 147, 187]. Thus, using classical stability tools may provide stability criteria which are too conservative, or of difficult practical application. Often, to solve this problem, modelers and control designers often resort to simulations in order to show the existence of some specific system's behavior. Simulations, however, can never provide effective algebraic conditions, and they are subject to numerical errors.

From a mathematical viewpoint, the problem of formally showing stability is known to be extremely difficult. One approach it to analyze the convergence behavior of nonlinear dynamical systems using Lyapunov functions [103, 108, 109, 45, 18]. However, in biological and network applications, the appropriate Lyapunov functions are not always easy to find and, moreover, convergence is not guaranteed in general in the presence of noise and/or uncertainties. Also, such an approach can provide un-effective algebraic conditions, or conditions which can be hardly verifiable and applicable.

The above limitations can be overcome if the convergence problem is interpreted as a property of all trajectories, asking that all solutions converge towards one another (contraction) [111, 194, 161]. This is the viewpoint of contraction theory, and more generally incremental stability methods, [7]. Global results are possible, and these are robust to noise, in the sense that, if a system satisfies a contraction property then trajectories remain bounded in the phase space. Contraction theory has a long history. Contractions in metric functional spaces can be traced back to the work of Banach and Caccioppoli [74] and, in the field of dynamical systems, to [79] and even to [99] (see also [138], [7], and e.g. [113] for a more exhaustive list of related references).

The aim of the Thesis is that of providing a coherent theoretical framework for the study of networked systems, modeled by means of Ordinary Differential Equations (ODEs) with applications to biochemical networks, see e.g. [155, 157, 12]. In particular, our interest is twofold. For interconnected systems, we explore the dynamical mechanisms which are responsible for the emergence of some coherent (coordinated) network dynamics. From the control viewpoint, we are interested in providing guidelines for the design of decentralized communication strategies (or protocols) for the network nodes which ensure some desired form of coordination. For biochemical systems, the analysis is focussed on understanding the key dynamical properties which are *responsible* for the system's behavior, or functionality. The main results for the analysis/control of interconnected systems that are presented in the Thesis are based on the use of a generalized version of contraction theory, [161, 163]. A detailed description of the contents of the Thesis is provided in the next Section.

1.1 Thesis Outline

Chapter 2 and Chapter 3 of the Thesis are introductory chapters. Specifically, in Chapter 2 the basic notions and definitions of contracting dynamical system are reviewed, as presented in the work by Prof. Slotine and his co-authors, [111, 194, 142]. Then, in Chapter 3 the main definitions are given of interconnected system [70] used in the rest of the Thesis. At the same time, in this Chapter, the main network control problems addressed in the rest of the Thesis are introduced. Examples of such network coordination problems are consensus, rendezvous, synchronization and cluster synchronization, [135, 157, 164, 163].

In Chapter 4, the notion of contracting dynamical system is redefined and extended. Indeed, intuitively contraction of a dynamical system of interest depends on *how distances in the system's phase space are measured.* That is, contraction is a property that depends on the particular norm being chosen for defining distances in the system phase space: it can be indeed found that the results of Chapter 2 make implicitly use of the Euclideann norm. From the methodological viewpoint, one of the major results obtained in the Thesis, and presented in this Chapter, is that of extending the notion of contracting system to the use of arbitrary norms (non-Euclidean norms). In the same Chapter, it is also shown that the algebraic conditions for contraction (using arbitrary norms) can be considerably relaxed if some structural properties of the vector field of interest are considered (symmetries). The results of this Chapter have been obtained in collaboration with Prof. E. D. Sontag and Prof. J. J. E. Slotine, [161, 163].

A first implication of the use of non-Euclidean norms is shown in Chapter 5. Specifically, it is shown that the use of such norms lead to the possibility of checking contraction using a graphical approach, both for continuous-time and discrete-time systems. Such an approach is shown to be particularly convenient for particular classes of biochemical systems arising in transcriptional networks. The *algorithmic* procedure for checking contraction presented in this Chapter has been obtained in collaboration with Prof. J. J. E. Slotine, [154, 160, 159]. A preliminary version of the algorithm can be found in [156].

In Chapter 6, it is shown how the mathematical tools developed in Chapter 4 can be used to study stability of interconnected systems. The first result presented in Chapter 6 is a *multi-scale* approach for network contraction. Its main feature is that contraction analysis for a network of interest can be broke down in two steps: a local level, where nodes are seen as black boxes and are characterized by some contraction estimate and an interconnection level, where such estimates are used to design couplings. The Chapter is then closed by presenting an approach making use of symmetries and contraction. Specifically, it is shown that network topology is linked to a particular class of symmetries (*permutations* of network nodes). Such properties are then used to generate different symmetry patterns. The results are of wide applications which range from control over networks, design of neural networks and *multi-purpose* networks, where a specific pattern of synchrony is associated to a particular set of inputs. The stability results presented in this Chapter arose, out from a collaboration with Prof. Sontag and Slotine, [162, 163].

In Chapter 7 some results for the analysis and control of (cluster) synchronization are presented. In particular, we consider a general model of interconnected system, and show that this emerging (coordinated) behavior can be ensured by a contraction property of some particular directions of the network phase space. We then specialize this result to some classes of systems, providing sufficient conditions for (cluster) synchronization based on matrix measures. This Chapter is then closed with a result for the analysis of network synchronization, linking contraction to Lyapunov based synchronization techniques and to the Master Stability Function. The main papers where those results appeared are [155, 157, 41] (see also [42]).

All the networks and systems considered in the above chapters were made up by nodes being continuous-time systems. In Chapter 8 we extend our study to networks of discrete-time and asynchronous nodes. By the word *asynchronous* it is meant here that information between network nodes occurs at time instants which are not predetermined. In this Chapter, after generalizing the notion of contraction to the use of arbitrary norms for discrete-time systems, we turn our attention to the study of asynchronous networks. Specifically, we show how our results can be applied to the design of communication protocols that allow to solve some coordination problems, like e.g. consensus and cluster-synchronization, [158].

In Chapter 9 some applications of our mathematical tools to biochemical systems are presented. Specifically, an approach is shown that allows to analyze/control entrainment of transcription networks, [161] and a study is presented on quorum-sensing networks [164]. Finally, the behavior of some important network motif is explained [163].

Chapter 2

Nonlinear Contraction Theory: a brief overview

In this introductory chapter we review some basic results on Contraction theory which are systematically extended, and proved under different technical assumptions in Chapter 4. The results presented can be found in various forms in [111], [194], [142] to which the reader is referred for further details. This Chapter is then closed by presenting some results linking contracting, Lipschitz and $QUAD$ vector fields, which can be partly found in [41].

2.1 Introduction

One of the most important problems arising in both the control and the analysis of dynamical systems is that of determining if the system of interest is *stable.* Typically, stability is defined in the sense of Lyapunov [175], [169] and it is intended as a property of some invariant set. For example, a set is said to be globally (asymptotically) stable if all the trajectories of the system of interest converge towards the set.

Contraction theory (or contraction analysis) is based on a different view of stability, which is inspired by fluid mechanics. Rather than viewing stability as *relative* to some nominal motion, or equilibrium point, in Contraction theory a system is said to be stable (or contracting) if initial conditions (or temporary disturbances) are *forgotten exponentially fast*, i.e. if the final behavior of the system is independent on initial conditions. In other words, the viewpoint of contraction theory is that of analyzing stability *incrementally* (or differentially): a system is contracting if trajectories converge towards each other. In many cases, this differential approach is significantly simpler than its *integral* counterpart both for the analysis and control of nonlinear dynamical systems. Indeed, there is no need for finding some implicit motion integral as in Lyapunov theory, or some global state transformation as in feedback linearization.

More generally, interpreting stability as a property of solutions (or trajectories) of a dynamical system and asking that all solutions converge towards each other is a viewpoint which is typical of incremental stability methods [7].

Contraction theory has a long history. Contractions in metric functional spaces can be traced back to the work of Banach and Caccioppoli (see e.g. [74] for further details). In the field of dynamical systems theory, ideas closely related to contraction can be traced back to [79] and even to [99] (see also [138], [7], and e.g. [113] for a more exhaustive list of related references and [89] for an historical overview).

In this Chapter we review some of the basic results of Contraction theory. The Chapter is organized as follows: we start in Section 2.2 with presenting the basic contraction analysis for a dynamical system. Such analysis is then generalized in Section 2.3 and some properties of contracting systems are presented in Section 2.4. Finally, motivated by the fact that sometimes a relaxed version of contraction is required for applications, we present the concept of partial contraction in Section 2.5 and that of contraction towards invariant subspaces in Section 2.6.

2.2 Basic convergence result

We consider generic n-dimensional deterministic dynamical systems of the form

$$\dot{x} = f\left(t, x\right), x(t_0) = x_0, \quad t_0 \geq 0 \tag{2.1}$$

The vector field $f : \mathbb{R}^+ \times \mathbb{R}^n \rightarrow \mathbb{R}^n$ is assumed to be smooth. The key idea is to find local conditions on the vector field guaranteeing convergence of nearby trajectories towards each other. The next step is then to show that such conditions guarantee global convergence properties.

Notice that (2.1) can be thought of as an n-dimensional fluid flow, with $\dot{x}$ being the n-dimensional *velocity* vector at the *position* x and time t. Since $f(t, x)$ is continuously differentiable, the following exact differential relation can be obtained:

$$\delta\dot{x} = \frac{\partial f}{\partial x}(t, x)\delta x \tag{2.2}$$

where δx is a virtual displacement. (This terminology comes from mechanics [13], where a virtual displacement is an infinitesimal displacement at *fixed time*: formally it may be thought of as a tangent differential form, differentiable with respect to time.)

Consider two neighboring trajectories of (2.1) and the virtual displacement, δx, between them. The squared (Euclidean) distance between these trajectories is $\delta x^T \delta x$

can be derived from (2.2):

$$\frac{d}{dt}\left(\delta x^T \delta x\right) = 2\delta x^T \delta \dot{x} = 2\delta x^T \frac{\partial f}{\partial x}(t,x)\delta x$$

Let $\lambda_{\max}(t,x)$ the largest eigenvalue of the symmetric part of $\frac{\partial f}{\partial x}$ (i.e., the largest eigenvalue of $\frac{1}{2}\left(\frac{\partial f}{\partial x} + \frac{\partial f}{\partial x}^T\right)$) we have:

$$\begin{aligned}
&\tfrac{d}{dt}\left(\delta x^T \delta x\right) = 2\delta x^T \tfrac{\partial f}{\partial x}(t,x)\delta x = \\
&= 2\left(\tfrac{1}{2}\delta x^T \left(\tfrac{\partial f}{\partial x} - \tfrac{\partial f}{\partial x}^T\right)\delta x + \tfrac{1}{2}\delta x^T \left(\tfrac{\partial f}{\partial x} + \tfrac{\partial f}{\partial x}^T\right)\delta x\right) \leq \\
&\leq 2\lambda_{\max}(t,x)\delta x^T \delta x
\end{aligned}$$

Thus:

$$\delta x(t)^T \delta x(t) \leq \delta x(t_0)^T \delta x(t_0) e^{\int_{t_0}^{t} \lambda_{\max}(\tau,x)d\tau} \tag{2.3}$$

Now, assume that $\lambda_{\max}(t,x)$ is uniformly negative definite, i.e.:

$$\exists c \neq 0 : \quad \forall x, \forall t \geq t_0, \quad \lambda_{\max}(t,x) \leq -c^2 \tag{2.4}$$

Then, (2.3) implies that any infinitesimal length converges exponentially to zero with a rate (contraction rate) given by c^2. By path integration this implies that the length of any finite path converges exponentially to zero. This motivates the following definition.

Definition 2.2.1. *An open connected region in state space $\mathcal{C} \subseteq \mathbb{R}^n$, is called a contraction region of (2.1) if system Jacobian is uniformly negative definite in $\mathcal{C}$, i.e. if:*

$$\exists c \neq 0 : \quad \forall x, \forall t \geq t_0, \quad \frac{1}{2}\left(\frac{\partial f}{\partial x} + \frac{\partial f}{\partial x}^T\right) \leq -c^2 I$$

Notice that the above condition is in turn implied by (2.4). We remark here that in this Chapter all matrix inequalities are referred to the *symmetric part* of square matrices.

Now, consider a *ball* of constant radius (defined by the Euclidean norm) about a given trajectory for which $\mathcal{C}$ is forward invariant (that is, the trajectory remains in $\mathcal{C}$ for any $t \geq t_0$). Since $\mathcal{C}$ is a contraction region, then any length within the ball decreases exponentially: that is, any trajectory starting in the ball remains in the ball and converges exponentially to the given trajectory. This leads to the following result (see [111] for a proof).

Theorem 2.2.1. *Any trajectory of (2.1) starting in a ball of constant radius centered around a given trajectory and contained at all times in a contraction region, remains in that ball and converges exponentially to this trajectory. Furthermore, global exponential convergence to the given trajectory is guaranteed if the whole state space is a contraction region.*

2.3 Generalized convergence analysis

Theorem 2.2.1 can be extended by using a more general definition of differential length. Specifically, the vector δx between nearby trajectories can be expressed using a differential coordinate transformation:

$$\delta z = \Theta(t,x)\delta x \tag{2.5}$$

with $\Theta(t,x)$ being a square uniformly invertible matrix. This leads to the generalization of a squared length as:

$$\delta z^T \delta z = \delta x^T M(t,x)\delta x \tag{2.6}$$

where $M(t,x) = \Theta^T\Theta$ is continuously differentiable and formally defines a Riemann space. In what follows, $M(t,x)$ will be termed as *metric* and it will be assumed to be uniformly positive definite. Indeed, in this case, exponential convergence of $\delta z^T \delta z$ to zero implies exponential convergence of $\delta x^T \delta x$ to zero.

The time derivative of $\delta z(t) = \Theta(t,x)\delta x(t)$ can be computed as:

$$\frac{d}{dt}\delta z = \dot{\Theta}\delta x + \Theta\delta\dot{x} = \left(\dot{\Theta} + \Theta\frac{\partial f}{\partial x}\right)\Theta^{-1}\delta z \tag{2.7}$$

where the matrix

$$F := \left(\dot{\Theta} + \Theta\frac{\partial f}{\partial x}\right)\Theta^{-1}$$

is termed in what follows as *generalized Jacobian*. Using (2.7), the rate of change of the squared (Euclidean) length δz can be computed as

$$\frac{d}{dt}\left(\delta z^T \delta z\right) = 2\delta z^T F \delta z$$

Therefore, if F is uniformly negative definite, then $\delta z^T \delta z$ exponentially converges to zero, implying in turn that $\delta x^T \delta x$ exponentially converges to zero. This leads to the following definition.

Definition 2.3.1. *A region is state space, $\mathcal{C}$, is a contraction region for (2.1) if $F(t,x)$ is uniformly negative definite in $\mathcal{C}$.*

The following result holds:

Theorem 2.3.1. *Any trajectory of (2.1) starting in a ball of constant radius (with respect to the metric $M(t,x) = \Theta(t,x)\Theta(t,x)^T$), centered around a given trajectory and contained at all times in a contraction region (with respect to $M(t,x)$), remains in that ball and converges exponentially to this trajectory. Furthermore, global exponential convergence to the given trajectory is guaranteed if the whole state space is a contraction region with respect to $M(t,x)$.*

We close this Section with the following remarks:

- for linear time-invariant systems, contraction in the sense of Theorem 2.3.1 is equivalent to strict stability, and Θ can be chosen as the transformation matrix which diagonalizes the system or puts it in Jordan form [111];

- a convex contraction region contains at most one equilibrium point;

- in an autonomous contracting dynamical system, all trajectories converge exponentially to a unique equilibrium point;

- for autonomous systems, Theorem 2.3.1 is a sufficient condition for the existence of a Lyapunov function.

2.4 Some properties of contracting systems

We shall also use the following two properties of contracting systems, whose proofs can be found in [111], [170]. Proofs generalized to the use of arbitrary metrics and norms can be found in Chapter 4

Hierarchies of contracting systems. Assume that the Jacobian of (2.1) is in the form

$$\frac{\partial f}{\partial x}(t,x) \;=\; \begin{bmatrix} J_{11} & J_{12} \\ 0 & J_{22} \end{bmatrix} \tag{2.8}$$

corresponding to a hierarchical dynamic structure. The J_{ii} may be of different dimensions. Then, a sufficient condition for the system to be contracting is that (i) the Jacobians J_{11}, J_{22} are contracting (possibly with different Θ's), and (ii) the matrix J_{12} is bounded.

Periodic inputs. Consider the system

$$\dot{x} = f\,(x, r(t)) \tag{2.9}$$

where the input vector $r(t)$ is periodic, of period T. Assume that the system is contracting (i.e., that the Jacobian matrix $\frac{\partial f}{\partial x}(x, r(t))$ is contracting for any $r(t)$). Then the system state $x(t)$ tends exponentially towards a periodic state of period T. A generalized version of this result will be presented in Chapter 4. In the same Chapter, it is shown that under some structural condition on the vector field, all system trajectories converge towards a periodic orbit with period being an integer multiplier of T.

2.5 Partial contraction

As shown in the previous Section, a nonlinear dynamical system is contracting if all of its trajectories converge exponentially towards each other. Often, in applications, one is interested in showing that, after some transient, system trajectories exhibit some specific behavior (which may consist of e.g. relationships between state variables). An example of such a situation is the study of synchronization/consensus of an interconnected systems. Indeed, in this case one is typically interested in showing that, after some transient, all trajectories of the nodes in the network exhibit a common behavior (see Chapter 3 for further details).

A simple yet powerful extension to nonlinear contraction theory is the concept of *partial* contraction [194]. This approach is based on the use of some auxiliary or virtual system which embeds the trajectories of the system of interest and that is contracting. Thus, the system of interest is not contracting, but convergence of its trajectories towards some specific behavior is ensured by contraction of this auxiliary system.

The basic result of partial contraction can be stated as follows [194] (see Chapter 4 for a different version and relative proof).

Theorem 2.5.1. *Consider a smooth nonlinear n-dimensional system of the form $\dot{x} = f(t, x, x)$ and assume that the so-called virtual system $\dot{y} = f(t, y, x)$ is contracting with respect to y. If a particular solution of the auxiliary y-system verifies a smooth specific property, then all trajectories of the original x-system verify this property exponentially. The original system is said to be* partially contracting.

Indeed, the virtual y-system has two particular solutions, namely $y(t) = x(t)$ for all $t \geq 0$ and the particular solution with the specific property. Since all trajectories of the y-system converge exponentially to a single trajectory, this implies that $x(t)$ verifies the specific property exponentially.

Example

In order to clarify the notion of virtual system, we use as a representative example the synchronization of two bidirectionally coupled oscillators. Consider the two systems:

$$\dot{z} = f(t, z) + h(w) - h(z), \tag{2.10}$$

$$\dot{w} = f(t, w) + h(z) - h(w), \tag{2.11}$$

where h is some coupling function.

A suitable virtual system can be chosen as

$$\dot{y} = f(t, y) - 2h(y) + h(z) + h(w) := \varphi(y, z, w). \tag{2.12}$$

Trajectories of the nodes are particular solutions of the y-system, i.e. $\varphi(t, z, z, w) = f(z) + h(w) - h(z)$ and $\varphi(t, w, z, w) = f(w) + h(z) - h(w)$. Hence, according to Theorem 2.5.1, if (2.12) is contracting with respect to the y state variable, the two particular solutions z and w will converge to each other. Thus, to prove synchronization of (2.10) and (2.11), it will suffice to show that (2.12) is contracting with respect to the y state variable. In turn, according to Theorem 2.5.1 this is implied by requiring uniform negativity of the matrix:

$$\frac{\partial f(t, y)}{\partial y} - 2\frac{\partial h(y)}{\partial y}. \tag{2.13}$$

2.6 Contraction towards linear flow invariant subspaces

Often, in applications, one is interested in proving contraction of (2.1) of only some *directions* in phase space. Again, this may be the case of interconnected systems: to prove synchronization, one has to show that all system trajectories converge towards some linear flow invariant subspace. For example, for a network of N identical nodes, such a subspace is

$$\mathcal{M} := \{x_i = x_j, \quad i, j = 1, \ldots, N\}$$

where x_i's denote the set of the state variables of a node (see Chapter 3 for the formalization of interconnected system).

We now review a result which allows to prove contraction towards some linear flow-invariant subspace for (2.1). See Chapter 4 for an alternative proof where arbitrary norms are considered.

Assume that there exists a linear flow invariant subspace, say $\mathcal{M}$, for system (2.1). By flow invariant subspace we mean that: $f(t, x) \subset \mathcal{M}$ for any t and for any $x \in \mathcal{M}$: that is, any trajectory with initial conditions on $\mathcal{M}$ remains in $\mathcal{M}$. Let p be the dimension of $\mathcal{M}$ and consider an orthonormal basis of phase space: $(e_1, \ldots, e_n)$. In such a basis, the first p vectors form a basis of $\mathcal{M}$, while the remaining $n - p$ vectors are a basis of $\mathcal{M}^\perp$. Define the $(n - p) \times n$ matrix V, whose rows are $e_{p+1}^T, \ldots, e_n^T$, i.e. $V^T V$ is a projection on $\mathcal{M}^T$ and (see [82], [85]):

$$V^T V + U^T U = I_n \quad V V^T = I_{n-p} \quad x \in \mathcal{M} \leftrightarrow Vx = 0$$

with U being the matrix whose rows are the basis of $\mathcal{M}$ and I_s be the s-dimensional identity matrix.

Let $z = Vx$. Notice that, by construction, x converges to $\mathcal{M}$ if z converges to 0. The convergence of z to 0 can be in turn assessed by studying the contraction properties of the reduced order dynamics

$$\dot{z} = Vf\left(t, V^T z + U^T U x\right)$$

Now, consider the following virtual system (see Theorem 2.5.1):

$$\dot{y} = Vf\left(t, V^T y + U^T U x\right) \tag{2.14}$$

Notice that, in the spirit of Theorem 2.5.1, $y(t) = z(t)$ is a particular solution of the virtual system. Moreover, since $U^T U x \in \mathcal{M}$, and since $\mathcal{M}$ is flow invariant, we have that $y(t) = 0$ is also a solution of (2.14). Therefore, contraction of (2.14) implies that $z(t)$ converges exponentially to zero, and hence that $x(t)$ converges exponentially to $\mathcal{M}$. This leads to the following result [142]:

Theorem 2.6.1. *Assume that for system (2.1) a linear flow invariant subspace exists and that $V\frac{\partial f}{\partial x}V^T$ is uniformly negative definite. Then, all the solutions of (2.1) exponentially converge towards $\mathcal{M}$.*

2.7 Contracting, Lipschitz and $QUAD$ vector fields

We now systematically derive the links between QUAD and contraction first, and then between the Lipschitz and QUAD conditions. In particular, it will be shown that contraction of the vector field is a sufficient condition for it to be QUAD and that, under certain conditions, a Lipschitz vector field is also QUAD. Moreover, we prove that the vector field being QUAD implies under certain conditions that the system is also contracting.

2.7.1 QUAD condition

The QUAD condition is an assumption on the vector field f in (2.1) usually made in the literature to prove network synchronization by means of appropriate Lyapunov functions, see for example [108, 109, 115, 106, 46, 45, 107, 48, 18]. A condition closely related can be found in [56] and can be traced back to the 1955 paper [95]. The QUAD condition can be stated as follows:

Definition 2.7.1. *A function, $f : \mathbb{R}^+ \times \mathbb{R} \rightarrow \mathbb{R}^n$ is QUAD(Δ, ω) if and only if, for any $x, y \in \mathbb{R}^n$:*

$$(x-y)^T[f(t,x) - f(t,y)] - (x-y)^T\Delta(x-y) \leq -\omega(x-y)^T(x-y) \tag{2.15}$$

where Δ is an $n \times n$ diagonal matrix and ω is a real positive scalar.

Dynamical system (2.1) is said to be QUAD or to *satisfy the QUAD condition* if f is QUAD(Δ, ω) for some Δ and ω.

This condition is used in a number of theoretical papers on synchronization to prove (semi-)negativity of some appropriate global Lyapunov function. For example, this condition, together with some *dissipativity* property of the nodes' vector field, is shown in [18] to guarantee global asymptotic synchronization of the network. In [108], after proving that the Lorenz system is QUAD, authors use this property to derive a proof of synchronization of linearly coupled Lorenz systems, while in [109] the analysis is extended to the case of asymmetrically coupled systems. Sufficient conditions are given in [115] for the synchronization of QUAD systems in the presence of time delays, and in [106] the QUAD condition is used to prove synchronizability of networks in the presence of a unique centralized adaptive coupling gain. This is then generalized in [46, 45] to the case of QUAD systems where the adaptive coupling gains evolve according to local decentralized laws firstly presented in [47]. It is worth emphasizing here that the QUAD condition does not necessarily rely on the assumption of *smoothness* of the vector field. In fact, in [45] it has been proved that the Chua's circuit is QUAD$(0,\omega)$. Finally, we remark here that the QUAD condition is also a key assumption often considered in pinning control problems, e.g. [76, 101, 32, 145, 199, 200].

2.7.2 Linking QUAD and contraction

Theorem 2.7.1. *If (2.1) is contracting with contraction rate*

$$\beta := \max\{\beta(t,x)\} < 0, \quad x \in \mathbb{R}^n,\, t \geq 0 \tag{2.16}$$

where $\beta(t,x) = \lambda_{\max}\left(0.5\left(\frac{\partial f}{\partial x}^T + \frac{\partial f}{\partial x}\right)\right)$*, then it is QUAD*$(\Delta,\omega)$ *for any arbitrary* Δ *and* ω *such that* $\Delta - \omega I_n \geq \beta I_n$.

Proof. The QUAD condition (2.15), can be simply rewritten as

$$(x-y)^T\left[f(t,x) - f(t,y)\right] \leq (x-y)^T\left(\Delta - \omega I_n\right)(x-y) \tag{2.17}$$

Now, define the following function of the scalar quantity $\xi \in [0,1]$

$$\Psi(\xi) = (x-y)^T f(t, y + \xi(x-y)) \tag{2.18}$$

which is continuous and differentiable by hypothesis. By virtue of the mean value theorem we have:

$$\exists\tilde{\xi} \in [0,1] : \Psi(1) - \Psi(0) = \frac{d\Psi\left(\tilde{\xi}\right)}{d\xi} \tag{2.19}$$

and therefore:

$$(x-y)^T\left[f\left(t,x\right)-f\left(t,y\right)\right]=\frac{d\Psi\left(\tilde{\xi}\right)}{d\xi} \tag{2.20}$$

from which it immediately follows

$$(x-y)^T\left[f\left(t,x\right)-f\left(t,y\right)\right]=(x-y)^T\,\frac{\partial f\left(t,y+\tilde{\xi}(x-y)\right)}{\partial x}\left(x-y\right) \tag{2.21}$$

By hypothesis, the system is contracting, that is, the symmetric part of the system Jacobian is negative definite in the whole state space. Thus:

$$(x-y)^T\,\frac{\partial f\left(t,y+\tilde{\xi}(x-y)\right)}{\partial x}\left(x-y\right)\leq-\left(x-y\right)^T\beta I_n\left(x-y\right) \tag{2.22}$$

Now, using (2.21), it immediately follows that system (2.1) is QUAD(Δ,ω) with $\Delta-\omega I_n\geq\beta I_n$ and the theorem remains proved. □

Theorem 2.7.2. *Given the dynamical system (2.1) and some positive scalar c, if the vector field f is differentiable and QUAD(Δ,ω) with $(\Delta-\omega I_n)\leq-cI_n$, then system (2.1) is contracting with contraction rate $\beta\leq-c$.*

Proof. From Definition 2.7.1, we have:

$$(x-y)^T\left[f\left(t,x\right)-f\left(t,y\right)\right]\leq(x-y)^T\left(\Delta-\omega I_n\right)\left(x-y\right) \tag{2.23}$$

$\forall x,y\in\mathbb{R}^n$, $\forall t\geq0$. Then, using (2.21), the above inequality becomes:

$$(x-y)^T\,\frac{\partial f\left(t,y+\tilde{\xi}(x-y)\right)}{\partial x}\left(x-y\right)\leq(x-y)^T(\Delta-\omega I_n)(x-y) \tag{2.24}$$

$\forall x,y\in\mathbb{R}^n$, $\forall t\geq0$. Since by hypothesis $\Delta-\omega I_n\leq-cI_n$, we have:

$$\frac{1}{2}(x-y)^T\left(J\left(t,\tilde{\xi}\right)+J^T\left(t,\tilde{\xi}\right)\right)(x-y)\leq-c(x-y)^T(x-y) \tag{2.25}$$

with:

$$J\left(\tilde{\xi}\right):=\frac{\partial f\left(t,y+\tilde{\xi}\left(x-y\right)\right)}{\partial x}$$

As x and y are arbitrary points in phase space, it immediately follows that $\beta(t,x)$, as defined in Theorem 2.7.1, is such that:

$$\beta(t,x)\leq-c \tag{2.26}$$

for all $x\in\mathbb{R}^n$ and $t\geq0$. The theorem is then proved. □

The following two corollaries are straightforward consequences of Theorem 2.7.1 and Theorem 2.7.2, giving necessary and sufficient conditions linking the QUAD assumption to contracting and semi-contracting systems.

Corollary 2.7.1. *A system is contracting with contraction rate β if and only if it is $QUAD(\Delta, \omega)$ with $\Delta - \omega I_n = \beta I_n$.*

Corollary 2.7.2. *A system is $QUAD(\Delta, \omega)$ with $\Delta = \omega I_n$ if and only if it is semi-contracting.*

2.7.3 Linking the Lipschitz and QUAD conditions

We examine now the relationship between the Lipschitz and QUAD conditions.

Theorem 2.7.3. *If f is Lipschitz, with Lipschitz constant equal to $\alpha > 0$, then f is $QUAD(\Delta, \omega)$, with $\Delta - \omega I_n \geq \alpha I_n$.*

Proof. To prove the Theorem we will use again the definition of QUAD, written as in (2.17). From trivial algebra and using the Cauchy-Schwarz inequality, we can write:

$$(x-y)^T(f(t,x) - f(t,y)) \leq \|x-y\|\|f(t,x) - f(t,y)\| \tag{2.27}$$

$\forall x, y \in \mathbb{R}^n$ and $\forall t \geq 0$. Since f is Lipschitz by hypothesis, we then have:

$$(x-y)^T(f(t,x) - f(t,y)) \leq \alpha\|x-y\|^2 \tag{2.28}$$

which is equivalent to write:

$$(x-y)^T(f(t,x) - f(t,y)) \leq (x-y)^T \alpha I_n (x-y) \tag{2.29}$$

Thus, (2.17) and (2.29) yield that f is QUAD(Δ, ω), for any Δ and ω such that

$$\Delta - \omega I_n \geq \alpha I_n \tag{2.30}$$

□

Remarks

- Corollary 2.7.1 establishes that contracting systems are only a subset of the more general QUAD vector fields.

- If system (2.1) is QUAD(Δ, ω), with $\Delta - \omega I_n \leq -cI_n$, $c > 0$, and f is differentiable, then trajectories in phase space converge to each other; this immediately implies that differentiable chaotic systems cannot satisfy this condition as they are characterized by local divergence of nearby trajectories. Thus, chaotic systems cannot be contracting (see also [155]). Conversely, if system (2.1) is QUAD(Δ, ω), with $\Lambda := \Delta - \omega I_n > 0$, then (2.15) implies $(x-y)^T(f(t,x) - f(t,y)) \leq (x-y)^T\Lambda(x-y)$, $\Lambda > 0$ and there might be regions in phase space in which nearby trajectories diverge (that is, regions where $(x-y)^T(f(t,x)-f(t,y)) > 0$) and regions where they converge ($(x-y)^T(f(t,x)-f(t,y)) < 0$), as for instance in chaotic systems.

- If system (2.1) is Lipschitz, then it can be made contracting by means of a simple (static) state feedback, implying the possibility of designing simple observer/controllers. This property will be also used to synchronize complex dynamical networks by means of an appropriately chosen constant coupling strength.

- We remark here that an alternative way of proving Theorem 2.7.1 and Theorem 2.7.2 can be obtained by rewriting the QUAD condition as in equation (8) of [18].

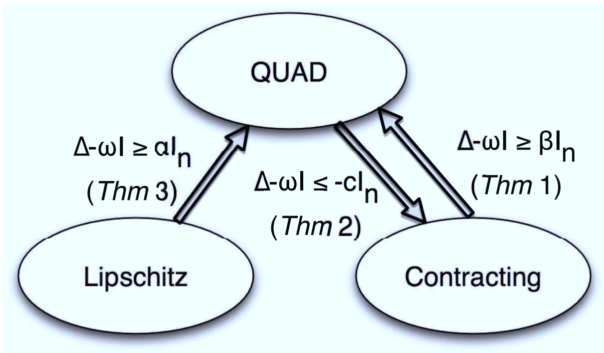

Figure 2.1: Relationship between QUAD and Lipschitz assumptions and contractivity formalized in Section 2.7

A summarizing schematic of the relationships discussed above between the QUAD, Lipschitz and contracting assumptions is depicted in Figure 2.1.

2.8 Concluding remarks

In this Chapter, we briefly introduced the notion of contracting dynamical system and reviewed the basic results used for determining if a system is contracting, as presented in [111]. We also introduced the notions of partial contraction and contraction towards linear flow invariant subspaces (see [194], [142]). A relationship between QUAD, Lipschitz and contracting vector fields was also shown. These results will be then used in Chapter 7We remark here that all the results of this Chapter make use of the Euclidean norm for *measuring* the distance between two nearby trajectories of a dynamical system. However, other norms can be used to this aim, leading to similar results but conditions in different algebraic forms. In Chapter 4, we explore in more detail this avenue and provide alternative proofs (generalized to the use of arbitrary norms and weaker constraints on the region $\mathcal{C}$)

to all the results briefly presented in this Chapter. These generalized versions of the above results are then used in the rest of Thesis to analyze/control networked systems and biochemical networks.

Chapter 3

Network coordination problems

This Chapter introduces the notion of *network* (or interconnected system) that is used in the rest of the Thesis. The problem of *network coordination* is also introduced. By network coordination it is meant here the emergence of a coherent dynamics from the interaction of the elements composing the network. Such an emerging dynamics can then be used to achieve some desired steady state behavior. Three coordination problems are introduced in this Chapter, which will be addressed in Chapter 7.

3.1 Introduction

Roughly speaking, a network is a set of *items* which communicate and interact by means of some *link*. Networks are all around us: we are ourselves, as individuals, units of a network of social relationships. But networks are also *inside* us: our lives are regulated at the molecular level by networks of biochemical reactions. Other examples of networks include: electric power grids, the Internet, subway systems, neural networks, ensembles of robots, [25], [132], [1].

Historically, the study of networks can be traced back to 1736, when Leonhard Euler published the solution of the famous *Konigsberg bridge problem*. The formalization proposed by Euler gave rise to *graph theory*, which has been established as an invaluable tool for answering many practical questions, like e.g.: determine the maximum flow per unit time from source to sink in a network of pipes,how to fill n jobs by n people with maximum total *utility*.

The last decade has seen the birth of a renewed research interest in the study of *complex networks*: networks whose structure is irregular, dynamically evolving in time, *populated* by entities which are dynamical systems. In this Thesis, we will use the term *interconnected system* (typically used within the Control-Theoretic community) as a synonymous of *complex network* (mainly used within the Physics community).

A particular important problem in the field of networked systems is that of analyzing/controlling the behavior emerging from the interactions of the network nodes (or emerging dynamics), and to explore its links with the network topology. For example, recently in [45] it has been proved that the interconnections between the elements of a network can be adapted so as guarantee a common behavior of the nodes. Such a coordinated behavior is termed as *synchronization*. Another kind of coordinated behavior is *consensus*, where the nodes of the network agree upon some quantity so as to perform some computation. For example, in [135], it was shown that it is possible to properly design decentralized coupling protocols for a network of integrators so as to satisfy the *average consensus problem*, where network nodes agree upon the average of their initial conditions.

This Chapter is organized as follows. We first formally define an interconnected system in Section 3.2, while in Section 3.3 we present the mathematical models of interconnected systems which are used in the rest of the Thesis. Finally, in Section 3.4 we introduce three coordination problems which are addressed in Chapter 7. The mathematical tools used to address such coordination problems are introduced in Chapter 4.

3.2 Basic notions of graph theory

In this Section, we briefly review some of the main notions of graph theory [26], [196], which shall be used in the rest of this Thesis, for more details see [66].

An *undirected (directed) graph*, $\mathcal{G} = \{\mathcal{N}, \mathcal{E}\}$ consists of two sets, $\mathcal{N}$, $\mathcal{E}$, such that $\mathcal{N} \neq \emptyset$, and $\mathcal{E}$ is a set of unordered (ordered) pairs of elements of $\mathcal{N}$. The elements of $\mathcal{N} := \{n_1, \dots, n_N\}$ are the nodes of the graph, while the elements of $\mathcal{E} := \{e_1, \dots, e_k\}$ are the edges (or links) of the graph. A node is usually referred to by its order, say i, in the set $\mathcal{N}$. In an undirected graph, each of the edges is defined by a couple of nodes, i and j, and is denoted as (i, j). The edge is said to be *incident* in nodes i and j that is, the two nodes are bidirectionally coupled. Two nodes are said to be *adjacent* or *neighboring* if they are linked by an edge. The set of the neighbors to node i is denoted with N_i.

In a *directed graph*, the order of the two nodes i, j is important. Indeed, in this case (i, j) stands for an edge from node i to node j (the edge is incident in i) and $(i, j) \neq (j, i)$, that is, the existence of an edge between node i and node j does not imply the existence of an edge from j to i. In a directed graph, the number of edges incident in node i is termed as *in-degree* of the node and denoted as $d_{i,in}$. Analogously, the number of edges starting from node i is termed as *out-degree* of the node and is denoted as $d_{i,out}$. Notice that $d_{i,in}$ is the cardinality of N_i. For an undirected graph we have $d_{i,in} = d_{i,out}$: this common value is simply termed as degree of node i and indicated with d_i.

A central concept in graph theory is that of *reachability* of two different nodes of a graph. Indeed, two nodes that are not adjacent may be reachable from one node to another. A *path* between node i and node j is a sequence of adjacent nodes that begins with i and ends with j. An undirected (directed) graph is said to be *connected* (*strongly connected*) if there exists a path between each pair of its nodes.

It is useful for the work presented in the Thesis to represent a graph by means of matrices. The *adjacency* matrix, A, of a graph is an $N \times N$ matrix whose element a_{ij} is positive if the edge (i, j) exists or zero otherwise. If the entries of A are either 1 or 0, we say that the graph is unweighted. On the other hand, A is said to be a *weighted adjacency matrix* if each element of A, say a_{ij}, can assume any nonnegative value (such a value is then termed as weight of the edge (i, j)). Graphs to which a weighted adjacency matrix is associated, are termed as weighted graphs and denoted as $\mathcal{G} = (\mathcal{N}, \mathcal{E}, A)$. From the definition above, it is straightforward to notice that the matrix A offers a matricial representation of the topology of some graph of interest. Sometimes, graphs whose edges are time-varying will be considered (that is, the graph topology changes in time). In this case, the adjacency matrix is time varying, i.e. $A := A(t)$.

An important matrix which will be used in the what follows is the so-called *Laplacian matrix*, denoted as L (see [66] for a detailed survey of the properties of such a matrix). Here, we briefly review the definition and some of the properties of L used in the rest of the Thesis.

Let D be the $N \times N$ diagonal matrix having on its main diagonal the out degree of the nodes, i.e. $D_{ii} = d_{i,out}$. The (weighted) Laplacian matrix associated to a graph is then defined as:

$$L := D - A \tag{3.1}$$

By definition, the row sum of the Laplacian matrix is zero. Thus, L has always a zero eigenvalue, i.e. $rank(L) = N - 1$. Moreover, the eigenvector corresponding to the zero eigenvalue is the vector $1_N := [1, \dots 1]^T$. By construction, it is also clear that the Laplacian matrix associated to an undirected graph is symmetric.

Using a classical result from linear algebra, i.e. Gershgorin circle theorem (see [82] and Chapter 5), it can be easily shown that all the eigenvalues of L as defined in (3.1) are nonnegative.

The following result can be found in [135].

Theorem 3.2.1. *Let $\mathcal{G} = (\mathcal{N}, \mathcal{E}, A)$ be a weighted (directed or undirected) graph with Laplacian L. Then, $\mathcal{G}$ is strongly connected if and only if $rank(L) = N - 1$.*

That is, Theorem 3.2.1 implies that if a graph is (strongly) connected, then only one eigenvalue, λ_1 is zero and all the other eigenvalue, λ_i, $i = 2, \dots, N$ are positive. In particular, for a directed graph, λ_2 is termed as *algebraic connectivity* of the graph and will play a key role in the dynamics of networked systems considered here [55].

(an analogous quantity to λ_2 for a directed graph is $\hat{\lambda}_2$ which is the second smallest eigenvalue of the symmetric part of L). For an undirected graph, it can be shown that [55]

$$\lambda_2 := \min_{x \neq 0, 1_N^T x = 0} \frac{x^T L x}{x^T x} \tag{3.2}$$

3.3 Networks of dynamical systems

Part of this Thesis is devoted to the study of dynamical systems interacting over a graph. That is, in terms of the notation introduced above: each node, of the graph $\mathcal{G}$ is characterized by some dynamics and the coupling between nodes is characterized by some algebraic function which depends on the state variables of the nodes.

Such systems will be termed as *interconnected systems*, or (complex) networks and we will refer to the framework introduced in [70]. We remark here that our formalism avoids the restrictions typically assumed in the literature like e.g. absence of self-couplings and multiple arrows, identical nodes, additive and/or diffusive coupling.

3.3.1 Definitions

In our framework the phase space of the i-th node (or cell, or neuron) is the set $P_i \subseteq \mathbb{R}^{n_i}$ (in the next Section further details on such sets will be specified), while its state at time t is denoted with $x_i(t) \in \mathbb{R}^{n_i}$. Each node has an intrinsic dynamics, which is affected by the state of some other nodes (i.e. the neighbors of i) by means of some coupling function. These interactions will be represented by means of directed graphs. In such a graph nodes sharing the same internal dynamics will be represented with the same symbol. Analogously, heterogeneous coupling functions can also be taken into account. Again, identical functions will be denoted by the same symbol.

This is formalized by the following definitions.

Definition 3.3.1. *An interconnected system consists of:*

1. *a set of nodes $\mathcal{N} := \{1, \ldots, N\}$;*
2. *an equivalence relation, $\sim_{\mathcal{N}}$ on $\mathcal{N}$;*
3. *a finite set, $\mathcal{E}$, of edges (arrows);*
4. *an equivalence relation, $\sim_{\mathcal{E}}$ on $\mathcal{E}$;*
5. *the maps $\mathcal{H} : \mathcal{E} \to \mathcal{N}$ and $\mathcal{T} : \mathcal{E} \to \mathcal{N}$ such that: for $e \in \mathcal{E}$, we have $\mathcal{H}(e)$ is the head of the arrow and $\mathcal{T}(e)$ the tail of the arrow;*

6. *equivalent arrows have equivalent tails and heads. That is, if* $e_1, e_2 \in \mathcal{E}$ *and* $e_1 \sim_{\mathcal{E}} e_2$, *then* $\mathcal{H}(e_1) \sim_{\mathcal{N}} \mathcal{H}(e_2)$ *and* $\mathcal{T}(e_1) \sim_{\mathcal{N}} \mathcal{T}(e_2)$.

Notice that the above definition coherently extends the definition of graph given in the previous Section.

The following set of edges, defining an important equivalence relation, is associated to each node, i.

Definition 3.3.2. *For any* $i \in \mathcal{N}$, *the input set of* i *is defined as*

$$\mathcal{I}(i) := \{e \in \mathcal{E} : \mathcal{H}(e) = i\}$$

Any element of $\mathcal{I}(i)$ *is termed as* input edge (or arrow) *of* i.

Definition 3.3.3. *The relation* $\sim_{\mathcal{I}}$ *(input equivalence) on* $\mathcal{N}$ *is defined by* $c \sim_{\mathcal{I}} d$ *if and only if there exists an arrow type preserving bijection* $\beta : \mathcal{I}(c) \to \mathcal{I}(d)$.

Finally, our set-up is completed by defining an interconnected system as follows:

Definition 3.3.4. *The dynamical system*

$$\dot{X} = \Phi(t, X) \tag{3.3}$$

defines an interconnected system if its phase space is defined as

$$P = \mathbb{R}^+ \times P_1 \times \dots P_N$$

where P_i *denotes the phase space of the* i*-th network node. Furthermore, let* $\pi_i : P \to P_i$ *be projections of (3.3), then it must hold that*

$$\pi_i(X(t)) = x_i(t)$$

3.3.2 Mathematical models

In this Section we present the mathematical models of networked systems used in the rest of the Thesis. All the mathematical models presented here are consistent with the general definition of interconnected system given above, i.e. Definition 3.3.1.

Let: $P_1 \subseteq \mathbb{R}^{n_1}$, $P_2 \subseteq \mathbb{R}^{n_2}$, ..., $P_N \subseteq \mathbb{R}^{n_N}$ be convex subsets (n_i is the dimension of the i-th node), $P := P_1 \times \ldots \times P_N$, $X := [x_1^T, \ldots, x_N^T]^T$, $x_i \in P_i$, $\phi_i(t, X) : \mathbb{R}^+ \times P \to P_i$ and $\Phi(t, X) := \left[\phi_1(t, X)^T, \ldots, \phi_N(t, X)^T\right]^T$. We assume that $\phi(t, X)$ is differentiable on X and that $\Phi(t, X)$ as well as $\frac{\partial \Phi}{\partial X}$ are both continuous on (t, X). In some applications it will be the case that P is some closed set, given e.g. by non-negativity constraints on variables and/or linear equalities representing mass-conservation laws. In general, for a non-open set, P, differentiability in X means that the vector field $\Phi(t,\cdot)$ can be extended as a differentiable function to some open set which includes P, with the continuity hypotheses with respect on (t, X) holding on such an open set.

The mathematical model for an interconnected system considered in this Thesis (see Chapter 6 and Chapter 7) is

$$\dot{x}_i = \phi_i(t, X) := f_i(t, x_i) + \tilde{h}_i(t, X) \tag{3.4}$$

with $i = 1, \ldots, N$, the function $f_i : \mathbb{R}^+ \times P_i \to P_i$ being the vector field associated to the intrinsic dynamics of the i-th node and the function $\tilde{h}_i : \mathbb{R}^+ \times P \to P_i$ (termed as input function, or coupling) describing the interaction of the i-th node with the other nodes composing the interconnected system. A particular choice for the coupling functions is:

$$\tilde{h}_i(t, X) = h_i(t, a_{i1}(t)x_1, \ldots, a_{iN}x_N)$$

where $A(t) := [a_{ij}(t)]$ is the $N \times N$ time varying adjacency matrix, with $a_{ij}(t) : \mathbb{R}^+ \to [0, 1]$ being smooth functions. That is, the above formalization allows us to consider within a unique framework directed and undirected networks, self-loops and multiple interactions. We will also consider networks with (smoothly) changing topology.

Sometimes, the compact form of (3.4) will be used, given by:

$$\dot{X} = \Phi(t, X) = F(t, X) + H(t, X)$$

with:

$$F(t, X) := \left[f_1(t, x_1)^T, \ldots, f_N(t, x_N)^T\right]^T$$

and

$$H(t, X) := \left[\tilde{h}_1(t, X), \ldots, \tilde{h}_N(t, X)\right]^T$$

A mathematical model similar to (3.4) will be also used for studying discrete-time and asynchronous systems (see Chapter 8).

In this Thesis, several *assumptions* on of the mathematical model (3.4) will be alternatively made. Namely:

- the case that all network nodes share the same dynamics will be studied. That is,

  $$f_1(t, \cdot) = \ldots = f_N(t, \cdot) = f(t, \cdot)$$

  and $F(t, X) := \left[f(t, x_1)^T, \ldots, f(t, x_N)^T\right]^T$, in (3.4).

- the case where the coupling functions are identical for all network nodes, i.e.

$$\tilde{h}_1(t,X) = \ldots = \tilde{h}_N(t,X) = \tilde{h}(t,X)$$

and $H(t,X) := \left[\tilde{h}(t,X)^T, \ldots, \tilde{h}(t,X)^T\right]^T$, in (3.4).

Sometimes, the coupling between nodes will be modeled as *diffusive*, i.e.

$$h_i(t,X) := \sum_{j \in N_i} \left[h_j(t,x_j) - h_j(t,x_i)\right]$$

In the next Section, we present some of the network coordination problems addressed in this Thesis. When needed, we will explicitly point out the assumptions made on (3.4)

3.4 Network coordination problems: a quick overview

In this Section we introduce some of the control/analysis problems that are addressed in the Thesis: consensus, synchronization and cluster synchronization. We refer to all such problems as *coordination* problems.

We remark here that all the coordination problems are stated for networks of continuous-time nodes. However, a formalization to the case of discrete-time networks is straightforward (see Chapter 8).

3.4.1 Consensus

One of the coordination problems which are addressed in Chapter 6 and Chapter 7 is the so-called consensus (or agreement) problem. Consensus problems have a long history in the field of computer science [117], where groups of *agents* have to agree upon certain quantities of interest in (3.4). Typically, in consensus problems, it is assumed that the dynamics of each network node is a simple integrator dynamics, i.e. $f_i(t,x_i) = 0$. Let $\xi : \mathbb{R}^N \to \mathbb{R}$ be a function of the network nodes' state variables, $x_1, \ldots, x_N$. The ξ consensus problem is then that of calculating $\xi\left(X(0)\right)$ by appropriately designing the coupling protocols $\tilde{h}_i$'s. In the special case where $\xi(X) := \frac{1}{N}\sum_{i=1}^N x_i$, the consensus problem is called *average consensus* problem. Sometimes, a slightly more complex dynamics at the nodes are considered: this is the case of e.g. higher order integrators dynamics. In this case, the consensus problem is termed as *higher order consensus* and becomes that of properly designing the coupling functions so as a subset of the state variables reach an agreement on $\xi\left(X(0)\right)$. An example of higher order consensus is the so-called rendezvous problem, see Chapter 7 for further details.

3.4.2 Synchronization

Another network coordination problem addressed in Chapter 7 is synchronization [25], [132]. In a classical context, synchronization means adjustment of rhythms of self-sustained oscillators due to some interaction. The study of synchronization can be traced back to Huygens in the 17th century and involves today a variety of research fields, such as mathematics [35], biology [198], neuroscience [29], robotics [33]. Typically, in network synchronization, all nodes are identical and the coupling between nodes is assumed to be diffusive and linear. That is, in (3.4):

$$h_i(t,X) := \Gamma \sum_{j \in N_i} (x_j - x_i)$$

in (3.4), where Γ is a constant coupling matrix. This choice for $h_i(t,X)$ models the fact that, when synchronization is achieved, the effects of coupling disappear. Notice that, in compact form, network dynamics can then be written by using the Laplacian matrix as:

$$\dot{X} = F(X) - (L \otimes \Gamma)X$$

where $\otimes$ denotes the Kronecker (or direct) product and

$$F(X) := \left[f(x_1)^T, \ldots, f(x_N)^T \right]^T$$

Notice that network synchronization is attained if all the trajectories of the above dynamics converge to the synchronization subspace

$$\mathcal{M} := \{x_1 = \ldots = x_N\}$$

3.4.3 Concurrent synchronization

In a network of dynamical elements which have different dynamics, *concurrent synchronization*, [142] is defined as the regime behavior where the whole network is *divided* into multiple groups of synchronized elements (in the literature this phenomenon is also known as cluster synchronization, or poli-synchronization). Sometimes, the term *cluster synchronization* will be used as a synonymous of concurrent synchronization. Concurrent synchronization phenomena are pervasive in the brain, where multiple *rhythms* are known to coexist [84] and may be useful for distributed algorithms or sensor networks, where different nodes of the network *process* different kinds of information. In terms of network dynamics, in (3.4) the coupling is assumed to be diffusive (not necessarily linear). Further details will be given in Chapter 6, Chapter 7, Chapter 8.

3.5 Concluding remarks

In this introductory Chapter, we briefly presented the main notions on networked systems used in the rest of the Thesis, together with some of the coordination problems addressed in what follows. The mathematical models and coordination problems introduced in this Chapter will be studied in Chapter 6, Chapter 7, Chapter 8. The main mathematical tools used to this aim are instead presented in the next Chapter.

Chapter 4

Extensions of Contraction Theory

In this Chapter we revisit and extend the ideas presented in Chapter 2. These extended results are then used in the rest of the Thesis. As pointed out in Chapter 2, contraction is dependent on the particular norm being considered for *measuring* the distances between trajectories and all of the results presented so far make implicitly use of the Euclidean norm. In this Chapter, arbitrary norms are instead used and a weaker condition is considered on the geometry of the subsets in phase space. Finally, some structural properties of the vector field together with contraction are used to determine the steady state behavior of a system of interest. The results presented in this Chapter were partly presented in [161], [163].

4.1 Introduction

As shown in Chapter 2, nonlinear contraction analysis [111] has been proposed as an effective tool to study the convergent properties of dynamical systems. The main idea of contraction theory (and more generally of incremental stability methods [7]) is to establish conditions in some phase space region of interest guaranteeing that neighboring trajectories converge exponentially towards each other. From such local result, global results can be obtained, and these are robust to noise, in the sense that, if a system satisfies a contraction property then trajectories remain bounded in the phase space [181].

As briefly pointed out in Chapter 2, applications to date of nonlinear contraction theory are based on the use of negative definite generalized Jacobians and Euclidians norms. As it was noticed in the original paper [111], other norms and their associated matrix measures [191] can also be used to quantify contraction, leading to similar results but conditions in different algebraic forms. The objectives of this Chapter can be summarized as follows:

- give a self-contained exposition, with all proofs included, of the results on contracting systems presented in Chapter 2 when arbitrary norms are considered.

In so doing, the definition of contracting system has to be slightly modified;

- derive a coherent theoretical framework where symmetries and contraction are used together to analyze (or control) dynamical systems. The approach is further generalized by showing that the above analysis can be performed on some auxiliary, or virtual, system, rather than the actual system itself. As such, our results provide a systematic framework extending and generalizing the results of [142, 64] in this context.;

- provide extensions to discrete-time systems.

All the results obtained in this Chapter are then used in the rest of the Thesis to analyze/control networks and biochemical systems (Chapter 6 - 9).

This Chapter is organized as follows. In Section 4.2 we define the notion of infinitesimally contracting system and prove that this *local* property implies a global property, i.e. contraction. The proof is given in a generalized form with respect to the one given in Chapter 2. In fact, convexity of the contraction region is replaced by a weaker constraint on the geometry of the space. In Section 4.3, we show that all the solutions of an infinitesimally contracting system, when forced by a periodic input, converge to a unique solution having the same period as the forcing. This is an extension of the result on periodic inputs presented in Section 2.4. In Sections 4.4-4.6 we revisit the questions regarding combinations of contracting systems, partial contraction and contraction relative to flow invariant subspaces. Finally, in the subsequent Sections we provide a coherent theoretical framework that links symmetries of a dynamical system to its contracting properties. Section 4.8 extends the notion of contraction (using arbitrary norms) to discrete-time systems.

4.2 Contraction using arbitrary norms

4.2.1 Definitions and problem statement

Consider again the generic system of ordinary differential equations (2.1). We assume that such a system is defined for $t \in [0, \infty)$ and $x \in C$, where $C \subseteq \mathbb{R}^n$. It will be assumed that $f(t, x)$ is differentiable on x, and that $f(t, x)$, as well as the Jacobian of f with respect to x, denoted as $J(t, x) = \frac{\partial f}{\partial x}(t, x)$, are both continuous in (t, x). In applications of the theory, it is often the case that C will be a closed set, for example given by non-negativity constraints on variables as well as linear equalities representing mass-conservation laws. For a non-open set C, differentiability in x means that the vector field $f(t, \cdot)$ can be extended as a differentiable function to some open set which includes C, and the continuity hypotheses with respect to (t, x) hold on this open set.

We denote by $\varphi(t, s, \xi)$ the value of the solution $x(t)$ at time t of the differential equation (2.1) with initial value $x(s) = \xi$. It is implicit in the notation that $\varphi(t, s, \xi) \in C$ ("forward invariance" of the state set C). This solution is, in principle, defined only on some interval $s \le t < s + \varepsilon$, but we will assume that $\varphi(t, s, \xi)$ is defined for all $t \ge s$. Conditions which guarantee such a "forward-completeness" property are often satisfied in biological applications, for example whenever the set C is closed and bounded, or whenever the vector field f is bounded. (See Appendix C in [175] for more discussion, as well as [9] for a characterization of the forward completeness property.) Under the stated assumptions, the function φ is jointly differentiable with respect to all of its arguments (this is a standard fact on well-posedness of differential equations, see for example Appendix C in [175]).

We recall (see for instance [124]) that, given a vector norm on Euclidean space ($|\cdot|$), with its induced matrix norm $\|A\|$, the associated *matrix measure* μ is defined as the directional derivative of the matrix norm, that is,

$$\mu(A) := \lim_{h \searrow 0} \frac{1}{h} \left(\|I + hA\| - 1 \right)$$

For example, if $|\cdot|$ is the standard Euclidean 2-norm, then $\mu(A)$ is the maximum eigenvalue of the symmetric part of A. As we shall see, however, different norms will be useful for our applications. Matrix measures are also known as "*logarithmic norms*", a concept independently introduced by Germund Dahlquist and Sergei Lozinskii in 1959, [38, 114]. The limit is known to exist, and the convergence is monotonic, see [179, 38]. Some matrix measures are reported in Table 4.1.

Table 4.1: Some matrix measures $n \times n$ matrix, $A = [a_{ij}]$. The i-th eigenvalue of A is denoted with $\lambda_i(A)$.

vector norm, $\lvert\cdot\rvert$	induced matrix measure, $\mu(A)$
$\lvert x\rvert_1 = \sum_{j=1}^n \lvert x_j\rvert$	$\mu_1(A) = \max_j \left(a_{jj} + \sum_{i \ne j} \lvert a_{ij}\rvert \right)$
$\lvert x\rvert_2 = \left(\sum_{j=1}^n \lvert x_j\rvert^2 \right)^{\frac{1}{2}}$	$\mu_2(A) = \max_i \left(\lambda_i \left\{ \frac{A + A^T}{2} \right\} \right)$
$\lvert x\rvert_\infty = \max_{1 \le j \le n} \lvert x_j\rvert$	$\mu_\infty(A) = \max_i \left(a_{ii} + \sum_{j \ne i} \lvert a_{ij} \rvert \right)$

We will say that system (2.1) is *infinitesimally contracting* on a convex set $C \subseteq \mathbb{R}^n$ if there exists some norm in C, with associated matrix measure μ such that, for some constant $c \in \mathbb{R} - \{0\}$,

$$\mu(J(t, x)) \le -c^2, \quad \forall x \in C, \quad \forall t \ge 0. \tag{4.1}$$

Let us discuss the motivation for this concept. Since by assumption $f(t, x)$ is continuously differentiable, the following exact *differential* relation can be obtained from (2.1):

$$\delta \dot{x} = J\,(t, x)\,\delta x \tag{4.2}$$

where, as before, $J = J\,(t, x)$ denotes the Jacobian of the vector field f, as a function of $x \in C$ and $t \in \mathbb{R}^+$, and where δx denotes a small change in states and "$\delta \dot{x}$" means $d\delta x/dt$, evaluated along a trajectory. (In mechanics, as in [13], δx is called "virtual displacement", and formally it may be thought of as a linear tangent differential form, differentiable with respect to time.) Consider now two neighboring trajectories of (2.1), evolving in C, and the virtual displacements between them. Note that (4.2) can be thought of as a linear time-varying dynamical system of the form:

$$\delta \dot{x} = J\,(t)\,\delta x$$

once that $J(t) = J(t, x(t))$ is thought of as a fixed function of time. Hence, an upper bound for the magnitude of its solutions can be obtained by means of the Coppel inequality [191], yielding:

$$|\delta x| \leq |\delta x_0|\, e^{\int_0^t \mu(J(\xi))d\xi}, \tag{4.3}$$

where $\mu\,(J)$ is the matrix measure of the system Jacobian induced by the norm being considered on the states and $|\delta x\,(0)| = |\delta x_0|$. Using (4.3) and (4.1), we have that

$$\exists \quad \beta > 0: \quad |\delta x\,(t)| \leq \beta e^{-c^2 t}$$

Thus, trajectories starting from infinitesimally close initial conditions converge exponentially towards each other. In what follows we will refer to c^2 as *contraction (or convergence) rate.*

4.2.2 Main convergence result

The key theoretical result about contracting systems links infinitesimal and global contractivity, and is stated below. This result can be traced, under different technical assumptions, to e.g. [111], [138], [99], [79].

Theorem 4.2.1. *Suppose that C is a convex subset of $\mathbb{R}^n$ and that $f(t, x)$ is infinitesimally contracting with contraction rate c^2. Then, for every two solutions $x(t) = \varphi(t, 0, \xi)$ and $z(t) = \varphi(t, 0, \zeta)$ of (2.1), it holds that:*

$$|x(t) - z(t)| \;\leq\; e^{-c^2 t}\,|\xi - \zeta|\,, \qquad \forall\, t \geq 0 \tag{4.4}$$

In other words, infinitesimal contractivity implies global contractivity. Motivated by this, in the rest of this Thesis, we will use the word *contracting* to denote an *infinitesimal contracting* system. We now provide a self-contained proof of Theorem 4.2.1. In fact, the result is shown here in a generalized form, in which convexity is replaced by a weaker constraint on the geometry of the space.

K-reachable sets

We will make use of the following definition:

Definition 4.2.1. *Let $K > 0$ be any positive real number. A subset $C \subset \mathbb{R}^n$ is K-*reachable *if, for any two points x_0 and y_0 in C there is some continuously differentiable curve $\gamma : [0, 1] \to C$ such that:*

1. $\gamma(0) = x_0$,
2. $\gamma(1) = y_0$ *and*
3. $|\gamma'(r)| \le K |y_0 - x_0|$, $\forall r$.

For convex sets C, we may pick $\gamma(r) = x_0 + r(y_0 - x_0)$, so $\gamma'(r) = y_0 - x_0$ and we can take $K = 1$. Thus, convex sets are 1-reachable, and it is easy to show that the converse holds as well.

Notice that a set C is K-reachable for some K if and only if the length of the geodesic (smooth) path (parametrized by arc length), connecting any two points x and y in C, is bounded by some multiple K_0 of the Euclidean norm, $|y - x|_2$. Indeed, re-parametrizing to a path γ defined on $[0, 1]$, we have:

$$|\gamma'(r)|_2 \le K_0 |y - x|_2$$

Since in finite dimensional spaces all the norms are equivalent, then it is possible to obtain a suitable K for Definition 4.2.1.

Remark 4.2.1. *The notion of K-reachable set is weaker that that of convex set. Nonetheless, in Theorem 4.2.2, we will prove that trajectories of a smooth system, evolving on a K-reachable set, converge towards each other, even if C is not convex. This additional generality allows one to establish contracting behavior for systems evolving on phase spaces exhibiting "obstacles", as are frequently encountered in path-planing problems, for example. A mathematical example of a set with obstacles follows.*

Example 4.2.1. *Consider the two dimensional set, C, defined by the following constraints:*

$$x^2 + y^2 \ge 1, \quad x \ge 0, \quad y \ge 0 \ .$$

Clearly, C is a non-convex subset of $\mathbb{R}^2$. We claim that C is K-reachable, for any positive real number $K > \frac{2}{\pi}$. Indeed, given any two points a and b in C, there are two possibilities: either the segment connecting a and b is in C, or it intersects the unit circle. In the first case, we can simply pick the segment as a curve ($K = 1$).

In the second case, one can consider a straight segment that is modified by taking the shortest perimeter route around the circle; the length of the perimeter path is at most $\frac{2}{\pi}$ times the length of the omitted segment. (In order to obtain a differentiable, instead of merely a piecewise-differentiable, path, an arbitrarily small increase in K is needed.)

Using the concept of K-reachable sets we can now relax the assumptions of Theorem 2.3.1 in Chapter 2 and prove the following result.

Theorem 4.2.2. *Suppose that C is a K-reachable subset of $\mathbb{R}^n$ and that $f(t,x)$ is infinitesimally contracting with contraction rate c^2. Then, for every two solutions $x(t) = \varphi(t,0,\xi)$ and $z(t) = \varphi(t,0,\zeta)$ it holds that:*

$$|x(t) - z(t)| \leq Ke^{-c^2 t} |\xi - \zeta| \qquad \forall\, t \geq 0\,. \tag{4.5}$$

Proof of Theorem 4.2.2

We now prove the main result on contracting systems, i.e. Theorem 4.2.1, under the hypotheses that the set C, i.e. the set on which the system evolves, is K-reachable.

Proof. Given any two points $x\,(0) = \xi$ and $z\,(0) = \zeta$ in C, pick a smooth curve $\gamma : [0,1] \to C$, such that $\gamma\,(0) = \xi$ and $\gamma\,(1) = \zeta$. Let $\psi\,(t,r) = \varphi(t,0,\gamma\,(r)$, that is, the solution of system (2.1) rooted in $\psi\,(0,r) = \gamma\,(r)$, $r \in [0,1]$. Since φ and γ are continuously differentiable, also $\psi\,(t,r)$ is continuously differentiable in both arguments. We define

$$w(t,r) := \frac{\partial \psi}{\partial r}(t,r)$$

It follows that

$$\frac{\partial w}{\partial t}(t,r) = \frac{\partial}{\partial t}\left(\frac{\partial \psi}{\partial r}\right) = \frac{\partial}{\partial r}\left(\frac{\partial \psi}{\partial t}\right) = \frac{\partial}{\partial r} f(\psi\,(t,r)\,,t)$$

Now,

$$\frac{\partial}{\partial r} f(\psi\,(t,r)\,,t) = \frac{\partial f}{\partial x}(\psi\,(t,r)\,,t)\frac{\partial \psi}{\partial r}(t,r)$$

so, we have:

$$\frac{\partial w}{\partial t}(t,r) = J(\psi\,(t,r)\,,t)w(t,r) \tag{4.6}$$

where $J(\psi\,(t,r)\,,t) = \frac{\partial f}{\partial x}(\psi\,(t,r)\,,t)$. Using Coppel's inequality [191], yields

$$|w(t,r)| \leq |w(0,r)|\, e^{\int_0^t \mu(J(\tau))d\tau} \leq K\,|\xi - \zeta|\, e^{-c^2 t} \tag{4.7}$$

$\forall x \in C$, $\forall t \in \mathbb{R}^+$, and $\forall r \in [0,1]$. Notice the Fundamental Theorem of Calculus, we can write

$$\psi\,(t,1) - \psi\,(t,0) = \int_0^1 w(t,s)ds$$

Hence, we obtain

$$|x(t) - z(t)| \leq \int_0^1 |w(t,s)|ds$$

Now, using (4.7), the above inequality becomes:

$$|x(t) - z(t)| \leq \int_0^1 \left(|w(0,s)| \, e^{\int_0^t \mu(J(\tau))d\tau} \right) ds \leq K \, |\xi - \zeta| \, e^{-c^2 t}$$

The Theorem is then proved. □

Proof of Theorem 4.2.1: The proof follows trivially from Theorem 4.2.2, after having noticed that in the convex case, we may assume $K = 1$. □

4.3 Contracting systems forced by periodic inputs

In actual applications, often one is given a system which depends implicitly on the time, t, by means of a continuous function $u(t)$, i.e. systems dynamics are represented by $\dot{x} = f(x, u(t))$. In this case, $u(t) : \mathbb{R}^+ \to U$ (where U is some subset of $\mathbb{R}$), represents an external input. It is important to observe that the contractivity property does not require any prior information about this external input. In fact, since $u(t)$ does not depend on the system state variables, when checking the property, it may be viewed as a constant parameter, $u \in U$. Thus, if contractivity of $f(x, u)$ holds uniformly $\forall u \in U$, then it will also hold for $f(x, u(t))$.

Given a number $T > 0$, we will say that system (2.1) is T-*periodic* if it holds that

$$f(t + T, x) \; = \; f(t, x) \qquad \forall \, t \geq 0, \, x \in C$$

Notice that the system $\dot{x} = f(x, u(t))$ is T-periodic, if the external input, $u(t)$, is itself a periodic function of period T.

The following is a theoretical result about periodic orbits which is an analogous of the result on periodic inputs presented in Section 2.4. It may be found, under various different technical variants, in the references given above, e.g. [111].

Theorem 4.3.1. *Suppose that:*

- *C is a closed convex subset of $\mathbb{R}^n$;*
- *f is infinitesimally contracting with contraction rate c^2;*
- *f is T-periodic.*

Then, there is a unique periodic solution $\alpha(t) : [0, \infty) \to C$ of (2.1) of period T and, for every solution $x(t)$, it holds that $|x(t) - \alpha(t)| \to 0$ as $t \to \infty$.

Now, we provide a self-contained proof of Theorem 4.3.1, in a generalized form which does not require convexity.

4.3.1 Proof of Theorem 4.3.1

In this Section we assume that the vector field f is T-periodic and prove Theorem 4.3.1.

Remark 4.3.1. *Periodicity implies that the initial time is only relevant modulo T. More precisely:*

$$\varphi(kT+t, kT, \xi) = \varphi(t, 0, \xi) \qquad \forall\, k \in \mathbb{N}, t \geq 0,\, x \in C \tag{4.8}$$

Indeed, let $z(s) = \varphi(s, kT, \xi)$, $s \geq kT$, and consider the function $x(t) = z(kT+t) = \varphi(kT+t, kT, \xi)$, for $t \geq 0$. So,

$$\dot{x}(t) = \dot{z}(kT+t) = f(kT+t, z(kT+t)) = f(kT+t, x(t)) = f(t, x(t))$$

where the last equality follows by T-periodicity of f. Since $x(0) = z(kT) = \varphi(kT, kT, \xi) = \xi$, it follows by uniqueness of solutions that $x(t) = \varphi(t, 0, \xi) = \varphi\,(kT+t, kT, \xi)$, which is (4.8). As a corollary, we also have that

$$\varphi(kT+t, 0, \xi) = \varphi(kT+t, kT, \varphi(kT, 0, \xi)) = \varphi(t, 0, \varphi(kT, 0, \xi)) \tag{4.9}$$

$\forall\, k \in \mathbb{N}, t \geq 0,\, x \in C$, where the first equality follows from the semigroup property of solutions (see e.g. [175]), and the second one from (4.8) applied to $\varphi(kT, 0, \xi)$ instead of ξ.

Define now

$$P(\xi) = \varphi(T, 0, \xi)$$

where $\xi = x\,(0) \in C$. The following Lemma will be useful in what follows.

Lemma 4.3.1. *$P^k(\xi) = \varphi(kT, 0, \xi)$ for all $k \in \mathbb{N}$ and $\xi \in C$.*

Proof. We will prove the Lemma by recursion. In particular, the statement is true by definition when $k = 1$. Inductively, assuming it true for k, we have:

$$P^{k+1}(\xi) = P(P^k(\xi)) = \varphi(T, 0, P^k(\xi)) = \varphi(T, 0, \varphi(kT, 0, \xi)) = \varphi(kT+T, 0, \xi)$$

as wanted. □

Theorem 4.3.2. *Suppose that:*

- *C is a closed K-reachable subset of $\mathbb{R}^n$;*

- *f is infinitesimally contracting with contraction rate c^2;*
- *f is T-periodic;*
- $Ke^{-c^2T} < 1$.

Then, there is a unique periodic solution $\alpha(t) : [0,\infty) \to C$ of (2.1) having period T. Furthermore, every solution $x(t)$, such that $x(0) = \xi \in C$, converges to $\alpha(t)$, i.e. $|x(t) - \alpha(t)| \to 0$ as $t \to \infty$.

Proof. Observe that P is a contraction with factor $Ke^{-c^2T} < 1$: $|P(\xi) - P(\zeta)| \leq Ke^{-c^2T}|\xi - \zeta|$ for all $\xi, \zeta \in C$, as a consequence of Theorem 4.2.2. The set C is a closed subset of $\mathbb{R}^n$ and hence complete as a metric space with respect to the distance induced by the norm being considered. Thus, by the contraction mapping theorem, there is a (unique) fixed point $\bar{\xi}$ of P. Let $\alpha(t) := \varphi(t, 0, \bar{\xi})$. Since $\alpha(T) = P(\bar{\xi}) = \bar{\xi} = \alpha(0)$, $\alpha(t)$ is a periodic orbit of period T. Moreover, again by Theorem 4.2.2, we have that $|x(t) - \alpha(t)| \leq Ke^{-c^2t}\left|\xi - \bar{\xi}\right| \to 0$. Uniqueness is clear, since two different periodic orbits would be disjoint compact subsets, and hence at positive distance from each other, contradicting convergence. This completes the proof. □

Proof of Theorem 4.3.1: It will suffice to note that the assumption $Ke^{-c^2T} < 1$ in Theorem 4.3.2 is automatically satisfied when the set C is convex (i.e. $K = 1$) and the system is infinitesimally contracting. □

Notice that, even in the non-convex case, the assumption $Ke^{-c^2T} < 1$ can be ignored, if we are willing to assert only the existence (and global convergence to) a unique periodic orbit, with some period kT for some integer $k > 1$. Indeed, the vector field is also kT-periodic for any integer k. Picking k large enough so that $Ke^{-c^2kT} < 1$, we have the conclusion that such an orbit exists, applying Theorem 4.3.2.

4.3.2 A simple example

As a first example to illustrate the application of the concepts introduced so far, we choose a simple bimolecular reaction, in which a molecule of A and one of B can reversibly combine to produce a molecule of C.

This system can be modeled by the following set of differential equations:

$$\begin{aligned} \dot{A} &= -k_1AB + k_{-1}C \\ \dot{B} &= -k_1AB + k_{-1}C \\ \dot{C} &= k_1AB - k_{-1}C \end{aligned} \tag{4.10}$$

where we are using $A = A(t)$ to denote the concentration of A and so forth. The system evolves in the positive orthant of $\mathbb{R}^3$. Solutions satisfy (stoichiometry) constraints:

$$\begin{aligned} A(t) + C(t) &= \alpha \\ B(t) + C(t) &= \beta \end{aligned} \tag{4.11}$$

for some constants α and β.

We will assume that one or both of the "kinetic constants" k_i are time-varying, with period T. Such a situation arises when the k_i's depend on concentrations of additional enzymes, which are available in large amounts compared to the concentrations of A, B, C, but whose concentrations are periodically varying. The only assumption will be that $k_1(t) \geq k_1^0 > 0$ and $k_{-1}(t) \geq k_{-1}^0 > 0$ for all t.

Because of the conservation laws (4.11), we may restrict our study to the equation for C. Once all solutions of this equation are shown to globally converge to a periodic orbit, the same will follow for $A(t) = \alpha - C(t)$ and $B(t) = \beta - C(t)$. We have that:

$$\dot{C} = k_1 (\alpha - C)(\beta - C) - k_{-1} C \tag{4.12}$$

Because $A(t) \geq 0$ and $B(t) \geq 0$, this system is studied on the subset of $\mathbb{R}$ defined by $0 \leq C \leq \min\{\alpha, \beta\}$. The equation can be rewritten as:

$$\dot{C} = k_1 \left(\alpha\beta - \alpha C - \beta C + C^2\right) - k_{-1} C \tag{4.13}$$

Differentiation with respect to C of the right-hand side in the above system yields this (1×1) Jacobian:

$$J := k_1 \left(-(\alpha + \beta) + 2C - k_{-1}\right) \tag{4.14}$$

Since we know that $-\alpha + C \leq 0$ and $-\beta + C \leq 0$, it follows that

$$J \leq -k_1 k_{-1} \leq -k_1^0 k_{-1}^0 := -c^2$$

for $c = \sqrt{k_1^0 k_{-1}^0}$. Using any norm (this example is in dimension one) we have that $\mu(J) < -c^2$. So (4.10) is contracting and, by means of Theorem 4.3.1, solutions will globally converge to a unique solution of period T (notice that such a solution depends on system parameters).

Figure 4.1 shows the behavior of the dynamical system (4.13), using two different values of k_{-1}. Notice that the asymptotic behavior of the system depends on the particular choice of the biochemical parameters being used. Furthermore, it is worth noticing here that the higher the value of k_{-1}, the faster will be the convergence to the attractor.

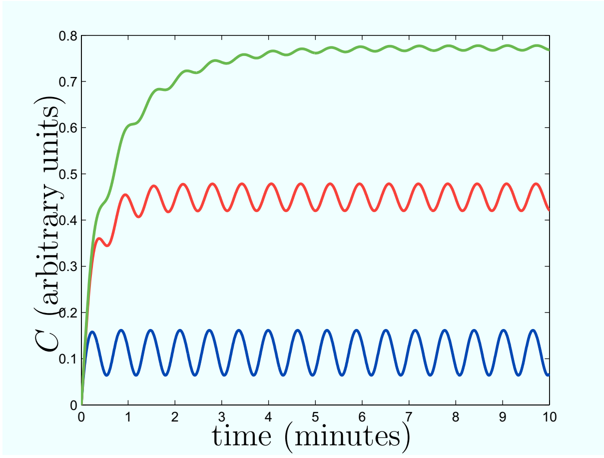

Figure 4.1: Entrainment of (4.13) to the periodic input $u(t) = 1.5 + \sin(10t)$ for $k_{-1} = 10$ (blue), $k_{-1} = 1$ (green), $k_{-1} = 0.1$ (red). Notice that an increase of k_{-1}, causes an increase of the contraction rate, hence trajectories converge faster to the system unique periodic attractor. The other system parameters are set to: $\alpha = \beta = 1$, $k_2 = 0.1$.

4.4 Hierarchies of contracting systems

An interesting property of contracting systems is that cascades of contracting systems remain contracting, it is enough to show this, inductively, for a cascade of two systems.

Consider a system of the following form:

$$\begin{aligned}\dot{x} &= f(t,x)\\ \dot{y} &= g(t,x,y)\end{aligned}$$

where $x(t) \in C_1 \subseteq \mathbb{R}^{n_1}$ and $y(t) \in C_2 \subseteq \mathbb{R}^{n_2}$ for all t (C_1 and C_2 are two K-reachable sets). We write the Jacobian of f with respect to x as $A(t,x) = \frac{\partial f}{\partial x}(t,x)$, the Jacobian of g with respect to x as $B(t,x,y) = \frac{\partial g}{\partial x}(t,x,y)$, and the Jacobian of g with respect to y as $C(t,x,y) = \frac{\partial g}{\partial y}(t,x,y)$,

We assume the following:

1. The system $\dot{x} = f(t,x)$ is infinitesimally contracting with respect to some norm (generally indicated as $|\cdot|_*$), with some contraction rate c_1^2, that is, $\mu_*(A(t,x)) \leq -c_1^2$ for all $x \in C_1$ and all $t \geq 0$, where μ_* is the matrix measure associated to $|\cdot|_*$.

2. The system $\dot{y} = f(t,x,y)$ is infinitesimally contracting with respect to some norm (which is, in general different from $|\cdot|_*$, and is denoted by $|\cdot|_{**}$), with contraction rate c_2^2, when x is viewed a a parameter in the second system, that is, $\mu_{**}(C(t,x,y)) \leq -c_2^2$ for all $x \in C_1$, $y \in C_2$ and all $t \geq 0$, where μ_{**} is the matrix measure associated to $|\cdot|_{**}$.

3. The mixed Jacobian $B(t,x,y)$ is bounded: $\|B(t,x,y)\| \leq k^2$, for all $x \in C_1$, $y \in C_2$ and all $t \geq 0$, for some real number k, where "$\|\cdot\|$" is the operator norm induced by $|\cdot|_*$ and $|\cdot|_{**}$ on linear operators $\mathbb{R}^{n_1 \times n_2 \times 1} \to \mathbb{R}^{n_1 \times n_2}$. (All norms in Euclidean space being equivalent, this can be verified in any norm.)

We claim that, under these assumptions, the complete system is infinitesimally contracting. More precisely, pick any two positive numbers p_1 and p_2 such that

$$c_1^2 - \frac{p_2}{p_1} k^2 \; > \; 0$$

and let

$$c^2 := \min\left\{c_1^2 - \frac{p_2}{p_1} k^2, c_2^2\right\}$$

We will show that $\mu(J) \leq -c^2$, where J is the full Jacobian:

$$J = \begin{bmatrix} A & 0 \\ B & C \end{bmatrix} \tag{4.15}$$

with respect to the matrix measure μ induced by the following norm in $\mathbb{R}^{n_1 \times n_2}$:

$$|(x_1, x_2)| = p_1 \left|x_1\right|_* + p_2 \left|x_2\right|_{**}$$

Since

$$(I + hJ)x = \begin{bmatrix} (I + hA)x_1 \\ hBx_1 + (I + hC)x_2 \end{bmatrix}$$

for all h and x, we have that:

$$\begin{aligned} |(I + hJ)x| &= p_1 \left|(I + hA)x_1\right| + p_2 \left|hBx_1 + (I + hC)x_2\right| \\ &\leq p_1 \left|I + hA\right| \left|x_1\right| + p_2 \left|hB\right| \left|x_1\right| + p_2 \left|I + hC\right| \left|x_2\right| \end{aligned}$$

where from now on we drop subscripts for norms. Pick now any $h > 0$ and a unit vector x (which depends on h) such that $\|I + hJ\| = |(I + hJ)x|$. Such a vector x exists by the definition of induced matrix norm, and we note that $1 = |x| = p_1 \left|x_1\right|_* + p_2 \left|x_2\right|_{**}$, by the definition of the norm in the product space. Therefore:

$$\begin{aligned} \frac{1}{h}\left(\|I + hJ\| - 1\right) &= \frac{1}{h}\left(|(I + hJ)x| - |x|\right) \\ &\leq \frac{1}{h}\left(p_1 \left|I + hA\right| \left|x_1\right| + p_2 \left|hB\right| \left|x_1\right| + p_2 \left|I + hC\right| \left|x_2\right| - p_1 \left|x_1\right| - p_2 \left|x_2\right|\right) \\ &= \frac{1}{h}\left(\left|I + hA\right| - 1 + \frac{p_2}{p_1} h \left|B\right|\right) p_1 \left|x_1\right| + \frac{1}{h}\left(\left|I + hC\right| - 1\right) p_2 \left|x_2\right| \\ &\leq \max\left\{\frac{1}{h}\left(\left|I + hA\right| - 1\right) + \frac{p_2}{p_1} k^2 \, , \, \frac{1}{h}\left(\left|I + hC\right| - 1\right)\right\} \end{aligned}$$

where the last inequality is a consequence of the fact that $\lambda_1 a_1 + \lambda_2 a_2 \leq \max\{a_1, a_2\}$ for any nonnegative numbers with $\lambda_1 + \lambda_2 = 1$ (convex combination of the a_i's). Now taking limits as $h \searrow 0$, we conclude that

$$\mu(J) \leq \max\left\{-c_1^2 + \frac{p_2}{p_1}k^2, -c_2^2\right\} = -c^2$$

as desired.

4.5 Partial contraction

The notion of partial contraction can also be extended when using arbitrary norms. Consider, again the system (2.1) and construct an auxiliary system as follows:

$$\dot{y} = v\,(t, y, x(t)) \tag{4.16}$$

with the property that

$$v\,(t, x, x) = f\,(t, x) \tag{4.17}$$

We say that (4.16) is a *virtual system* for (2.1). Now, notice that (4.17) implies that the solutions of (4.16) are also solutions of (4.17). Furthermore, $x(t)$ is an input to (4.16). Now, if the virtual system is contracting uniformly in $x(t)$, then all of its solutions contract towards a unique solution, say $y_c(t)$. This, in turn, implies that for any solution of (4.16), say $z(t)$:

$$|z(t) - y_c(t)| \to 0, \quad t \to +\infty$$

4.6 Contraction towards linear flow invariant subspaces

We now revisit the question of contractions relative to a linear flow invariant subspace $\mathcal{M}$ originally posed in [142] (we will also term this as *relative contractions*)

Let us pick any orthogonal matrix Q ($QQ^{\mathrm{T}} = Q^{\mathrm{T}}Q = I$), and partition Q as:

$$Q = (VW) \in \mathbb{R}^{n\times n}$$

with $V^T = (v_1, \ldots, v_q) \in \mathbb{R}^{n\times q}$ and $W^T = (w_1, \ldots, w_m) \in \mathbb{R}^{n\times m}$. Since Q is orthogonal, $V^TV + W^TW = I$, $WW^T = I$, $VV^T = I$, $WV^T = 0$, and $VW^T = 0$ (zero and identity matrices of appropriate sizes). Let $\mathcal{M}$ be the linear subspace of $\mathbb{R}^n$ spanned by the rows of $W \in \mathbb{R}^{n\times m}$, say w_i, $i = 1, \ldots m$. Equivalently, the rows of V, say v_i, constitute an orthogonal basis of $\mathcal{M}^\perp$, i.e. $\mathcal{M} = \ker V$,. In applications to interconnected systems, $\mathcal{M}$ will typically be the synchronization manifold (see Chapter 3). We consider the following conditions on C:

$$V^T\mathbb{R}^q + W^T WC \ \subseteq\ C \tag{4.18}$$

(this condition is satisfied in the special case that $C = \mathbb{R}^n$) and on f:

$$Vf(t, W^T WC) \ \subseteq\ C \tag{4.19}$$

Since $\mathcal{M}$ is the range of W^T and the kernel of V, condition (4.19) is satisfied if we know that $\mathcal{M}$ is a forward-invariant set, $f(t, M) \subseteq \mathcal{M}$.

We say that system (2.1) is *infinitesimally contracting to* $\mathcal{M}$ if there exists some norm in $\mathbb{R}^n$, with associated matrix measure μ, such that, for some constant $c^2 \neq 0$, the *contraction rate*:

$$\mu\left(VJ\left(t,x\right)V^T\right) \leq -c^2, \quad \forall x \in C, \quad \forall t \geq 0 \tag{4.20}$$

We can then state the main result as follows.

Theorem 4.6.1. *Suppose that C, M, V satisfy conditions (4.18) and (4.19), and that $f(t,x)$ is infinitesimally contracting to $\mathcal{M}$ with contraction rate c. Consider any solution $x(t) = \varphi(t, 0, \xi)$ of (2.1). Then*

$$|Vx(t)| \ \leq\ e^{-c^2 t}\,|V\xi|\,, \qquad \forall\, t \geq 0 \tag{4.21}$$

Since $Vx(t) \to 0$ as $t \to \infty$ is equivalent to $x(t) \to \ker V = \mathcal{M}$, this result implies that every trajectory of (2.1) approaches $\mathcal{M}$ exponentially.

Proof. Fix the particular solution $\bar{x}(t) = \varphi(t, 0, \xi)$ of (2.1) of interest. Let $\eta := V\bar{x}(0) \in \mathbb{R}^q$. We consider the following system of differential equations in $\mathbb{R}^q$:

$$\dot{y} \ =\ g(t,y) \ :=\ Vf(t, V^T y + W^T W\bar{x}(t)) \tag{4.22}$$

For each $r \in [0, 1]$, let

$$\psi\,(t,r) \ :=\ \text{solution of (4.22) with } \ \psi\,(0,r) \ =\ r\,\eta$$

The function $\psi\,(t,r)$ is continuously differentiable jointly on (t,r).

Observe that $\bar{x}(t) = (V^T V + W^T W)\bar{x}(t) = V^T\bar{y}(t) + W^T W\bar{x}(t)$, where $\bar{y}(t) := V\bar{x}(t)$. Since $\bar{x}$ satisfies $\dot{x} = f(t,x)$, it follows that $\dot{\bar{y}} = Vf(t,\bar{x}) = g(t, \bar{y}(t))$. This means that $\bar{y}(t)$ is a solution of (4.22). Since $\bar{y}(0) = V\bar{x}(0) = \eta$, it follows by uniqueness of solutions that $\psi\,(t,1) = \bar{y}(t)$ for all $t \geq 0$.

Similarly, $y \equiv 0$ is also a solution, because $Vf(t, W^T W\bar{x}(t)) \equiv 0$ (by condition (4.19). Thus, $\psi(t,0) = 0$ for all $t \geq 0$.

We define

$$w(t,r) := \frac{\partial \psi}{\partial r}(t,r)$$

Since $\psi(0,r) = r\eta$, we have that $w(0,r) = \eta$ for all r. Furthermore,

$$\begin{aligned} \frac{\partial w}{\partial t}(t,r) &= \frac{\partial}{\partial t}\left(\frac{\partial \psi}{\partial r}\right) = \frac{\partial}{\partial r}\left(\frac{\partial \psi}{\partial t}\right) \\ &= \frac{\partial}{\partial r} g(t, \psi(t,r)) = A(t,r)\, w(t,r) \end{aligned}$$

where,

$$A(t,r) = VJ(t, x(t,r))V^T$$

and where, using (4.18)

$$x(t,r) := V^T \psi(t,r) + W^T W \bar{x}(t) \in C$$

Coppel's inequality [191] yields:

$$|w(t,r)| \leq |w(0,r)|\, e^{\int_0^t \mu(A(\tau,r))d\tau} \leq |\eta|\, e^{-c^2 t} \tag{4.23}$$

for all $t \geq 0$ and all $r \in [0,1]$. From

$$\bar{y}(t) - 0 = \psi(t,1) - \psi(t,0) = \int_0^1 w(t,r)\, dr$$

it now follows that

$$|\bar{y}(t)| \leq \int_0^1 |w(t,r)|\, dr \leq |\eta|\, e^{-ct}$$

and the proof is complete because $\eta = V\bar{x}(0) = V\xi$ and $\bar{y}(t) = V\bar{x}(t)$. □

4.7 Contraction and symmetries of dynamical systems

We now turn our attention to the study of the effects of symmetries of vector fields on their contraction properties.

In this Section, we consider operators acting over the state space of (2.1). It will be often the case that such operators are linear: in this case, they belong to GL, the *general linear group*.

The *effects* of the operators on the *structure* of the solutions of (2.1) can be specified in terms of a group of transformations, see e.g. [69]. In what follows, we will denote with the term *symmetries* of a system of ODEs the transformations that preserves the *structure* of solutions of (2.1).

We will extensively use the following definitions:

Definition 4.7.1. *Let Γ be a group of operators acting on $\mathbb{R}^n$. We say that $\gamma \in \Gamma$ is a symmetry of (2.1) if for any solution, $x(t)$, $\gamma x(t)$ is also a solution. Furthermore, if $\gamma x = x$, we say that the solution $x(t)$ is γ-symmetric.*

Definition 4.7.2. *Let Γ be a group of operators acting on $\mathbb{R}^n$, and $f : \mathbb{R}^+ \times \mathbb{R}^n \to \mathbb{R}^n$. The vector field, f, is said to be γ-equivariant if $f(t, \gamma x) = \gamma f(t, x)$, for any $\gamma \in \Gamma$ and $x \in \mathbb{R}^n$.*

Thus, γ-equivariance in essence means that γ "commutes" with f.

Definition 4.7.3. *We say that a solution of (2.1) is h-symmetric, if there exist some $T > 0$ such that $x(t) = \gamma x(t + T)$. The vector field, f, is said to be h-equivariant if $f(t, \gamma x) = \gamma f(t + T, x)$.*

In what follows we will refer to γ and h as actions, and *id* will denote the identity action.

Symmetries, equivariance and invariant subspaces

We first review the relationship [69] between symmetries, equivariance, and the existence of flow-invariant linear subspace.

If f is γ-equivariant, then γ is a symmetry of (2.1). Indeed, letting $y(t) = \gamma x(t)$, we have

$$\dot{y} = \gamma \dot{x} = \gamma f(t, x) = f(t, \gamma x) = f(y, t)$$

so that $y(t)$ is also a solution of (2.1).

If the operator γ is linear, this in turn immediately implies that the subspace $\mathcal{M}_\gamma = \{x \in \mathbb{R}^n : \gamma x = x\}$ is flow-invariant under the dynamics (2.1). Thus, solutions having symmetric initial conditions, $x_0 = \gamma x_0$, preserve that symmetry for any $t \geq 0$. Note that $\mathcal{M} \neq \emptyset$ since $\mathbf{0} \in \mathcal{M}$.

In the rest of the Thesis we assume γ to be any linear operator (under simple conditions specified in the next section) and give some extensions for nonlinear operators. Therefore, our framework is somewhat broader than that typically considered in the literature on symmetries of dynamical systems, where it is typically assumed that γ describes finite groups or compact Lie Groups, see e.g. [69] and references therein.

Basic results on symmetries and contraction

We first review some results from [64] which this Section shall generalize. Those results can be summarized as follows:

- If the dynamical system of interest is contracting, then γ and h symmetries of the vector fields are transferred onto symmetries of trajectories.
- if f presents some spatial symmetry, then this property can be transferred to the solutions x be only requiring contraction towards a properly defined subspace; this condition is less strict than the previous one.

Note that, although the proofs in [64] are presented in the context of Euclidian norms, they generalize straightforwardly to other norms as they just use the definition of contraction.

Theorem 4.7.1. *Assume that $f(t,x)$ in (2.1) is γ-equivariant. Then, all the solutions of (2.1) globally exponentially converge towards a unique γ-symmetric solution if one of the following conditions hold:*

1. *f is contracting;*
2. *f is contracting towards $\mathcal{M}_\gamma$, where $\mathcal{M}_\gamma := \{x \in \mathbb{R}^n : x = \gamma x\}$.*

Proof. First, recall that if f is γ-equivariant, and $x(t)$ is a solution of (2.1), then also $\gamma x(t)$ is a solution of the system.

Therefore, if the system is contracting, then for any solution, $a(t)$, of (2.1), we have that for all $t \geq 0$,

$$|a(t) - \gamma x(t)| \to 0, \quad t \to +\infty$$

That is, $a(t) \to \gamma x(t)$ a $t \to +\infty$.

We will now prove the result under hypothesis 2, i.e. f is contracting towards $\mathcal{M}_\gamma$. Recall that $\mathcal{M}_\gamma$ is a linear flow invariant subspace for (2.1). Now, let $a(t) \notin \mathcal{M}_\gamma$ be a solution of (2.1). By the hypothesis, we have that $a(t) \to \mathcal{M}_\gamma$ as $t \to +\infty$. This, in turn, implies that:

$$a(t) \to x(t) = \gamma x(t), \quad t \to +\infty$$

That is, $a(t)$ globally exponentially converges to a γ-symmetric solution. This proves the Theorem. ☐

An important class of systems to which Theorem 4.7.1 can be applied is that of Lagrangian systems. For such systems, it can be easily shown that the symmetries of the Lagrangian function transfer onto the equations of motion, making them invariant under the same symmetry (see e.g. [176] in the context of motion control).

A similar property (i.e. transfer of symmetries of the vector field onto symmetries of x) holds for spatio-temporal symmetries. Let p_γ be the order of γ, i.e. $\gamma^{p_\gamma} = id$. The following result holds:

Theorem 4.7.2. *If f is h-equivariant and contracting, then x is h-symmetric. Furthermore, at steady state the solutions are periodic of period $p_\gamma T$.*

Proof. Indeed, $\gamma x(t+T)$ is a solution of (2.1):

$$\frac{d\gamma x(t+T)}{dt} = \gamma\dot{x}(t+T) = f(t, \gamma x(t+T))$$

Since (2.1) is contracting, there exist some $K > 0$ such that

$$|x(t) - \gamma x(t+T)| \leq Ke^{-c^2 t}$$

i.e. $x(t) \to \gamma x(t+T)$ exponentially fast. By recursion:

$$x(t) \to \gamma^{p_\gamma} x(t + p_\gamma T) = x(t + p_\gamma T)$$

Notice that for any $t \in [0, p_\gamma T]$, $x(t + np_\gamma T)$ is a Cauchy sequence. Since $\mathbb{R}^n$, equipped with the (weigthed) 1, 2 and ∞ norm is a complete space, we have that

$$\lim_{n\to+\infty} x(t + np_\gamma T)$$

exists. This completes the proof. □

Note that $p_\gamma T$ may actually be an integer multiple of the *smallest* period of the solutions.

4.7.1 Coexistence of multiple spatial symmetries

In the previous Section, we showed that the symmetries of the vector field of (2.1) are transformed in symmetries of its solutions, $x(t)$, if the system is contracting (towards some linear invariant subspace). We now assume that f is equivariant with respect to a number of $s > 1$ actions: the aim of this Section is to provide sufficient conditions determining the steady state behavior of the system.

Let:

- $\mathcal{M}_i$ be the linear subspace defined by γ_i;
- $\dot{x}^i = f^i(t, x^i)$ be the dynamics of (2.1) on $\mathcal{M}_i$;
- $\gamma_1, \ldots, \gamma_s$ be the symmetries showed by f^i;

Theorem 4.7.3. *Assume that $\mathcal{M}_1 \subset \mathcal{M}_2 \subset \ldots \subset \mathcal{M}_s$. Then, all the solutions of (2.1) exhibit the symmetry γ_j ($1 \leq j \leq s$) if:*

1. *(2.1) contracts towards $\mathcal{M}_s$;*
2. *$\forall i = j+1, \ldots, s$, $\dot{x}^i = f^i(t, x^i)$ is contracting towards $\mathcal{M}_{i-1}$.*

Proof. By assumptions we know that the sets $\mathcal{M}_i$ are all linear invariant subspaces. Denote with c_i^2 the contraction rates of $\dot{x}^i = f^i(t, x^i)$ towards $\mathcal{M}_{i-1}$. Let $a_i(t)$ be solutions of (2.1) such that $a_i(t_0) \in \mathcal{M}_i$, and let $b(t)$ be a solution of (2.1) such that $b(t_0) \notin \mathcal{M}_s$.

We have:

$$|b(t) - a_j(t)| = \left| b(t) + \sum_{i=j+1}^{s} a_i(t) - \sum_{i=j+1}^{s} a_i(t) - a_j(t) \right| \le |b(t) - a_s(t)| + \\ + \sum_{i=j+1}^{s} |a_i(t) - a_{i-1}(t)|$$

Now, by hypotheses, the dynamics of (2.1) reduced on each of the subspaces $\mathcal{M}_i$ $(i = j+1, \ldots, s)$, i.e. $\dot{x}^i = f^i(t, x^i)$, is contracting towards $\mathcal{M}_{i-1}$. Thus, we have that there exist some $K_i > 0$, $i = 1, \ldots, j-1$, such that:

$$\begin{aligned} &|b(t) - a_s(t)| \le K_{s+1} e^{-c_{s+1}^2 t} \\ &|a_i(t) - a_{i-1}(t)| \le K_i e^{-c_i^2 t} \qquad i = j+1, \ldots, s \end{aligned}$$

This implies that

$$|b(t) - a_j(t)| \to 0$$

exponentially. The Theorem is then proved. □

With the following result, we show that if (2.1) is contracting towards $\mathcal{M}_\gamma$, then the only symmetries that the vector field, f, can eventually exhibit are those defining invariant subspaces strictly contained in $\mathcal{M}_\gamma$.

Theorem 4.7.4. *Assume that (2.1) exhibits a symmetry, γ, and that it is contracting towards $\mathcal{M}_\gamma$. Then there does not exist any other symmetry, β, such that $\mathcal{M}_\gamma \cap \mathcal{M}_\beta = \{0\}$.*

Proof. The proof of this result is straightforward, by contradiction. In fact, assume that there exist two symmetries, γ and β, such that $\mathcal{M}_\gamma \cap \mathcal{M}_\beta = \{0\}$. That is, let

$$d(a, b, t) := |a(t) - b(t)|$$

be the distance between $a(t) \in \mathcal{M}_\gamma$ and $b(t) \in \mathcal{M}_\beta$. We have that

$$\inf_{a \in \mathcal{M}_\gamma, b \in \mathcal{M}_\beta, t \in \mathbb{R}^+} \{d(a, b, t)\} = D > 0$$

since both $\mathcal{M}_\gamma$ and $\mathcal{M}_\beta$ are invariant subspaces. This in turn implies that $a(t)$ and $b(t)$ cannot globally exponentially converge towards each other. That is, the system is not contracting towards $\mathcal{M}_\gamma$. This contradicts the hypotheses. Hence, the result remains proved. □

With the following result we address the case where the invariant subspaces defined by the symmetries are not strictly contained in each other but intersect:

Theorem 4.7.5. *Assume that* $\mathcal{M}_\cap := \cap \mathcal{M}_i \neq \{0\}$. *Then, all solutions of (2.1) exhibit the symmetry defined by* $\mathcal{M}_\cap$ *if one of the two conditions holds:*

- f *is contracting toward each subspace* $\mathcal{M}_i$*;*
- f *is contracting.*

Proof. Let x_i, $i = 1, \dots, s$, be solutions of (2.1), such that $x_i(t_0) \in \mathcal{M}_i$, and $a(t)$ be a solution of the system such that $a(t_0) \notin \mathcal{M}_i$. Now, if f is contracting towards each $\mathcal{M}_i$, we have, by definition, that there exists$K_i > 0$, $c_i^2 \neq 0$, $i = 1, \dots, s$, such that:

$$|a(t) - x_i| \leq K_i e^{-c^2 t}$$

This, in turn, implies that there exists some $K > 0$, $c^2 \neq 0$ such that:

$$|x_i - x_j| \leq K e^{-c^2 t}, \quad \forall i \neq j$$

Now, since $\mathcal{M}_i$ are flow invariant, we have that $x_i \in \mathcal{M}_i$, for all $t \geq t_0$. Thus, $x_i \to \mathcal{M}_\cap$, as $t \to +\infty$, implying that also $a \to \mathcal{M}_\cap$, as $t \to +\infty$.

By using similar arguments, it is possible to prove the result under the stronger hypothesis of f being contracting. □

An example: synchronizing networks with chain topologies

The aim of this Example is to: i) introduce an important γ-symmetry for the study of networked systems (analyzed in a broader framework in Section 6.5); ii) show how the above results can be used to obtain convergence conditions for a system of interest. Specifically, we show that Theorem 4.7.3 allows to study network synchronization iteratively reducing the dimensionality of the problem. On the other hand, Theorem 4.7.4 can be used to conclude that the synchronization subspace is unique.

Consider, for instance, the diffusively coupled network represented in Figure 4.2, whose dynamics are described by:

$$\begin{aligned}
\dot{x}_1 &= f_1(X) := g(x_1) + h(x_2) - h(x_1) \\
\dot{x}_2 &= f_2(X) := g(x_2) + h(x_1) + h(x_3) - 2h(x_2) \\
\dot{x}_3 &= f_3(X) := g(x_4) + h(x_2) + h(x_4) - 2h(x_3) \\
\dot{x}_4 &= f_4(X) := g(x_4) + h(x_3) - h(x_4)
\end{aligned} \tag{4.24}$$

where: $x_i \in \mathbb{R}^n$, $X := [x_1^T, x_2^T, x_3^T, x_4^T]^T$, all the nodes have the same intrinsic dynamics, g and are coupled by means of the output function, h. We assume that all the components of $h(\cdot)$ are strictly increasing and that its Jacobian is a bounded diagonal matrix. Now, consider the following action:

$$\gamma_2 : \quad (x_1, x_2, x_3, x_4) \to (x_4, x_3, x_2, x_1) \tag{4.25}$$

That is, γ_2 permutes x_1 with x_4 and x_2 with x_3. Let

$$F(X) := [f_1(X)^T, f_2(X)^T, f_3(X)^T, f_4(X)^T]^T$$

it is straightforward to check that $\gamma_2 F(X) = F(\gamma_2 X)$. That is, F is γ_2-equivariant. This, in turn, implies that the subspace

$$\mathcal{M}_2 := \left\{X \in \mathbb{R}^{4n} : (x_1, x_2, x_3, x_4) = (x_4, x_3, x_2, x_1)\right\}$$

is flow invariant. Notice that such a subspace corresponds to the poly-synchronous subspace, where node 1 is synchronized to node 4 and node 2 is synchronized to node 3 (synchronous nodes are also pointed out in Figure 4.2). Let $J_2(X)$ be the Jacobian of the network, and

$$V_2 := \frac{1}{\sqrt{2}} \begin{bmatrix} -1 & 0 & 0 & 1 \\ 0 & -1 & 1 & 0 \end{bmatrix}$$

be the matrix spanning the null of $\mathcal{M}_2$ (notice that the rows of $\mathcal{M}_2$ are orthonormal). All the trajectories of the network globally exponentially converge towards $\mathcal{M}_2$ if the matrix $V_2 J_2(X) V_2^T$ is contracting (see Theorem 4.7.1). It is straightforward to check that such a matrix is contracting if the function $g(\cdot) - h(\cdot)$ is contracting. Let $x_{1,4}, x_{2,3} \in \mathcal{M}_2$, with $x_{1,4} = x_1 = x_4$ and $x_{2,3} = x_2 = x_3$; the dynamics of (4.24) reduced on $\mathcal{M}_2$ is given by:

$$\begin{aligned} \dot{x}_{1,4} &= g(x_{1,4}) + h(x_{2,3}) - h(x_{1,4}) \\ \dot{x}_{2,3} &= g(x_{2,3}) + h(x_{1,4}) - h(x_{2,3}) \end{aligned} \tag{4.26}$$

which corresponds to an *equivalent* 2-nodes network (see Figure 4.2). It is straightforward to check that the above reduced dynamics is γ_1-equivariant with respect to the action

$$\gamma_1 : \quad (x_{1,4}, x_{2,3}) \to (x_{2,3}, x_{1,4})$$

Thus, the subspace

$$M_1 := \left\{X \in \mathbb{R}^{4n} : (x_{1,4}, x_{2,3}) = (x_{2,3}, x_{1,4})\right\}$$

is a flow invariant subspace. Furthermore, the trajectories of (4.26) globally exponentially converge towards $\mathcal{M}_1$ if $V_1 J_1(X) V_1^T$ is contracting, where $V_1 = \frac{1}{\sqrt{2}}[-1, 1]$

and $J_1(X)$ is the Jacobian of (4.26). Now, $V_1 J_1 V_1^T = \frac{1}{2}(\frac{\partial g}{\partial x_{1,4}} - 2\frac{\partial h}{\partial x_{1,4}} + \frac{\partial g}{\partial x_{2,3}} - 2\frac{\partial h}{\partial x_{2,3}})$, which is contracting if $g(\cdot) - h(\cdot)$ is contracting.

Thus, using Theorem 4.7.3, we can finally conclude that the network synchronizes if the function $g(\cdot) - h(\cdot)$ is a contracting function. Furthermore, the synchronization subspace is unique by means of Theorem 4.7.4.

We remark here that:

- the dimensionality-reduction methodology presented above can also be extended to the more generic case of chain topologies of length 2^r, for any integer, r;
- the same methodology can be used to prove synchronization of networks having *hypercube* topologies, as they can be seen as *chains* of *chains*. Hence, the above approach can be used to find condition for the synchronization of *lattices*. Such a topology typically arise from e.g. the discretization of partial differential equations. In this view, our results provide a sufficient condition for the spatially uniform behavior in reaction diffusion PDEs, similarly to [11];
- the synchronization condition obtained above is less stringent than that obtained by proving contraction of (4.24) towards the synchronization subspace

$$\mathcal{M} := \left\{ X \in \mathbb{R}^{4n} : x_1 = x_2 = x_3 = x_4 \right\}$$

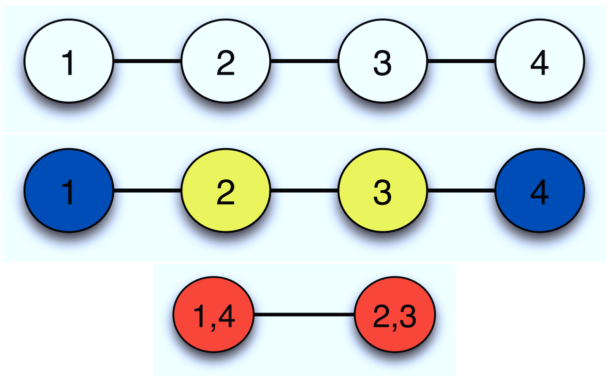

Figure 4.2: Top panel: the chain topology network of 4 nodes. Middle panel: poly-synchronous subspace identified by $\mathcal{M}_2$. Bottom panel: equivalent network and synchronous subspace identified by $\mathcal{M}_1$.

4.7.2 Generalizations using virtual systems

The results presented in the previous sections link the symmetries of a dynamical system and contraction. Specifically, they show that if a system presents a set of

$s > 1$ symmetries, then the steady state behavior is determined by the contraction properties of the vector field.

In this Section, we extend the previous results and show that in order for the solutions of (2.1) to exhibit a specific symmetry, equivariance and contraction of f are not necessarily needed. Indeed, such a condition can be replaced by an equivariance condition on the vector field of some virtual system, similar in spirit to that of Section 4.5.

Theorem 4.7.6. *Assume that there exists some virtual system (4.16) for system (2.1) and such that:*

- *is h (or γ) equivariant;*
- *is contracting (or contracting towards $\mathcal{M}_\gamma$).*

Then, any solution of (2.1) globally exponentially converges towards a h (or γ) symmetric solution:

$$y_c(t) = \gamma y_c(t+T) \quad (y_c(t) = \gamma y_c(t))$$

Proof. Indeed, by assumption, all the solutions $y(t)$ of the virtual system globally exponentially converge towards some h (γ) symmetric solution, say $y_c(t)$. Now, notice that any solution of (2.1), say $z(t)$, is a particular solution of (4.16). This implies that:

$$|z(t) - x(t)| \to 0$$

as $t \to +\infty$. The result is then proved. □

Note that

- Any solution of the virtual system having symmetric initial conditions, i.e. $y(t_0) = \gamma y(t_0)$, preserves the symmetry for any $y > t_0$. In particular, if a solution of the *real* system has initial conditions verifying the symmetry of the *virtual* system, i.e. $x(t_0) = \gamma x(t_0)$, then it preserves this symmetry, i.e. $x(t) = \gamma x(t)$ for any $t \geq t_0$.
- Theorem 4.7.6 can be straightforwardly extended to the case where the virtual system presents a set of $s > 1$ spatial symmetries.

4.7.3 Extensions to control

In the above Section, we presented some results that can be used to analyze the steady state behavior of a system of interest. The main idea beyond such results is the use of contraction to study convergence of trajectories towards some invariant subspace. In turn, such a subspace is defined by some *structural* property of the vector field, i.e. a symmetry. In this Section, we show that this idea can be also used to control system (2.1). In particular, we show that by using some control inputs, it is possible to: i) generate some desired symmetries (and hence some desired invariant subspace) for the system; ii) *drive* all the trajectories towards the invariant subspace, imposing contraction.

The dynamical system considered here is

$$\dot{x} = f(x, \tilde{u}(x), \bar{u}(t), t) \tag{4.27}$$

That is, the input to system (2.1) consists of: i) a feedback component, $\tilde{u}(x)$; ii) an exogenous component, $\bar{u}(t)$.

Spatial symmetries

Theorem 4.7.7. *Assume that in system (4.27) the control input generates a spatial symmetry, γ, and ensures contraction towards $\mathcal{M}_\gamma$. Then, any solution of (4.27) is γ-symmetric.*

Proof. Let

$$g(x, \bar{u}(t), t) := f(x, \tilde{u}(x), \bar{u}(t), t)$$

By hypotheses, the vector field g is γ-equivariant. This implies that, if $x(t)$ is a solution of (4.27), then $\gamma x(t)$ is also a solution. Indeed:

$$\gamma \dot{x} = \gamma g(x, \bar{u}(t), t) = g(\gamma x, \bar{u}(t), t)$$

Furthermore, by hypotheses, the control input makes the vector field g contracting. Hence, for any solution of (4.27), $a(t)$, we have:

$$|a(t) - x(t)| \to 0$$

as $t \to +\infty$. □

The above analysis can be generalized to the case where the control inputs generate a set of $s > 1$ spatial symmetries. The following result provides a sufficient condition for selecting one of the possible steady state behaviors determined by the symmetries.

Theorem 4.7.8. *Assume that the inputs $\tilde{u}(x)$ and $\bar{u}(t)$ create $s > 1$ symmetries for system (4.27) and that $\mathcal{M}_1, \ldots \mathcal{M}_s$ are their associated invariant subspaces. Then, (4.27) exhibits symmetry γ_k if $\tilde{u}(x)$ and $\bar{u}(t)$ ensure contraction towards $\mathcal{M}_k$.*

Proof. The proof of this result is straightforward and it is omitted here. □

Spatiotemporal symmetries

We now extend the above results to the control of spatio-temporal symmetries. As formalized in the next result, we have now to impose some extra condition on $\tilde{u}(t)$.

Theorem 4.7.9. *Assume that*

$$\dot{x} = f(x, \tilde{u}(x), \bar{u}(t), t) = g(x, \tilde{u}(t), t)$$

is h-equivariant, i.e.

$$\gamma g(x, \tilde{u}(t), t) = g(\gamma x, \gamma \tilde{u}(t+T), t+T)$$

and that $\tilde{u}(t)$ is h-symmetric, i.e.

$$\tilde{u}(t) = \gamma \tilde{u}(t+T)$$

If g is contracting, then all the solutions of (4.27) globally exponentially converge towards a h-symmetric solution.

Proof. In fact $\gamma x(t+T)$ is a solution of the system:

$$\begin{aligned} &\tfrac{d\gamma x(t+T)}{dt} = \gamma \dot{x}(t+T) = \gamma g(x(t+T), \tilde{u}(t+T), t+T) = \\ &= g(\gamma x(t+T), \gamma \tilde{u}(t+T), t+T) = g(\gamma x(t+T), \tilde{u}(t), t+T) \end{aligned}$$

Since the system is contracting we have:

$$|x(t) - \gamma x(t+T)| \to 0$$

This proves the result. □

4.7.4 Controlling Symmetries of Virtual systems

In this Section, we present two results that can be used to determine the links between the trajectories of a system when forced by different inputs.

Consider a system described by:

$$\dot{x} = f(x, u(t), t) \tag{4.28}$$

Theorem 4.7.10. *Assume that (4.28) is contracting with respect to x, uniformly in $u(t)$, and that there exist some linear transformations γ_i, ρ_i, $i \geq 1$, such that:*

$$\gamma_i f(x, u(t), t) = f(\gamma_i x, \rho_i u(t), t)$$

Let $x_i(t)$ be solutions of (4.28) when forced by $u(t) = u_i(t)$, i.e.

$$\dot{x}_i = f(x_i, u_i(t), t), \quad x_i(t=0) = x_{0,i}$$

Then, for any $u_i(t)$, $u_j(t)$ such that $\rho_i u_i(t) = \rho_j u_j(t)$

$$|\gamma_i x_i - \gamma_j x_j| \to 0$$

as $t \to +\infty$. Moreover, let x_i^k and x_j^k the k-th component of x_i and x_j respectively and γ_i^k, (γ_j^k) be the k-th component of γ_i (γ_j). If

$$\gamma_i^k x_{0,i}^k = \gamma_j^k x_{0,j}^k$$

then $\gamma_i^k x_i^k(t) = \gamma_j^k x_j^k(t)$, for any $t \geq 0$.

The second statement of the above Theorem implies that if the system when forced by two different inputs starts with certain symmetries, then the symmetries are preserved.

Proof. Indeed, let $u_v = \rho_i u_i = \rho_j u_j$ and consider the following virtual system:

$$\dot{y} = f(y, u_v, t) \tag{4.29}$$

Notice that, for any i, j, $\gamma_i x_i$ and $\gamma_j x_j$ are particular solutions of such a system. Indeed:

$$\gamma_i \dot{x}_i = \gamma_i f(x_i, u_i, t) = f(\gamma_i x_i, \rho_i u_i, t) = f(\gamma_i x_i, u_v, t)$$
$$\gamma_j \dot{x}_j = \gamma_j f(x_j, u_j, t) = f(\gamma_j x_j, \rho_j u_j, t) = f(\gamma_j x_j, u_v, t)$$

Now, since $f(x, u_v, t)$ is contracting by hypotheses, we have, for any i, j, there exists some C such that:

$$|\gamma_i x_i - \gamma_j x_j| \leq C \, |\gamma_i x_{0,i} - \gamma_j x_{0,j}| \, e^{-\lambda t}, \quad \lambda > 0$$

This proves the first part of the result. To conclude the proof it suffices to notice that exponential convergence of $|\gamma_i x_i - \gamma_j x_j|$ to 0 implies that all of its components exponentially converge to 0. In particular, this implies that there exists some C_k, λ_k such that:

$$\left|\gamma_i^k x_i^k - \gamma_j^k x_j^k\right| \leq C_k \left|\gamma_i^k x_{0,i}^k - \gamma_j^k x_{0,j}^k\right| e^{-\lambda t_k}, \quad \lambda_k > 0$$

Since $\left|\gamma_i^k x_{0,i}^k - \gamma_j^k x_{0,j}^k\right| = 0$ by hypotheses, we have that

$$\left|\gamma_i^k x_i^k(t) - \gamma_j^k x_j^k(t)\right|, \quad \forall t \geq 0$$

□

Theorem 4.7.10 can be extended by replacing the linear operators γ_i, ρ_i by more general nonlinear transformations acting on the system

$$\dot{x} = f(t, u(t, x), x) \tag{4.30}$$

The transformations considered are smooth nonlinear functions of the state and of time,

$$\gamma = \gamma(t, x) \qquad\qquad \rho = \rho(t, u(t, x), x)$$

Following the same arguments as in Theorem 4.7.10, it is then straightforward to show,

Theorem 4.7.11. *Assume that (4.30) is contracting uniformly in $u(t, x)$ and that there exist some $\gamma_i(t, x)$, $\rho_i(t, u(t, x), x)$, $i \geq 1$, such that:*

$$\frac{\partial \gamma_i}{\partial x} f(t, u(t, x), x) = f(t, \rho_i(u(x, t), x, t), \gamma_i(x))$$

Let $x_i(t)$ be solutions of (4.30) when forced by $u(t) = u_i(x_i, t)$, i.e.

$$\dot{x}_i = f(x_i, u_i(x_i, t), t), \quad x_i(t = 0) = x_{0,i}$$

Then, for any $u_i(x_i, t)$, $u_j(x_j, t)$ such that $\rho_i(u(x_i, t), x_i, t) = \rho_j(u_j(x_j, t), x_j, t)$

$$|\gamma_i(x_i) - \gamma_j(x_j)| \to 0$$

as $t \to +\infty$. Moreover, let x_i^k and x_j^k the k-th component of x_i and x_j respectively and γ_i^k, (γ_j^k) be the k-th component of γ_i (γ_j). If

$$\gamma_i^k \left(x_{0,i}^k \right) = \gamma_j^k \left(x_{0,j}^k \right)$$

then $\gamma_i^k \left(x_i(t)^k \right) = \gamma_j^k \left(x_j(t)^k \right)$, for any $t \geq 0$.

Proof. The proof follows exactly the same steps as those used to prove Theorem 4.7.10, with u_v in virtual system (4.29) now being chosen as $u_v = \rho_i(u(x_i, t), x_i, t) = \rho_j(u_j(x_j, t), x_j, t)$. □

We close this Section by pointing out some features of the above two theorems.

- the proofs of both Theorem 4.7.10 and Theorem 4.7.11 are based on the proof of contraction of some appropriately constructed virtual system of the form (4.29). We now show that, if some hypotheses are made on γ_i's, then the contraction condition can be weakened. Specifically, assume that all the intersection of the subspaces defined by γ_i, $\mathcal{M}_i$, is nonempty. Then, it is straightforward to check that $|\gamma_i x_i - \gamma_j x_j| \to 0$ if: (i) f is contracting towards each $\mathcal{M}_i$, or (ii) contracting towards $\mathcal{M}_\cap$. Notice that, since our results make use of symmetries of virtual systems, they extend those in [64];

- Analogously, Theorem 4.7.10 and Theorem 4.7.11 can also be extended to study the case where the input u_i *selects* one specific symmetry γ_i. Indeed, let $u_v = \rho_i u_i$. In this case, it can be shown that symmetry γ_i is shown by the solutions of (4.28) if $f(x, u_v, t)$ is contracting towards $\mathcal{M}_i$.

- A particularly interesting case for Theorem 4.7.10 is when some of the components of $x_{0,i}$ and $x_{0,j}$ are the same and the actions γ_i and γ_j leave such components unchanged. That is, in view of the notations above $\gamma_i^k = id = \gamma_j^k$ and $x_{0,i}^k = x_{0,j}^k$. Indeed, in this case Theorem 4.7.10 implies that

$$x_i^k(t) = x_j^k(t) \quad \forall t \geq 0$$

  That is, the k-th components of the trajectories of (4.28) have identical temporal evolutions even if forced by different inputs. A similar result holds for Theorem 4.7.11 .This consequence of the above two results is used in Section 9.4.1.

A discussion on symmetries of virtual systems

Let us briefly discuss some of the main features of our results involving the use of virtual systems.

We showed that a given dynamical system of interest can exhibit some symmetric steady state behavior even if the corresponding vector field is not equivariant and/or contracting. Indeed, a sufficient condition for a system to exhibit a symmetric final behavior is the symmetry of the vector field of some appropriately constructed virtual system. Of course, an interesting general question is that of identifying a virtual system explaining the final behavior of a real system, an aspect is reminiscent of the process of identifying a Lyapunov function in stability analysis.

We also used the concept of virtual system to solve the problem of relating the trajectories of a system when forced by two different inputs. Indeed, while the forced systems of interest are not equivariant with respect to the same action, we showed that it is possible to construct a symmetric and contracting virtual system which allows us to relate the steady state behavior of the two systems.

In particular, the virtual system is constructed in a way such that it embeds as particular solutions $\gamma_i x_i$. In this view, the construction of the virtual system presented above is a generalization of the results presented in [194]. In that paper, where virtual systems and partial contraction were first introduced, the virtual system is constructed in a way such that it embeds the solutions of the real systems, x_i. Clearly, our results reduce to the results presented in [194] when $\gamma_i = \gamma_j = id$ and $u_i(t) = u_j(t)$.

The idea of relating non-symmetric behaviors of real systems using a symmetric *virtual* system, possibly of different dimension, presents analogies with the concept of *supersymmetry* in modern particle physics (see e.g. [59, 165] and references therein). The motivation beyond the concept of supersymmetry is that non-symmetric transformations of an object (the real system in our framework) in a finite dimensional space, may be explained by a symmetric transformation of another, possibly higher-dimensional, object (the virtual system in our framework). In particle physics, supersymmetry can e.g. relate elementary particles characterized by a given spin to particles differing by half a unit of spin.

4.8 Discrete-time contraction theory

We now consider the discrete-time m-dimensional nonlinear dynamical system

$$x\left(k+1\right) = f\left(k, x\left(k\right)\right), \quad x\left(k_0\right) = x_0, \quad k_0 \geq 0 \tag{4.31}$$

subject to appropriate regularity constraints. The following definitions are used throughout the Thesis:

Definition 4.8.1. *We say that two trajectories, say $x(k)$ and $y(k)$, of (4.31) converge asymptotically towards each other if*

$$|x(k) - y(k)| \rightarrow 0, \quad k \rightarrow +\infty$$

Definition 4.8.2. *We say that a matrix $\Theta\left(x\left(k\right), k\right)$ is a uniformly invertible matrix in some region $\mathcal{R} \subseteq \mathbb{R}^m$ if for any $x \in \mathcal{R}$ and for any $k \in \mathbb{N}$, the matrix $\Theta^{-1}\left(x\left(k\right), k\right)$ exists. When $\mathcal{R} \equiv \mathbb{R}^m$ we will simply say that $\Theta\left(x\left(k\right), k\right)$ is a uniformly invertible matrix.*

Let

$$J(k) := \frac{\partial f\left(k, x(k)\right)}{\partial x}$$

Differentiation of (4.31) gives the dynamics of the virtual displacements, say $\delta x(k)$, between two nearby trajectories (see [111]) $\delta x\left(k+1\right) = J(k)\delta x\left(k\right)$, $\delta x\left(k_0\right) = \delta x_0$. Thus, an upper bound for the distance between any two trajectories of the above equation can be obtained as $\left|\delta x\left(k\right)\right| \leq \prod_{r=1}^{k} \left\|J(k-r)\right\| \left|\delta x_0\right|$. It immediately follows that (see [160]), if there exist a scalar $d \in [0, 1[$ such that $\|J(k)\| \leq d$, $\forall k \geq k_0$, then $|\delta x\left(k\right) \rightarrow 0|$ as $k \rightarrow +\infty$. An immediate extension, similar to that proposed in [111], gives a condition on the so-called generalized Jacobian,

$$f(k) = \Theta(k+1, x(k+1)) J(k) \Theta^{-1}(k, x(k))$$

where $\Theta(x(k), k)$ is a uniformly invertible matrix. This motivates the following result (see [111], [160]).

Theorem 4.8.1. *Consider the discrete-time m-dimensional deterministic dynamical system (4.31) and let $\mathcal{C}$ be a convex open subset of phase space. If there exist a uniformly invertible matrix in $\mathcal{C}$, $\Theta(k, x(k))$, and some $0 \leq d < 1$ such that, $\|f(k)\| \leq d, \quad \forall k \geq k_0, \quad \forall x(k) \in \mathcal{C}$, then all system trajectories rooted in $\mathcal{C}$ converge asymptotically towards each other. Furthermore, there exists some $0 < \chi_1 < 1$ and some $\chi_2 > 0$ such that, for any two solutions of (4.31), say $x(k), y(k) \in \mathcal{C}$, $|x(k) - y(k)| \leq \chi_2 \cdot \chi_1^k \, |x(k_0) - y(k_0)|$.*

If the hypotheses of Theorem 4.8.1 are all fulfilled, we say that the system is contracting in $\mathcal{C}$. If $\mathcal{C} \equiv \mathbb{R}^m$ we simply say that the system is contracting and that all of its trajectories converge towards each other.

As pointed out in [142] for continuous time systems, contraction theory can be used to analyze the convergent behavior of systems trajectories towards a linear invariant subspace, $\mathcal{M}$, embedded in the m-dimensional system phase space, i.e. a linear subspace such that $\forall x \in \mathcal{M}$, $x(k+1) = \phi(k, x) \in \mathcal{M}$, $\forall k \geq k_0$. The following definition formalizes the notion of convergence towards a subspace, used in the rest of the Thesis

Definition 4.8.3. *Let $\mathcal{M}$ be a linear invariant subspace for (4.31). We say that all the trajectories of (4.31) are contracting (or simply converge) towards $\mathcal{M}$ if for any $y(k) : y(k_0) \notin \mathcal{M}$ there exist some $x(k) : x(k_0) \in \mathcal{M}$ such that:*

$$|x(k) - y(k)| \to 0, \quad k \to +\infty$$

Theorem 4.8.2. *Assume that the linear subspace, $\mathcal{M}$, is flow invariant for the discrete time dynamical system (4.31). Let V be the matrix whose rows are an orthonormal basis of $\mathcal{M}^\perp$. Then, all the solutions of (4.31) converge towards $\mathcal{M}$ if there exist a norm such that $\left\|V J(k) V^T\right\| \leq d < 1$ for any $k \geq k_0$ and $\forall x \in \mathbb{R}^m$.*

Proof. Define $z(k) = V x(k)$. All system trajectories converge towards $\mathcal{M}$ if and only if for any $z(k)$ such that $z(k_0) \neq 0$, $z(k) \to 0$, as $k \to +\infty$. Now:

$$V^T V x + W^T W x = x$$

That is,

$$x = V^T z + W^T W x$$

and hence it follows that

$$z\,(k+1) = Vf\left(k, V^T z + W^T W x\right)$$

As in [194], [142], we construct the auxiliary system

$$\mathbf{y}\,(k+1) = Vf\left(k, V^T \mathbf{y} + W^T W x\right)$$

which is contracting by hypotheses. Furthermore, notice that such a system has $\mathbf{y} = z$ and $\mathbf{y} = 0$ as particular solutions. Thus, contraction of the virtual system immediately implies that $z(k) \to 0$. $\square$

4.9 Concluding remarks

In this Chapter we derived some extensions of nonlinear contraction theory. Specifically, we revisited (and extended) the main results on contraction and contraction towards subspaces presented in Chapter 2 were obtained using non-Euclidean norms. At the same time, we presented novel results that make use of both contraction and symmetries to determine the steady state behavior of a dynamical system of interest. All the results presented in this Chapter are used in the rest of the Thesis. In Chapter 5 we show that the use of non-Euclidean matrix measures and norms can be effectively used to obtain a graphical procedure for imposing/checking contraction of a given system of interest. Later, in Chapter 6 and Chapter 7 we show that non-Euclidean norms and measures can be used to provide sufficient condition for the stability and synchronization of networked systems with nodes being both continuous-time and discrete-time systems. In Chapter 8 we show that the results obtained here can be used to design/analyze decentralized control strategies for asynchronous networks.

Chapter 5

A graphical approach to prove contraction

This Chapter presents an approach to prove contraction of nonlinear dynamical systems, based on the use of non-Euclidean norms and their associated matrix measures, introduced in Chapter 2. A graphical procedure is proposed to derive conditions for a system to be contracting. Such conditions can also be used to design control strategies to make a system contracting, or to design consensus and synchronization strategies for networks of nonlinear oscillators. After presenting the main steps of the approach and its proof, both for continuous-time and discrete-time systems, we illustrate the theoretical derivations on a set of representative examples. The results presented in this Chapter were partly presented in [154], [160], [159]. Another version of the proposed graphical approach can instead be found in [156].

5.1 Introduction

Applications to date of nonlinear contraction theory are based on the use of negative definite generalized Jacobians and Euclidians norms. As shown in Chapter 4, other norms and their associated matrix measures [191] can also be used to quantify contraction, leading to similar results but conditions in different algebraic forms. The aim of this Chapter is to explore in more detail this avenue showing that, as suggested in [156], it represents a natural approach for particular classes of systems; in particular those encountered in biochemistry and in some network coordination problems. Specifically, some *graphical* tools are developed for establishing contraction both for continuous-time and discrete-time systems. By using vector-1 or vector-∞ norms and their associated matrix measure, a procedure is derived to check the existence of a constant diagonal metric in which the system of interest is contracting. Such a procedure results in a graphical condition to be verified on a directed graph whose topology is determined by the dynamics of the system of interest. Thus, the outcome of our procedure, if the state variables of the system are all homogeneous, is a set of well defined physical constraints on the system dynamics that ensure it to be contracting. This is the case, for example, of systems of biochemical reactions where conditions provided by our approach are equivalent to requiring a balance between the species involved in the reactions. We will also show that the proposed procedure can be effectively applied to synchronization problems providing guidelines for the design of both linear and nonlinear coupling protocols ensuring asymptotic synchronization.

One of the main advantages of the proposed procedure is that it makes proving contraction possible without the need of identifying explicitly a suitable metric in which all trajectories converge. Simply, the aim of the graphical approach is to give sufficient conditions that ensure that such a metric exists, thus extending the class of systems to which contraction can be easily and successfully applied.

We present the procedure both for continuous-time and discrete-time systems, validating the theoretical results on a set of representative examples. The new graphical approach for proving contraction is presented and derived in Section 5.2. Geometric interpretation and robustness are discussed in Section 5.3. Some applications both in continuous-time and in discrete-time are presented in Section 5.4. Concluding remarks are offered in Section 5.5.

5.2 A graphical tool for proving contraction

We show now that by means of matrix measures and norms induced by non-Euclidean vector norms, (such as μ_1, μ_∞, $\|\cdot\|_1$, $\|\cdot\|_\infty$: see Chapter 2), it is possible to obtain a graphical procedure for checking if a system is contracting or for imposing such property. Formally, the conditions required by the procedure for a system to be contracting are sufficient conditions. This means that, if the conditions are satisfied, then the system is contracting, while the vice-versa is not true.

Given a nonlinear vector field, $f(t,x)$, let $J(t,x) := \frac{\partial f}{\partial x}(t,x)$ be its time varying Jacobian matrix. The outcome of the procedure is to provide a set of conditions on the elements of J, (and hence on the dynamics of $f(\cdot,\cdot)$) that can be used to prove contraction. Thus, the procedure presented here can be used both for checking if a system is contracting and for designing some coupling function guaranteeing contractivity (and hence some desired behavior).

In this Section, we present an outline of the proposed procedure for both continuous-time and discrete-time systems. Then, in Section 5.2.2, proofs are given of the results on which our approach is based.

5.2.1 Outline

The first step of the procedure is to differentiate the system of interest, in order to obtain the Jacobian matrix, $J := \frac{\partial f}{\partial x}$:

$$\begin{bmatrix} J_{1,1}(t,x) & J_{1,2}(t,x) & \dots & J_{1,m}(t,x) \\ J_{2,1}(t,x) & J_{2,2}(t,x) & \dots & J_{2,m}(t,x) \\ \dots & \dots & \dots & \dots \\ J_{m,1}(t,x) & J_{m,2}(t,x) & \dots & J_{m,m}(t,x) \end{bmatrix} \tag{5.1}$$

which is, in general, state/time dependent.

The next step is then to construct a directed graph from the system Jacobian. To this aim, we first derive an adjacency matrix from J, say $\mathcal{A}$, using the following rules:

1. initialize $\mathcal{A}$ so that $\mathcal{A}(i,j) = 0$, $\forall i,j$;
2. for all $i \neq j$, set $\mathcal{A}(i,j) = \mathcal{A}(j,i) = 1$ if either $J_{i,j}(t,x) \neq 0$, or $J_{i,j}(t,x) \neq 0$.

Such a matrix describes an undirected graph (see e.g. [66]), say $\mathcal{G}(\mathcal{A})$. The second step in the procedure is then to associate directions to the edges of $\mathcal{G}(\mathcal{A})$ to obtain a directed graph, say $\mathcal{G}_d(\mathcal{A})$. This is done by computing the quantity

$$\alpha_{i,j}(t,x) = \frac{|J_{i,j}(t,x)|}{|J_{i,i}(t,x)|}(m - n_{0i} - 1) \tag{5.2}$$

for continuous-time systems, or the quantity

$$\hat{\alpha}_{i,j}(t,x) = |J_{i,j}(t,x)|(m - n_{0i} - 1) \tag{5.3}$$

for discrete-time systems. In the above expressions n_{0i} is the number of zero elements on the i-th row of $\mathcal{A}$. (Note that if $J_{i,i}(t,x) = 0$ for some i, then, before computing (5.2), the system parameters/structure must be engineered so that $J_{i,i}(t,x) \neq 0$, for all i.)

The directions of the edges of $\mathcal{G}_d(\mathcal{A})$ are then obtained using the following simple rule:

> *the edge between node i and node j is directed from i to j if the quantity $\alpha_{i,j}(t,x) < 1$ (or $\hat{\alpha}_{i,j}(t,x) < 1$) while it is directed from j to i if $\alpha_{i,j}(t,x) \geq 1$ (or $\hat{\alpha}_{i,j}(t,x) \geq 1$).*

Note that, the quantities $\alpha_{i,j}(t,x)$ (or $\hat{\alpha}_{i,j}(t,x)$) will be in general time-dependent, therefore the graph directions might be time-varying.

Once the directed graph $\mathcal{G}_d(\mathcal{A})$ has been constructed, contraction is then guaranteed under the following conditions:

1. uniform negativity of all the diagonal elements of the Jacobian, i.e. $J_{i,i}(t,x) < 0$ for all i, for continuous-time systems or $\hat{\alpha}_{i,i}(t,x) < 1$ for discrete-time systems;

2. for all t, the directed graph $\mathcal{G}_d(\mathcal{A})$ does not contain loops of any length and $\alpha_{ij}(t,x)\alpha_{ji}(t,x) \leq 1$ ($\hat{\alpha}_{ij}(t,x)\hat{\alpha}_{ji}(t,x) \leq 1$) for any $i \neq j$.

Note that, when the above conditions are not satisfied, our approach can be used to impose contraction for the system of interest by:

1. using, if possible, a control input to impose the first condition of the above procedure for all the elements $J_{i,i}(t,x)$ that do not fulfill it;

2. *re-direct* (using an appropriate control input, or tuning system parameters) some edges of the graph $\mathcal{G}_d(\mathcal{A})$ in order to satisfy the *loopless* condition;

3. associate to each reverted edge (e.g. the edge between node i and node j) one of the following inequalities:

   - $\alpha_{i,j}(t,x) \geq 1$ ($\hat{\alpha}_{i,j}(t,x) \geq 1$), if the edge is reverted from j to i;
   - $\alpha_{i,j}(t,x) < 1$ ($\hat{\alpha}_{i,j}(t,x) < 1$), if the edge is reverted from i to j;
   - ensure that $\alpha_{ij}(t,x)\alpha_{ji}(t,x) \leq 1$;
   - (or, for discrete-time systems, $\hat{\alpha}_{ij}(t,x)\hat{\alpha}_{ji}(t,x) \leq 1$).

5.2.2 Proof

In this Section, we state and prove the basic theoretical results used to derive the procedure presented in Section 5.2.1. The main idea for the following proofs is to ensure contraction using μ_∞ and $\|\cdot\|_\infty$. Notice that, in what follows, we do not need the matrix Θ to be state/time dependent as often required when contraction is proved using the Euclidean matrix norm/measure (see e.g. [112]). This makes contraction theory even more powerful and, at the same time, of simpler application.

As the matrix Θ is constant, the generalized Jacobian is given by $F = \Theta J \Theta^{-1}$. In what follows we also assume that Θ is diagonal:

$$\Theta := \begin{bmatrix} p_1 & 0 & \dots & \dots & 0 \\ 0 & p_2 & 0 & \dots & 0 \\ \dots & \dots & \dots & \dots & \dots \\ 0 & \dots & \dots & \dots & p_m \end{bmatrix} \tag{5.4}$$

with p_i, $i = 1, \dots, m$ being arbitrary positive scalars.

Continuous-time systems

Theorem 5.2.1. *The continuous-time m-dimensional dynamical system (2.1) is contracting, if its Jacobian matrix, J, is such that*

1. $J_{i,i}(t,x) < 0, \ \forall \quad i = 1, \ldots, m;$
2. *the graph $\mathcal{G}_d(\mathcal{A})$ constructed from J as detailed above does not contain (directed) loops and $\alpha_{ij}(t,x)\alpha_{ji}(t,x) \leq 1$.*

Proof. From the discussion outlined in the above Section, to prove contraction we have to show that there exists a negative matrix measure for J. Namely, we use $\mu_\infty(\Theta J \Theta^{-1})$, where Θ is defined as in (5.4). Such a measure is negative if and only if:

1. $\forall \ i = 1, \ldots, m, \ J_{i,i}(t,x) < 0;$
2. $\forall x$, $\forall t \in R^+$ and $\forall \ i = 1, \ldots, m$, $\exists \ p_1, \ldots, p_m$ such that

$$\sum_{j=1, j\neq i}^{m} \frac{p_i}{p_j} |J_{i,j}(t,x)| < |J_{i,i}(t,x)| \tag{5.5}$$

Now, the first set of inequalities is satisfied from the hypotheses, as $J_{i,i}(t,x) < 0$ for all i. Then, to complete the proof, we have to show that, if the loopless condition on $\mathcal{G}_d(\mathcal{A})$ is satisfied, then there exists a set of positive scalars $p_1, p_2, \ldots, p_m$ satisfying the second set of inequalities.

Note that, if we indicate with n_{0i} the number of null elements on the i-th row of (5.1), then such a set is fulfilled if $\forall x$, $\forall t \geq 0$ and $\forall \ i, j = 1, \ldots, m$, $i \neq j$ the set of inequalities

$$|J_{i,i}(t,x)| > \frac{p_i}{p_j} |J_{i,j}(t,x)| (m - n_{0i} - 1) \tag{5.6}$$

is satisfied. Inequalities (5.6) can also be recast as:

$$p_j > \alpha_{i,j}(t,x) \, p_i \tag{5.7}$$

where $\alpha_{i,j}(t,x)$ is defined as in (5.2). Now, if the set of inequalities (5.7) is consistent, there exists some set of (positive) scalars $p_1, p_2, \ldots, p_m$ satisfying (5.6). Hence, the existence of a diagonal metric in which the system is contracting is guaranteed.

We now prove that, if hypothesis 2 holds, then the set of inequalities (5.7) is consistent.

Recall that directions of the edges of $\mathcal{G}_d(\mathcal{A})$ are determined by the coefficients $\alpha_{i,j}(t,x)$, given in (5.2). In particular, node i and node j are linked if and only if $\alpha_{i,j}(t,x)$ and/or $\alpha_{j,i}(t,x)$ are different from 0. The direction of the edges linking i and j are instead assigned by some conditions on $\alpha_{i,j}(t,x)$ (or $\alpha_{j,i}(t,x)$). In particular, from (5.7) we have that:

- the edge is from j to i if $\alpha_{i,j}(t,x) - 1 \geq 0$;
- the edge is from i to j if $\alpha_{i,j}(t,x) - 1 < 0$;

Notice that, if the elements $J_{i,j}(t,x)$ and $J_{j,i}(t,x)$ are both different from 0, then both $\alpha_{i,j}(t,x)$ and $\alpha_{j,i}(t,x)$ are defined, yielding the following inequalities:

$$\begin{aligned} p_j &> \alpha_{i,j}(t,x)\, p_i \\ p_i &> \alpha_{j,i}(t,x)\, p_j \end{aligned} \tag{5.8}$$

In terms of the graph, this means that the direction between node i and node j is determined by both $\alpha_{i,j}(t,x)$ and $\alpha_{j,i}(t,x)$. Since by hypotheses no loops are present in $\mathcal{G}_d(\mathcal{A})$, then it must be

$$(\alpha_{i,j}(t,x) - 1)(\alpha_{j,i}(t,x) - 1) \leq 0 \tag{5.9}$$

with $\alpha_{ij}(t,x)\alpha_{ji}(t,x) \leq 1$, thus making the set of inequalities (5.8) consistent. Notice that violating a such condition would imply the presence of loops of length 2 (i.e. of loops consisting of bidirectional links between two nodes) and would make the above two inequalities inconsistent.

In what follows, we will assume (5.9) to hold. If no loops are present in the undirected graph $\mathcal{G}(\mathcal{A})$, then $\mathcal{G}_d(\mathcal{A})$ will be by construction an acyclic directed graph, describing a consistent set of inequalities between its nodes. Hence contraction is guaranteed.

Assume now that some cycle of length greater than 2 is instead present in $\mathcal{G}(\mathcal{A})$. By hypotheses, we have that no cycles must be present in $\mathcal{G}_d(\mathcal{A})$. Therefore when assigning directions to the edges of $\mathcal{G}(\mathcal{A})$, no loops of any length are formed. That is, loops of any length in the undirected graph $\mathcal{G}(\mathcal{A})$, will cause the presence in the directed graph $\mathcal{G}_d(\mathcal{A})$ of at least one node, say j, with incoming links from two of its adjacent edges (see e.g. Figure 5.1 for a schematic loop of length 3, where the nodes adjacent to j are labeled as i and k).

By construction, such a node will then be associated to one of the following set of inequalities:

$$\begin{aligned} p_j &> \alpha_{i,j}(t,x)\, p_i \quad \alpha_{i,j}(t,x) \geq 1 \\ p_j &> \alpha_{k,j}(t,x)\, p_k \quad \alpha_{k,j}(t,x) \geq 1 \end{aligned}$$

or

$$\begin{aligned} p_j &> \alpha_{i,j}(t,x)\, p_i \quad \alpha_{i,j}(t,x) \geq 1 \\ p_k &> \alpha_{j,k}(t,x)\, p_j \quad \alpha_{j,k}(t,x) < 1 \end{aligned}$$

(Notice that only the above conditions need to be considered, since loops of length 2 must be excluded.) The above conditions then exclude the case that vertices of a loop in the undirected graph could be associated to inconsistent inequalities between the scalars $p_1, p_2, \dots, p_m$ and therefore guarantee that a solution exists for inequalities (5.7). Hence, the Theorem remains proved. □

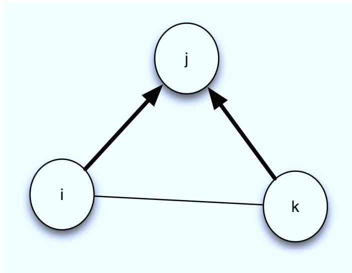

Figure 5.1: A schematic representation of a loop of length 3 in $\mathcal{G}(\mathcal{A})$. Notice that, in general the loop-less condition on the graph $\mathcal{G}_d(\mathcal{A})$, causes the presence o at least one vertex with all incoming links (in this case, j).

Discrete-time systems

Theorem 5.2.2. *A discrete-time m-dimensional dynamical system (4.31) is contracting if its Jacobian matrix, J, is such that*

1. $\forall i = 1, \ldots, n$, $\hat{\alpha}_{i,i}(t,x) < 1$;
2. *the graph $\mathcal{G}_d(\mathcal{A})$ does not contain (directed) loops and* $\hat{\alpha}_{ij}(t,x)\hat{\alpha}_{ji}(t,x) \le 1$

Proof. As for the continuous-time case, the idea of the proof is to derive a set of inequalities ensuring contraction of (4.31). These inequalities are again translated into some topological condition on the graph $\mathcal{G}_d(\mathcal{A})$. In particular, to prove contraction, we will now use $\|\Theta J \Theta^{-1}\|_\infty$, where Θ is defined as in (5.4).

By definition, such a norm is smaller than unity if:

$$\sum_{j=1}^{n} \frac{p_i}{p_j} |J_{i,j}(t,x)| < 1 \quad \forall i = 1, \ldots, n \tag{5.10}$$

The above set of inequalities is satisfied if:

$$\frac{p_i}{p_j} |J_{i,j}(t,x)| < \frac{1}{m - n_{0i} - 1}, \quad \forall i, j = 1, \ldots, n \tag{5.11}$$

where n_{0i} denotes the number of zero elements on the i-th row.

Notice that, when $i = j$, the above conditions can be rewritten as $\hat{\alpha}_{i,i}(t,x) < 1$ and hence are satisfied by hypotheses.

Thus, to complete the proof, we have to show that, if the loopless condition on $\mathcal{G}_d(\mathcal{A})$ is satisfied, then the remaining set of inequalities is fulfilled. Specifically, such inequalities are all fulfilled if

$$p_j > \hat{\alpha}_{i,j}(t,x)\, p_i \quad \forall i, j = 1, \ldots, n \quad i \neq j \tag{5.12}$$

It is then clear that, as in the continuous-time case, if the set of inequalities represented by (5.6) is consistent (i.e. there exists some set of values for $p_1, \ldots, p_n$ satisfying such inequalities), then contraction will be immediately proven. We have then to show that the loopless condition on $\mathcal{G}_d(\mathcal{A})$ implies consistency of (5.12). We start by constructing a graph in which a node is associated to each parameter $p_1, \ldots, p_n$ in (5.6) and labeled as $1, \ldots, n$. The topology of the graph is then determined by the coefficients $\hat{\alpha}_{i,j}(t,x)$, given in (5.3). In particular, node i and node j are linked if and only if $\hat{\alpha}_{i,j}(t,x) \neq 0$. The direction of the edge linking i and j are instead assigned from (5.12) according to the *magnitude* of $\hat{\alpha}_{i,j}(t,x)$:

- the edge is from j to i if $\hat{\alpha}_{i,j}(t,x) \geq 1$;
- the edge is from i to j if $\hat{\alpha}_{i,j}(t,x) < 1$;

The proof then follows using the same steps as those for the continuous-time case.

□

5.2.3 Remarks

- Notice that the procedure presented above is based on the use of $\mu_\infty(\Theta J \Theta^{-1})$ and $\|\Theta J \Theta^{-1}\|_\infty$ for proving contraction. Other matrix measures and norms can also be used. In particular, for the continuous-time case, it is easy to prove that, using $\mu_1(\Theta J \Theta^{-1})$, yields the same procedure applied on J^T. If this is the case, the resulting procedure will follow the same logical steps as that of Section 5.2.1, with the only difference being the expression of $\alpha_{i,j}(t,x)$:

$$\alpha_{i,j}(t,x) := \frac{|J_{j,i}(t,x)|(m - c_{0i} - 1)}{|J_{i,i}(t,x)|} \tag{5.13}$$

  where c_{0i} denotes the number of zero elements of the i-th column of J. Analogously, for discrete-time systems, using $\|\Theta J \Theta^{-1}\|_1$ also yields the same steps as those presented in Section 5.2.1 with the only difference being again the definition of $\hat{\alpha}_{i,j}(t,x)$:

$$\hat{\alpha}_{i,j}(t,x) := |J_{j,i}(t,x)|(m - c_{0i} - 1); \tag{5.14}$$

- The key idea for our graphical approach is to formulate contraction using non-Euclidean norms and a metric, Θ, which is diagonal, with positive and constant diagonal elements. We remark here that it is possible to extend the use of our approach to more generic metrics $\Theta(t,x)$. Specifically, this can be done by first performing a smooth change of variables on the system of interest and by applying the presented methodology on the transformed system;

- An interesting open problem is that of identifying the *most convenient* metric $\Theta(t, x)$ to solve the problem of interest. As with any other method for the analysis of nonlinear systems, like e.g. Lyapunov approaches, finding such a metric may need a substantial amount of trial and error, intuition, numerics and *experience* with a set of already-studied systems (like e.g. the ones analyzed in this Chapter);

- While it possible to devise an algorithm to detect the presence of loops in the graph $\mathcal{G}_d(\mathcal{A})$, an open problem is to define a general algorithm for the automatic construction and analysis of such a graph;

- The procedure presented here can have a clear physical interpretation. This is the case, for example, of molecular systems, i.e. systems composed by genes and proteins, where the state variables represent the concentrations of the species involved into the system. In this case, each term $\alpha_{i,j}(t, x)$ represent a *normalized production rate* between species i and species j and the resulting set of inequalities provided in Section 5.2.1 points towards a balance of some *flow-like* quantities in the system (see e.g. [156], [154] and Section 5.4.1);

- Note that our approach can also be used to check partial contraction of the virtual system describing a network of oscillators. In this case, the approach presented in Section 5.2.1 is applied to the Jacobian of such a system and can be used to analyze synchronization phenomena in networks of coupled dynamical systems (e.g. networks of biological oscillators in Section 5.4);

- The procedure can also be used to study the convergence properties of all trajectories towards a linear invariant subspace, M. This, in turn, can be done by applying the steps of Section 5.2.1 to the matrix

$$V \frac{\partial f}{\partial x} V^T$$

as required from Theorem 4.6.

Example 5.2.1. *As an elementary illustration, consider again the general externally-driven transcriptional module (9.2) [40] (see Chapter 9 for further details and extensions of the contraction analysis). Note that the term $(E_T - y)$ is a concentration and therefore must be non-negative. The parameters k_1 and k_2 are positive constants.*

We will show, using the procedure presented in Sec. 5.2.1, that this system is contracting. As proved in [111] (Section 3.7.vi), this in turn implies that, when forced by a periodic input $u(t)$, system (9.2) tends globally exponentially to a periodic solution of the same period as $u(t)$. That is, the system becomes entrained to any periodic input. This property is often a desirable property for biological systems: many important activities of life are, in fact, regulated by periodic, clocklike *rhythms. We can think for example of the suprachiasmatic nucleus (SCN), whose activity is regulated by daily dark-light cycles (see e.g. [177]). Contraction analysis of more general transcriptional modules is presented and extensively studied in [161]. Computing the Jacobian of (9.2) yields*

$$J = \begin{bmatrix} -\delta - k_2 (E_T - y) & k_1 + k_2 x \\ k_2 (E_T - y) & -k_1 - k_2 x \end{bmatrix} \tag{5.15}$$

In this case, the graph $G_d(A)$ associated to J contains only two nodes, labeled as 1 and 2. Thus, the only possible loop in such a graph has length 2. To avoid the presence of such a loop, we have to ensure that the direction determined by $\alpha(1,2)$ is the same as that determined by $\alpha(2,1)$. Computation of these two quantities in accordance with (5.13) yields

$$\alpha(1,2) = \frac{k_2 (E_T - y)}{\delta + k_2 (E_T - y)} < 1$$

and

$$\alpha(2,1) = \frac{k_1 + k_2 x}{k_1 + k_2 x} = 1$$

Following the schematic procedure of Section 5.2.1, this in turn implies that the directions determined by $\alpha(1,2)$ and $\alpha(2,1)$ are the same. In particular, the unique edge of the graph is directed from node 1 to node 2 and no loop can be present. Contraction is then proven.

5.3 A geometric interpretation of the conditions

In this Section we give a geometrical interpretation of our results.

We recall here Gershgorin disk theorems, a set of classical results from linear algebra, which are typically used to provide an estimate of the location of the eigenvalues of a generic matrix, [82].

Theorem 5.3.1. *Let A be a square $m \times m$ matrix, and let p_1, p_2, ..., p_m be some positive real numbers. Then all eigenvalues of A lie in the region*

$$G_P(A) = \bigcup_{i=1}^{m} \left\{ z \in C : |z - a_{ii}| \leq \sum_{\substack{j=1 \\ j \neq i}}^{m} \frac{p_j}{p_i} |a_{ij}| \right\} \tag{5.16}$$

as well as in the region

$$G_P\left(A^T\right) = \bigcup_{j=1}^{m} \left\{ z \in C : |z - a_{jj}| \leq \sum_{\substack{i=1 \\ i \neq j}}^{m} \frac{p_j}{p_i} |a_{ij}| \right\} \tag{5.17}$$

It is worth emphasizing here that both the regions $G_P(A)$ and $G_P\left(A^T\right)$ can be represented as unions of m disks (Gershgorin disks) in the complex plane. Furthermore, the i-*th* Gershgorin disk is centered in a_{ii} with radius given by the weighted sum of the i-th row (or column) off-diagonal elements.

Now notice that for continuous-time systems, the conditions provided in Section 5.2.1 imply that each Gershgorin disk must be completely enclosed in the left-hand side of the complex plane. In fact, uniform negativity of the diagonal elements of the system Jacobian, J, implies that all Gershgorin disks are centered in the left hand-side of the complex plane. Our approach applied to J (or equivalently, the contraction condition given by using μ_∞), the loop-less condition on the directed graph $\mathcal{G}_d(\mathcal{A})$ implies consistency of the set of inequalities (5.6). It is worth noticing here that the consistency of such inequalities implies consistency of (5.5). From a geometrical viewpoint, (5.5) is a straightforward condition on the radius of the i-th Gershgorin disk. Namely, the radius of such a disk must be smaller than the distance of its center from the origin of the complex plane.

An identical interpretation can be given for the procedure involving J^T. In fact, in this case the conditions in Section 5.2.1 ensure uniform negativity of μ_1. This condition, in turn, is equivalent to requiring that the region $G_P\left(J^T\right)$ must be completely enclosed in the left-hand side of the complex plane.

Similarly, it is also possible to give a geometrical interpretation of the contraction rate, c, defined as the maximum of the matrix measure identified by our graphical approach. In particular, the contraction rate can be seen as the distance on the real axis between the origin of the complex plane and the intersection with such axis of the Gershgorin disk closer to the imaginary axis (see Figure 5.2).

Similar considerations can be made for discrete-time systems. In particular, Gershgorin disks need now to be completely enclosed within the unit circle in the complex plane. In analogy with the continuous-time case, the contraction rate is given by the minimum of the distances between the disks and the unitary circle.

Interestingly, both for continuous-time and discrete-time systems, our conditions yield the existence of a metric in which the system Jacobian is diagonally-dominant. Note that one of the main advantages of the presented approach is that such a metric does not need to be computed explicitly. In fact, the results presented in this Chapter ensure that such a metric exists by requiring that the scalars p_i are such that the loop-less condition is satisfied.

It is worth emphasizing here that the stronger the diagonal-dominance of the Jacobian is, the larger is the system contraction rate. Now, as discussed in [181], [181], a higher contraction rate corresponds to better noise rejection properties.

Finally, note that in the case of the Euclidean norm, similar arguments could be used by constructing the Gershgorin disks of the symmetric part of the generalized Jacobian.

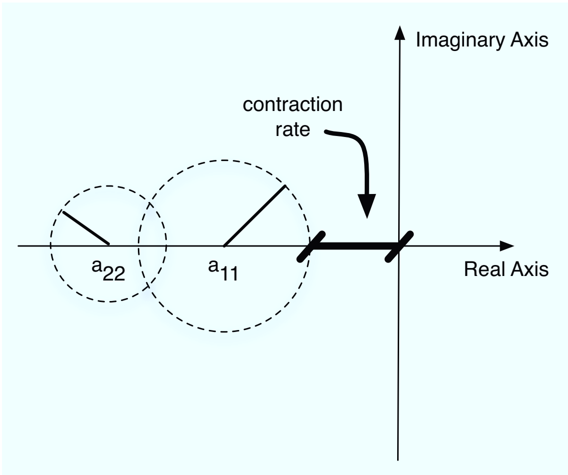

Figure 5.2: A schematic representation of a Gershgorin region (for a real matrix A) composed by two disks. The geometrical interpretation for the contraction rate is pointed out (continuous-time case).

5.4 Applications

In this Section, we illustrate the application of our results to a set of representative problems. Namely, we will first show how a set of constraints on the biochemical parameters of a synthetic biological circuit can be derived by means of our approach, so that it spontaneously synchronizes when coupled to other circuits. We then turn our attention to the problem of synchronizing two chaotic discrete systems coupled in a master-slave configuration.

5.4.1 Networks of Biological Oscillators

The problem that we address in this Section is that of using our approach to tune the parameters of synthetic biological circuits so that, when coupled, they self synchronize.

The Repressilator is a synthetic biological circuit of three genes inhibiting each other in a cyclic way [52]. As shown in Figure 5.3, gene *lacI* (associated to the state-variable c_i in our model) expresses protein LacI (C_i), which inhibits transcription of gene *tetR* (a_i). This translates into protein TetR (A_i), which inhibits transcription of gene *cI* (b_i). Finally, the protein CI (B_i) translated from *cI* inhibits expression of *lacI*, completing the cycle. In [61], a modular addition to the *classical* Repressilator circuit is proposed with the aim of coupling different oscillators using the quorum sensing mechanism. Specifically, the module makes use of two proteins: (i) LuxI, which synthesizes the auto-inducer; (ii) LuxR, with which the auto-inducer synthesized by LuxI forms a complex that activates the transcrpition of various genes.

Quorum sensing is the process by which many bacteria coordinate gene expression according to the local density of signaling molecules produced by other bacteria. It provides a broadcast strategy for the exchange of information between bacteria. One could think of bacteria as nodes in a network that becomes fully connected via an all-to-all topology when quorum sensing is present (see Chapter 9).

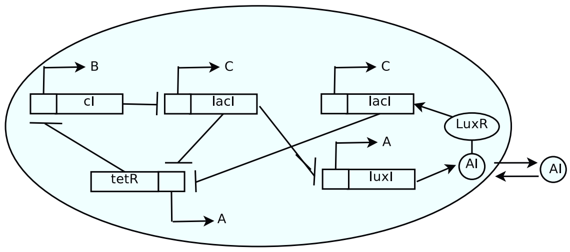

Figure 5.3: Repressilator circuit and coupling mechanism

To model the dynamics of gene expression in the cell, one must keep track of the temporal evolution of all $mRNA$ and protein concentrations. Note that, for the sake of simplicity, variations in the cell density are neglected here. The resulting mathematical model for the network is

$$\begin{aligned}
\dot{a}_i &= -a_i + \tfrac{\alpha}{1+C_i^2} \\
\dot{b}_i &= -b_i + \tfrac{\alpha}{1+A_i^2} \\
\dot{c}_i &= -c_i + \tfrac{\alpha}{1+B_i^2} + \tfrac{kS_i}{1+S_i} \\
\dot{A}_i &= \beta_A a_i - d_A A_i \\
\dot{B}_i &= \beta_B b_i - d_B B_i \\
\dot{C}_i &= \beta_C c_i - d_C C_i \\
\dot{S}_i &= -k_{s0} S_i + k_{s1} A_i - \eta \left(S_i - S_e\right) \\
\dot{S}_e &= -k_{se} S_e + \eta_{ext} \sum_{j=1}^{N} \left(S_j - S_e\right)
\end{aligned} \tag{5.18}$$

having chosen the Hill coefficients equal to 2 as in [61]. We remark here that the above model is dimensionless. This is done by: (i) measuring time in units of $mRNA$ lifetime (which is assumed equal for the three genes), and (ii) expressing the protein levels in units of their Michaelis constant. The parameter α represents the dimensionless transcription rate in the absence of self-repression, while k denotes the maximum contribution of the auto-inducer to the expression of *lacI*.

We first assume that the Repressilator circuits on which the procedure of Section 5.2.1 is applied are all identical. According to [61], we set parameters $\beta_A = \beta_B = \beta_C = 2$. In (5.18) the dynamical equations corresponding to the Repressilator circuits, i.e. the intracellular species concentrations, are denoted with the subscript i, while S_e is the dynamical equation for the coupling auto-inducer.

The network of interest is an all-to-all network. Hence, the virtual system can be chosen as having the same dynamics as the individual Repressilator circuit, forced by the external coupling signal S_e (see e.g. [155], [156], [154] for further examples), i.e.

$$\begin{array}{l} \dot{a} = -a + \frac{\alpha}{(1+C^2)} \\ \dot{b} = -b + \frac{\alpha}{(1+A^2)} \\ \dot{c} = -c + \frac{\alpha}{(1+B^2)} + \frac{(kS_i)}{(1+S_i)} \\ \dot{A} = \beta_A a - d_A A \\ \dot{B} = \beta_B b - d_B B \\ \dot{C} = \beta_C c - d_C C \\ \dot{S} = -k_{s0} S + k_{s1} A - \eta\left(S - S_e\right) \\ \dot{S}_e = -k_{se} S_e + \eta_{ext}\left(S_1 + ... + S_N\right) - \eta_{ext} N S_e \end{array} \tag{5.19}$$

Indeed, by direct inspection it is easy to check that, by substituting the state variables of the nodes dynamics for the virtual variables (i.e. $[a_i, b_i, c_i, A_i, B_i, C_i, S_i, S_e]$ for $[a, b, c, A, B, C, S, S_e]$), gives the equations of the each Repressilator circuit in the network. In this sense, the virtual system embeds the trajectories of all network oscillators.

We can now check contraction of the virtual system (5.19) using the steps presented in Section 5.2.1. Differentiation of (5.19) yields the following Jacobian matrix, J

$$\begin{bmatrix} -1 & 0 & 0 & 0 & 0 & f_1(C) & 0 & 0 \\ 0 & -1 & 0 & f_1(A) & 0 & 0 & 0 & 0 \\ 0 & 0 & -1 & 0 & f_1(B) & 0 & f_2(S) & 0 \\ \beta & 0 & 0 & -\beta & 0 & 0 & 0 & 0 \\ 0 & \beta & 0 & 0 & -\beta & 0 & 0 & 0 \\ 0 & 0 & \beta & 0 & 0 & -\beta & 0 & 0 \\ 0 & 0 & 0 & k_{s1} & 0 & 0 & -k_{s0}-\eta & \eta \\ 0 & 0 & 0 & 0 & 0 & 0 & 0 & -K_q \end{bmatrix} \tag{5.20}$$

where f_1 and f_2 denote the partial derivatives of decreasing and increasing Hill functions with respect to the state variable of interest, $k_{diff} = \eta_{ext} N$ and $K_q =$

$k_{se} + k_{diff}$. Note that the Jacobian matrix J has the the following structure:

$$J = \begin{bmatrix} J_{11} & J_{12} \\ 0 & J_{22} \end{bmatrix}$$

with

$$J_{11} = \begin{bmatrix} -1 & 0 & 0 & 0 & 0 & f_1(C) & 0 \\ 0 & -1 & 0 & f_1(A) & 0 & 0 & 0 \\ 0 & 0 & -1 & 0 & f_1(B) & 0 & f_2(S) \\ \beta & 0 & 0 & -\beta & 0 & 0 & 0 \\ 0 & \beta & 0 & 0 & -\beta & 0 & 0 \\ 0 & 0 & \beta & 0 & 0 & -\beta & 0 \\ 0 & 0 & 0 & k_{s1} & 0 & 0 & -k_{s0} - \eta \end{bmatrix}$$

and $J_{12} = \begin{bmatrix} 0 & 0 & 0 & 0 & 0 & 0 & \eta \end{bmatrix}^T$, $J_{22} = -K_q$. Thus it represents a hierarchical combination of dynamical systems, see Chapter 4. Furthermore, notice that J_{22} (associated to the quorum sensing dynamics) is negative, i.e. such dynamics is contracting. This implies that the overall dynamics of the virtual system is contracting if the submatrix J_{11} is contracting (see Section 4.4). Thus, our approach can be applied directly onto the submatrix $\tilde{J} = J_{11}$. The diagonal elements of $\tilde{J}$ are all negative, thus (see Section 5.2.1), $\mathcal{G}_d(\mathcal{A})$ has to be constructed. In so doing, matrix $\mathcal{A}$ is derived:

$$\mathcal{A} = \begin{bmatrix} 0 & 0 & 0 & 1 & 0 & 1 & 0 \\ 0 & 0 & 0 & 1 & 1 & 0 & 0 \\ 0 & 0 & 0 & 0 & 1 & 1 & 1 \\ 1 & 1 & 0 & 0 & 0 & 0 & 1 \\ 0 & 1 & 1 & 0 & 0 & 0 & 0 \\ 1 & 0 & 1 & 0 & 0 & 0 & 0 \\ 0 & 0 & 1 & 1 & 0 & 0 & 0 \end{bmatrix} \tag{5.21}$$

From (5.21), $\mathcal{G}(\mathcal{A})$ is obtained as shown in Figure 5.4 (left panel).

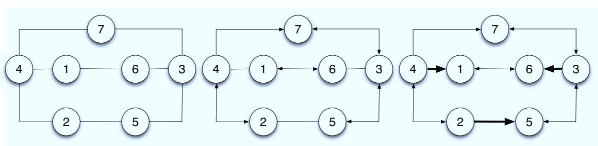

Figure 5.4: Graphs associated to J: $\mathcal{G}(\mathcal{A})$ (left panel); $\mathcal{G}_d(\mathcal{A})$ with state dependent edges (central panel); choice for $\mathcal{G}_d(\mathcal{A})$ (right panel)

Then, computation of coefficients $\alpha_{i,j}(t,x)$ (reported in Table 5.1) provides the directions of the edges of $\mathcal{G}(\mathcal{A})$. Notice that the elements of the left column of Table 5.1 are all state dependent. This implies that the directions of the corresponding edges in $\mathcal{G}_d(\mathcal{A})$ can be time-varying as they are associated to conditions which are

Table 5.1: Set of coefficients $\alpha_{i,j}(t,x)$

$\alpha_{i,j}(t,x)$	Algebraic expression	$\alpha_{i,j}(t,x)$	Algebraic expression
$\alpha_{1,6}$	$\frac{2\alpha C}{(1+C^2)^2}$	$\alpha_{4,1}$	$\frac{d_A}{\beta_A}$
$\alpha_{2,4}$	$\frac{2\alpha A}{(1+A^2)^2}$	$\alpha_{5,2}$	$\frac{d_B}{\beta_B}$
$\alpha_{3,5}$	$\frac{4\alpha B}{(1+B^2)^2}$	$\alpha_{6,3}$	$\frac{d_C}{\beta_C}$
$\alpha_{3,7}$	$\frac{2K}{(1+S_i)^2}$	$\alpha_{7,4}$	$\frac{K_{s1}}{K_{s0}+\eta}$

Table 5.2: Constraints on the biochemical parameters

direction between node i and node j	Constraint
from node 4 to node 1	$\frac{d_A}{\beta_A} > 1$
from node 2 to node 5	$\frac{d_B}{\beta_B} < 1$
from node 3 to node 6	$\frac{d_C}{\beta_C} < 1$

functions of the state. Moreover, due to biochemical constraints [61], $\alpha_{7,4} < 1$. However, the other coefficients in the table (right column) can be easily tuned since they depend only on biochemical parameters of the network (recall that in this case we can tune only the biochemical parameters of the circuits, since no control input is available). In Figure 5.4 (central panel), a *partially directed* graph is shown, obtained by assigning directions to the edges between nodes corresponding to the first four rows and the last row of Table 5.1. Notice that the edges associated to state-dependent conditions are all denoted with a double arrow as the directions of these links might vary in time. The design task is then to use coefficients $\alpha_{4,1}$, $\alpha_{5,2}$, $\alpha_{6,3}$ to avoid the formation of loops at all time as required by the conditions given in Section 5.2.1. A possible choice is presented in the right panel of Figure 5.4, where the edges corresponding to the above coefficients are directed to avoid loops. The inequalities associated to the new directions are reported in Table 5.2. To satisfy these constraints we can choose $d_a = 2\beta_A$, $d_B = 0.5\beta_B$, $d_C = 0.4\beta_C$. Simulation results, shown in Figure 5.5 (top), confirm that, under these conditions, complete asymptotic synchronization is indeed achieved. In Figure 5.5 (bottom), the case is considered of non-identical Repressilators having slightly different parameters from each other. It is shown that, if this occurs, our results then provide conditions for synchronization towards a boundary layer around the nominal synchronization trajectory, [181]. Notice that, as stated in Section 5.3, the stronger the contraction rate is, the thinner is the boundary layer. That is, the better the constraints of Table 5.2 are satisfied, the smaller this set will be, i.e. trajectories will be better synchronized.

From a physical viewpoint, the conditions derived above can be interpreted as follows:

- the constraints on the biochemical parameters imposed by our approach are given in Table 5.2. They imply a *balance* between the production and degradation rates of the protein concentrations involved into the reactions;

- for the system of interest, all state variables are homogeneous quantities. Hence, each of the terms $\alpha_{i,j}(t,x)$'s, which were used to determine the directions of the edge in $\mathcal{G}_d(\mathcal{A})$, can be thought of as a *normalized production rate* between species i and species j. Thus, in this special case, the loop-less condition on $\mathcal{G}_d(\mathcal{A})$ implies a balance of *flows* in the system (see e.g. [156] and [154]).

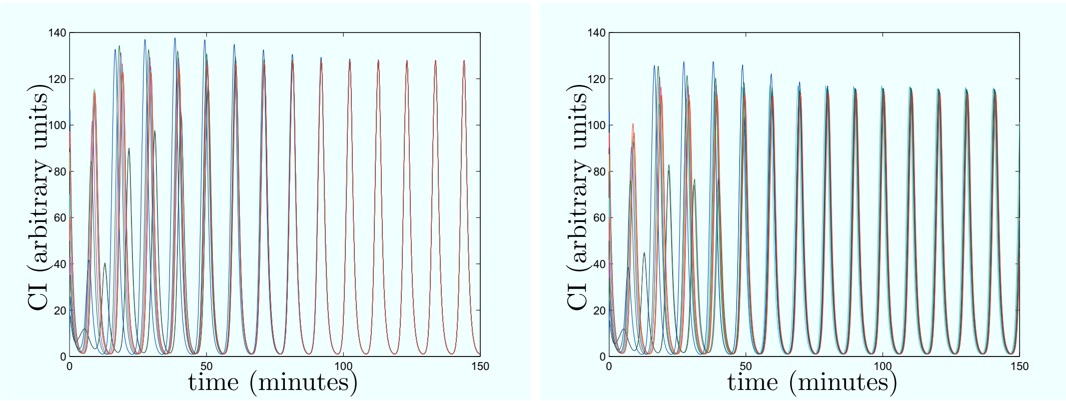

Figure 5.5: Complete (left panel) and robust (right panel) synchronization regimes.

5.4.2 Master-Slave synchronization of discrete-time chaotic systems

To illustrate our approach to the case of discrete-time systems, we consider the problem of synchronizing two chaotic Henon maps [136] using a master-slave synchronization strategy.

In what follows, we denote the set of the state variables of the driving map by y_1, y_2 and the states of the receiver map by x_1 and x_2. The mathematical model of the master-slave configuration is then represented by 4 coupled difference equations:

$$\begin{aligned} y_1(k+1) &= a - y_1(k)^2 + by_2(k) \\ y_2(k+1) &= y_1(k) \\ x_1(k+1) &= a - x_1(k)^2 + bx_2(k) + h(y_1(k)) - h(x_1(k)) \\ x_2(k+1) &= x_1(k) + g(y_2(k)) - g(x_2(k)) \end{aligned} \tag{5.22}$$

where $a = 1.4$ and $b = 0.3$ are system parameters, and the functions $h(\cdot)$, $g(\cdot)$ are the coupling functions. We will now show how to use the proposed procedure, in order to design the coupling so that $(x_1, x_2) \to (y_1, y_2)$, as $k \to +\infty$.

Notice that, in this case, we have to ensure that the slave Henon map is contracting by appropriately choosing the coupling functions. In fact, its contraction will imply that all of its trajectories converge towards the particular solution $(x_1, x_2) = (y_1, y_2)$. Now, according to Section 5.2.1, differentiation of the slave system with respect to its state variables yields:

$$J := \begin{bmatrix} -2x_1 - \frac{\partial h(x_1)}{\partial x_1} & b \\ 1 & -\frac{\partial g(x_2)}{\partial x_2} \end{bmatrix} \tag{5.23}$$

where, for the sake of brevity, the dependence on the discrete time-variable, k, has been omitted.

We now use our approach in order to obtain guidelines for the design of the (nonlinear) protocols g and h ensuring synchronization.

In this case, the graph $\mathcal{G}_d(\mathcal{A})$ is composed by just two nodes (see Section 5.2.1) with the edge between them going from node 1 to node 2. In fact, such direction is determined by the values of $\hat{\alpha}_{1,2}(t,x)$ and $\hat{\alpha}_{2,1}(t,x)$ as:

$$\hat{\alpha}_{1,2} = b < 1 \quad \hat{\alpha}_{2,1} = 1$$

Thus, the loop-less condition on the graph $\mathcal{G}_d(\mathcal{A})$ is already satisfied; we need only to impose the condition on the diagonal elements of J; namely:

$$\begin{aligned} \hat{\alpha}_{1,1}(t,x) &= \left| -2x_1 - \frac{\partial h(x_1)}{\partial x_1} \right| < 1 \\ \hat{\alpha}_{2,2}(t,x) &= \left| -\frac{\partial g(x_2)}{\partial x_2} \right| < 1 \end{aligned} \tag{5.24}$$

A possible choice for satisfying the above conditions is simply to set $\alpha_{1,1}(t,x) = \alpha_{2,2}(t,x) = 0$. These constraints then imply that the protocol functions must fulfill the following conditions:

$$\begin{aligned} \frac{\partial h(x_1)}{\partial x_1} &= -2x_1 \\ \frac{\partial g(x_2)}{\partial x_2} &= 0 \end{aligned} \tag{5.25}$$

Thus, it immediately follows that $h(\cdot)$ and $g(\cdot)$ can be chosen as:

$$\begin{aligned} h(x) &= -x^2 + K_1 \\ g(x) &= K_2 \end{aligned} \tag{5.26}$$

where K_1 and K_2 are constants (in what follows we will choose $K_1 = K_2 = 0$).

Interestingly, using our approach, we find that in order to synchronize the master slave system, we need to (appropriately) couple only the first state variable. Thus, the outcome of the procedure outlined in Section 5.2.1 indicates the *minimal* number of states that we need to couple in order to synchronize the maps.

Using the above results, the model of the two coupled maps becomes:

$$\begin{aligned} y_1(k+1) &= a - y_1(k)^2 + by_2(k) \\ y_2(k+1) &= y_1(k) \\ x_1(k+1) &= a - x_1(k)^2 + bx_2(k) + \left(x_1(k)^2 - y_1(k)^2\right) \\ x_2(k+1) &= x_1(k) \end{aligned} \tag{5.27}$$

In Figure 5.6 (top panel) the behavior of the synchronization error is shown, i.e. $y_1 - x_1$, when the coupling protocol is set to zero. Notice that, in this case, the error as expected does not decrease to zero and synchronization is not attained. The bottom panel of Figure 5.6 shows, instead, the dynamics of the error when the coupling is chosen as in (5.26). Notice that, in this case, the error decreases uniformly to zero, indicating that synchronization between the master and the slave is achieved.

Notice that the choice of coupling functions above suggests a cancelation of some of the dynamics of the slave system. It is important to note that the algebraic conditions (5.24) can also be used to design more sophisticated coupling functions. For instance, consider the following structure for the coupling function h in (5.26):

$$h(x) = -\gamma(k)\, x \tag{5.28}$$

where $\gamma(k)$ is a time varying adaptive gain.

With this choice of coupling, the slave map equations become

$$\begin{aligned} x_1(k+1) &= a - x_1(k)^2 + bx_2(k) + \gamma(k)(x_1 - y_1) \\ x_2(k+1) &= x_1(k) \end{aligned} \tag{5.29}$$

Now, it is straightforward to notice that all conditions of Section 5.2.1 can be satisfied if the time-varying coupling gain is in the range $[2x_1, 2x_1 + 1]$, $\forall k$. To satisfy this condition, we consider for the time-varying coupling gain an adaptation law depending on x_1, so that $\gamma(k) \in [2x_1, 2x_1 + 1]$, $\forall k$. In particular, we choose as a possible adaptation law:

$$\gamma(k+1) = 2x_1(k) + \bar{c}\, e(k), \quad e(0) = x_1(0) \tag{5.30}$$

where $e(k) := x_1 - y_1$ and $\bar{c}$ is a real number such that $|\bar{c}| < 1$. The performance of this adaptive coupling scheme is shown in Figure 5.7, where synchronization error (top) and the gain (bottom) evolutions are shown. We notice that as expected the strategy guarantees convergence of the slave map onto the master trajectory.

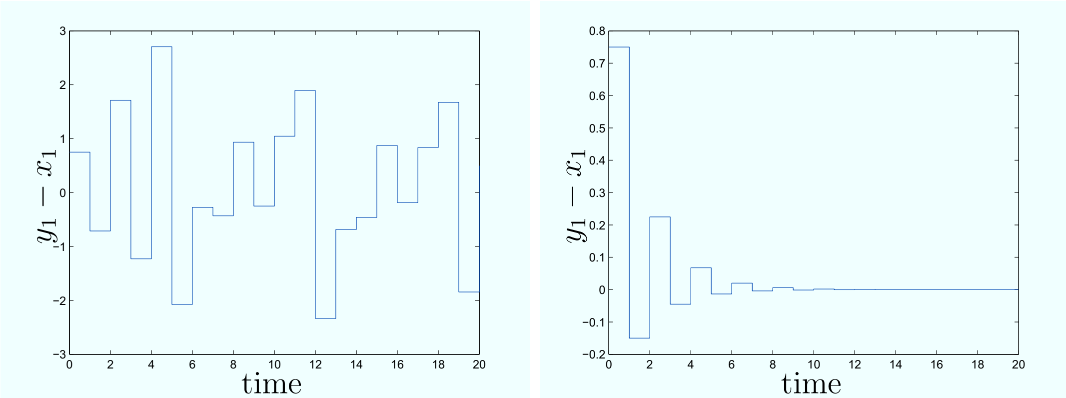

Figure 5.6: Temporal behavior of the mismatch between the first state variables of the master and slave systems when 1) no coupling is present (left panel) and 2) the communication protocol is set as in (5.26) (right panel).

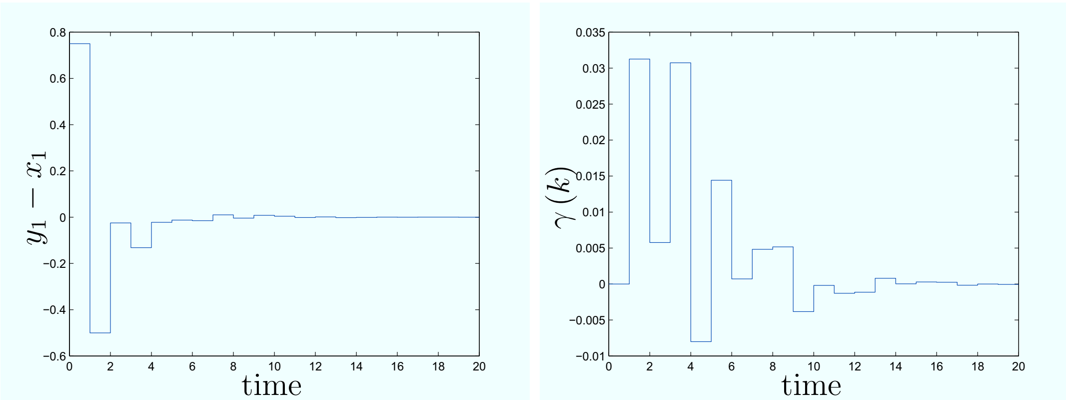

Figure 5.7: Evolution of (left panel) the mismatch between the first state variables of the master and slave systems when coupling (5.30) is used; (right panel) the evolution of the adaptive gain, $\gamma(k)$.

5.5 Concluding remarks

We presented a procedure to prove or impose contraction, for both continuous-time and discrete-time nonlinear dynamical systems. The key idea is to use matrix norms and measures induced by non-Euclidean norms, allowing the resulting set of algebraic conditions to be turned into a set of graphical conditions. At the core of our approach is the construction of a directed graph from the generalized Jacobian, which is then required to be loopless in order for the system to be contracting. One of the main advantages of using the presented graphical procedure is that we do not need to find explicitly an appropriate metric to show contraction. The possible implications of our approach for both circuits and control system design are discussed, and are shown to be particularly effective on a set of representative examples coming from different areas and involving the design of circuits as well as the design of control strategies. We illustrated the approach on a transcriptional module (that, in analogy with the operational amplifier, could be thought of as a basic building block for synthetic and natural molecular circuits). We then considered the following two problems: 1) tuning the parameters of a synthetic biological circuit so that it self-synchronizes when coupled to similar circuits; 2) design a nonlinear communication protocol for the master-slave synchronization of Henon maps (a discrete-time chaotic system). The new graphical approach can have broad applications, particularly for systems whose stability is most easily described using non-Euclidean norms, as in the examples we studied. In the next chapters, we will show that such norms and measures provide an effective tool for the analysis/control of networks with both continuous-time and discrete-time nodes.

Chapter 6

Stability of interconnected systems

In this Chapter we present some results useful for studying the emerging behavior of networked systems by means of Contraction Theory. One of the main features of these results is that they allow to break down the analysis in two different, independent steps. Sometimes, in network coordination problems like e.g. (cluster) synchronization, one is interested in proving that all network trajectories converge towards a subspace of the network phase space rather than proving that all network trajectories converge towards each other. Motivated by this, we present a methodology for studying contraction of an interconnected system towards linear invariant subspaces. We start with introducing the problem in Section 6.1 and present a general Lemma in Section 6.2. Such a result is then used to develop a *multi-scale* approach for the study of interconnected systems (Section 6.3). After some numerical examples (Section 6.4) we turn our attention to the problem of studying contraction of a networked system towards poli-synchronous subspaces in Section 6.5 and finally present two applications in Section 6.6. The results presented in this chapter have been recently published in [162], [163].

6.1 Introduction

It is often useful to break down the analysis and design of large-scale systems into two independent steps:

(a) At a "global" level, properties of a network or interconnection graph are imposed so as to guarantee a desired behavior for the full interconnected system. In this analysis, subsystems may be characterized as "black boxes" with assumed input-output characteristics, but detailed knowledge of their internal structure is not required.

(b) At a "local" level of analysis, one imposes constraints on the structure and behavior of individual subsystems (components), so as to fit the requirements of the global approach. These requirements are verified independently of the overall network structure.

This "multi-scale" or hierarchical methodology is robust in so far as a large degree of uncertainty can be tolerated in the components, only constrained by meeting appropriate behavioral requirements.

There are many examples of such approaches in control theory, including among others (1) the use of small-gain theorems to guarantee stability of a negative feedback loop provided that the components are individually stable (qualitative property of components) and the overall loop H_∞ gain is less than one, as well as nonlinear generalizations based on input to state stability [173, 39]; (2) input/output monotone systems theory [10, 174, 8], in which input-output characteristics are the only required "quantitative" data; (3) the use of passivity-based tools [190, 127, 12].

In Section 6.2 and Section 6.3 we present yet another example of the general principle, this time in the framework of contractive systems discussed in [111]. We show that contractivity of the overall system can be guaranteed if the matrix measures of Jacobians of individual components are upper bounded and a reduced-order matrix associated to the interconnection is contractive. Note that the construction of such reduced-order matrix uses only norm and matrix-measure estimates, but no precise knowledge, of components. No assumptions are made on the networks. Directed networks, self-loops, and multiple regulatory interactions are allowed.

This Chapter is then concluded by presenting a methodology for controlling networked systems based on the combined use of symmetries and contraction. Specifically, we present some results that allow to impose some desired pattern of synchrony for a network of interest (multi purpose networks).

6.2 A globalization result with matrix measures

We assume given:

- k spaces $\mathbb{R}^{n_i}$ endowed respectively with "local" norms $|\xi_i|_{\mathrm{L,i}}$, $i = 1, \ldots, k$, and
- an "interconnection" or "structure" norm $|x|_{\mathrm{S}}$ on $\mathbb{R}^k$.

The structure norm is assumed to be *monotone*, meaning that, for any two vectors $x, y \in \mathbb{R}^k$, we have

$$0 \le x \le y \quad \Rightarrow \quad |x|_{\mathrm{S}} \le |y|_{\mathrm{S}}$$

where an inequality such as "$x \le y$" between vectors is understood coordinate-wise, that is, $x_i \le y_i$ for all indices i. All the usual L^p norms, with $1 \le p \le \infty$ are monotone.

Let

$$N := n_1 + n_2 + \ldots + n_k$$

and introduce a "global" norm on $\mathbb{R}^N$ as follows. Given any vector $\xi = (\xi_1, \ldots, \xi_k)^{\mathrm{T}} \in \mathbb{R}^N$, with $\xi_i \in \mathbb{R}^{n_i}$, $i = 1, \ldots, k$,

$$|\xi|_{\mathrm{G}} := \left| \left(|\xi_1|_{\mathrm{L},1}, \ldots, |\xi_k|_{\mathrm{L},k} \right)^{\mathrm{T}} \right|_{\mathrm{S}}$$

That is, the global norm is obtained by first computing the local norms $x_i = |\xi_i|_{\mathrm{L,i}}$, and then evaluating the structure norm of the resulting vector x with components x_i. Using the fact that the structure norm is assumed to be monotone, it is easy to show that this is indeed a norm.

For example, if all local norms as well as structure norms are L^p norms, with the same p, then the global norm is again the same L^p norm (on a larger space). However, more generally one may mix different norms.

Given two norms, say $|x|_1$ and $|y|_2$, in $\mathbb{R}^q$ and $\mathbb{R}^p$ respectively, we may consider the usual induced operator norm on matrices $A \in \mathbb{R}^{p\times q}$, $\|A\|_{12} := \sup_{|x|_1=1} |Ax|_2$. In particular, for the special cases when $p = n_i$ and $q = n_j$ and the above norms, we denote this norm as $\|A\|_{\mathrm{L,i,j}}$:

$$\|A\|_{\mathrm{L,i,j}} := \sup_{|x|_{\mathrm{L,i}}=1} |Ax|_{\mathrm{L,j}}$$

When $p = q = k$ we write:

$$\|A\|_{\mathrm{S}} := \sup_{|x|_{\mathrm{S}}=1} |Ax|_{\mathrm{S}}$$

and when $p = q = N$:

$$\|A\|_{\mathrm{G}} := \sup_{|x|_{\mathrm{G}}=1} |Ax|_{\mathrm{G}}$$

We use the notations $\mu_{\mathrm{L,i}}[\cdot]$, $\mu_{\mathrm{S}}[\cdot]$, and $\mu_{\mathrm{G}}[\cdot]$ for the matrix measures (logarithmic norms) associated to $\|\cdot\|_{\mathrm{L,i,i}}$, $\|\cdot\|_{\mathrm{S}}$, and $\|\cdot\|_{\mathrm{G}}$ respectively.

Given any "global" matrix $A_{\mathrm{G}} \in \mathbb{R}^{N\times N}$, we define its associated "structure" matrix $A_{\mathrm{S}} \in \mathbb{R}^{k\times k}$ as follows. We start by partitioning A_{G} in the form:

$$A_{\mathrm{G}} = \begin{pmatrix} A_{11} & A_{12} & \ldots & A_{1k} \\ A_{21} & A_{22} & \ldots & A_{2k} \\ \vdots & \vdots & \ddots & \vdots \\ A_{k1} & A_{k2} & \ldots & A_{kk} \end{pmatrix} \tag{6.1}$$

and for each $i = 1, \ldots, k$, we define the following numbers:

$$\widetilde{A}_{ii} := \mu_{\mathrm{L,i}}[A_{ii}]$$

and for each $i, j \in \{1, \ldots, k\}$ with $i \neq j$, we let:

$$\widetilde{A}_{ij} := \|A_{ij}\|_{\mathrm{L,i,j}}$$

Finally, we define:

$$A_{\mathrm{S}} := \begin{pmatrix} \widetilde{A}_{11} & \widetilde{A}_{12} & \ldots & \widetilde{A}_{1k} \\ \widetilde{A}_{21} & \widetilde{A}_{22} & \ldots & \widetilde{A}_{2k} \\ \vdots & \vdots & \ddots & \vdots \\ \widetilde{A}_{k1} & \widetilde{A}_{k2} & \ldots & \widetilde{A}_{kk} \end{pmatrix} \tag{6.2}$$

(The proofs will actually show a little more, namely that upper bounds on the $\widetilde{A}_{ij}$ could be used, instead.)

Our main result is as follows:

Theorem 6.2.1. *For every set of "local" norms on $\mathbb{R}^{n_i}$, every "structure" norm on $\mathbb{R}^k$, and every matrix $A_{\mathrm{G}} \in \mathbb{R}^{N \times N}$,*

$$\mu_{\mathrm{G}}[A_{\mathrm{G}}] \leq \mu_{\mathrm{S}}[A_{\mathrm{S}}]$$

This Theorem follows from:

Lemma 6.2.1. *For every set of "local" norms on $\mathbb{R}^{n_i}$, every "structure" norm on $\mathbb{R}^k$, and every matrix $A_{\mathrm{G}} \in \mathbb{R}^{N \times N}$:*

$$\|I + hA_{\mathrm{G}}\|_{\mathrm{G}} \leq \|I + hA_{\mathrm{S}}\|_{\mathrm{S}} + g(h) \qquad \text{for all } h > 0 \tag{6.3}$$

where $g : \mathbb{R}_{>0} \to \mathbb{R}_{>0}$ is such that $g(h) = o(h)$ as $h \searrow 0$.

To see how Theorem 6.2.1 follows from Lemma, we recall that

$$\mu_{\mathrm{G}}[A_{\mathrm{G}}] = \lim_{h \searrow 0} \frac{1}{h} \left(\|I + hA_{\mathrm{G}}\|_{\mathrm{G}} - 1\right)$$

and similarly for $\mu_{\mathrm{S}}[A_{\mathrm{S}}]$. Subtracting 1 from both sides in (6.3), dividing by h, and taking the limit as $h \searrow 0$, the Theorem results.

We now prove the Lemma.

Proof. Pick any vector $\xi \in \mathbb{R}^N$. We will show that

$$|(I + hA_{\mathrm{G}})\xi|_{\mathrm{G}} \leq \left[\|I + hA_{\mathrm{S}}\|_{\mathrm{S}} + g(h)\right] |\xi|_{\mathrm{G}} \tag{6.4}$$

for some function g as above. Since this holds in particular for all ξ with $|\xi|_{\mathrm{G}} = 1$, the Lemma will follow.

We need the following observation. Since, for any norm $|\cdot|$ and induced matrix norm $\|\cdot\|$, by definition the matrix measure of a matrix B is $\mu(B) = f'(0)$, where

$f(h) = \|I + hB\|$, there is a function $g(h) = o(h)$ such that $\|I + hB\| = 1 + h\mu(B) + g(h)$. In particular, there are such functions $g_i(h)$ associated to the "local" norms $|\cdot|_{\mathrm{L,i}}$. We let $g(h) := \max\{g_1(h), \ldots, g_k(h)\}$. Thus,

$$\|1 + hA_{ii}\|_{\mathrm{L,i}} \;\leq\; 1 + h\mu_{\mathrm{L,i}}[A_{ii}] + g(h),\; i = 1, \ldots, k \tag{6.5}$$

Note that $g(h) = o(h)$.

We start the proof of the Lemma by writing in block form $\xi = (\xi_1, \ldots, \xi_k)^{\mathrm{T}}$, with $\xi_i \in \mathbb{R}^{n_i}$, $i = 1, \ldots, k$, and denote

$$\eta \;:=\; (I + hA_{\mathrm{G}})\,\xi$$

In block form, we have $\eta = (\eta_1, \ldots, \eta_k)^{\mathrm{T}}$, with $\eta_i \in \mathbb{R}^{n_i}$, $i = 1, \ldots, k$, where

$$\eta_i \;=\; (1 + hA_{ii})\xi_i \,+\, \sum_{j \neq i} hA_{ij}\xi_j$$

By definition of the global norm,

$$|\eta|_{\mathrm{G}} \;=\; |x|_{\mathrm{S}}$$

where we denote $x_i := |\eta_i|_{\mathrm{L,i}}$ for each $i = 1, \ldots, k$ and $x = (x_1, \ldots, x_k)^{\mathrm{T}}$. Similarly,

$$|\xi|_{\mathrm{G}} \;=\; |y|_{\mathrm{S}}$$

where we denote $y_i := |\xi_i|_{\mathrm{L,i}}$ for each $i = 1, \ldots, k$ and $y = (y_1, \ldots, y_k)^{\mathrm{T}}$.

Using the triangle inequality, we have that, for every $i = 1, \ldots, k$:

$$\begin{aligned}
x_i \;&\leq\; |(1 + hA_{ii})\xi_i|_{\mathrm{L,i}} \,+\, \sum_{j \neq i} |hA_{ij}\xi_j|_{\mathrm{L,i}} \\
&\leq\; \|1 + hA_{ii}\|_{\mathrm{L,i}}\, |\xi_i|_{\mathrm{L,i}} \,+\, \sum_{j \neq i} h\, \|A_{ij}\|_{\mathrm{L,i,j}}\, |\xi_j|_{\mathrm{L,j}} \\
&\leq\; \Big[1 + h\mu_{\mathrm{L,i}}[A_{ii}]\Big]\, |\xi_i|_{\mathrm{L,i}} \,+\, \sum_{j \neq i} h\, \|A_{ij}\|_{\mathrm{L,i,j}}\, |\xi_j|_{\mathrm{L,j}} \\
&\qquad\qquad\qquad\qquad + g(h)\, |\xi_i|_{\mathrm{L,i}} \\
&=\; z_i \;:=\; \Big[1 + h\widetilde{A}_{ii}\Big]\, y_i \,+\, \sum_{j \neq i} h\widetilde{A}_{ij} y_j \,+\, g(h) y_i
\end{aligned}$$

where we used (6.5). In terms of the following vector $z \in \mathbb{R}^k$:

$$z \;:=\; (I + hA_{\mathrm{S}})\, y \,+\, g(h)\, y$$

we can summarize the above inequality as "$x \leq z$" (in the coefficient-wise order), and hence, using monotonicity of the "structure" norm, we know that $|x|_{\mathrm{S}} \leq |z|_{\mathrm{S}}$. By the triangle inequality,

$$|x|_{\mathrm{S}} \;\leq\; \|I + hA_{\mathrm{S}}\|_{\mathrm{S}}\, |y|_{\mathrm{S}} \;+\; g(h)\; |y|_{\mathrm{S}}$$

Recalling that $|x|_{\mathrm{S}} = |\eta|_{\mathrm{G}} = |(I + hA)\,\xi|_{\mathrm{G}}$ and $|y|_{\mathrm{S}} = |\xi|_{\mathrm{G}}$, we have that

$$|(I + hA_{\mathrm{G}})\,\xi|_{\mathrm{G}} \;\leq\; [\|I + hA_{\mathrm{S}}\|_{\mathrm{S}} + g(h)]\,|\xi|_{\mathrm{G}}$$

which is (6.4) and hence the Lemma is proved. □

6.3 Application to structured systems

The above general results on contraction can be immediately applied to the study of global stability of interconnected systems. For example, if the interconnection structure is a graph with pure diffusion among components, then it is convenient to employ Euclidean norm for the structure norm. The structure measure will evaluate to zero, which implies that the interconnection structure does not destroy contraction.

6.3.1 Stability of interconnected systems

We now sketch several ways in which the contraction results presented in this Chapter can be applied to networked control systems.

We consider the interconnected system (3.4). Recall that, a particular choice for the functions $\tilde{h}_i(t,x)$ is:

$$\tilde{h}_i(t,x) = h_i(t, a_{i1}(t)x_1, a_{i2}(t)x_2, \ldots, a_{iN}(t)x_N)$$

where $A(t) := [a_{ij}(t)]$ is the $N \times N$ time-varying adjacency matrix, with $a_{ij}(t) : \mathbb{R}^+ \to [0,1]$ being smooth functions. Notice that the above formalization allows us to consider within a unique framework directed and undirected networks with (smoothly) changing topology, self loops and multiple interactions. Of course, one could incorporate the time-varying coefficients $a_{ij}(t)$ directly into the functions h_i, redefining this function, so that there is no need for the "tilde" in Equation (3.4). However, we prefer to write things in this form in order to emphasize that the entries of $A(t)$ may be uncertain.

We denote with $J := [J_{ij}]$ the Jacobian of the interconnected system composed by the N subsystems in (3.4), i.e.

$$J_{ij} := \frac{\partial f_i}{\partial x_j} + \frac{\partial \tilde{h}_i}{\partial x_j} \tag{6.6}$$

In what follows, the Jacobian matrix will play the role of the *global* matrix, A_{G}, as defined in Section 6.2, with $A_{ij} = J_{ij}$. The elements $\tilde{A}_{ij}$ of the structure matrix, A_{S}, can then be defined as follows:

- $\tilde{A}_{ii} := \mu_{L,i}(J_{ii}(t,x))$;
- $\tilde{A}_{ij} := \|J_{ij}(t,x)\|_{L,i,j}$, $i \neq j$;

where the local norms can be chosen arbitrarily. Notice that in the above notation we omitted the dependence of the global and structure matrices on the time and state variables.

The following result shows that (3.4) is contracting if there exist a uniformly negative matrix measure for the reduced order matrix A_{S}, obtained as described above.

Theorem 6.3.1. *The interconnected system (3.4) is contracting if there exist some matrix measure such that*

$$\mu_S\left(A_{\mathrm{S}}\right) \leq -c, \quad c \in \mathbb{R}^+$$

Proof. The proof of this result is a straightforward consequence of Theorem 6.2.1. Indeed, it suffices to recall that $\mu_S\left(A_{\mathrm{S}}\right)$ upper bounds $\mu_G\left(J\left(t,x\right)\right)$. Thus, by hypotheses, we have:

$$\mu_G\left(J\left(t,x\right)\right) \leq \mu_S\left(A_{\mathrm{S}}\right) \leq -c$$

That is, (3.4) is contracting and all of its trajectories converge towards each other by means of Theorem 4.2.1. □

Now, assume that only upper bounds of the elements $\tilde{A}_{ij}$ are known. That is, only some $c_i \in \mathbb{R}$ and $m_{ij} \geq 0$, such that $\tilde{A}_{ii} \leq c_i$ and $\tilde{A}_{ij} \leq m_{ij}$, uniformly, are known. All norms in Euclidean space being equivalent, the finiteness of the upper bounds m_{ij} for one norm will imply the existence of such upper bounds for any other norm. However, the actual values are critical for the estimates.

Construct the matrix $\hat{A}_{\mathrm{S}} := [\hat{A}_{ij}]$ as follows:

- $\hat{A}_{ii} := c_i$;
- $\hat{A}_{ij} := m_{ij}$.

Then, Theorem 6.3.1 immediately implies that the interconnected system (3.4) is contracting if there exist some matrix measure such that

$$\mu_S\left(\hat{A}_{\mathrm{S}}\right) < 0$$

We now present some consequences of the results presented in this Section.

- Assume that matrix measure estimates of the intrinsic nodes dynamics and the coupling function are known. That is,

$$\mu_{L,i}\left(\frac{\partial f_i}{\partial x_i}\right) \leq \alpha, \text{ and } \mu_{L,i}\left(\frac{\partial \tilde{h}_i}{\partial x_i}\right) \leq m_{ii} \tag{6.7}$$

  Then, we can take $c_i = \alpha + m_{ii}$. It follows that we can write $\hat{A}_{\mathrm{S}} = \alpha I + M$, where $M = [m_{ij}]$ and I is the identity matrix of appropriate dimensions. Now, using Theorem 6.3.1 and the sub-additivity property of matrix measures it is straightforward to prove that the entire system is contracting if

$$\alpha + \mu_S(M) < 0 \tag{6.8}$$

- We will now discuss (6.8) by distinguishing between two cases:

  1. nodes dynamics are contracting, i.e. $\alpha < 0$;
  2. nodes dynamics are not contracting, i.e. $\alpha \geq 0$.

  Case 1. As a very special consequence of (6.8), if $\alpha < 0$, we have that contraction of the networked system is ensured by any coupling such that the associated matrix, M, fulfills the following condition:

$$\mu_S\left(M\right) < |\alpha|$$

  This means that a network of contracting nodes remains contracting even if the coupling strategy introduces some instability (which may be due e.g. to the presence of some noise), or the nodes become disconnected. In turn, this leads to the conclusion that there is no *diffusion-driven instability* possible for contractive systems, in the sense that contraction of the individual systems, when coupled by diffusive terms, ensures contraction of the entire network. (This can be easily shown by noticing that the matrix M in this case has zero row and column sums.)

  Case 2. If $\alpha \geq 0$, from (6.8) we can immediately conclude that contraction of the interconnected system is ensured by any coupling strategy such that

$$\mu_S\left(M\right) < -\alpha$$

  That is, the functions $h_i\left(t, x\right)$, $i = 1, \ldots, N$, have to *compensate* the (possible) instabilities intrinsic to the nodes.

- When applied to synchronization/consensus problems, our results ensure that all nodes globally exponentially converge to a unique point on the synchronization manifold $x_1 = \ldots = x_N$ as in our case such a manifold is embedded into a contracting space. In this sense, our results guarantee a stronger result than just convergence of all trajectories towards the synchronization manifold in state space.

6.4 Applications

A possible application of the results derived in Section 6.2 and Section 6.3 is the synthesis of appropriate decentralized strategies ensuring stability of networks of dynamical systems. We consider the problem of designing a distributed control strategy ensuring convergence of either Hopfield (HN for short) [81] or Fitzhugh-Nagumo (FN) systems, see e.g. [151]. We remark here that by *convergence* we mean that all trajectories of the network nodes converge towards each other.

In both cases, we will assume that the coupling functions are not necessarily diffusive and that the network topology is directed. We remark here that in our approach the individual subsystems are considered as black boxes, characterized by their contraction estimates. Hence, the same coupling functions derived below can be used to ensure convergence of networks of different subsystems characterized by the same contraction estimates. For the sake of brevity the illustration of the *design process* is omitted here and will be presented elsewhere.

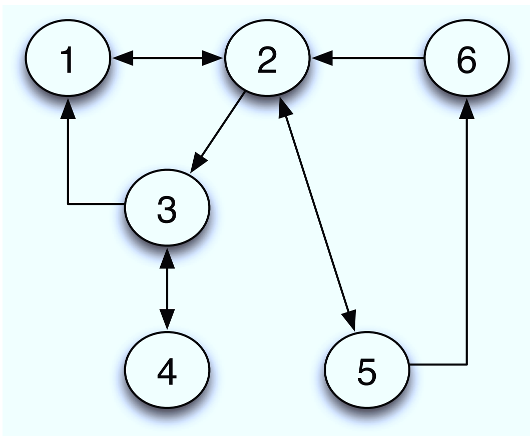

Figure 6.1: Network used for the simulations of HN and FN

Convergence of networked HNs and FNs

We start by considering the network topology of Figure 6.1. The first model we consider is a network of HN [81] given by:

$$\dot{x}_i = -\frac{x_i}{R} + \sum_{j \in N_i} (h_{ij}(x_j) - h_{ij}(x_i)) + u(t) \tag{6.9}$$

Table 6.1: Coupling function for network (6.9)

edge	$h_{ij}(x)$
$1 \leftrightarrow 2,\ 6 \rightarrow 2,\ 2 \rightarrow 3,\ 5 \rightarrow 6$	$G\arctan(x)$
$3 \rightarrow 1,\ 5 \leftrightarrow 2$	Kx
$3 \leftrightarrow 4$	$\frac{1-e^{-x}}{1+e^{-x}}$

where $i = 1, \ldots, N$. Here, x_i denote the neural voltages, R is the resistance, h_{ij} are the coupling functions, N_i is the set of neighbours of node i and $u(t)$ represents some periodic external input acting on all nodes. It is straightforward to check that the synchronization subspace $\{x_1 = x_2 = \ldots = x_n\}$ is an invariant subspace for (6.9). Thus, contraction of the networked system immediately implies that all of its trajectories converge towards such a manifold. This, in turn is implied by the existence of some structure matrix measure, μ_S, such that $\mu_S(A_{\mathrm{S}})$ is uniformly negative.

Some recent results on the synchronization/consensus of networks of identical systems with diffusive coupling and fixed topology can be found in [194], [142], [155], [157], [159].

Note that this network has:

$$f_i(x_i, t) = -\frac{x_i}{R} + u(t) \quad \text{and} \quad \tilde{h}_i(x) := \sum_{j \in N_i} \left(h_{ij}(x_j) - h_{ij}(x_i)\right)$$

Deriving the Jacobian of the interconnected system as in (6.6), we then have

$$J(x) = A_{\mathrm{G}} = A_{\mathrm{S}} = -\frac{1}{R} I + M(x)$$

where I is the identity matrix of appropriate dimensions and $M(x) := \left[\frac{\partial h_{ij}}{\partial x_j}\right]$. In order to guarantee convergence, we need to show now that the network is contracting. To this aim, we choose the coupling functions so as to to fulfill the conditions of Theorem 6.3.1. Specifically, the coupling functions are those reported in Table 6.1 and use Theorem 6.3.1 to find simple conditions on the coupling gains G and K in order to ensure contraction of the network. Using as structure matrix measure the one induced by the weighted vector-1 norm, we have:

$$\mu_S\left(A_{\mathrm{S}}\right) = \mu_{1,P}\left(A_{\mathrm{S}}\right) \leq -\frac{1}{R} + \mu_{1,P}\left(M(x)\right)$$

The simplest choice for the matrix measure $\mu_{1,P}$ is that induced by the weights $p_1 = \ldots = p_N$, obtaining:

$$\mu_{1,P}\left(M(x)\right) \leq \max\left\{-G + K, G\right\}$$

Now, if we set $G < 1/R$ and $K - G < 1/R$, then the Jacobian measure is uniformly negative definite, making the network contracting. Since each node is forced by the periodic function $u(t)$, this implies that there exist a unique periodic orbit towards which all trajectories of (6.9) converge (see Chapter 4 and [161]). Furthermore, the synchronization manifold is flow invariant for network dynamics. Thus, we can conclude that contraction of (6.9) implies that all of its trajectories converge towards a unique solution which is embedded into the synchronization manifold. That is, at steady state network nodes are synchronized onto a periodic orbit having the same period as $u(t)$.

We now turn our attention to the problem of ensuring convergence of a network of FN oscillators described by [58]:

$$\begin{aligned} \dot{v}_i &= c\left(v_i + w_i - \tfrac{1}{3}v_i^3 + u(t)\right) \\ \dot{w}_i &= -\tfrac{1}{c}\left(v_i - a + bw_i\right) \end{aligned} \tag{6.10}$$

where v_i is the membrane potential, w_i is a recovery variable and $u(t)$ is the magnitude of the stimulus current. The parameters are set to: $c = 6$, $a = 0$, $b = 2$. We will now design a non-diffusive coupling strategy, similar to the so-called excitatory-only coupling, which may play an important role for the synchronization of neurons in the brain (see e.g. [197]). Specifically, we couple FN oscillators in the network only on the state variable v_i, via the additive coupling function:

$$\tilde{h}_i(v_i.w_i) := -\gamma_1 \sum_{j\in N_i} v_j - (\gamma_2 + c)v_i \tag{6.11}$$

which is added to the first state equation in (6.10).

Notice that, as in this case for HN, the subspace (or synchronization manifold)

$$\mathcal{M} := \{x_i = x_j, \quad i,j = 1,\dots,6\}$$

is flow invariant for the network of our interest. Thus, contraction of the network implies that all of its trajectories converge towards a unique solution, embedded in $\mathcal{M}$.

We will use Theorem 6.3.1 to obtain a sufficient condition on the coupling functions $\tilde{h}_i(t, x_i, x_j)$ ensuring contraction. In so doing, we use as *local* matrix measure, $\mu_{L,i}$ the one induced by the ∞-norm, while we use as *structure* matrix measure, μ_S, the one induced by the vector 1-norm.

If we set the gains of the coupling function (6.11) so as to fulfill

$$\gamma_2 > c + \frac{b-1}{c} \tag{6.12}$$

we obtain

$$\alpha = -\frac{b-1}{c}$$

with α defined as in (6.7).

Now, constructing the matrix M as in (6.7) and using μ_∞ as local matrix measure, $\mu_{L,i}$, yields:

$$\begin{bmatrix} 0 & \gamma_1 & \gamma_1 & 0 & 0 & 0 \\ \gamma_1 & 0 & 0 & 0 & \gamma_1 & \gamma_1 \\ 0 & \gamma_1 & 0 & \gamma_1 & 0 & 0 \\ 0 & 0 & \gamma_1 & 0 & 0 & 0 \\ 0 & \gamma_1 & 0 & 0 & 0 & 0 \\ 0 & 0 & 0 & 0 & \gamma_1 & 0 \end{bmatrix}$$

Therefore, using Theorem 6.3.1, we can conclude that all network trajectories converge towards each other (and therefore converge towards the synchronization manifold) if

$$3\gamma_1 < \frac{b-1}{c} \tag{6.13}$$

Figure 6.2 shows a simulation for such a network, confirming the theoretical predictions.

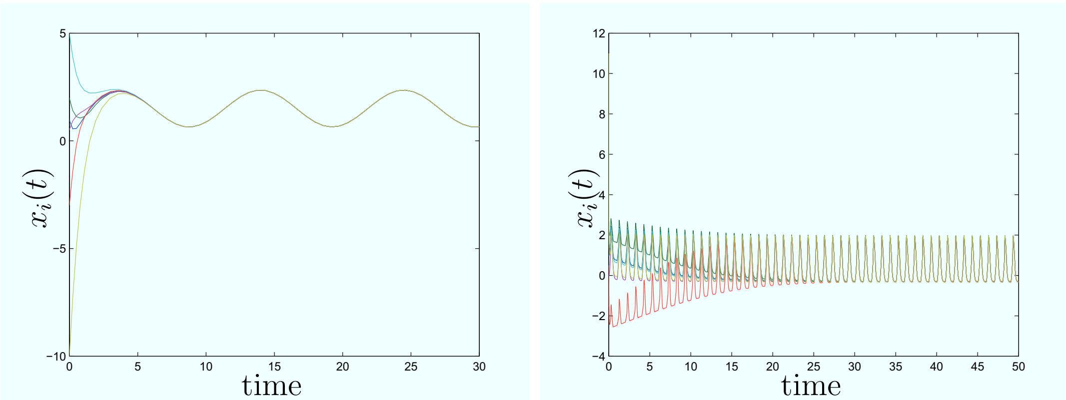

Figure 6.2: Simulation of: (left panel) network (6.9) with $R = 1$, $G = K = 0.9$; (right panel) network (6.10) with $\gamma_1 = 0.05$ and $\gamma_2 = 7$.

6.5 Contraction towards poli-synchronous subspaces

In Section 6.2 we presented a *multiscale* methodology for studying contraction of the interconnected system (3.4). That is, we presented a result for the convergence of all network trajectories towards each other. Often, in network coordination problems like e.g. concurrent synchronization, one is interested in proving the stability of some invariant subset of the phase space, termed as poli-synchronous manifold (see Chapter 3). In this Section we present an approach for studying contraction of (3.4) towards such poli-synchronous subspaces.

6.5.1 Analysis and control

In this Section, the objective is now that of studying the collective behavior emerging in network described by (3.4). Our main idea can then be summarized as follows:

1. study the symmetries of (3.4) to determine the possible poli-synchronous subspaces (defining the possible patterns of synchrony);

2. determine among the possible patterns, the one exhibited by (3.4) using contraction.

Consider a partition of the N nodes of a network into k groups, $\mathcal{G}_1, \ldots, \mathcal{G}_k$, characterized by the same intrinsic dynamics. We define the following subspaces associated to each group of nodes:

$$\mathcal{M}_{p,s} := \{x_i = x_j, \quad \forall i, j \in \mathcal{G}_s\}, \quad s = 1, \ldots, k$$

Notice that all the nodes of the i-th group are synchronous if and only if network dynamics evolve onto the associated subspace $\mathcal{M}_{p,i}$. The *poli-synchronous subspace*, say $\mathcal{M}_p$, is then defined as the intersection of all $\mathcal{M}_{p,k}$, i.e. $\mathcal{M}_p := \bigcap_k \mathcal{M}_{p,k}$, or equivalently

$$\mathcal{M}_p := \{x_i = x_j, \forall i, j \in \mathcal{G}_m, 1 \le m \le k\}$$

We a say that a given pattern of synchrony is possible for the network of interest if its corresponding poli-synchronous subspace is flow invariant. In this view, a useful result is the following:

Theorem 6.5.1. *The set $\mathcal{M}_p$ is invariant for network (3.3) if the nodes belonging to group $\mathcal{G}_p$: i) have the same uncoupled dynamics; ii) are input symmetric.*

The proof of the above Theorem can be found in e.g. [69, 70]. In terms of network synchronization/control, intuitively such a result implies that a specific pattern of synchrony is possible if the aspiring synchronous nodes have synchronous input sets.

The following result is a straightforward consequence of the results presented in Section 4.7.

Corollary 6.5.1. *Assume that for network (3.4) the sets $\mathcal{M}_{p,k}$ exist. Then, the synchrony pattern exhibited by the network is given by:*

1. *the intersection $\mathcal{M}_p$, if the network is contracting (or contracting towards each $\mathcal{M}_{p,k}$);*

2. *$\mathcal{M}_{p,k}$, if the network is contracting only towards $\mathcal{M}_{p,k}$.*

Chain topologies: revised

Consider, again, the network topology in Figure 4.2. Recall that in Section 4.7.1 we proved network synchronization in two subsequent steps. Specifically, we first proved that all network trajectories are globally exponentially convergent towards the poly-synchronous subspace where $x_1 = x_4$, $x_2 = x_3$. We then showed that network dynamics reduced on such a subspace were globally exponentially convergent towards the synchronous subspace.

The subspaces $\mathcal{M}_2$ and $\mathcal{M}_1$ towards which convergence was proved were, in turn, determined by equivariance of network dynamics with respect to some permutation action. Notice that this equivariance property is a direct consequence of the fact that node 1 of the network is input-equivalent to node 4 and node 2 is input-equivalent to node 3. Moreover, the *equivalent* nodes of the 2-nodes reduced network are also input-equivalent.

6.5.2 Controlling symmetry patterns

We now turn our attention to the problem of imposing some desired behavior for (3.4). The set-up that we have in mind is that of a network that can be *programmed* to perform different tasks, by controlling few interconnections: in this sense, a similar result is given in [64], where the input continuity formalism was used.

Let $X := \left[x_1^T, \dots, x_N^T\right]^T$ and $\Phi(t,X) := \left[\phi_1(t,X)^T, \dots, \phi_N(t,X)^T\right]^T$. Network dynamics (3.4) can then be written as:

$$\dot{X} = \Phi(t,X) \tag{6.14}$$

Now, let $F(t,X)$ be the stacks of all the functions $f_i(t,x_i)$ and $\tilde{H}(t,X)$ be the stack of all the $\tilde{h}_i(t,X)$. We assume that the function Φ has the following form:

$$\Phi(t,X) := F(t,X) + \tilde{H}(t,X,\tilde{U}(X),\bar{U}(t))$$

Where the possible presence of inputs to the network (6.14) is emphasized. Indeed, $\tilde{U} := [\tilde{u}_1, \dots, \tilde{u}_N]$ and $\bar{U} := [\bar{u}_1, \dots, \bar{u}_N]$, represents two types of inputs that can be used to control network dynamics:

- $\tilde{U}(X)$ can be thought of as a feedback control input: physically, it can affect the structure of the couplings between nodes;
- $\tilde{U}(t)$ denotes an exogenous input, which can be used to e.g. switch between different coupling functions and/or to directly affect the intrinsic dynamics of the nodes.

We define the following *control task*:

ensure a desired pattern of synchrony for the interconnected system (6.14).

Recall that a pattern of synchrony is identified in phase space by a linear subspace: the subspace associated to the *desired* pattern is denoted with $\mathcal{M}_d$. We say that the network control problem is solved if all the trajectories of (6.14) globally exponentially converge towards $\mathcal{M}_d$. The following results is a straightforward consequence of the results obtained in Chapter 4.

Theorem 6.5.2. *The control problem is solved if the inputs $\tilde{U}$ and $\bar{U}$:*

1. *ensure the input equivalence to which $\mathcal{M}_d$ is associated;*
2. *ensure contraction towards $\mathcal{M}_d$.*

6.6 Applications

We now present two possible applications of the results derived in Section 6.5. Specifically, we will show how our results can be used to analyze and/or design networks so as to achieve some desired *functionality*. In Chapter 9 we will present a further application of the above results to the analysis of network motifs arising in transcriptional networks.

6.6.1 Multilayer perceptrons

Our first example is the analysis/control of a multilayer perceptron network. Such a system can be seen as a generalization of feedforward loops (see e.g. [4] and Chapter 9), where a set of inputs is mapped onto a set of outputs. Examples of multilayer systems can be found in e.g. artificial neural networks [168] and protein-protein interaction networks [3]. A schematic representation of a multilayer perceptron system is given in Figure 6.3. The network consists of k layers: the i-th layer consists of n_i nodes and the total number of nodes is $N := \sum_{i=1}^{k} n_i$. Each of the nodes of the i-th layer communicates unidirectionally with a subset of the nodes belonging to the layer $(i+1)$-th. Only the dynamics of the nodes of the first layer are affected by some exogenous input, i.e. $u_i(t)$, $i = 1, \dots, n_1$. Thus, the information provided by the inputs is *enconded* by the state variables of the first layer which in turn affect the dynamics of the nodes belonging to the second layer. In this way, the *hierarchical* structure of the network allows to *transfer* the information provided by the inputs $u_i(t)$ to some set of outputs, represented by the state variables of the k-th layer.

It is then clear that if the coupling functions between nodes are *properly designed*, then it is possible to *program* the network so that it can perform some desired task. Now, we show that the results derived so far can be used to this aim. The mathematical model considered here is:

$$\begin{aligned} \dot{x}_i &= g(t, x_i) + u_i & i &= 1, \dots, n_1 \\ \dot{x}_i &= g_i(t, x_i) + h_i(t, x_i, x_j) & i &= n_1 + 1, \dots, N, \quad j \in N_i \end{aligned} \tag{6.15}$$

where N_i denotes set of nodes unidirectionally coupled to node i.

A first step for the analysis/control of the network of interest is that of determining the possible invariant poli-synchronous subspaces. To make this point clear, assume that all the nodes belonging to the same layer share the same dynamics and that the coupling functions between the nodes of the i-th layer and the nodes of the $i+1$-th layer are identical. In this case, it is straightforward to check that the nodes within the same layer are input symmetric if they have the same number of inputs. Thus, two nodes, say i and j, belong to the same group, $\mathcal{G}_p$, if they both belong to the layer s and if they have the same number of inputs. This implies that it is possible to ensure the existence of some invariant subspace (corresponding to some desired task) by simply designing the number of inputs to each node.

As a second step, we have to ensure that the network dynamics is contracting towards the (desired) poli-synchronous subspace. Notice that the specific hierarchical topology of the network implies a lower triangular structure for system Jacobian (see Section 4.4 in Chapter 4). That is, differentiation of (6.15) yields a Jacobian matrix representing an hierarchy of the form (4.15). Therefore, the network dynamics is contracting if:

1. $g_i(t, x_i)$ is contracting;
2. $g_i(t, x_i) + h_i(t, x_i, x_j)$ is contracting (with respect to x_i);
3. $h_i(t, x_i, x_j)$ has bounded partial derivatives.

To show the effectiveness of the procedure outlined above, we now consider the network in Figure 6.4. The inputs are increasing step functions with final value equal to 1. The control task is that of ensuring, by means of the coupling functions, that $x_{12} = 1$ if and only if $u_i = 1$, for any $i = 1, \dots, 6$. In what follows, we assume that the intrinsic dynamics of each node is linear and stable (even if more complicated, e.g. nonlinear, dynamics can also be taken into account), i.e.

$$\dot{x}_i = -x_i$$

Since our task is that of providing an high output only when all the inputs are high, we found that a simple input function satisfying all of the requirements**1. - 3.** is

$$h_i(t, x_i, x_j) = \prod_{j \in N_i} x_j$$

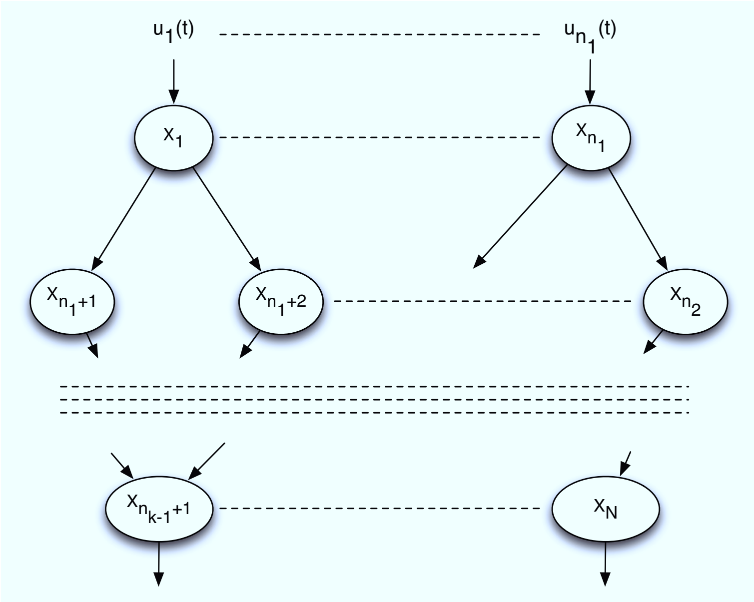

Figure 6.3: A schematic representation of a multilayer perceptron network

Now, the individual nodes are linear systems and thus the state variables of the first layer increase to 1 when the corresponding inputs are equal to 1. Moreover, for all the other layers, $x_i \to 1$ if and only if $x_j = 1$, for all $j \in N_i$. This in turn implies that $x_{12} = 1$ if and only if $u_i = 1$, $i = 1, \ldots, 6$, as wanted. We remark here that the above choice for the input function is similar to the input functions arising in biochemical protein-protein interaction networks, [3].

Figure 6.5 shows simulation results for the above network. Notice that x_{12} is activated only when the above condition is satisfied.

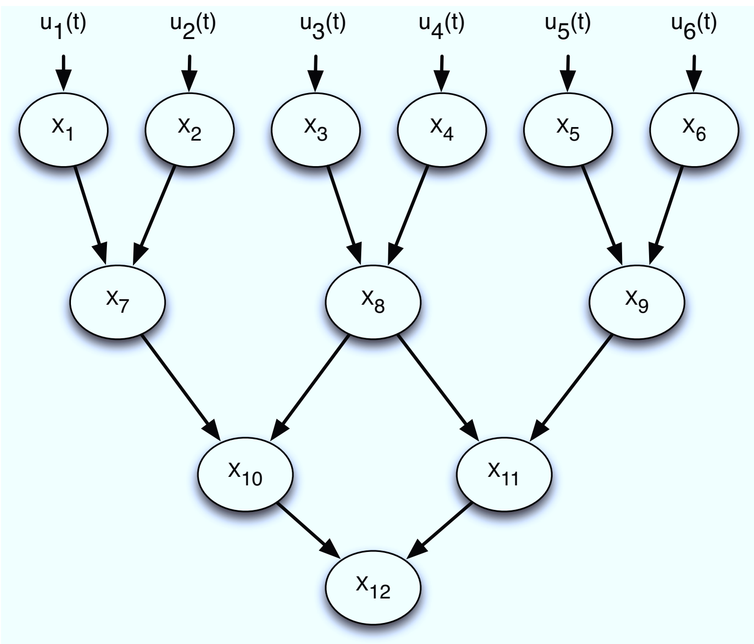

Figure 6.4: Multilayer perceptron network designed in Section 6.6.1

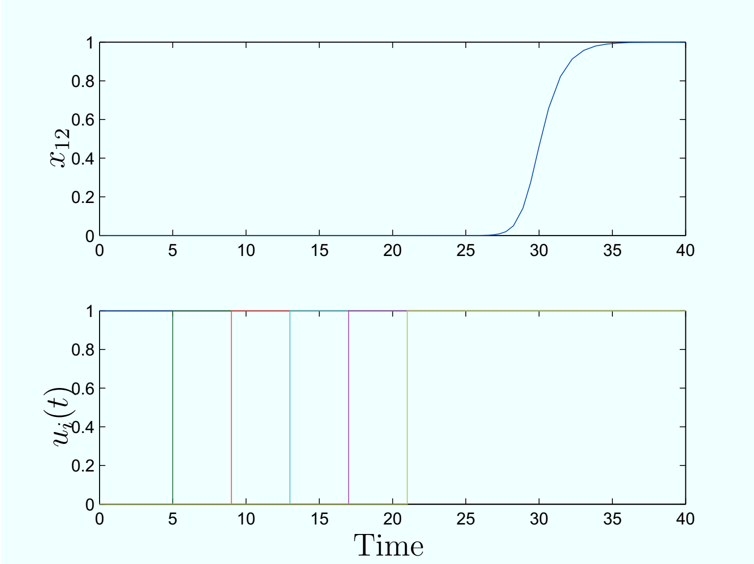

Figure 6.5: Behavior of x_{12} in the multilayer perceptron network in Figure 6.4 (top panel). The input functions, $u_i(t)$, are increasing step functions, activated at different times (bottom panel).

6.6.2 Synchrony patterns for distributed computing

We now turn our attention to the problem of imposing some poli-synchronous behavior for a network of interest. Specifically, we will impose different patterns of synchrony for a network composed of Hopfield models. The motivation that we have in mind here is that of *multi-purpose* networks, i.e. networks that can be *reused* to perform different tasks. For example, this may be the case of sensor networks ([120], [204]) where each poli-synchronous steady steady is associated to a specific set of inputs. A further notable example is the brain, where different poli-synchronous behaviors are believed to play a key role in e.g. learning processes (see e.g. [84]).

The dynamics that we consider here is similar to (6.9) and represents a network of HN models coupled by means of a nonlinear (not necessarily diffusive) coupling, with a time-varying topology. Namely:

$$\dot{x}_i = -x_i + \sum_{j\in N_i} a_{ij}(t)h_{ij}(t, x_i, x_j) + u_i \tag{6.16}$$

where $a_{ij}(t)$ is the i-th element of the time-varying interconnection matrix $A(t)$, h_{ij} represents the interconnection function from node j to node i and u_i in an exogenous input to the i-th node.

We start with the network in Figure 6.6. Nodes denoted by the same shape are forced by the same exogenous input. Specifically:

- $u_i(t) = 1 + \sin(0.7t)$ for the circle nodes;

- $u_i(t) = 5 + 3\sin(0.5t)$ for the square nodes;
- $u_i(t) = 0$ for node 13.

Analogously, identical arrows denote identical coupling functions:

- the coupling between circle nodes is diffusive, bidirectional and linear:

$$h_{ij}(t, x_i, x_j) = a_{ij}(t)(x_j - x_i)$$

- the coupling between square nodes is diffusive, unidirectional and linear;
- the coupling between circle and square nodes is diffusive, bidirectional and nonlinear:

$$h_{ij}(t, x_i, x_j) = a_{ij}(t)\left(\arctan(x_j) - \arctan(x_j)\right)$$

- the square nodes affect the dynamics of node 13 unidirectionally. Specifically, the dynamics of x_{13} is given by:

$$\dot{x}_{13} = -x_{13} + (1 - b(t)) \sum_{j=9}^{12} \frac{x_j}{1 + x_j} + b(t) \sum_{j=9}^{12} \frac{1}{1 + x_j} \tag{6.17}$$

  where $b(t)$ is a parameter that is smoothly increased between 0 and 1. Notice that $b(t)$ can be used to switch between two different coupling functions.

We remark here that the input to node 13 is a well known coupling mechanism in the literature on neural networks, and is termed as *excitatory-only* coupling, see e.g. [153].

It is straightforward to check that network dynamics are contracting (using e.g. the matrix measure induced by the 1-norm).

In Figure 6.7 the input symmetric nodes are pointed out by means of colors: the associated linear poli-synchronous subspace is

$$\mathcal{M}_1 = \{x_i = x_j, i, j = 1, \dots, 8\} \bigcap \{x_i = x_j, i, j = 9, \dots, 12\}.$$

Furthermore, it is easy to check that $\mathcal{M}_1$ is flow invariant. Now, since network dynamics are contracting, all of its trajectories converge towards a unique solution embedded into $\mathcal{M}_1$. That is, at steady state all the nodes having the same *color* in Figure 6.6 are synchronized. Figure 6.8 clearly confirms the theoretical analysis, showing the presence of the three synchronized clusters, when $b(t) = 0$.

The same synchronized behavior is kept even when $b(t)$ smoothly varies from 0 to 1. Indeed, network dynamics is still contracting and the input symmetry defining $\mathcal{M}_1$ is preserved. In Figure 6.9 the behavior of the network is shown when at $t = 50$, $b(t)$ is set to 1.

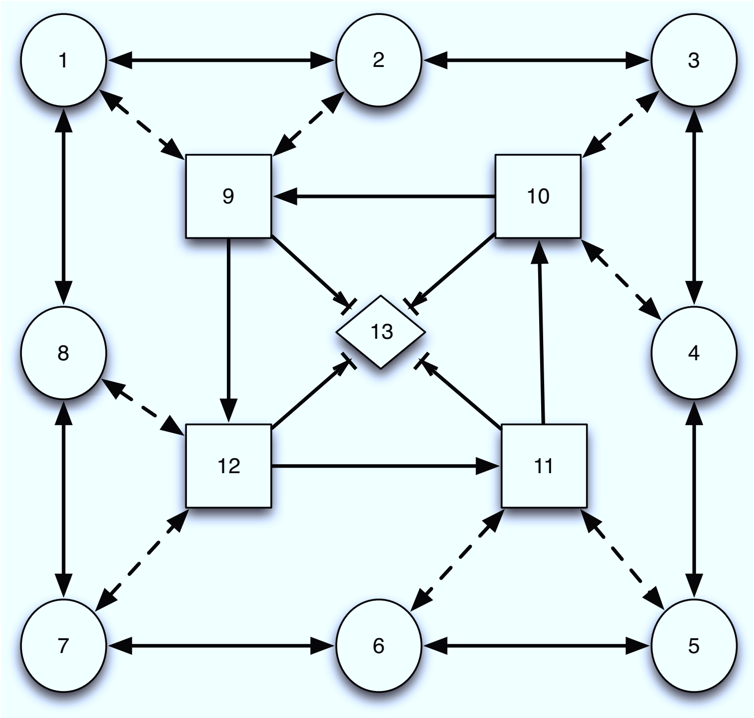

Figure 6.6: Network of Hopfield models used in Section 6.6.2

Notice that the variation of $b(t)$ from 0 to 1 causes an *inhibitory* effect of the level of x_{13}. This is due to the fact that, when $b(t) = 0$, x_{13} is forced by the sum of increasing sigmoidal functions. Vice-versa, when $b(t) = 1$, x_{13} is forced by the sum decreasing sigmoidal functions. We will analyze in more detail such functions in Chapter 9, where it will be pointed out that sigmoids play a key role in the modeling of biochemical systems.

Now, assume that we need to create a new synchronized cluster consisting of e.g. nodes 2, 4, 6, 8. A way to achieve this task is that of modifying the input symmetry defining $\mathcal{M}_1$ and to impose a new input symmetry defining the subspace

$$\mathcal{M}_2 = \{x_i = x_j, i, j = 1, 3, 5, 7\} \bigcap \{x_i = x_j, i, j = 2, 4, 6, 8, \} \bigcap \{x_i = x_j, i, j = 9, \ldots, 12\}$$

In turn, this can be done by smoothly varying the topology of the network, e.g. by diffusively coupling node 13 to the nodes 2, 4, 6, 8. The coupling function used to this aim, which preserves the contracting property, is:

$$h_i(t, x_i, x_j) = h(x_j) - h(x_i), \quad h(x) := \frac{1 - e^{-x}}{1 + e^{-x}}$$

In Figure 6.10 the new topology is shown, together with the class of input equivalence. Figure 6.11 shows the behavior of the network, pointing out that a new cluster of synchronized nodes arises.

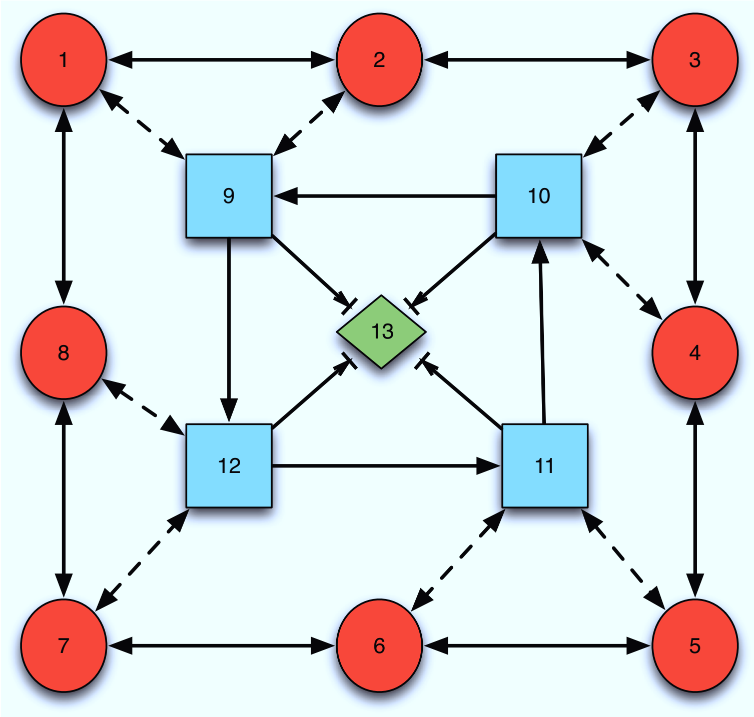

Figure 6.7: Network of Hopfield models used in Section 6.6.2: input equivalent nodes are pointed out by means of identical colors

6.7 Concluding remarks

We presented a set of sufficient conditions ensuring stability of networked systems, using contraction. The analysis is multi-scale, and is robust in the sense that a large degree of uncertainty can be tolerated in the components, as long as the contraction estimates are met for the network subsystems and their couplings. Indeed, only the knowledge of the upper bound of matrix measures and norms are required for applying our results. Computationally, one only needs to perform the maximizations involved in the computation of measures for individual (lower-dimensional) subsystems and couplings. In fact, applied recursively, one could even reduce the problem to a set $\log n$ computations for 2×2 matrices (for a system of dimension n). Among other features, contraction-based analysis has the advantage that no *a priori* knowledge is required of an attractor in order to perform stability analysis. Moreover, the approach can be also turned into *design* tool. For example, for set-point regulation or synchronization, once a system has been designed so that a particular state or subspace is flow-invariant, contraction ensures that all system trajectories converge to this desired point. The Chapter was then closed by presenting some results that can be used to impose, by means of decentralized communication protocols, arbitrary synchrony patterns to a network of interest. All the results of this Chapter were obtained by proving contraction of the network of interest. In the next Chapter we will address the problems of coordinating and (cluster) synchronizing a network

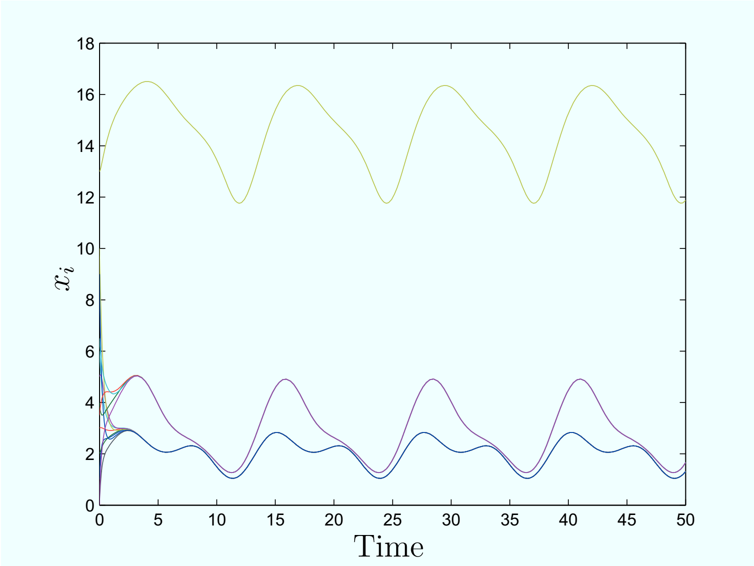

Figure 6.8: Network of Hopfield models (6.16) when $b(t)$ in (6.17) is equal to 0

of interest. It will be shown that solving those problems is equivalent in showing that the network dynamics is contracting towards a properly defined subspace.

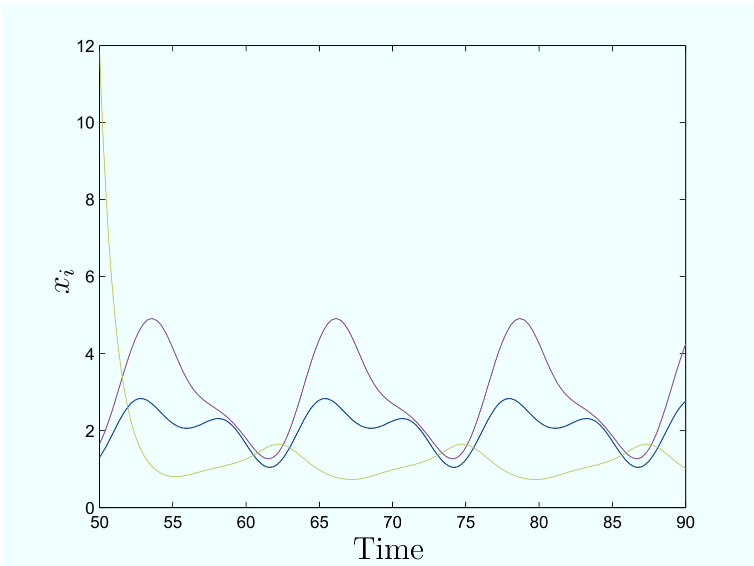

Figure 6.9: Network of Hopfield models (6.16) when $b(t)$ in (6.17) is equal to 0

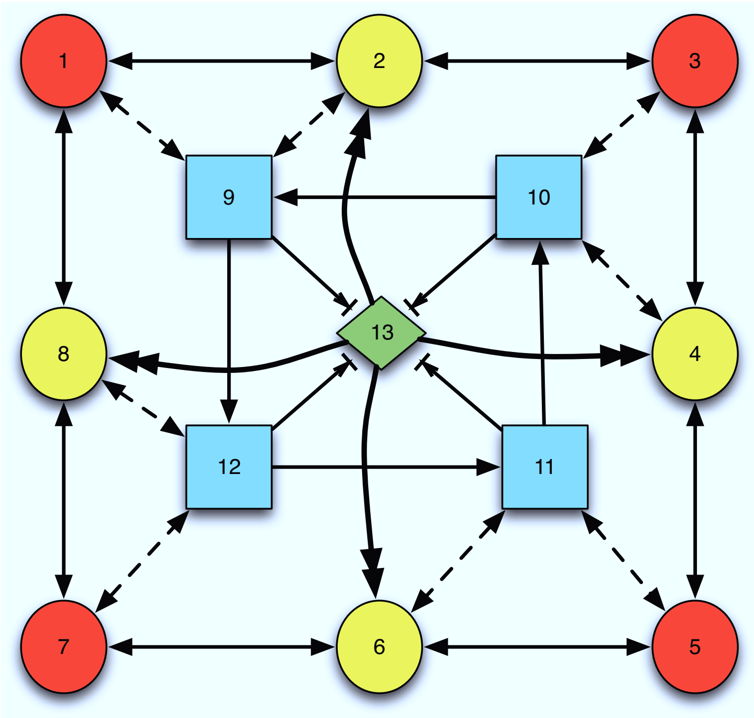

Figure 6.10: Network of Hopfield models used in Section 6.6.2: two new links are activated by node 13, creating a new class of input equivalent nodes (in yellow)

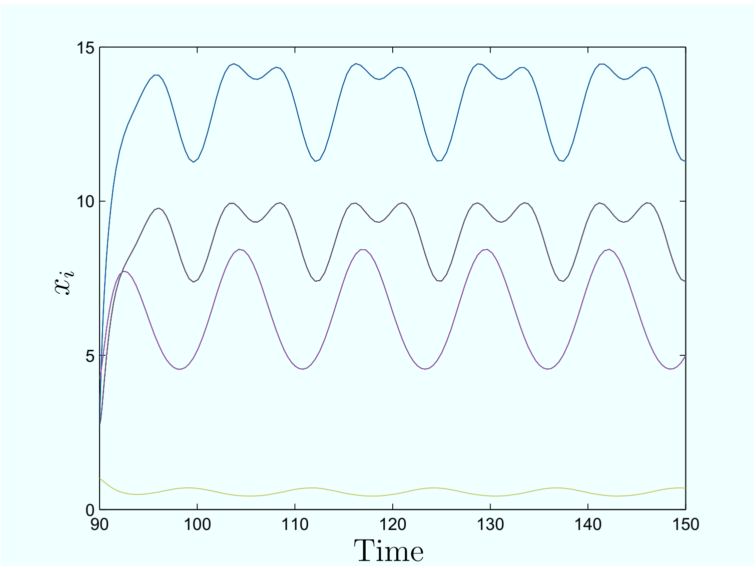

Figure 6.11: Network of Hopfield models

Chapter 7

Contraction-based synchronization and control of networks

In this Chapter we apply contraction analysis to the problem of synchronizing a complex network. Specifically, after presenting a general result for convergence of all network trajectories towards some (poli-) synchronous subspace, we derive some useful results for coordinating diffusively networked systems. We start by presenting a result on the synchronization of networks of diffusively coupled linear time-varying systems. This is then used to solve a testbed problem in decentralized control theory, i.e. the rendezvous problem. Then, using the matrix measure induced by the vector-two norm we present a sufficient condition for synchronization of coupled nonlinear systems. After presenting sufficient conditions for the stability of the synchronized evolution, we establish some links between contracting, Lipschitz and QUAD vector fields to study analyze network synchronization and consensus. The analysis is then completed by presenting the relationships between contraction and the Master Stability Function approach. The results presented in this chapter have appeared in [155, 157, 41] (see also [42]).

7.1 Introduction

Two of the key problems which are currently subject of much ongoing research in the field of networks are the study of the emergent, coordinated, behavior and the design of distributed algorithms for the coordination of networks of dynamic agents (see e.g. [135], [144]).

In particular, much attention has been focussed on synchronization and consensus of all agents towards some common asymptotic evolution are two notable examples of coordinated emerging behavior, see e.g. [133, 25, 139, 143, 195, 103, 146, 210, 88, 116, 209, 31, 43]. It has been found that these phenomena can be used to explain the behavior of natural systems and engineered in applications, e.g.

for secure communications, image processing, flocking and swarming behavior in robots, synchronization in power grids [73, 80, 201].

A typical example of coordination, that has also been used as a testbed problem in the literature, is the so called *rendezvous problem*. Namely, the problem is that of designing a distributed control strategy driving all the agents towards a common point in space, where they all have zero velocities (see for example [49], [104] and references therein).

Different approaches have been proposed in the literature to solve those problems. The typical approach makes use of Lyapunov functions, as network analysis/-control can be reduced to a stability problem of some invariant set in network phase space.

In this Chapter, the above two problems are addressed by means of Contraction Theory which has been introduced in Chapter 4. Indeed, in both analysis and control of networks we are typically interested in finding conditions guaranteeing the evolution of all trajectories of the nodes of a network towards each other. For this reason, a viable approach to study agents cooperation is that of investigating the convergence properties of all solutions.

The aim of this Chapter is to derive novel stability criteria using contraction. These results will be then used to analyze the steady state behavior of a network of interest and to design coupling protocols ensuring the achievement of some desired *task*.

The main topics addressed in this Chapter can be summarized as follows:

1. A general result for the coordination of a network is presented where no assumptions are made on nodes dynamics and topology. Then, such a result is specialized to the case where both linear and nonlinear identical nodes are diffusively coupled and a sufficient condition is obtained for synchronization involving: i) network topology; ii) nodes dynamics; iii) coupling strength.

2. We then show how to use our results in order to design decentralized control strategies guaranteeing some desired task for the network. As a representative example, we show how to design a decentralized control strategy to solve the rendezvous problem for a network of mobile agents. We wish to emphasize that the *design procedure* is general and can be effectively extended to solve other problems such as flocking and synchronization in complex networks of dynamical systems.

3. Typically, when studying synchronization and consensus by means of Lyapunov techniques, some assumptions are made on the dynamics of each node in the network. For instance, to prove asymptotic synchronization, the nodes' vector fields are supposed to be Lipschitz or to satisfy some other nonlinear inequality, upper bounding the rate of change of the vector field in phase space.

For example, the so-called QUAD condition (see Section 2.7 for further details) is often assumed to be satisfied as a starting point to derive conditions for synchronization of the network of interest. Using the matrix measure induced by the Euclidean norm, we use the links between the above hypotheses (see Section2.7) to study synchronization, consensus and pinning control of complex networks.

4. Finally, we obtain a link between contraction theory and the Master Stability Function, an approach used for the local analysis of synchronization mainly used within the Physics community, see e.g. [15]. Such a result represents an improvement to the results presented in [155].

7.2 Network control

In this Section we provide a sufficient condition for the convergence of the networked systems of the form (3.4) that is reported here for the sake of clarity

$$\dot{x}_i = \phi_i(t, X) := f_i(t, x_i) + \tilde{h}_i(t, X)$$

The main result of this Section are based on the use of Theorem 4.6.1 (see Chapter 4). Later, we will also show how to specify such a result to the case of undirected diffusively coupled systems.

In this Section, we present a sufficient condition for network (3.4) ensuring that all the nodes sharing the same dynamics converge towards the same steady state behavior. Recall that in Chapter 6 we showed that the invariant poli-synchronous subspaces of a network are determined by its symmetries and that the steady state behavior can be determined using contraction. Now, we provide a sufficient condition for all the trajectories of (3.4) to contract towards a poli-synchronous subspace.

Let $\mathcal{G}_i$, $i = 1, \ldots, k \leq N$ be the groups of agents sharing the same dynamics. We then say that the network achieves cluster (or concurrent) synchronization if all of its trajectories globally exponentially converge towards the poli-synchronous subspace

$$\mathcal{M}_p := \{x_i = x_j, \forall i, j : \phi_i(x, t) = \phi_j(x, t)\}$$

That is, all the nodes sharing the same dynamics are synchronized. Sometimes, we will also say that, in this case, network nodes are coordinated.

We will now present a condition ensuring that all network trajectories globally exponentially converge towards $\mathcal{M}_p$. The setup that we have in mind here is that of coordination of networks, where different agents process different information. This is the case e.g. of distributed algorithms [23]. A further notable example is the brain, which is composed by neurons that sense and process different kind of informations [84].

7.2.1 Convergence towards a poli-synchronous subspace

Let X be stack of all the x_i's in (3.4), i.e. $X := [x_1^T, \ldots, x_N^T]^T$ and:

$$\begin{aligned} F(t,x) &:= \left[f_1(t,x_1)^T, \ldots, f_N(t,x_N)^T\right]^T \\ \tilde{H}(t,X) &:= \left[\tilde{h}_1(t,X)^T, \ldots, \tilde{h}_N(t,X)^T\right]^T \end{aligned} \tag{7.1}$$

Our first result can be stated as follows.

Theorem 7.2.1. *Assume that for network (3.4) the subspace $\mathcal{M}_p$ exists. Let V be the orthonormal matrix spanning $\mathcal{M}_p^{\perp}$. Network coordination is attained if there exist some matrix measure such that*

$$\mu\left(V\frac{\partial F}{\partial X}V^T\right) < -\mu\left(V\frac{\partial \tilde{H}}{\partial X}V^T\right)$$

Proof. Indeed, from Theorem 4.6.1 we have that all networks trajectories converge towards the poli-synchronous subspace, $\mathcal{M}_p$, if:

$$\mu\left(V\left(\frac{\partial F}{\partial X} + \frac{\partial \tilde{H}}{\partial X}\right)V^T\right) < 0$$

i.e. is uniformly negative definite. Now, by the subadditivity property of matrix measure we have that the above condition is satisfied if:

$$\mu\left(V\frac{\partial F}{\partial X}V^T\right) + \mu\left(V\frac{\partial \tilde{H}}{\partial X}V^T\right)$$

is uniformly negative definite. This proves the result. □

The above result shows that in order for a decentralized control strategy to solve a coordination task (i.e. convergence towards $\mathcal{M}_p$) two conditions have to be satisfied:

- the subspace $\mathcal{M}_p$ exists;
- the network is contracting towards such a subspace.

We remark here that the former requirement can be ensured by properly designing the network topology and the coupling functions $\tilde{h}_i$'s, i.e. by requiring that nodes sharing the same dynamics are all input symmetric (see Chapter 6 and [142],[71] for further details).

7.2.2 Networks of diffusively coupled linear systems

We now turn our attention to the problem of coordinating an undirected network of diffusively coupled identical linear systems.

We consider undirected networks of $N > 1$, n-dimensional smooth continuous time dynamical systems of the form:

$$\dot{x}_i = A(t)x_i + \Gamma \sum_{j \in N_i} [x_j - x_i] \tag{7.2}$$

where the intrinsic dynamics at the nodes is linear, N_i denotes the set of the neighbors of the i-th network node. In what follows, the cardinality of N_i, i.e. the degree of the i-th network node, is denoted with d_i. In (7.2), Γ is some coupling matrix. In what follows, the eigenvalues of network Laplacian are denoted with $\lambda_i(L)$. The algebraic connectivity is denoted as $\lambda_2(L)$, [55].

Let $s(t)$ be a generic solution of an isolated node of (7.2), i.e. $\dot{s}(t) = A(t)s(t)$. We look for a sufficient condition ensuring that

$$\lim_{t \to +\infty} |x_i(t) - s(t)| = 0, \quad \forall i = 1, \dots, N$$

In this case, we will say that network coordination is fulfilled for network (7.2). That is, all network trajectories converge towards the synchronization manifold

$$\mathcal{S} := \{x \in R^{nN} : x_1 = ... = x_N\} \tag{7.3}$$

Theorem 7.2.2. *Network coordination is fulfilled for network (7.2) if there exist a matrix measures, μ, such that:*

$$\mu\left(A(t) - \lambda_2(L)\Gamma\right) \leq -c, \quad c > 0 \tag{7.4}$$

Before starting with the proof of the Theorem, we report here two useful results (see. e.g. [17], chapter 20, [22], chapter 5 and [82], Theorem 2.3.1).

Lemma 7.2.1. *Let $\otimes$ denote the Kronecker product. The following properties hold:*

- $(A \otimes B)(C \otimes D) = (AC) \otimes (BD)$*;*
- *if A and B are invertible, then $(A \otimes B)^{-1} = A^{-1} \otimes B^{-1}$;*

Lemma 7.2.2. *For any $n \times n$ real symmetric matrix, A, there exist an orthogonal $n \times n$ matrix, Q, such that*

$$Q^T A Q = U \tag{7.5}$$

where U is an $n \times n$ diagonal matrix.

Proof of Theorem 7.2.2

Define:

$$X := \left[x_1^T, \ldots, x_N^T\right]^T, \quad S := 1_N \otimes s \quad E := X - S$$

where 1_N denotes the N-dimensional vector consisting of all ones. The network dynamics can then be written as:

$$\dot{X} = (I_N \otimes A(t))X - (L \otimes \Gamma)X$$

Thus, we have:

$$\dot{E} = (I_N \otimes A(t))E - (L \otimes \Gamma)X$$

Furthermore, notice that

$$\begin{aligned}
&(L \otimes \Gamma)X = \\
&(L \otimes \Gamma)(E + S) = \\
&(L \otimes \Gamma)E + (L \otimes \Gamma)S = \\
&(L \otimes \Gamma)E + (L \otimes \Gamma)(1_N \otimes s) = \\
&(L \otimes \Gamma)E
\end{aligned}$$

where the last equality follows from Lemma 7.2.1 and from the fact that $L \cdot 1_N = 0$ (see e.g. [66]). Thus:

$$\dot{E} = (I_N \otimes A(t))E - (L \otimes \Gamma)E \tag{7.6}$$

Since L is symmetric, by means of Lemma 7.2.2 we have that there exist an $N \times N$ orthonormal matrix Q such that:

$$\Lambda = Q^T L Q$$

where Λ is the $N \times N$ diagonal matrix, having on its main diagonal the eigenvalues of L, $\lambda_i(L)$.

Define the following coordinate transformation:

$$Z = (Q \otimes I_n)^{-1} E$$

In the new coordinates (7.6) becomes

$$\dot{Z} = (Q \otimes I_n)^{-1} \left[(I_N \otimes A(t)) - (L \otimes \Gamma)\right] (Q \otimes I_n) Z$$

Then, using Lemma 7.2.1, we have:

$$\begin{aligned}
&(Q \otimes I_n)^{-1} (I_N \otimes A(t)) (Q \otimes I_n) = \\
&(Q^{-1} \otimes I_n) (I_N \otimes A(t)) (Q \otimes I_n) = \\
&(Q^{-1} \otimes A(t)) (Q \otimes I_n) = \\
&(I_N \otimes A(t))
\end{aligned}$$

Analogously:

$$\begin{aligned}
&(Q \otimes I_n)^{-1} (L \otimes \Gamma) (Q \otimes I_n) = \\
&(Q^{-1} \otimes I_n) (L \otimes \Gamma) (Q \otimes I_n) = \\
&(Q^{-1} L \otimes \Gamma) (Q \otimes I_n) = \\
&Q^{-1} L Q \otimes \Gamma = \\
&\Lambda \otimes \Gamma
\end{aligned}$$

That is, network dynamics can be written as:

$$\dot{Z} = [I_N \otimes A(t) - \Lambda \otimes \Gamma] Z \tag{7.7}$$

It is straightforward to check that the above dynamics consists of N uncoupled n-dimensional dynamics, of the form:

$$\dot{z}_i = [A(t) - \lambda_i(L)\Gamma] z_i, \quad i = 1, \ldots, N, \quad z_i \in \mathbb{R}^n$$

Now, recall that (see e.g. [66]) the eigenvector associated to $\lambda_1(L) = 0$, is 1_N. Therefore, the dynamics along $\mathcal{S}$ is

$$\dot{z}_1 = [A(t)] z_1$$

i.e. it is a solution of the uncoupled nodes' dynamics, $s(t)$. On the other hand, the dynamics transversal to the invariant subspace are:

$$\dot{z}_i = [A(t) - \lambda_i(L)\Gamma] z_i, \quad i = 2, \ldots, N$$

Now, notice that all network trajectories globally exponentially converge towards $\mathcal{S}$ if all of the $N-1$ above dynamics are contracting. Indeed, contraction of such dynamics implies that

$$|z_i| = |x_i - s(t)| \to 0, \quad t \to +\infty, \quad \forall i = 2, \ldots, N$$

Now, it is straightforward to check that such a condition is automatically fulfilled if

$$\dot{z}_2 = [A(t) - \lambda_2(L)\Gamma] z_2$$

is contracting. This is true by hypothesis and the result is then proved.

We remark here two implications of Theorem 7.2.2:

1. assume that network nodes are not contracting. Then, condition (7.4) implies that the network can be synchronized if the topology is connected (i.e. $\lambda_2(L) \neq 0$) and Γ is a matrix having all of its elements positive;

2. if, on the other hand, the network nodes are contracting, then all network trajectories converge towards each other even if the topology is not connected, i.e. $\lambda_2(L) = 0$;

3. the above result can be straightforwardly extended to the case of directed balanced networks.

One application of Theorem 7.2.2 is the design of decentralized control strategies solving the n-th order consensus problem []. In Section 7.3 we will show one of such applications, where a decentralized strategy is designed in order to solve the rendezvous problem in a network of agents moving in a plane.

7.2.3 Networks of diffusively coupled nonlinear nodes

We now specialize the general result of Section 7.2.1 by using the matrix measure induced by the vector-2 norm. Using such a measure, we obtain a criterion for network synchronization of nonlinear diffusively coupled systems.

Again, we study undirected graphs in which each node is a nonlinear n-dimensional possibly non-autonomous system. Specifically we consider

$$\dot{X} = F\left(t, X\right) - \alpha \left(L \otimes I_n\right) X \tag{7.8}$$

where $F(t,X)$ is defined in (7.1) and α denotes the coupling strength. The network is said to be synchronized if all oscillators converge towards the same synchronous state, i.e. if all network trajectories converge towards the synchronization manifold, $\mathcal{S} := \{x_1 = \ldots = x_N\}$.

Theorem 7.2.3. *Network (7.8) synchronizes if:*

$$\max_{x,t} \lambda_{\max}\left(\frac{\partial f}{\partial x}\right) \leq \alpha \lambda_2(L)$$

Proof. Let V be the orthonormal matrix spanning $\mathcal{S}^{\perp}$ and let J be the Jacobian of (7.8), i.e.

$$J := \frac{\partial F}{\partial X} - \alpha \left(L \otimes I_n\right)$$

By means of Theorem 4.6.1 we have that all network trajectories converge towards

$\mathcal{S}$ if $\mu_2\left(VJV^T\right)$ is uniformly negative definite. That is,

$$\mu_2\left(V\frac{\partial F}{\partial X}V^T - V(\alpha(L\otimes I_n))V^T\right) \leq -c \quad c>0.$$

Now, using the subadditivity property of matrix measures [191]:

$$\begin{aligned}&\mu_2\left(V\tfrac{\partial F}{\partial X}V^T - V(\alpha(L\otimes I_n))V^T\right) \leq \\ &\mu_2\left(V\tfrac{\partial F}{\partial X}V^T\right) + \mu_2\left(-V(\alpha(L\otimes I_n))V^T\right)\end{aligned}$$

Notice that L is a symmetric matrix with $L\cdot 1_N = 0$. Thus, analogously to the proof of Theorem 7.2.2, we can choose V such that:

$$\mu_2\left(-V(\alpha(L\otimes I_n))V^T\right) = \alpha\mu_2\left(-\Lambda\right) := -\alpha\lambda_2(L)$$

Furthermore:

$$\mu_2\left(V\frac{\partial F}{\partial X}V^T\right) := \lambda_{\max}\left(V\left[\frac{\partial F}{\partial X}\right]_s V^T\right)$$

where $\left[\frac{\partial F}{\partial X}\right]_s$ denotes the symmetric part of $\frac{\partial F}{\partial X}$. To evaluate the above matrix measure, consider the quadratic form:

$$v^T V\frac{\partial F}{\partial X}V^T v = a^T\frac{\partial F}{\partial X}a$$

Notice that for any $a\neq 0$, we have:

$$\min_{x,t}\lambda_{\min}\left(\frac{\partial f}{\partial x}\right)a^Ta \leq a^T\frac{\partial F}{\partial X}a \leq \max_{x,t}\lambda_{\max}\left(\frac{\partial f}{\partial x}\right)a^Ta$$

where $\partial f/\partial x$ is the Jacobian of the intrinsic node's dynamics. On the other hand $a^Ta = v^TVV^Tv = v^Tv$. Thus:

$$\begin{aligned}&\mu_2\left(V\tfrac{\partial F}{\partial X}V^T - V(\alpha(L\otimes I_n))V^T\right) \leq \\ &\max_{x,t}\lambda_{\max}\left(\tfrac{\partial f}{\partial x}\right) - \alpha\lambda_2(L)\end{aligned}$$

Since the above quantity is uniformly negative definite by hypotheses, we have that all of network trajectories globally exponentially converge towards $\mathcal{S}$. This proves the result. □

7.3 Solving the rendezvous problem

As an application of the results presented in Section 7.2, we consider the problem of imposing a desired task to a set of $N>1$ mobile agents moving in the plane. In accordance with the existing literature [98], [182], we choose the agent dynamics given by

$$\begin{aligned} \dot{r}_i &= v_i \\ \dot{v}_i &= u \end{aligned} \tag{7.9}$$

where $r_i = (x_i, y_i)$ and $v_i = (v_{ix}, v_{iy})$ represent the position and velocity vectors of agent i in a fixed reference frame. The agents are controlled via an appropriate acceleration vector, $u = (u_{ix}, u_{iy})$.

We will consider the rendezvous problem, i.e. the problem of finding an appropriate (distributed) control strategy which guides all agents towards a common position, say $\bar{r}$, i.e. such that $\lim_{t\to\infty} r_i(t) = \bar{r}$, $\forall i = 1, \ldots, N$.

As we will see, the proposed communication protocol is composed by: (i) a local decentralized term based on the positions of the neighbors of each node; (ii) a local feedback function of each agent velocity.

Theorem 7.3.1. *Consider a connected network of mobile agents modeled by (7.9). Then, the following distributed strategy*

$$\begin{array}{l} u_{ix} = \sigma_1 \sum_{j\in N_i} (x_j - x_i) - (\sigma_1 + \sigma_{2i})\, v_{ix} \\ u_{iy} = \sigma_3 \sum_{j\in N_i} (y_j - y_i) - (\sigma_3 + \sigma_{4i})\, v_{iy} \end{array}, \tag{7.10}$$

solves the rendezvous problem if all the σ's are positive. Furthermore, the point in which all the agents meet is $(\bar{x}, \bar{y})$*:*

$$\begin{array}{l} \bar{x} = \frac{avg(x_i(0))}{\sigma_1} + \frac{1}{\sigma_1} avg\left(\frac{v_{ix}(0)}{\sigma_{2i}}\right) \\ \bar{y} = \frac{avg(y_i(0))}{\sigma_3} + \frac{1}{\sigma_3} avg\left(\frac{v_{ix}(0)}{\sigma_{4i}}\right) \end{array} \tag{7.11}$$

where $avg\,(\cdot)$ *is the average operator.*

Proof. We will prove the result for the x-component of (7.9), as the same proof holds for the y-component.

Consider the following coordinate transformation:

$$x_i^t = x_i + \varepsilon v_{ix} \tag{7.12}$$

where ε is a scalar that will be chosen later. Using (7.12), the dynamics of (7.9) controlled by (7.10) becomes:

$$\begin{array}{l} \dot{x}_i^t = (1 + \varepsilon N_i - \sigma_1 - \sigma_{2i})\, v_{ix} + \varepsilon\sigma_1 \sum_{j\in N_i} (x_j - x_i^t) \\ \dot{v}_{ix} = (\varepsilon N_i - \sigma_1 - \sigma_{2i}) + \sigma_1 \sum_{j\in N_i} (x_j - x_i^t) \end{array} \tag{7.13}$$

Now, let $z_i := [x_i^t, v_{ix}]^T$. The dynamics (7.13) can then be written in compact form as

$$\dot{z}_i = \begin{bmatrix} 0 & 1+\varepsilon d_i - \sigma_1 - \sigma_{2i} \\ 0 & \varepsilon d_i - \sigma_1 - \sigma_{2i} \end{bmatrix} z_i + \begin{bmatrix} \varepsilon\sigma_1 & 0 \\ \sigma_1 & 0 \end{bmatrix} \sum_{j\in N_i} (x_j - x_i) \tag{7.14}$$

(recall that d_i is the cardinality of N_i.) Since ε is an arbitrary scalar, we have that for any σ_1, σ_{2i},

$$\exists\varepsilon : \sigma_1 + \sigma_{2,i} = \varepsilon d_i + 1$$

Thus, we have that there exist some ε such that (7.14) becomes

$$\dot{z}_i = \begin{bmatrix} 0 & 0 \\ 0 & -1 \end{bmatrix} z_i + \begin{bmatrix} \varepsilon\sigma_1 & 0 \\ \sigma_1 & 0 \end{bmatrix} \sum_{j\in N_i} (x_j - x_i) \tag{7.15}$$

Notice that the rendezvous problem is solved if all network trajectories converge towards the subspace

$$\mathcal{R} := \{r_i = r_j, \quad v_i = v_j = 0, \quad \forall i,j = 1,\dots,N\}$$

Now, the above subspace is flow invariant for network dynamics and (7.15) is in the same form as (7.2) with:

$$A := \begin{bmatrix} 0 & 0 \\ 0 & -1 \end{bmatrix}, \quad \Gamma := \begin{bmatrix} \varepsilon\sigma_1 & 0 \\ \sigma_1 & 0 \end{bmatrix}$$

This implies that Theorem 7.2.2 can be applied and, hence, the rendezvous (or, equivalently, contraction towards $\mathcal{R}$) is attained if there exists a negative matrix measure for the matrix $A - \lambda_2(L)\Gamma$. It Now, it is straightforward to check that the matrix

$$A - \lambda_2(L) = \begin{bmatrix} -\varepsilon\lambda_2(L)\sigma_1 & 0 \\ -\lambda_2(L)\sigma_1 & -1 \end{bmatrix}$$

is contracting. Specifically, to this aim the matrix measure $\mu_{\infty,\Theta}$ can be used, with

$$\Theta := \begin{bmatrix} \theta_1 & 0 \\ 0 & \theta_2 \end{bmatrix}$$

and $\theta_2/\theta_1 < 1/(\lambda_2(L)\sigma_1)$. The second part of the statement, i.e. convergence of network trajectories to the fixed point (7.11), is straightforward. Indeed, it suffices to notice that such a point belongs to $\mathcal{R}$ and that the quantities

$$\bar{x} = \frac{avg(x_i(t))}{\sigma_1} + \frac{1}{\sigma_1} avg\left(\frac{v_{ix}(t)}{\sigma_{2i}}\right)$$
$$\bar{y} = \frac{avg(y_i(t))}{\sigma_3} + \frac{1}{\sigma_3} avg\left(\frac{v_{ix}(t)}{\sigma_{4i}}\right)$$

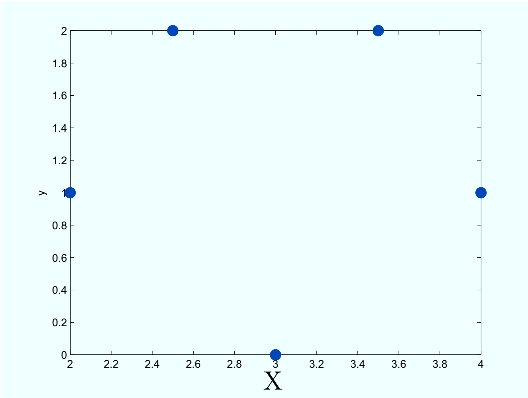

Figure 7.1: Initial agents' positions in the space

are invariant for the network dynamics. □

Numerical example

We now validate the strategy developed above, taking as a representative example a network of 5 agents modeled by (7.9) and controlled by the decentralized control strategy (7.10). The initial positions of the agents are arranged along a pentagon (see Figure 7.1). The initial velocities were picked randomly from a normal distribution with mean 0 and standard deviation 1. The temporal evolution of nodes' positions and velocities, confirming the theoretical analysis, are shown in Figure 7.2.

7.4 Linking QUAD, Lipschitz and contracting vector fields

In this Section the study of networked systems is continued by using the links between QUAD, Lipschitz and contracting vector fields presented in Chapter 2. Recall that in Section 2.7 we linked the contracting properties of a dynamical system to the Lipschitz and QUAD properties of its vector field, by using the Euclidean matrix measure, μ_2. We now use those links to study synchronization and consensus of a complex network modeled as:

$$\dot{x}_i = f\left(t, x_i\right) + \sigma \sum_{j \in \mathcal{N}_i} (x_j - x_i), \quad i = 1, \ldots, N \tag{7.16}$$

where σ is the unique coupling strength, N_i is the set of neighbors of the node i.

Before illustrating our result, we need to state the following Lemma.

Lemma 7.4.1. *[82] Denote by L the Laplacian matrix of an undirected network. The following properties hold*

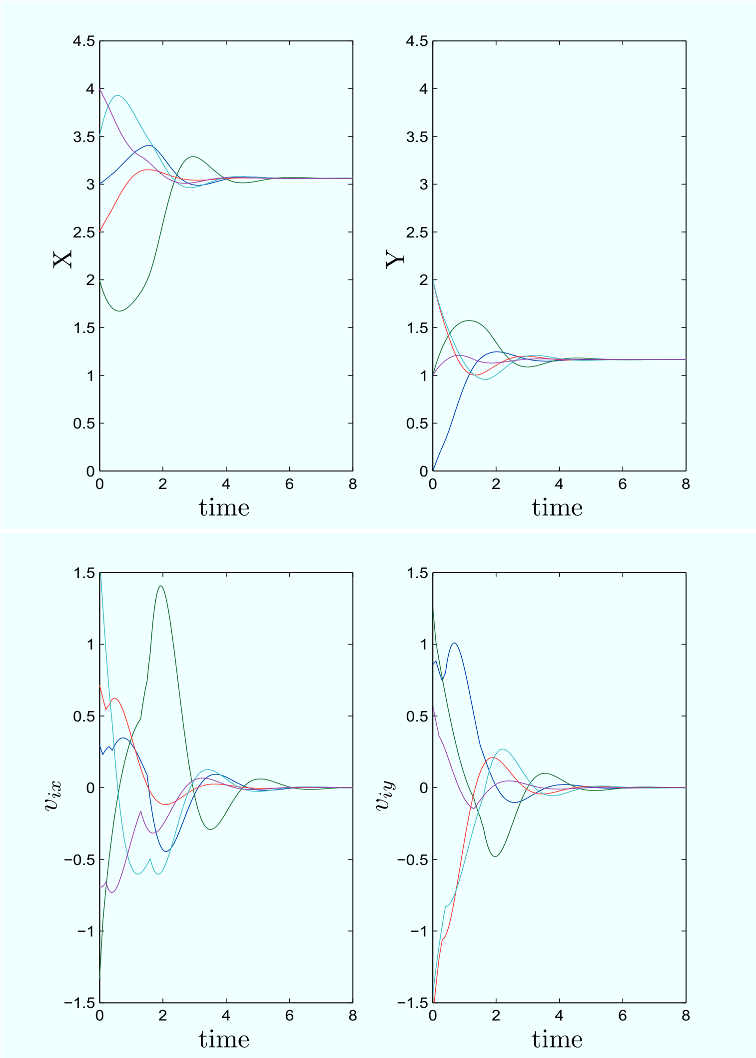

Figure 7.2: Evolutions of the positions (top) and velocities (bottom) of the agents controlled by (7.10)

1. *L has a simple zero eigenvalue and all the other eigenvalues are positive if and only if the network is connected;*

2. *the smallest nonzero eigenvalue $\lambda_2(L)$ satisfies*

$$\lambda_2(L) = \min_{v^T 1_N = 0, v \neq 0} \frac{v^T L v}{v^T v}$$

We are now ready to state the following result.

Theorem 7.4.1. *Given a network of N nodes described by (7.16), if:*

H1 *the vector field of the uncoupled nodes is Lipschitz (with Lipschitz constant $\alpha > 0$);*

H2 $\sigma > \max\left\{\alpha, \frac{\alpha}{\lambda_2(L)}\right\}$*;*

H3 *the network is connected;*

then the network synchronizes.

Proof. Note that (7.16) can be rewritten as

$$\dot{x}_i = f\left(t, x_i\right) + \sigma \sum_{j \in \mathcal{N}_i} x_j - \sigma d_i x_i, \quad i = 1, \ldots, N \tag{7.17}$$

where d_i represents the degree of node i. By hypothesis $f\left(t,x\right)$ is Lipschitz, and so, from Theorem 2.7.3, $f\left(t,x\right)$ is also QUAD(Δ, ω), with $\Delta \geq \left(\alpha + \omega\right) I_n$. Let us define a new function:

$$g\left(t,x\right) = f\left(t,x\right) - \sigma x.$$

Clearly, we have that g is QUAD(Δ, ω), with $(\Delta - \omega I_n) \geq (\alpha - \sigma) I_n$. Now, since by hypotheses $\sigma > \max\left\{\alpha, \frac{\alpha}{\lambda_2(L)}\right\}$ and the matrix Δ is an arbitrary diagonal matrix, we can choose Δ so that $\left(\omega + \alpha - \sigma\right) I_n \leq \Delta < \omega I_n$. Thus, by means of Theorem 2.7.2, we can then conclude that the function $g\left(t,x\right)$ is contracting, i.e. there exists some positive scalar β such that

$$\lambda_{\max}\left\{\frac{1}{2}\left(J + J^T\right)\right\} \leq -\beta$$

with

$$J := \frac{\partial g}{\partial x} = \left(\frac{\partial f}{\partial x} - \alpha I\right) \tag{7.18}$$

Now, we show that the above condition ensures network synchronization.

To this aim, define the following quantity

$$x^* := \frac{1}{N}\sum_{j=1}^{N} x_j(t).$$

Let $e_i := x_i - x^*$ and consider the following candidate Lyapunov function

$$V = \frac{1}{2}\sum_{i=1}^{N} e_i^T e_i \tag{7.19}$$

The time derivative $\dot{V}$ of the above function along the network dynamics is:

$$\sum_{i=1}^{N} e_i^T \left[f\left(t, x_i\right) - \sigma \sum_{j=1}^{N} L_{ij} x_j - \frac{1}{N}\sum_{j=1}^{N} f\left(t, x_j\right)\right] \tag{7.20}$$

Now, adding and subtracting $f(t, x^*)$, and noticing that (since $\sum_{i=1}^{N} e_i(t) = 0$,)

$$\sum_{i=1}^{N} e_i(t) \left[f(t, x^*) - \frac{1}{N} \sum_{j=1}^{N} f(t, x_j) \right] = 0$$

we get:

$$\dot{V} = \sum_{i=1}^{N} e_i^T \left[f(t, x_i) - f(t, x^*) - \sigma \sum_{j=1}^{N} L_{ij} x_j \right] \tag{7.21}$$

Recall, now, that the function $g(t, x)$ defined above is $QUAD$, and that we can choose Δ in the set $[(\omega + \alpha - \sigma) I_n, \omega I_n]$. This implies that, for any two vectors $a, b \in \mathbb{R}^n$, we have:

$$(a - b)^T [f(t, a) - f(t, b)] \leq (a - b)^T (\Delta - \omega I_n + \sigma I_n)(a - b)$$

Now, choosing $\Delta = (\omega + \alpha - \sigma) I_n$, the above inequality becomes:

$$(a - b)^T [f(t, a) - f(t, b)] \leq \alpha (a - b)^T (a - b) \tag{7.22}$$

Using (7.22) with $a = x_i$, $b = x^*$, from (7.21) we obtain

$$\dot{V} \leq \alpha \sum_{i=1}^{N} e_i^T e_i - \sigma e_i^T \sum_{j=1}^{N} L_{ij} e_j$$

That is,

$$\dot{V} \leq \alpha e^T e - \sigma e^T (L \otimes I_n) e$$

and thus

$$\dot{V} \leq \alpha e^T e - \sigma \min_{e \neq 0} \left[e^T (L \otimes I_n) e \right] \tag{7.23}$$

where e denotes the stack of e_i.

Notice now that $e^T 1_{Nn} = 0$. By means of Lemma 7.4.1 we have:

$$\min_{e \neq 0} \left[e^T (L \otimes I_n) e \right] = \lambda_2(L) e^T e$$

Thus,

$$\dot{V} \leq (\alpha - \sigma \lambda_2(L)) e^T e$$

which is negative definite since, by hypotheses, $\sigma > \max\{\alpha, \alpha/\lambda_2(L)\}$. □

Theorem 7.4.1 provides a sufficient condition for the global synchronization of a complex network. We wish to emphasize here that one of the key steps in our proof was that of using Theorem 2.7.2 and Theorem 2.7.3 in order to link hypothesis $(H1)$ of Theorem 7.4.1 to contraction of the function $g(t, x) = f(t, x) - \alpha x$. Notice that this key step allowed us to prove synchronization without requiring boundedness of nodes' dynamics, as instead required in some papers addressing the synchronization problem (see e.g. [18]). Indeed, as we *translate* the Lipschitz condition onto a contracting condition, knowledge of the specific attractor where all nodes converge is not required any longer.

Note that Theorem 7.4.1 can be used as an effective tool to analyze synchronization properties of a network such as its synchronizability and can be easily extended to the case of non-unique coupling gains, say α_{ij}, between pairs of mutually coupled nodes.

7.4.1 Adaptive synchronization

So far, we assumed a fixed and unique coupling strength between nodes. We now consider the case in which such coupling strength evolves in time following the adaptation law:

$$\begin{aligned} \dot{x}_i &= f\left(t, x_i\right) + \sum_{j \in \mathcal{N}_i} \sigma_{ij}\left(t\right)\left(x_j - x_i\right) && (7.24) \\ \dot{\sigma}_{ij} &= \gamma \|x_j - x_i\| && (7.25) \end{aligned}$$

with $\gamma > 0$, $\sigma_{ij}\left(0\right) \geq 0$. Such a strategy was introduced and analyzed in [46], [45] and [44]. Specifically, it was shown that global asymptotic stability is dependent on the characteristics of the vector field f. In fact, in [44] it was shown that a sufficient condition for stability was for the vector field f to be QUAD(Δ, ω), with $(\Delta - \omega I_n) \leq 0$.

In general, proving that a system is QUAD(Δ, ω) is not straightforward. We now show that the mathematical tools developed in the previous Section can be useful to immediately determine if a particular system can synchronize under the adaptive strategy (7.24), without verifying the QUAD property.

As a representative example we use the driven damped Van der Pol oscillator, for which proving the QUAD property is non-trivial. Nevertheless, we know from [194] that it is semi-contracting and so, from Corollary 2.7.2 we can say that it is also QUAD(Δ, ω), with $\Delta = \omega I_n$. Thus, using the theorem in [44], which requires the node vector field to be QUAD to guarantee network synchronization and convergence of the gain to finite values, we can immediately conclude that applying the adaptive coupling law to a network of driven damped Van der Pol oscillators yields a globally asymptotically stable synchronous regime.

We validate numerically the above result, by considering a scale-free network (for further details on this topology see for example [133, 25]) of 1000 identical driven damped Van der Pol oscillators coupled through an adaptive edge-based strategy. The initial condition were chosen randomly from a uniform distribution between 0

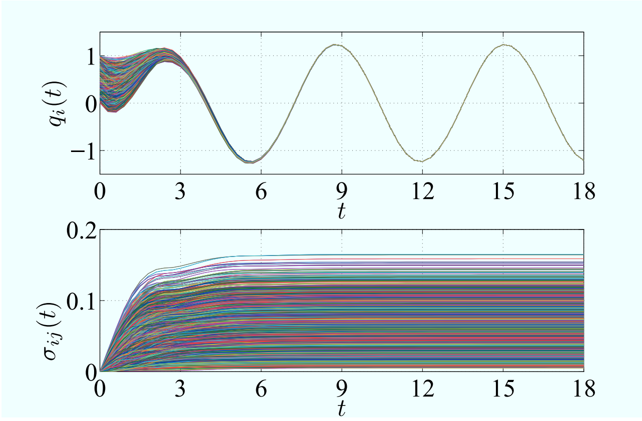

Figure 7.3: Evolution of 1000 Van der Pol oscillators connected through a scale-free network with adaptive coupling gains: q state variable (top), α (bottom)

and 1, while the average degree of the network was set to 5. According to [194] and denoting the state of the i-th node by $x_i = [p_i, q_i]^T$, the governing equations of the network are:

$$\dot{p}_i = a_3 q_i - \frac{a_1}{3} p_i^3 - a_2 p_i \tag{7.26}$$

$$\dot{q}_i = -a_3 p_i + \frac{u(t)}{a_3} + \frac{1}{a_3} \sum_{j \in \mathcal{N}_i} \sigma_{ij}(q_j - q_i) \tag{7.27}$$

$$\dot{\sigma}_{ij} = \gamma \|q_i - q_j\| \tag{7.28}$$

where a_1, a_2 and a_3 are strictly positive constants and $u(t)$ is a periodic forcing. In our simulation we choose $a_1 = a_2 = a_3 = 1$, $\gamma = 0.1$ and $u(t) = \sin(t)$. Figure 7.3 clearly shows that all oscillators converge as expected onto a common evolution, while the adaptive gains settle to constant values.

7.4.2 Design of decentralized control strategies

Above, we used the results presented in Chapter 4 to analyze network synchronization. That is, once the nodes dynamics were given together with a communication strategy, we were able to predict synchronization if the node vector fields satisfied certain conditions.

In this Section, we show that the results presented in this paper can also be used as an effective tool for designing decentralized (nonlinear) protocols for synchronization.

In particular, we will focus on generic networks described by the equation

$$\dot{x}_i = f(t, x_i) + \sigma \sum_{j \in N_i} \left(\tilde{h}(x_j) - \tilde{h}(x_i) \right), i = 1, \ldots, N \tag{7.29}$$

where $\tilde{h} : \mathbb{R}^n \to \mathbb{R}^n$ is some smooth nonlinear function of the system states and σ is a positive scalar.

The following result can then be stated.

Theorem 7.4.2. *Consider a network, whose nodes dynamics are given by (7.29). If:*

- *the network is connected;*
- *h is such that $\frac{\partial \tilde{h}}{\partial x} > 0$;*
- *the function $f(t, x_i) - \sigma d_i h(x_i)$, with d_i being the degree of node i, is QUAD(Δ, ω), with $\Delta - \omega I_n \leq c I_n$ for some $c < 0$,*

then, the network synchronizes.

Proof. The proof follows trivially from Theorem 2.7.2. In particular, it suffices to note that, if a system is QUAD(Δ, ω), with $\Delta - \omega I_n \leq c I_n < 0$, then it is also contracting with rate $\beta \leq c$. Thus, using the same line of argument as in Theorem 7.4.1 (see also [159, 194, 157]), it is possible to show that, if the topology is connected and the coupling protocol is strictly increasing, that is,

$$\frac{\partial \tilde{h}}{\partial x} > 0$$

then the network nodes synchronize. The Theorem is then proved. □

Consensus of N integrators

A direct straightforward application of Theorem 7.4.2 is the average consensus problem, in which the nodes are assumed to be simple integrators. In particular, it is easy to show that the *classical* communication strategy (see e.g. [135, 102])

$$\dot{x}_i = \sigma \sum_{j \in \mathcal{N}_i} (x_j - x_i)$$

satisfies all the hypotheses of Theorem 7.4.2. Thus, trajectories of all network nodes converge towards each other. Moreover, since the quantity

$$\tilde{x} := \frac{1}{N} \sum_{i=1}^{N} x_i(t)$$

is invariant for the network dynamics, then all trajectories will converge to it. That is, the average consensus problem is solved.

Notice that the same result can also be proven by means of Theorem 7.4.1. In fact, for the integrator dynamics at the nodes, the Lipschitz constant is equal to 0, and thus the nodes converge towards each other for any positive value of σ.

7.4.3 Pinning control

We now turn our attention to the study of pinning control schemes where we assume that a *master* node is attached only unidirectionally to the rest of the network (e.g. see [76, 101, 32, 145, 199, 200] for further details). The equations of motion of the controlled network then become:

$$\begin{aligned} &\dot{s} = f(s,t) \\ &\dot{x}_i = f(x_i,t) - \sigma \textstyle\sum_{j \in \mathcal{N}_i} (x_i - x_j) - \delta_i q (x_i - s) \end{aligned} \tag{7.30}$$

with

$$\delta_i = \begin{cases} 1, & i = 1, \ldots, N_{pin} \\ 0, & i = N_{pin+1}, \ldots, N \end{cases} \tag{7.31}$$

where N_{pin} is the number of pinned nodes, q is the constant control gain and s the desired synchronous solution to be achieved.

Theorem 7.4.3. *Given the controlled network (7.30), all nodes trajectories converge towards $s(t)$ if:*

- *the vector field of the uncoupled nodes is Lipschitz (with Lipschitz constant $\alpha > 0$);*
- $\sigma > \max \left\{ \alpha, \frac{\alpha}{\lambda_2(L)} \right\}$*;*
- *the function $g(x,t) = f(x,t) - \sigma x$ is QUAD(Δ, ω), with $\Delta - \omega I_n < 0$;*
- *the network is connected.*

Proof. Following the same arguments used earlier, it is easy to show that the network is made contracting by the choice of σ. Hence, all nodes converge exponentially towards each other, that is, $x_1 = \ldots = x_N$. On the synchronization manifold, trajectories then must converge towards the desired trajectory s as the pinning node is only coupled unidirectionally to the rest of the network. □

Note that, as observed in the existing literature on pinning control (see e.g. [171] and references therein), it suffices for just one node in the connected network to be directly controlled. Indeed, $s(t)$ acts as an exogenous forcing signal on the rest of the (contracting) network.

We wish to emphasize that similar results can be extended to the case of adaptive coupling gains, see [48] for further details.

7.5 Linking Contraction Theory and the Master Stability Function

In this Section we establish a link between contraction (using μ_2) and a well known approach, used within the Physics community, for analyzing local network synchronization, the Master Stability Function (MSF). We first present a brief review of the MSF approach and then present some results showing that if a (virtual) system associated to the network is contracting (see Chapter 2), then the MSF is negative, implying synchronization.

Throughout this Section, we will consider the network of N diffusively coupled nonlinear autonomous systems, i.e.

$$\dot{X} = F\left(X\right) - \alpha\left(L \otimes I\right)\tilde{H}\left(X\right) \tag{7.32}$$

with X, $F(X)$, $\tilde{H}(X)$ defined as usual. Recall that the network is said to be synchronized if all oscillators converge towards the same synchronous state, characterized by the stability properties of the synchronization manifold, defined as $\{x \in \mathbb{R}^{mN} : x_1 = ... = x_N\}$.

7.5.1 The Master Stability Function approach

Let $s\left(t\right)$ be a trajectory of $\dot{x} = f(x)$ with initial conditions $s(0) = x_{s0}$. In [2] the Lyapunov exponents for $s\left(t\right)$ are defined as follows.

Definition 7.5.1. *The Lyapunov exponents of the flow $\phi\left(x_{s0}\right)$ are defined to be the Lyapunov exponents of the associated stroboscopic time-T map.*

Thus, the Lyapunov exponents of a flow are defined in terms of the Lyapunov exponents of a map, i.e. the time-T map. Namely, let $g : \mathbb{R}^m \to \mathbb{R}^m$ be a smooth map and say $g^{(n)}$ the n-th iterate of g. Define $J_n = \frac{\partial g^{(n)}}{\partial x^n}$ and let Σ be the m-dimensional sphere of unitary radius with $J_n\Sigma$ representing the deformation of the sphere after n iterations of the map. Also, let r_k^n be the length of the k-th longest orthogonal axis of the ellipsoid $J_n\Sigma$ for an orbit with initial point $x_{s0} \in \Sigma$, for $k = 1, ..., m$.

Definition 7.5.2. *The* k*-th Lyapunov number, L_k, of x_{s0} is defined as*

$$L_k = \lim_{n\to\infty} \left(r_k^n\right)^{1/n} \tag{7.33}$$

if this limit exists. The k*-th Lyapunov exponent of x_{s0} is $h_k = \ln L_k$. Notice that by definition $L_1 \geq L_2 \geq ... \geq L_m$ and $h_1 \geq h_2 \geq ... \geq h_m$.*

Thus, the Lyapunov exponents measure the rates of divergence of nearby points along m orthogonal directions determined by the dynamics of the flow. The MSF approach makes use of the following assumptions, as shown in [57] and [140]: (i) the coupled oscillators (nodes) and the coupling functions are all identical; (ii) the synchronization manifold is an invariant manifold; (iii) the coupling functions are well approximated near the synchronous state by a linear operator. The main idea in [15] is to derive the variational equation from equation (7.32) describing small variations, ξ_k, of the trajectories of (7.32) from the synchronous evolution, say $s(t)$. This equation is then block diagonalized to give:

$$\dot{\xi}_k = \left[\frac{\partial f(x_s)}{\partial x} - \alpha\lambda_k(L)\frac{\partial \tilde{H}(x_s)}{\partial x}\right]\xi_k \tag{7.34}$$

For $k = 0$, we have the variational equation along the synchronization manifold; all other ks correspond to transverse eigenmodes to such manifold. Hence, it is shown that local stability of the synchronous evolution can be captured by the computation of the maximum Lyapunov exponent as a function of α, i.e. the MSF.

A first example

We start by looking at the representative example of two coupled Rossler oscillators of the form:

$$\begin{cases} \dot{x}_1 = -(y_1 + z_1) + \varepsilon_x(\alpha(x_2 - x_1)) \\ \dot{y}_1 = x_1 + ay_1 + \varepsilon_y(\alpha(y_2 - y_1)) \\ \dot{z}_1 = b + z_1(x_1 - c) + \varepsilon_z(\alpha(z_2 - z_1)) \end{cases}, \tag{7.35}$$

$$\begin{cases} \dot{x}_2 = -(y_2 + z_2) + \varepsilon_x(\alpha(x_1 - x_2)) \\ \dot{y}_2 = x_2 + ay_2 + \varepsilon_y(\alpha(y_1 - y_2)) \\ \dot{z}_2 = b + z_2(x_2 - c) + \varepsilon_z(\alpha(z_1 - z_2)) \end{cases} \tag{7.36}$$

We study the cases when coupling is active only on the x-variable ($\varepsilon_y = \varepsilon_z = 0$), or only on the y-variable ($\varepsilon_x = \varepsilon_z = 0$), or on all variables ($\varepsilon_x \neq 0$, $\varepsilon_y \neq 0$, $\varepsilon_z \neq 0$). As shown in Section 2.5, a possible virtual system is:

$$\begin{cases} \dot{x} = -(y + z) + \varepsilon_x(-2\alpha x + \alpha x_1 + \alpha x_2) \\ \dot{y} = x + ay + \varepsilon_y(-2\alpha y + \alpha y_1 + \alpha y_2) \\ \dot{z} = b + z(x - c) + \varepsilon_z(-2\alpha z + \alpha z_1 + \alpha z_2) \end{cases} \tag{7.37}$$

We assume $a = 0.2$, $b = 0.2$, $c = 2.5$, so that each Rossler system has a chaotic attractor. The virtual velocities of (7.37) are expressed as:

$$\begin{bmatrix} \delta\dot{x} \\ \delta\dot{y} \\ \delta\dot{z} \end{bmatrix} = \begin{bmatrix} -2\alpha\varepsilon_x & -1 & -1 \\ 1 & 0.2 - 2\alpha\varepsilon_y & 0 \\ z & 0 & x - 2.5 - 2\alpha\varepsilon_z \end{bmatrix} \begin{bmatrix} \delta x \\ \delta y \\ \delta z \end{bmatrix} \tag{7.38}$$

The symmetric part of the Jacobian in (7.38), in the case of coupling on the x-variable ($\varepsilon_x = 1$), is:

$$J_s = \begin{bmatrix} -2\alpha & 0 & (z-1)/2 \\ 0 & 0.2 & 0 \\ (z-1)/2 & 0 & x - 2.5 \end{bmatrix} \tag{7.39}$$

Analytical computation of the eigenvalues of (7.39) reveals that an eigenvalue is always positive, implying that (7.37) is not contracting. However, it is well known that the two systems can be synchronized for small coupling strengths: indeed in [140] it is shown that the MSF is negative for small α. The symmetric part of the Jacobian in (7.38) in the case of coupling on the y-variable ($\varepsilon_y = 1$) is:

$$J_s = \begin{bmatrix} 0 & 0 & (z-1)/2 \\ 0 & 0.2 - 2\alpha & 0 \\ (z-1)/2 & 0 & x - 2.5 \end{bmatrix} \tag{7.40}$$

The analytical expressions of the eigenvalues of J_s, in (7.40), reveals that an eigenvalue is positive definite and independent on α, implying that (7.37) is not contracting. However, we know that chaotic Rossler systems can be synchronized for a sufficiently large coupling strength, i.e. their MSF is negative for large coupling strengths. The symmetric part of the Jacobian in (7.38) in the case of coupling on all the state variables ($\varepsilon_x = \varepsilon_y = \varepsilon_z = 1$) is:

$$J_s = \begin{bmatrix} -2\alpha & 0 & (z-1)/2 \\ 0 & 0.2 - 2\alpha & 0 \\ (z-1)/2 & 0 & x - 2\alpha - 2.5 \end{bmatrix} \tag{7.41}$$

The eigenvalues of (7.41) are all dependent on the coupling strength: particularly, the increase of the coupling strength causes the decrease of the eigenvalues. Thus, for large enough coupling strengths, the system is contracting and the two Rossler systems synchronize. This result is confirmed by studying the MSF, which is negative for large α. The example indicates that if a virtual system is contracting, the MSF is negative, but that the viceversa, as expected, is not true.

Remark 7.5.1. *The MSF provides local conditions for synchronization that need to* *be checked numerically, the construction of a virtual system and the ensuing analysis provide a stronger stability result which is global and can be proven analytically.*

Remark 7.5.2. *The MSF approach requires a priori knowledge of the existence of the synchronization manifold. Contraction theory, instead, does not require the knowledge of a specific attractor to perform the stability analysis.*

7.6 Contraction and MSF

We now first present a result linking contracting systems and Lyapunov exponent and finally show some links between contraction theory and the MSF. We remark here that in this Section the *classical* notion of contracting dynamical system (based on the Euclidean norm, see Chapter 2 and Chapter 4) will be used.

7.6.1 Lyapunov exponents and Contraction theory

Corollary 7.6.1. *If Theorem 2.2.1 holds with* $\mathcal{C} \equiv \mathbb{R}^m$ *then the transverse Lyapunov exponents to all the system trajectories are negative.*

Proof. Given a generic trajectory, $x_s(t)$, from Definition 7.5.1 and Definition 7.5.2, in [2] (page 382) we have:

$$\dot{J}_t = A(t)\, J_t \tag{7.42}$$

where $J_t = \frac{\partial \phi(x_{s0})}{\partial x}$ and $A(t) = \frac{\partial f}{\partial x}$. To prove the theorem, we show that if the contracting property holds, then the volume of any given ball of initial conditions in state space shrinks. To do this, we use the Liouville's formula, given by:

$$\begin{aligned} \Delta_t' &= Tr\,(A(t))\,\Delta_t \\ \Delta_0 &= 1 \end{aligned} \tag{7.43}$$

where $\Delta_t = \det(J_t)$. From (7.43) the following result can be obtained:

$$\Delta_t = \exp\left(\int_0^t Tr\,(A(t))\,dt\right) \tag{7.44}$$

If the system is contracting, then:

$$\frac{1}{2}\left(\frac{\partial f}{\partial x}^T + \frac{\partial f}{\partial x}\right) \leq -\beta I \tag{7.45}$$

This hypothesis holds for all $x(t)$ and for all $t \in \mathbf{R}^+$: particularly it will be true for x_s. From [82] (page 398) we know that the trace, the determinant and all principal minors of a negative definite matrix are negative. Thus, the integral in

(7.44) is negative, meaning that the volume of any given ball in the phase space decreases. □

7.6.2 Synchronization of all to all networks

Theorem 7.6.1. *Consider a network of N nodes with an all-to-all topology. If the network dynamics are contracting for some range of the coupling strength, A, then the master stability function will be negative in the same range.*

Proof. The virtual system corresponding to a network of N elements with all-to-all topology is:

$$\dot{x} = f(x) - \alpha N h(x) + \alpha h(x_1) + ... + \alpha h(x_N) \tag{7.46}$$

System (7.46) is contracting if:

$$\frac{\partial f}{\partial x} - \alpha N \frac{\partial h}{\partial x} \leq -\beta I \tag{7.47}$$

with $\beta > 0$. Since an all-to-all network can be viewed as a complete graph, and since the Laplacian matrix for such a graph has one zero eigenvalue (the first), while the others are all equal to N, as shown in [66] (page 280 Lemma 13.1.3), it is possible to rewrite (7.34) as:

$$\dot{\xi}_k = \left[\frac{\partial f(x_s)}{\partial x} - \alpha N \frac{\partial \tilde{h}(x_s)}{\partial x}\right] \xi_k \tag{7.48}$$

for each transverse mode, i.e. $k \neq 0$. The matrix in (7.48) has the same expression of the Jacobian (7.47). As the virtual system is contracting in some range A of the coupling strength by hypothesys, then system (7.48) will be contracting over the same range. Following Corollary 7.6.1, the maximum Lyapunov exponent of (7.48) is negative and the theorem remains proved. □

Example 7.6.1. *Theorem 7.6.1 is applied to reinterpret the behavior of two Rossler systems coupled on all state variables. We have already pointed out that the virtual system corresponding to the network of two coupled Rossler systems is contracting. From (7.34), the variational equations for the modes of the synchronous state of the network are:*

$$\dot{\xi}_0 = \left[\begin{pmatrix} 0 & -1 & -1 \\ 1 & 0.2 & 0 \\ z_s & 0 & x_s - 2.5 \end{pmatrix}\right] \xi_0 \tag{7.49}$$

$$\dot{\xi}_1 = \left[\begin{pmatrix} 0 & -1 & -1 \\ 1 & 0.2 & 0 \\ z_s & 0 & x_s - 2.5 \end{pmatrix} - 2\alpha \begin{pmatrix} 1 & 0 & 0 \\ 0 & 1 & 0 \\ 0 & 0 & 1 \end{pmatrix}\right] \xi_1 \tag{7.50}$$

Since the matrix in (7.50) is equal to the Jacobian matrix of the virtual system and *it is contracting for all (x, y, z) for large enough α, this will be true for (x_s, y_s, z_s). Thus, the dynamics of the transverse modes are contracting if α is sufficiently large, implying the negativeness of the master stability function in the same range of the parameter α.*

Remark 7.6.1. *Note that the higher is N (set equal to 2 in (7.50)), the lower will be the value of α that synchronizes the network, confirming what stated in the literature, see e.g. [53].*

7.6.3 Synchronization of networks with general topology

Assume now that $\tilde{H}(X)$ is linear. As shown in [194], we can associate to a generic connected network of the form (7.32) the following auxiliary, virtual, system:

$$\dot{Y} = F(Y) - \alpha (L \otimes I_n) Y - (1_{N\times N} \otimes K_0)(Y - X) \tag{7.51}$$

where $Y := \left[y_1^T, \ldots, y_N^T\right]^T$ is the set of virtual state variables, K_0 is some symmetric positive definite matrix and $1_{N\times N}$ is the $N \times N$ matrix whose elements are all equal to 1.

System (7.51) has $y = x$ as a solution and admits the particular solution $y_1 = \ldots = y_N = y_\infty$, with y_∞ such that:

$$\dot{y}_\infty = f(y_\infty) - nK_0 y_\infty + K_0 \sum_{j=1}^{N} x_j(t)$$

Thus, contraction of such a system immediately implies synchronization of (7.32) (see Section 4.5 and also [194]). We can then state the following result.

Theorem 7.6.2. *Consider a network with N identical nodes. If (i) the network is connected; (ii) the coupling functions are linear and increasing; (iii) the auxiliary system (7.51) is contracting for some range of the coupling strength, $\alpha \in A$; then the MSF will be negative in A, i.e. the network synchronizes.*

Proof. From the hypotheses, we have that system (7.51) is contracting, i.e. the symmetric part of its Jacobian, say J_s, given by

$$J_s := \left[\frac{\partial F}{\partial y}\right]_s - \alpha (L \otimes I_n) - 1_{N\times N} \otimes K_0$$

is negative definite $\forall \alpha \in A$.

Let $J_r = -\alpha (L \otimes I_n) - 1_{N\times N} \otimes K_0$. Then, its maximum eigenvalue can be computed, as shown in [194], using Courant-Fischer Theorem (see e.g. [82]):

$$\lambda_{\max}(J_r) = -\lambda_{m+1}(\alpha (L \otimes I_n))$$

Thus, if the auxiliary system is contracting then:

$$\lambda_{m+1}\left(\alpha\left(L\otimes I_n\right)\right) > \max_i \lambda_{\max}\left(\left[\frac{\partial f}{\partial y_i}\right]_s\right) \tag{7.52}$$

$\forall\alpha\in A$. We can then conclude that the matrix

$$\frac{\partial F}{\partial y} - \alpha\left(L\otimes I_n\right) \tag{7.53}$$

is negative definite $\forall\alpha\in A$. Hence, the linear system

$$\dot{\xi} = \left(\frac{\partial F}{\partial y} - \alpha\left(L\otimes I_n\right)\right)\xi$$

is contracting. The proof is then concluded by noticing that the dynamics of the above system around the synchronization manifold yields the variational equation used, according to the MSF approach [140], to calculate the Lyapunov exponents. Now, since the system is contracting, then its Lyapunov exponents will be negative as shown in [155], immediately implying negativity of the MSF. □

7.7 Numerical validations

To validate Theorem 7.6.2 we used the classical oscillator defined in e.g. [50] as:

$$\begin{aligned}\dot{x}_1 &= x_1 - x_2 - x_1\left(x_1^2 + x_2^2\right)\\ \dot{x}_2 &= x_1 + x_2 - x_1\left(x_1^2 + x_2^2\right)\end{aligned} \tag{7.54}$$

We assume that the coupling between nodes is linear and acting on both state variables. Using a virtual system constructed as in (7.51), it is easy to see that the second and third hypotheses of Theorem 7.6.2 are satisfied. We now consider two connected network topologies of $N = 1000$ nodes in order to satisfy the first hypothesis of Theorem 7.6.2.

7.7.1 Nearest neighbor network

This topology presents a small algebraic connectivity, thus, the coupling strength α, computed as required by Theorem 7.6.2 is expected to be large (in this case $\alpha \cong 12000$). In Figure 7.4 the behavior is shown of the network state variables when the coupling strength is increased from 0 to α at time $t = 10s$.

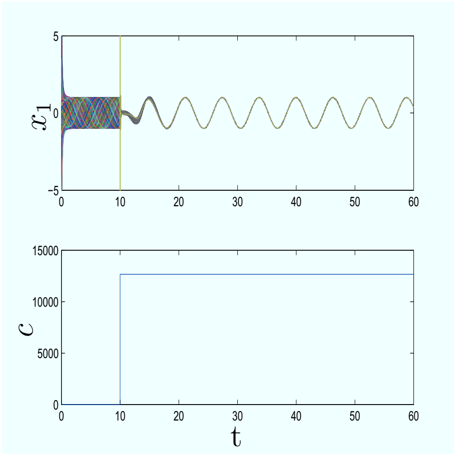

Figure 7.4: Evolution of the first state component for all oscillators (top) when the coupling strength (c) is varied between 0 and α at $t = 10s$.

7.7.2 Small world network

The algebaic connectivity is increased by adding new links, with uniform probability, to the nearest neighbor topology of Section 7.7.1. Then, the coupling strength computed using Theorem 7.6.2 decreases considerably with respect to the previous case. In Figure 7.5 the behavior is shown of the states of the network and the applied coupling strength (in this case $\alpha \cong 800$).

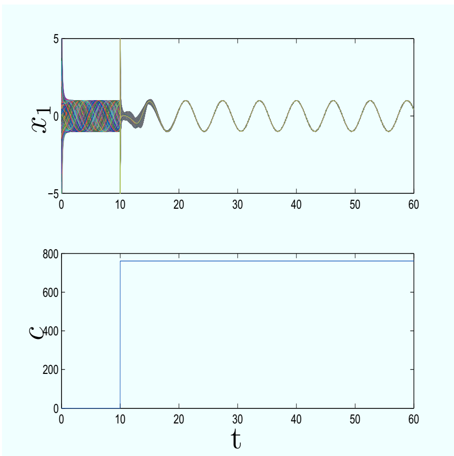

Figure 7.5: Evolution of the first state component for all oscillators (top) when the coupling strength (c) is varied between 0 and α at $t = 10s$.

7.8 Discussion

In this Chapter, we provided a coherent theoretical study for network coordination, based on the use of contraction theory. We first presented a generic lemma that can be used to analyze the convergence of a dynamical system of interest towards some linear invariant subspace. We then used such a result to coordinate complex dynamical networks consisting of both linear and nonlinear nodes. In order to show the effectiveness of our results as a design tool, we designed a decentralized strategy ensuring the rendezvous for a network of mobile agents. From the analysis viewpoint, instead, we obtained novel sufficient conditions for network synchronization by deriving some links between contraction analysis, Lyapunov-based techniques and the Master Stability Function. In the next chapter, we will present similar results for the analysis/control of discrete-time and asynchronous networks.

Chapter 8

Convergence of discrete-time and asynchronous systems and networks

All networks and systems analyzed in the previous chapters were characterized by a continuous-time dynamics. In this Chapter, we turn our attention to the problem of analyzing/controlling discrete time and asynchronous systems and networks. Specifically, after stating sufficient conditions for general smooth discrete-time dynamical systems, we show that these conditions can be easily specialized to the analysis and design of communication strategies ensuring consensus, synchronization and cluster-synchronization in discrete-time and asynchronous networks. The results presented in this Chapter were submitted for journal publication [158]

8.1 Introduction

In all the applications discussed so far, it is assumed that each agent in a network has the ability of performing some computation and share information with its neighbors. It is implicitly assumed that interactions between the network nodes occur synchronously. That is, all nodes only send/receive informations at predetermined time instants and use the most recent data for performing computations. One of the implications of this assumption is the need for each agent to be synchronized to a common clock, thus yielding the so-called synchronization penalty ([23], pag. 97). In applications, devices are often modeled by discrete-time systems which are asynchronous rather than synchronous, in the sense that each node transmits, receives or processes information in accordance to some individual internal clock. For example, in decentralized, digital or event-based control problems [14] [20], controllers often act independently at different times as this can have advantages on synchronous implementations of the distributed control strategy. The use of asynchronous protocols becomes even more crucial in the case of networks of systems interacting over the internet, for example, where transmission times vary and information becomes available to different nodes at different times (see e.g. [121] and references therein).

In the asynchronous framework no assumptions are made on the relative speeds and phases of the agents' clocks and no guarantee is given on the time of delivery or even on the delivery being successful. Thus, it is possible to easily take into account within the same framework heterogenous agents, time-varying communication delays, packet dropouts. The drawback, when dealing with asynchronism, lies in the fact that it dramatically affects and often destroys the convergence properties of the synchronous implementation of a system or network. Thus, solving consensus and synchronization problems in asynchronous networks becomes difficult by using traditional stability techniques, where such problems are formulated in terms of stability of some invariant set. To overcome this problem, our viewpoint is instead that of nonlinear contraction theory as discussed in Chapter 6 and Chapter 7.

The aim of this Chapter is that of proposing an effective methodology for the analysis and design of linear and nonlinear decentralized control strategies for the coordination of discrete time and asynchronous networks of both linear and nonlinear nodes. From the methodological viewpoint, the key idea is again that of using norms which are not induced by any scalar product to prove a contracting property on the synchronous version of the asynchronous network of interest. The approach is based on the idea (see [23]) of giving sufficient conditions on a synchronous system that ensure convergence to some fixed point of its asynchronous implementation. In this Chapter, we expand and generalize the methodology presented in [23] to generic networks of nonlinear discrete-time systems. In particular, the main contributions of the Chapter can be summarized as follows:

1. a coherent theoretical framework is derived for the control of discrete-time and asynchronous systems. Results are based on the use of nonlinear contraction of discrete-time dynamical systems both in the synchronous and asynchronous case;

2. several criteria are presented that can be used to design nonlinear distributed communication strategies for the coordination of networks, consisting of nonlinear discrete-time and asynchronous nodes.

3. The case where identical nodes are controlled by means of heterogeneous control strategies is also addressed. Specifically, some sufficient conditions are obtained for the coordination of networks of identical nodes where multiple communication protocols co-exist.

4. sufficient conditions are also provided for the coordination of networks consisting of multiple clusters of non-homogeneous nodes. That is, the problem

is addressed of designing (nonlinear) decentralized protocols ensuring cluster synchronization.

The theoretical results are illustrated by a set of representative examples of interest in both Control and Optimization.

8.2 Problem Statement

In this Section we introduce the basic mathematical model used in this Chapter and the problem statement.

Let $S_1, \ldots, S_N$ be connected sets in $\mathbb{R}$, and let $S := S_1 \times \ldots \times S_N$. For any $x \in S$, we write $x = [x_1, \ldots, x_N]^T$, where $x_i \in S_i$, $i = 1, \ldots, N$. Let $\Phi : S \times \mathbb{N} \to S$ be a smooth function defined by $\Phi(x, k) := [\phi_1(x, k), \ldots, \phi_N(x, k)]^T$, $\forall x \in S$, with $\phi_i : S \times \mathbb{N} \to S_i$. We assume that there exists a set of times $T = \{0, 1, 2, \ldots\}$ at which one or more components x_i of x update their values. Let T_i be the set of times at which the state variable x_i is updated. We will consider N-dimensional smooth dynamical systems of the form [23] (pages 426-428)

$$\begin{aligned} x_i\left(k+1\right) &= \phi_i\left(x\left(\tau^i\left(k\right)\right), k\right), \quad && \forall k \in T_i \\ x_i\left(k+1\right) &= x_i\left(k\right), && \forall k \notin T_i \end{aligned} \tag{8.1}$$

$i = 1, \ldots, N$, where $x\left(\tau^i\left(k\right)\right) := \left[x_1\left(\tau_1^i\left(k\right)\right), \ldots, x_N\left(\tau_N^i\left(k\right)\right)\right]^T$ and the quantity $\tau_j^i\left(k\right)$ corresponds to the time instant when information from x_j becomes available to x_i. Note that in network coordination problems, each x_i denotes the state of heterogeneous agents, with dynamics determined by ϕ_i, interacting with each others. Notice that $0 \leq \tau_j^i\left(k\right) \leq k$, $\forall k \in T$ and the difference $k - \tau_j^i\left(k\right)$ can be thought of as a form of communication delay. We are interested in the stability properties of trajectories of system (8.1). Notice that stability in this context is not intended as a property of some invariant set, but as a global property of solutions themselves. The key idea is to derive conditions on the stability of (8.1), by giving conditions on the stability of its *synchronous implementation*, i.e.

$$x_i\left(k+1\right) = \phi_i\left(x\left(k\right), k\right), \quad i = 1, \ldots, N \tag{8.2}$$

8.2.1 Related Work

The idea of studying the properties of an asynchronous discrete-time system in terms of those of its synchronous implementation has been presented in a number of papers in the existing literature. For instance in [23], Chapter 6 (and references therein) a criterion based on the contraction mapping theorem (see e.g. [74]) is obtained for finding the fixed point of the evolution operator of some asynchronous discrete-time system of interest. In this Chapter, by using nonlinear contraction analysis we give conditions for the convergence of all trajectories of a discrete-time asynchronous system towards some (possibly) non-stationary orbit. We then use such results to design nonlinear communication strategies to ensure *coordination* of a network of interest. Specifically, we consider networks whose nodes are discrete-time synchronous or asynchronous systems, possibly nonlinear, controlled by linear or nonlinear protocols.

Surprisingly, even when both nodes dynamics and coupling protocols are assumed to be linear, results on consensus and synchronization of asynchronous networks are relatively sparse, if compared to those on both continuous-time and discrete-time networks. A widely studied algorithm for consensus can be found in the seminal work [186] (see also [187]). In e.g. [186], the following network of m one-dimensional nodes is analyzed by using a different approach:

$$x_i(k+1) = u_i(x), \quad u_i := \sum_{j=1}^{m} a_{ij}(k) x_j(k - \tau_j^i(k)), \quad \forall k \in T_i \tag{8.3}$$

where $a_{ij}(k)$ is some nonnegative weight that agent i assigns to $x_j(k - \tau_j^i(k))$. The convergence properties of the above algorithm have also been studied under different assumptions on agent connectivity and information exchange in e.g. [24], [85], [131]. In Section 8.5 we show that our results are more generic than those presented in the above references as we consider a wider class of dynamical systems and networks. Moreover, as also shown in Section 8.5, the same convergence conditions derived in [186], [24], [85], [131] are obtained when our methodology is applied to (8.3).

In some recent works (see e.g. [54] and Section 8.6.2 for further details) the consensus problem of the following synchronous network is analyzed:

$$x_i(k+1) = x_i(k) + u_i(x), \quad u_i(x) = \xi_* \sum_{j \in N_i} (x_j - x_i)$$

where ξ_* is a positive scalar representing the coupling strength and N_i denotes the set of neighbors of node i. In Section 8.6.2 it is shown that our results can be used to provide sufficient conditions ensuring consensus of the above network and of its asynchronous implementation. Finally, we provide guidelines for the design of nonlinear communication strategies that ensure consensus for both the synchronous and asynchronous networks.

Another problem, related to our work and addressed in the literature, is the design of asynchronous consensus strategies in continuous-time multi-agent systems with time delays. In [202] (and references therein) such a problem has been addressed when the network has a switching topology. An interesting future research direction might be extending our results to the case of switching networks.

8.3 Mathematical preliminaries

In this Section we will introduce some results that will be used in the rest of the Chapter.

8.3.1 The joint spectral radius and primitive matrices

The *joint spectral radius* of a set of matrices was firstly introduced in [152]. Let Σ denote a nonempty set of $l \times l$ real matrices, A_i: $\Sigma := \{A_i : i \in \mathcal{I}\}$, where $\mathcal{I}$ is the set of indexes. Note that Σ is not necessarily bounded. Let's now define

$$\tilde{\rho}_k(\Sigma) := \sup \left\{ \rho \left(\prod_{i=1}^{k} A_i \right) : A_i \in \Sigma, \quad for \quad 1 \le i \le k \right\}$$

For any given k, the above quantity represents the largest possible spectral radius of all products of k matrices, chosen freely in the set Σ. We can now define the *generalized spectral radius* as $\tilde{\rho}(\Sigma) := \lim_{k \to +\infty} \sup \left(\tilde{\rho}_k(\Sigma)\right)^{1/k}$, which represents the maximal asymptotic spectral radius of the products of matrices that can be constructed using the set Σ. Analogously, the *joint spectral radius*, $\hat{\rho}(\Sigma)$, is defined as $\hat{\rho}(\Sigma) := \lim_{k \to +\infty} \sup \left(\hat{\rho}_k(\Sigma)\right)$, where

$$\hat{\rho}_k(\Sigma) := \sup \left\{ \left\| \prod_{i=1}^{k} A_i \right\| : A_i \in \Sigma, \quad for \quad 1 \le i \le k \right\}$$

In [21], it was shown that for any bounded set of matrices, the above limits exist and have a common value, denoted by $\rho(\Sigma)$. In the rest of the Chapter, we will refer to the above common value as *joint spectral radius*. Applications of the joint spectral radius to the stability of time varying linear systems and linear inclusions can be found in [37], [78], [166]. In [37], [78] the following result is proved.

Theorem 8.3.1. *Consider an l-dimensional discrete linear time varying system $x(k+1) = A_k x(k)$, $x(0) = x_0 \in \mathbb{R}^l$. Then, $\rho(\Sigma) < 1$ if and only if $\lim_{k \to +\infty} x(k) = 0$, for any x_0.*

We now present some definitions which will be used in the rest of the Chapter.

Definition 8.3.1 ([82]). *A square nonnegative matrix A, is said to be primitive if it is irreducible and has only one eigenvalue of maximum modulus.*

Lemma 8.3.1. *Consider two $n \times n$ square matrices, A and B, having constant column sums equal to $\bar{a}$ and $\bar{b}$ respectively. Then, AB has column sum equal for all the columns. Furthermore, this sum is equal to $\bar{a}\bar{b}$.*

Proof. Let $C := AB$. We have $c_{ij} = \sum_{r=1}^{n} a_{ir} b_{rj}$. Thus, the j-th column sum of the matrix C is given by

$$\sum_{i=1}^{n} \sum_{r=1}^{n} a_{ir} b_{rj} = \sum_{i=1}^{n} \left(b_{ij} \sum_{k=1}^{n} a_{ki}\right) = \sum_{i=1}^{n} \left(b_{ij} \bar{a}\right) = \bar{a}\bar{b}$$

□

Proofs of the following three lemmas can be found in e.g. [82], [149], and [23].

Lemma 8.3.2. *Let A be a nonnegative and irreducible matrix. If at least one main diagonal entry is positive, then A is primitive.*

Lemma 8.3.3. *If a nonnegative matrix $A \in \mathbb{R}^{n \times n}$ has the same positive constant column sums, given by $\mu > 0$, then μ is an eigenvalue of A with an associated eigenvector $\mathbf{1}$ and $\rho(A) = \mu$. Furthermore, if A is primitive, with $a_{ii} > 0$, for all i, then μ is the unique eigenvalue of maximum modulus.*

Lemma 8.3.4. *Given an $n \times n$ square nonnegative matrix, A, the following statements are equivalent: (i) $\rho(A) < 1$; (ii) there exists $\Theta = diag(\theta_1, \dots, \theta_n)$ such that $\|\Theta A \Theta^{-1}\| < 1$; (iii) there exist some $\lambda < 1$ and $\omega > 0$ such that $A\omega \leq \lambda\omega$.*

8.4 Global convergence of synchronous systems

Using the notation introduced above, the dynamics of (8.2) can then be written as

$$x(k+1) = \Phi(x(k), k) \tag{8.4}$$

Theorem 8.4.1. *Assume that for system (8.2) the linear subspace, say $\mathcal{M}$, spanned by the vector $\mathbf{1}$ is flow invariant. Let V be the matrix whose rows form a basis of $\mathcal{M}^{\perp}$. Then, all system trajectories globally converge towards $\mathcal{M}$ if the following set of conditions are satisfied for any $x \in \mathbb{R}^N$ and for any $k \geq k_0$ (possibly after some smooth coordinate transformation):* **(H1)** *the matrix $\frac{\partial \Phi(x(k),k)}{\partial x}$ is irreducible;* **(H2)** $\frac{\partial \phi_i(x(k),k)}{\partial x_i} > 0, \forall i$; **(H3)** $\frac{\partial \phi_i(x(k),k)}{\partial x_j} \geq 0, \forall i,j,\ i \neq j$; **(H4)** $\sum_{i=1}^{N} \frac{\partial \phi_i(x(k),k)}{\partial x_j} = \bar{c}(k) \leq 1$, $\forall j = 1, \dots, N$. *Furthermore, if $\sum_{i=1}^{N} \frac{\partial \phi_i(x(k),k)}{\partial x_j} = \bar{c}(k) > 1, \forall j = 1, \dots, N$, then convergence is ensured if* **H1 - H3** *hold and* **(H5)** $\left\| V \frac{\partial \Phi(x(k),k)}{\partial x} V^T \right\| < 1$.

Proof. Differentiation of (8.4), gives the dynamics of the system virtual displacements:

$$\delta x(k+1) = J(k)\, \delta x(k), \quad \delta x(k_0) = \delta x_0 \tag{8.5}$$

where $J(k) := \frac{\partial \Phi(x(k),k)}{\partial x}$. The evolution of δx can be written explicitly as $\delta x(k) = \prod_{r=1}^{k} J(k-r)\, \delta x_0$. Now, **H1**, **H2**, **H3** imply (Lemma 8.3.2) that J is primitive. Let $\Sigma^k := \left\{ \prod_{i=1}^{k} J_i, \quad J_i = J(i) \right\}$. We start with proving the Theorem when **H4** is satisfied. We have to distinguish between two cases.

Case 1: $\bar{c}(k) < 1$**.** From Theorem 8.3.1, we know that (8.5) is stable if and only if $\rho(\Sigma) < 1$. By definition we have $\rho(\Sigma) = \sup_{k\in\mathbb{N}} \sup_{J\in\Sigma^k} \rho(J)^{\frac{1}{n}}$. Now, from **H4** we know that all the column sums of all matrices J_i are equal to $\bar{c}(k) < 1$. Thus, by means of Lemma 8.3.1, we have that any product between matrices J_i has column sums lower than 1. This, in turn, implies that $\rho(\Sigma) < 1$. Convergence is then proved, i.e. $\delta x(k) \to 0$ as $k \to +\infty$ and for any $k \in \mathbb{R}^N$. Since $\mathcal{M}$ is flow invariant, this implies that system trajectories globally converge to $\mathcal{M}$.

Case 2: $\bar{c}(k) = 1$**.** In this case, from **H4** and Lemma 8.3.3, it follows that $\rho(J_i) = 1$, $\forall i$. Hence, as J_i is nonnegative, then $\|J_i\|_1 = 1$ and nearby trajectories cannot diverge from each other. Thus, the invariant subspace, $\mathcal{M}$, is unique and it is spanned by the eigenvector of J associated to the unique eigenvalue of maximum modulus. We will now prove that all trajectories of the system will converge towards $\mathcal{M}$. Denote with $\mathbf{e}_1$ the vector $\mathbf{1}$ and with $\mathbf{e}_2, \ldots, \mathbf{e}_N$ the vectors completing an orthogonal basis in $\mathbb{R}^N$. Then, in the basis $\mathbf{E}$, composed by the above vectors, every matrix J_i has the following block triangular form (see e.g. [148], page 3):

$$J_i = \begin{bmatrix} J_{i1} & J_{i2} \\ \mathbf{0} & J_{i3} \end{bmatrix} \tag{8.6}$$

where J_{i1} is 1×1, J_{i2} is $1 \times (N-1)$ and J_{i3} is $(N-1) \times (N-1)$. That is, the dynamics of the virtual displacements (8.5) in this new basis has the form

$$\begin{bmatrix} \delta x_{\mathcal{M}} \\ \delta x_{\perp} \end{bmatrix}(k) = \prod_{r=1}^{k} \begin{bmatrix} J_{i1}(k-r) & J_{i2}(k-r) \\ \mathbf{0} & J_{i3}(k-r) \end{bmatrix} \begin{bmatrix} \delta x_{\mathcal{M}} \\ \delta x_{\perp} \end{bmatrix}(k_0) \tag{8.7}$$

where $\delta x_{\mathcal{M}}$ represents the dynamics on $\mathcal{M}$ and $\delta x_{\perp}$ those transversal to $\mathcal{M}$. Thus, the evolution of $\delta x_{\perp}$is given by: $\delta x_{\perp}(k) = \prod_{r=1}^{k} J_{i3}(k-r)\delta x_{\perp}(k_0)$. Define now:

$$\Sigma_3^k := \left\{ \prod_{i=1}^{k} J_{i3}, \quad J_{i3} = J_{i3}(i) \right\}$$

Notice that, by means of **H4** and Lemma 8.3.3, the eigenvalues of J_{i3} are all in modulus strictly lower than 1, $\forall k$. Thus $\rho\left(\Sigma_3^k\right) < 1$: hence $\delta x_{\perp}(k) \to 0$ as $k \to +\infty$, **for any** $x \in \mathbb{R}^N$**.** This in turn implies that there exist a matrix norm, $\|\cdot\|$, such that $\|J_{i3}\| < 1$. That is, $\delta x_{\perp}(k) \to 0$ and hence all systems trajectories converge towards $\mathcal{M}$.

To conclude the proof, we have to show that if **H4** is violated, then convergence of the nodes is ensured if **H1**, **H2**, **H3**, **H5** are satisfied. The proof follows the same outline as the proof of the previous case (i.e. $\rho(\Sigma) = 1$). The additional hypothesis, **H5**, obviously implies that only one invariant subspace, $\mathcal{M}$, exists and that the dynamics transversal to $\mathcal{M}$ are contracting (see Theorem 4.8.2). $\square$

Remarks

- Notice that, in general, it is difficult to compute the joint spectral radius for a set of matrices (see e.g. [137]). However, for the case of our interest (i.e. nonnegative, irreducible matrix with constant column sum), the computation of $\rho(\Sigma)$ becomes straightforward, since it directly depends on the column sum of the set of matrices being considered;

- under the condition $\bar{c}(k) < 1$ in Theorem 8.4.1, we proved that all trajectories of system (8.4) converge towards each other for any $x \in \mathbb{R}^N$ and for any $k \in \mathbb{N}$. In the case $\bar{c}(k) \geq 1$ we proved that trajectories converge towards $\mathcal{M}$ for any $x \in \mathbb{R}^N - \{\mathcal{M}\}$ as $k \to +\infty$. This will be of fundamental importance for deriving stability conditions on asynchronous systems which can be easily checked on the synchronous implementation of the system;

- notice that, since the conditions of Theorem 8.4.1 are uniform conditions, they might appear restrictive at first, but are required to guarantee convergence of the asynchronous implementation of the system. Moreover, as shown in Section 8.6.2 ad Section 8.7.1, these conditions are not difficult to satisfy when the aim is the design of linear and nonlinear communication protocols ensuring consensus and synchronization of discrete time and asynchronous networked systems;

- the convergence rate towards $\mathcal{M}$ is given by: (i) $\rho\left(\Sigma_3^k\right)$ if the row column sum of system Jacobian is smaller or equal than unity; (ii) $\max_{x,k}\left\{\left\|V\frac{\partial\Phi(x,k)}{\partial x}V^T\right\|\right\}$ otherwise.

8.5 Global convergence of asynchronous systems

Now consider the asynchronous version of system (8.4), given by (8.1). In what follows, according to [23], we will say that x^* is a fixed point of $\phi(x,k)$ if:

$$x^* = \phi(x^*,k), \forall k$$

The following two assumptions can be found in [23].

Assumption 8.5.1. *The sets T_i are infinite, and if $\{t_k\}$ is a sequence of elements of T_i that tends to infinity, then $\lim_{k\to+\infty}\tau^i(t_k) = +\infty$.*

Assumption 8.5.2. *Let $x := [x_1,\dots,x_N]^T$, $\Phi(x,k) := [\phi_1,\dots,\phi_N]^T : S\times\mathbb{N}\to S$, with $S = S_1\times\ldots\times S_N$. There exist a sequence of non empty sets $\{X(k)\}$, with*

$$\ldots\subset X(k+1)\subset X(k)\subset\ldots\subset X(0)$$

and a sequence $\{s(k)\}$ *with* $s(k) \in \mathbb{N}$, $s(0) = 0$, $s(k) \to +\infty$ *as* $k \to +\infty$, *such that: 1)* $\Phi(x, \beta) \in X(k+1)$, $\forall k, x \in X(k), \beta \geq s(k)$, *; 2) if* $\{\mathbf{y}(m)\}$ *is a sequence such that* $\mathbf{y}(m) \in X(k)$, $\forall k$ *larger than some index* m_k, *then every limit point of* $\{y(m)\}$ *is a fixed point of* $\Phi(x, k)$*; 3) for all* k*, we have:*

$$\exists X_i(k) \subset X_i(0), i = 1, 2, \ldots, N: \quad X(k) = X_1(k) \times \ldots \times X_N(k)$$

The Asynchronous Convergence Theorem can then be stated as follows (see [23] for the proof):

Theorem 8.5.1. *Consider the asynchronous system (8.1). If the above assumptions hold, and the initial state* $x(0)$ *is such that* $x(0) = (x_1(0), \ldots, x_N(0)) \in X(0)$*, then every limit point of* $\{x(k)\}$ *is a fixed point of* $\Phi(x, k)$*.*

Our main result can then be stated as follows.

Theorem 8.5.2. *All trajectories of asynchronous system (8.1) will converge towards each other if: i) Assumption 8.5.1 holds; ii) the synchronous system (8.2) fulfills Theorem 8.4.1.*

Proof. We will prove the Theorem by showing that if Theorem 8.4.1 is satisfied by (8.2), then it is possible to construct an appropriate sequence of sets $X(k)$, so that Assumption 8.5.2 is verified. Thus, Theorem 8.5.1 can be used to prove convergence of (8.1).

We start with the case where the column sum of the system Jacobian is upper bounded by some positive constant $\bar{c}_1 < 1$. That is, in terms of the notation introduced in Theorem 8.4.1, we have $\bar{c}(k) \leq \bar{c}_1 < 1$. This implies that $\rho(J_i) < 1$, for any i. Since the Jacobian is a nonnegative matrix, this condition implies that $\|J_i\|_1 \leq \bar{c}_1 < 1$, $\forall i$. On the other hand, notice that the following inequality holds:

$$|\delta x(k)|_1 \leq \prod_{r=1}^{k} \|J(k-r)\|_1 |\delta x_0|_1 \leq \bar{c}_1^k |\delta x_0|_1$$

Now, from the norm equivalence in finite dimensional spaces, we have that for any vector $v \in \mathbb{R}^n$, there exist some α_1 such that $\|v\|_1 \leq \alpha_1 \|v\|_{\Theta,\infty}$. Thus, the sequence of sets, required by Theorem 8.5.1, can be defined as:

$$X^1(k) := \left\{\delta x(k) : |\delta x(k)|_{\Theta,\infty} \leq \bar{c}_1^k \alpha_1 |\delta x(k_0)|_{\Theta,\infty}\right\} \tag{8.8}$$

Furthermore, it is easy to show that such a sequence satisfies the conditions required by Assumption 8.5.2. In fact: 1) if $\delta x(k) \in X^1(k)$, then $\delta x(k+1) \in X^1(k+1)$; 2) the sequence $\{\delta x(k)\}$ belongs to $X^1(k)$, $\forall k \geq 0$, and its limit point is 0; 3) since the sets are defined using the weighted infinite norm, the third condition in Assumption

8.5.2 is automatically satisfied. Thus, Theorem 8.5.1 can be applied, implying that $\delta x \to 0$, as $k \to +\infty$.

We now prove the Theorem in the case where the column sum of the system Jacobian is equal to $\bar{c} = 1$, implying that $\rho(J_i) = 1$ for any i. Recall from the proof of Theorem 8.4.1 that there exist a matrix norm, $\|\cdot\|_*$, such that $\|J_{i3}\|_* = \bar{c}_2 < 1$, where J_{i3} denotes the Jacobian sub-matrix associated to the transversal dynamics (see equation (8.7)). Thus, it is always possible to find a positive (finite) scalar α_2 such that $\|J_{i3}\|_* \le \alpha_2 \|J_{i3}\|_{\Theta,\infty}$. We can then define

$$X^2(k) := \left\{ \delta x_\perp(k) : |\delta x_\perp(k)|_{\Theta,\infty} \le \bar{c}_2^k \alpha_2 |\delta x_\perp(k_0)|_{\Theta,\infty} \right\} \tag{8.9}$$

Finally, consider the case where the column sum of the system Jacobian is $\bar{c} > 1$ (notice that $\mathcal{M}$ is assumed to be unique in Theorem 8.4.1), implying that $\rho(J_i) > 1$. In this case, the dynamics transversal to $\mathcal{M}$ are contracting, since there exist a norm such that $\|VJ(k)V^T\| = c_3 < 1$. Then, we know that there exist an α_3, such that $\|VJ(k)V^T\| \le \alpha_3 \|VJ(k)V^T\|_{\Theta,\infty}$. Define now

$$X^3(k) := \left\{ \delta x_\perp(k) : |\delta x_\perp(k)|_{\Theta,\infty} \le \bar{c}_3^k \alpha_3 |\delta x_\perp(k_0)|_{\Theta,\infty} \right\} \tag{8.10}$$

It is easy to show that the sequences of sets in (8.9), (8.10) satisfy conditions required by Assumption 8.5.2, and hence can be used to analyze the convergent behavior of the asynchronous implementation (8.1) of system (8.4). In fact:

- if $\delta x_\perp(k) \in X^i(k)$, then $\delta x_\perp(k+1) \in X^i(k+1)$, $i = 2, 3$;
- the sequence $\{\delta x_\perp(k)\}$ belongs to $X^i(k)$, $\forall k \ge k_0$, $i = 2, 3$, and its limit point is 0, i.e. the virtual dynamics converge towards $\mathcal{M}$;
- since the sets are defined using the weighted infinite norm, the third condition in Assumption 8.5.2 is automatically satisfied.

Thus, Theorem 8.5.1 can be applied, implying that $\forall x \notin \mathcal{M}$, $\delta x_\perp \to 0$, as $k \to +\infty$, and thus that $x \to \mathcal{M}$. The Theorem is then proved. □

Analyzing convergence of a networked system

As a first application of our results, we now use Theorem 8.4.1 and Theorem 8.5.2 to analyze the convergence properties of the network of m nodes in (8.3), see e.g. [186], [24], [85], [131]. A possible approach for analyzing such a network is the one introduced in [131], where a convergence analysis of the above protocol was performed by using an *enlarged agent system*. Such a system was obtained by adding *new* agents to the original system, in order to deal with delays. In the above cited Chapter, it is shown that the above protocol ensures consensus if:

1. the graph is (strongly) connected;
2. $a_{ii}(k) \geq \eta$, for any $k \in \mathbb{N}$ (where $0 < \eta < 1$)
3. $a_{ij}(k) \geq \eta$ if agent i receives information from agent j at time k
4. $a_{ij}(k) = 0$ if agent i does not receive any information form agent j at time k
5. the following condition holds: $\sum_{j=1}^{m} a_{ij}(k) = 1$ for all i and for any k;
6. the delays are bounded.

We now show that by means of Theorem 8.4.1 and Theorem 8.5.2 it is possible to prove the same result without the need of using an enlarged system for the analysis. Indeed, consider the synchronous implementation of the above network, which is simply:

$$x_i(k+1) = \sum_{j=1}^{m} a_{ij}(k)x_j(k)$$

It is easy to check that a sufficient condition for $\mathcal{M} := \{x_1 = \ldots = x_m\}$ to be invariant is $\sum_{j=1}^{m} a_{ij}(k) = 1$. Furthermore, notice that the Jacobian associated to the above system is $J(k) := [a_{ij}(k)]$. Now, all the hypotheses of Theorem 4 are fulfilled if conditions 1)-6) are all satisfied. Indeed:

1. if the graph is strongly connected, then $J(k)$ is irreducible for any k;
2. condition 2) implies that all the diagonal elements of $J(k)$ are strictly positive for any k;
3. condition 3) implies that all the off diagonal elements of $J(k)$ are non-negative for any k
4. $\sum_{i=1}^{m} J_{ij}(k) = \bar{c}(k) = 1$ for any k (condition 5)).

Thus, using Theorem 8.4.1 it is possible to conclude that all trajectories of the network globally converge towards $\mathcal{M}$. That is, consensus is achieved for the synchronous network. Furthermore, if the delays are all bounded, Theorem 8.5.2 immediately implies that also all trajectories of the asynchronous implementation of the network globally converge towards $\mathcal{M}$. That is, the asynchronous network achieves consensus.

8.6 Networks of discrete time and asynchronous systems

We now further look at the convergence of networked systems and at the design of decentralized communication protocols. In what follows we will use standard definitions from graph theory (fur further details see e.g. [66]). Assume that in (8.2) the smooth functions ϕ_i are defined as:

$$\phi_i\left(x_i, k\right) := f\left(x_i(k), k\right) + \sum_{j \in N_i} \left[h\left(x_j(k)\right) - h\left(x_i(k)\right)\right] \tag{8.11}$$

where N_i is the set of neighbors of the i-th agent on the graph. The cardinality of N_i, denoted as D_i, is the degree of node i (for directed networks D_i denotes the in-degree of node i). Then, the dynamical equations (8.2) become

$$x_i\left(k+1\right) = f\left(x_i\left(k\right), k\right) + \sum_{j \in N_i} \left[h\left(x_j(k)\right) - h\left(x_i(k)\right)\right], \quad i = 1, \ldots, N \tag{8.12}$$

with initial conditions $x\left(k_0\right) = x_{k0}$, $k_0 \geq 0$. Notice that the above equations represent a network of agents interacting diffusively, by means of the output function h, see e.g. [83]. We will refer to (8.12) as a discrete time network, or synchronous implementation of a network of asynchronous systems. The following set of differential equations is termed as the asynchronous network, or asynchronous implementation of the network

$$\begin{array}{ll} x_i\left(k+1\right) = f\left(x_i\left(\tau_i^i\left(k\right)\right)\right) + \sum_{j \in N_i} \left[h\left(x_i\left(\tau_i^i\left(k\right)\right)\right) - h\left(x_j\left(\tau_j^i\left(k\right)\right)\right)\right] & \forall k \in T_i \\ x_i\left(k+1\right) = x_i\left(k\right) & \forall k \notin T_i \end{array} \tag{8.13}$$

where the set of times T_i and τ_j^i are defined as in Section 8.2. We can now give sufficient conditions on the function h that ensure nodes convergence for both undirected and directed discrete time networks of the form (8.12) and (8.13).

Theorem 8.6.1. *All trajectories of the (directed) undirected (strongly) connected network described by (8.12) converge towards each other if (possibly after some smooth coordinate transformation) the coupling functions and vector fields are such that, for any $x \in \mathbb{R}^N$ and for any $k \geq k_0$: 1) $\frac{\partial f(x_i,k)}{\partial x_i} - D_i \frac{\partial h(x_i)}{\partial x_i} > 0$, $\forall i$; 2) $\frac{\partial h(x_j)}{\partial x_j} \geq 0$, $\forall i, j$, $i \neq j$; 3) $\frac{\partial f(x_i,k)}{\partial x_i} - D_i \frac{\partial h(x_i)}{\partial x_i} + \sum_{j \in N_i} \frac{\partial h(x_j)}{\partial x_j} = \bar{c}(k) \leq 1$*

Proof. For the network of interest, the invariant subspace $\mathcal{M}$ in phase space is

$$\mathcal{M} := \left\{x_i = x_j, \quad i \neq j\right\} \tag{8.14}$$

To prove convergence of all trajectories towards $\mathcal{M}$, it suffices to notice that under hypotheses 1)-3) the network satisfies all the hypotheses of Theorem 8.4.1 (recall the definition of ϕ_i given in (8.11)). Indeed, note that the fact that J is primitive in Theorem 8.4.1 is automatically guaranteed by the connectivity property of the network and by the choice of the communication protocol. □

Corollary 8.6.1. *If all the hypotheses of Theorem 8.6.1 are satisfied, then all trajectories of the asynchronous implementation of the network given by (8.13), converge towards each other.*

Proof. The proof is obtained trivially from the application of Theorem 8.5.1 and Theorem 8.6.1.

8.6.1 Coexistence of multiple protocols

Our results can be easily extended to the case where the nodes of both the network (8.12) and its asynchronous implementation (8.13), are connected by means of heterogeneous (non-identical) coupling functions, h_{ij}. We will consider the following discrete time network

$$x_i\left(k+1\right)=f\left(x_i\left(k\right),k\right)+\sum_{j\in N_i}\left[h_{ij}\left(x_j(k)\right)-h_{ij}\left(x_i(k)\right)\right],\quad j\in N_i,\quad i=1,\ldots,N \tag{8.15}$$

and its asynchronous implementation

$$\begin{array}{ll} x_i\left(k+1\right)=f\left(x_i\left(\tau_i^i\left(k\right)\right)\right)+\sum_{j\in N_i}\left[h_{ij}\left(x_i\left(\tau_i^i\left(k\right)\right)\right)-h_{ij}\left(x_j\left(\tau_j^i\left(k\right)\right)\right)\right] & \forall k\in T_i \\ x_i\left(k+1\right)=x_i\left(k\right) & \forall k\notin T_i \end{array} \tag{8.16}$$

Theorem 8.6.2. *All trajectories of the undirected connected network (or of the strongly connected directed network), described by (8.15) converge towards each other if (possibly after some smooth coordinate transformation) the vector fields and the coupling functions are such that, for any $x\in\mathbb{R}^N$ and for any $k\geq k_0$: 1) $\frac{\partial f(x_i,k)}{\partial x_i}-\sum_{j\in N_i}\frac{\partial h_{ij}(x_i)}{\partial x_i}>0$, $\forall i$; 2) $\frac{\partial h_{ij}(x_j)}{\partial x_j}\geq 0$, $\forall i,j,\ i\neq j$; 3) $\frac{\partial f(x_i,k)}{\partial x_i}-\sum_{j\in N_i}\frac{\partial h_{ij}(x_i)}{\partial x_i}+\sum_{j\in N_i}\frac{\partial h_{ji}(x_j)}{\partial x_j}=\bar{c}(k)\leq 1$, $\forall i,j$*

Proof. It is straightforward to check that in this case, the subspace $\mathcal{M}$ is given by (8.14). The proof can then be concluded by noticing that in the above hypotheses, the conditions required by Theorem 8.4.1 are all satisfied. □

Corollary 8.6.2. *If all the hypotheses of Theorem 8.6.2 are satisfied for (8.15), then all trajectories of (8.16) converge towards each other.*

8.6.2 Example: discrete time and asynchronous consensus

We illustrate the application of the results derived so far to the problem of achieving consensus in discrete time networks. This problem is commonly addressed in synchronous networks ([203], [85], [105]), while only few papers in the literature deal with the asynchronous case, e.g. [54]). We analyze the convergent behavior of a set of $N > 1$ dynamical agents interacting with each other synchronously:

$$x_i(k+1) = x_i(k) + \sum_{j \in N_i} h_{ij}(x_j(k)) - h_{ij}(x_i(k)) \tag{8.17}$$

or asynchronously:

$$\begin{array}{ll} x_i(k+1) = x_i(k) + \sum_{j \in N_i} h_{ij}(x_j(\tau(k))) - h_{ij}(x_i(\tau(k))), & k \in T_i \\ x_i(k+1) = x_i(k), & k \notin T_i \end{array} \tag{8.18}$$

Discrete time consensus: directed and undirected networks

We start by analyzing the classical linear agreement protocol (see also Section 8.2.1); that is, $h_{ij}(x) = h(x) = \xi_* x$, with $\xi_* \in \mathbb{R}^+$, in (8.17). We assume that the network topology is a strongly connected one, represented in Figure 8.1. To prove convergence, we only have to satisfy hypotheses 1)-3) of Theorem 8.6.1. Notice that for the undirected network, such hypotheses are immediately satisfied if the couplings are chosen as $\xi_* := \frac{\bar{\xi}}{D_{\max}}$, with $0 < \bar{\xi} < 1$ and $D_{\max} := \max_i \{D_i\}$. Let's now consider a generic nonlinear protocol of the form $h_{ij}(x) = h(x)$. Now, the hypotheses of Theorem 8.6.1 are satisfied if: (i) $0 < 1 - D_i \frac{\partial h(x_i)}{\partial x_i} < 1, \quad \forall i = 1, \ldots, N$; (ii) $\frac{\partial h(x_i)}{\partial x_j} > 0$. A possible choice for h that satisfies such conditions is then:

$$h(\cdot) := G \arctan(\cdot) \tag{8.19}$$

In fact, the derivative of this function is positive, and the gain G can be chosen to satisfy (i). The above protocols can be slightly modified to achieve convergence for the directed network, using Theorem 8.6.2. Specifically, to easily satisfy the hypotheses of such a Theorem, we can choose $h(x) = K_{ij}x$ and $h(x) = G_{ij}\arctan(x)$, where the gains are chosen to fulfill condition 3) of Theorem 8.6.2. Figure 8.2 shows simulation results for the above choices of the protocols, with properly designed gains.

Asynchronous consensus, directed and undirected networks

Corollary 8.6.1 and Corollary 8.6.2 imply that the protocols derived above will work for the asynchronous network (8.18). We assume that the topology of the network is again that of Figure 8.1, while the sampling times are given in Table 8.1. Figure

Table 8.1: Values of the sampling times for each node

node	1	2	3	4	5	6	7	8
sampling time	1	0.3	2	3	0.5	2	0.4	1

8.3 shows the behavior of the state variables of the nodes in the asynchronous

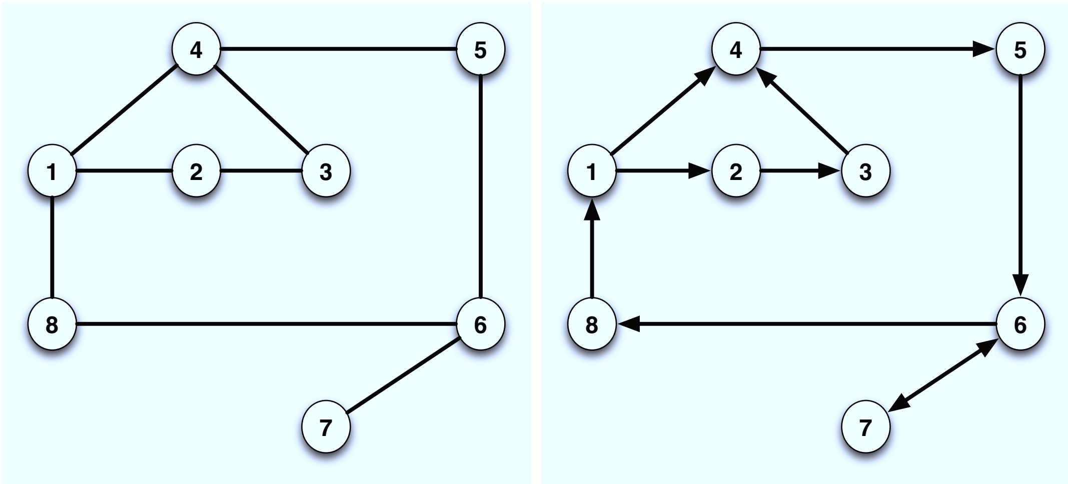

Figure 8.1: Undirected and directed networks used for the numerical validation.

network with the decentralized linear protocol (top panels), and the behavior of the same network, controlled by the asynchronous implementation of the nonlinear communication strategy in (8.19) (bottom panels).

Using mixed protocols to reach consensus

We now provide numerical validation for Theorem 8.6.2 and Corollary 8.6.2, by considering the networks in Figure 8.1. The coupling functions between the nodes of the networks are specified in Table 8.2. Figure 8.4 shows: simulation results for both the undirected and directed discrete time networks (top panels), and the behavior of for their asynchronous implementation (bottom panels). All the simulations confirm the theoretical predictions.

Table 8.2: Coupling functions

edge (undirected network)	edge (directed network)	$h(\cdot)$
$1-4$, $2-3$, $6-7$, $6-8$, $1-8$	$1 \to 4$, $2 \to 3$, $7 \to 6$, $6 \to 8$, $1 \to 8$	$G_{ij} \arctan(\cdot)$
$1-2$, $3-4$, $4-5$, $5-6$	$1 \to 2$, $3 \to 4$, $4 \to 5$, $5 \to 6$, $6 \to 7$	$K_{ij}x$

8.7 Cluster synchronization

We now consider the case of networks of heterogeneous nodes communicating by means of (possibly) heterogeneous coupling functions. Here the control task for the communication protocols is that of ensuring the so-called cluster synchronization regime (also termed as poly-rhythm or concurrent synchronization), see e.g. [142], [19]. At the best of our knowledge, there are currently no papers addressing the problem of finding conditions for cluster synchronization in discrete-time and asynchronous networks. Specifically, we will consider the following discrete time

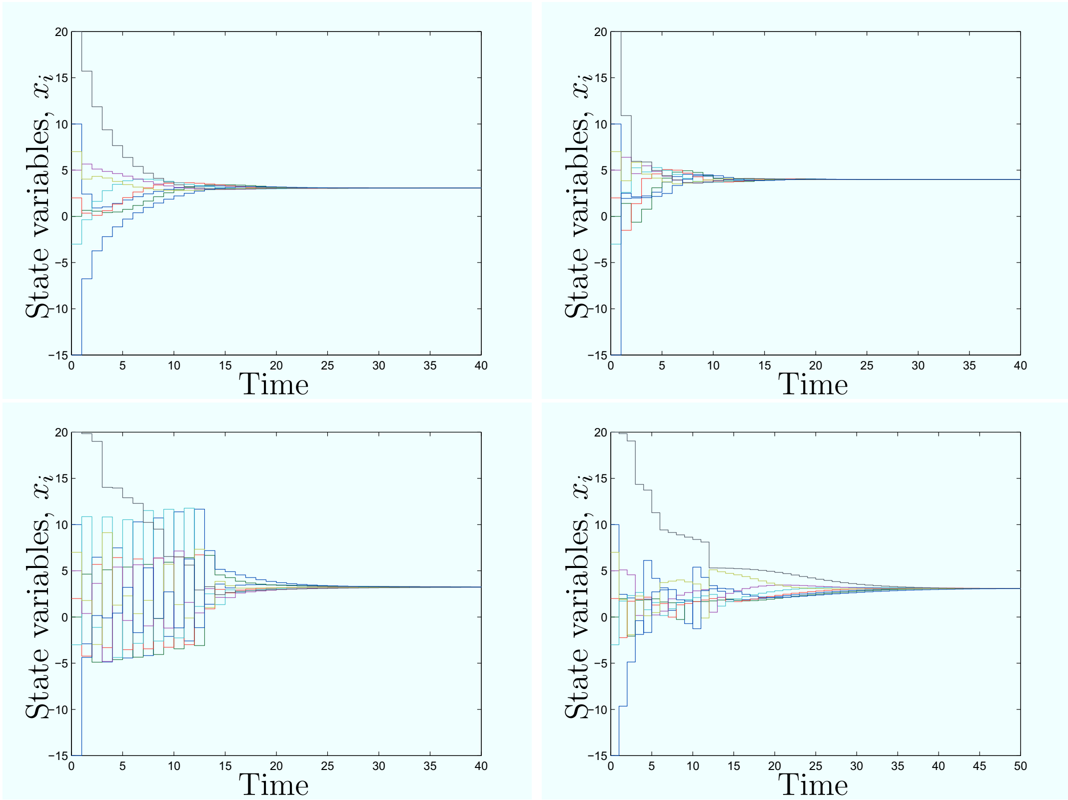

Figure 8.2: Simulation of the discrete-time undirected network (top-left panel) and the discrete-time directed network (top-right panel) in Figure 8.1, with agents controlled by the linear communication strategies. A consensus is also attained for the discrete-time undirected (bottom-left) and directed (bottom-right) network, when the nonlinear protocols are used.

network

$$x_i\,(k+1) = f_{\gamma(i)}\,(x_i\,(k)\,,k) + \sum_{j\in N_i} \left[h_{ij}\,(x_j(k)) - h_{ij}\,(x_i(k))\right], \quad j \in N_i, \quad i = 1,\ldots,N \tag{8.20}$$

and its asynchronous implementation

$$\begin{array}{ll} x_i\,(k+1) = f_{\gamma(i)}\,(x_i\,(\tau_i^i\,(k))\,,k) + \sum_{j\in N_i}\left[h_{ij}\,(x_i\,(\tau_i^i\,(k))) - h_{ij}\left(x_j\left(\tau_j^i\,(k)\right)\right)\right] & \forall k \in T_i \\ x_i\,(k+1) = x_i\,(k) & \forall k \notin T_i \end{array} \tag{8.21}$$

In both of the above equations, γ is defined between two set of indexes, $\gamma : \{1,\ldots,N\} \to v = \{1,\ldots,\Gamma\}$, $\Gamma \le N$ denoting the number of groups in the network. Two nodes, i.e. i and j, have the same dynamics if and only if $\gamma\,(i) = \gamma\,(j)$. Let now $G_1,\ldots,G_\Gamma$ be the groups of agents sharing the same dynamics:

$$G_l =: \{(x_1,\ldots,x_N): \quad \forall i,j = 1,\ldots,N, \quad \gamma\,(i) = \gamma\,(j) = l\}$$

Theorem 8.7.1. *All trajectories of the undirected connected network (or of the*

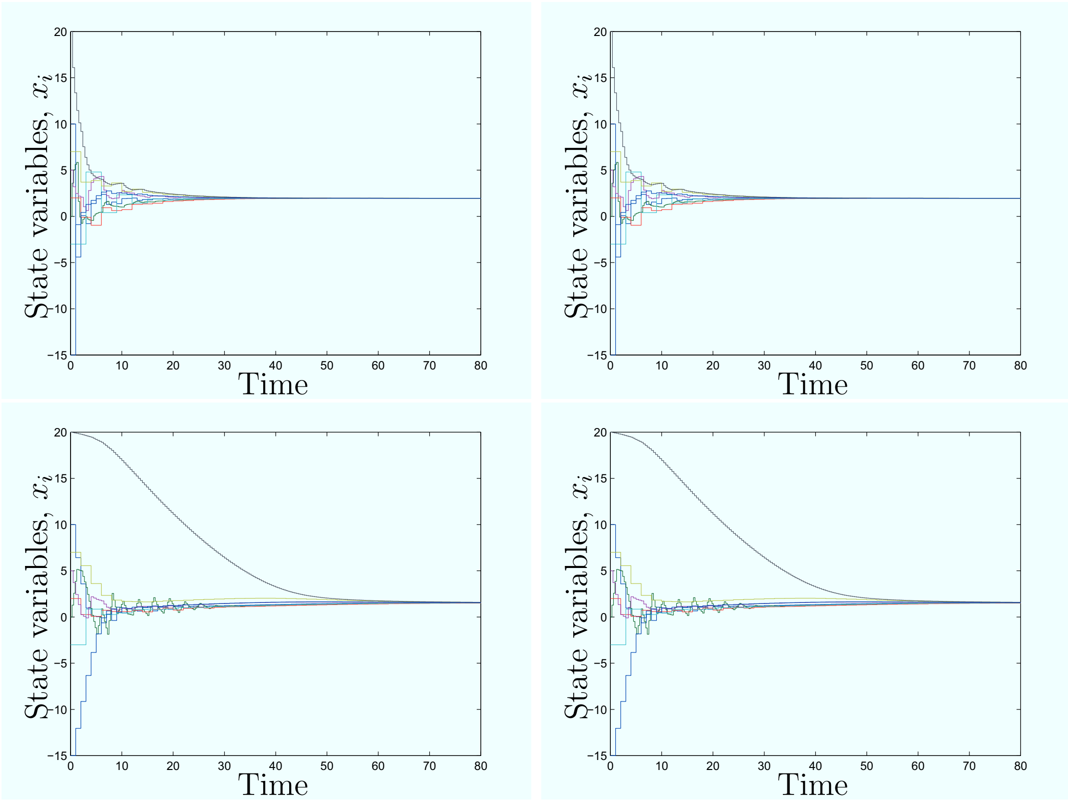

Figure 8.3: Simulation of the asynchronous undirected network (top-left panel) and of the asynchronous directed network (top-right panel) in Figure 8.1, with agents controlled by the linear communication strategy. A consensus is also attained when the agents of the undirected (bottom-left) and directed (bottom-right) are controlled by the asynchronous nonlinear communication protocol. The values of the sampling times are given in Table 8.1

strongly connected directed network), described by (8.20) converge towards each other if all nodes are input-symmetric and (possibly after some smooth coordinate transformation) the coupling functions are such that, for any $x \in \mathbb{R}^N$ *and for any* $k \geq k_0$*: 1)* $\frac{\partial f_{\gamma(i)}(x_i,k)}{\partial x_i} - \sum_{j \in N_i} \frac{\partial h_{ij}(x_i)}{\partial x_i} > 0$, $\forall i$*; 2)* $\frac{\partial h_{ij}(x_j)}{\partial x_j} \geq 0$, $\forall i,j,\ i \neq j$*; 3)* $\frac{\partial f_{\gamma(i)}(x_i,k)}{\partial x_i} - \sum_{j \in N_i} \frac{\partial h_{ij}(x_i)}{\partial x_i} + \sum_{j \in N_i} \frac{\partial h_{ji}(x_j)}{\partial x_j} = \bar{c}_{\gamma(i)}(k) < 1$, $\forall i,j : \gamma(i) = \gamma(j)$

Proof. Notice that under the input-symmetric hypothesis, the following linear invariant (poli-synchronous) subspace exists:

$$\mathcal{M} := \{x_i = x_j, \quad \forall i,j : \gamma(i) = \gamma(j)\}$$

We have to prove that all system trajectories converge towards $\mathcal{M}$. Let $J(k)$ be the Jacobian of network dynamics. Hypotheses 1) - 3) imply that $\|J(k)\|_1 < 1$ for any $x \in \mathbb{R}^N$ and for any $k \in \mathbb{N}$. That is, the network dynamics is contracting. Therefore, all system trajectories globally converge towards $\mathcal{M}$. □

Corollary 8.7.1. *If all hypotheses of Theorem 8.7.1 are satisfied for (8.20), then*

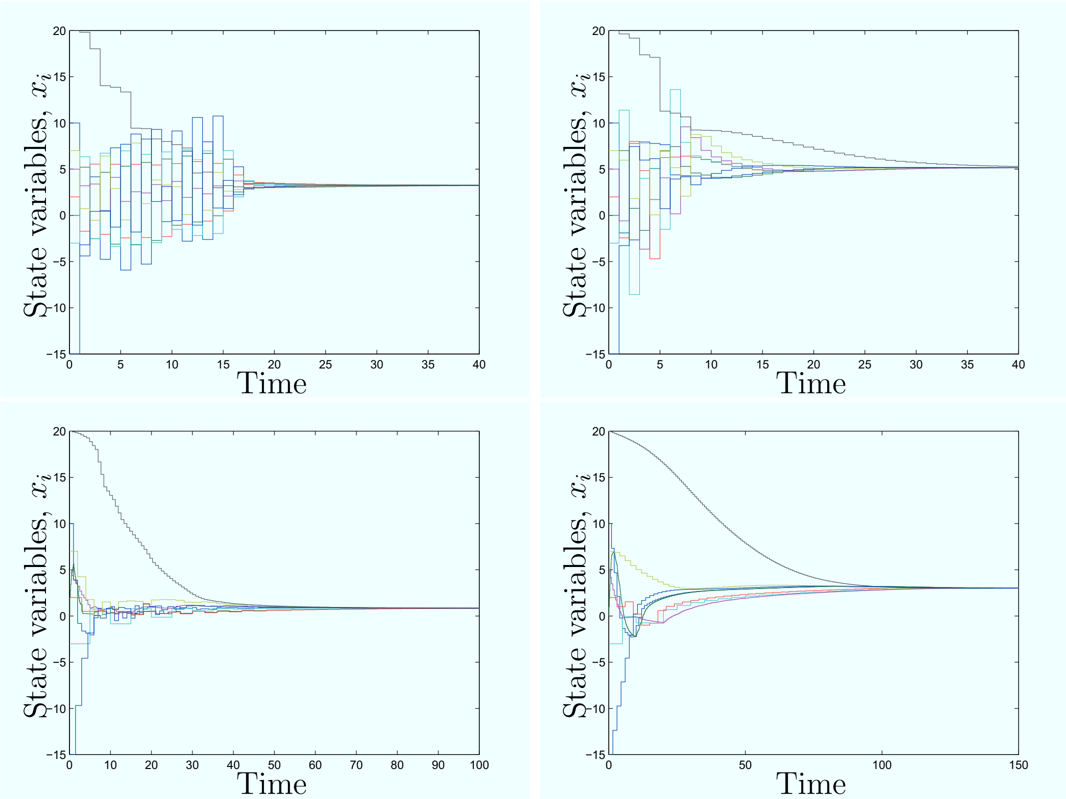

Figure 8.4: Simulation of the synchronous discrete-time undirected network (top-left panel) and the directed network (top-right panel) in Figure 8.1, with agents controlled by both the linear and nonlinear communication strategies. A similar behavior is obtained for the asynchronous undirected (bottom-left) and directed (bottom-right) networks (the sampling times for each node are in Table 8.1). The coupling functions are in Table 8.2.

all trajectories of (8.21) converge towards each other.

8.7.1 Example: cluster synchronization of Hopfield models

As an example, consider the problem of synchronizing a network of heterogeneous discrete time Hopfield models (see e.g. [207]). The network that we are going to analyze is composed by two groups of dynamical systems and is schematically represented in Figure 8.5. Thus, the objective of the decentralized control strategy is that of ensuring that, at steady state, two clusters of synchronized nodes emerge. In terms of the notation introduced above, the objective of the control is that of ensuring convergence of all network trajectories towards the poli-synchronous subspace

$$\mathcal{M} := \{x_1 = x_6 = x_7 = x_8 = x_9\} \bigcup \{x_2 = x_3 = x_4 = x_5\} \tag{8.22}$$

In Figure 8.5, the nodes indicated with a square have dynamics

$$x_i\left(k+1\right)=a\left(k\right)x_i\left(k\right)+b\left(k\right)g_1\left(x_i(k)\right)+u_i\left(k\right)+\sum_{l\in N_i}\left[h\left(x_l(k)\right)-h\left(x_i(k)\right)\right],\quad x_i\in\mathbb{R} \tag{8.23}$$

while the dynamics of nodes depicted by circles is given by

$$x_j\left(k+1\right)=c\left(k\right)x_j\left(k\right)+d\left(k\right)g_2\left(x_j(k)\right)+u_j\left(k\right)+\sum_{l\in N_j}\left[h\left(x_l(k)\right)-h\left(x_j(k)\right)\right],\quad x_j\in\mathbb{R} \tag{8.24}$$

In (8.23) and (8.24), the functions g_1 and g_2 denote some activation functions, the time-varying coefficients $a\left(k\right)$, $b\left(k\right)$, $c\left(k\right)$, $d\left(k\right)$ can be interpreted as the strength of the activations, while u_i and u_j are the inputs to each node of the network. We assume that the input is common to all nodes of the same group and that nodes can communicate to each other. The asynchronous implementation of (8.23) and (8.24) is given by:

$$\begin{aligned}
&x_i\left(k+1\right)=a\left(k\right)x_i\left(\tau_i^i(k)\right)+b\left(k\right)g_1\left(x_i(\tau_i^i(k))\right)+u_i\left(k\right)+\textstyle\sum_{l\in N_i}\left[h\left(x_l(\tau_l^i(k))\right)-h\left(x_i(\tau_i^i(k))\right)\right], && \forall k\in T_i\\
&x_i\left(k+1\right)=x_i\left(k\right), && \forall k\notin T_i\\
&x_j\left(k+1\right)=c\left(k\right)x_j\left(\tau_j^j(k)\right)+d\left(k\right)g_2\left(x_j(\tau_j^j(k))\right)+u_j\left(k\right)+\textstyle\sum_{l\in N_j}\left[h\left(x_l(\tau_l^j(k))\right)-h\left(x_j(\tau_j^j(k))\right)\right], && \forall k\in T_j\\
&x_j\left(k+1\right)=x_j\left(k\right), && \forall k\notin T_j
\end{aligned} \tag{8.25}$$

It is straightforward to check that the subspace defined in (8.22) is flow invariant for (8.23)-(8.24) (or (8.25 in the asynchronous case). In what follows, we set:

$$\begin{array}{lll}
a\left(k\right)=0.5+\frac{1}{1+k}, & b\left(k\right)=0.4+\frac{k}{k^2+1}\sin\left(\frac{k\pi}{2}\right), & g_1\left(x\right)=0.5\left(x-\sin\left(x\right)\right)\\
c\left(k\right)=0.5, & d\left(k\right)=0.3, & g_2\left(x\right)=0.5\left(x+\sin\left(x\right)\right)
\end{array}$$

Note that the linear and arctan control strategies derived in Section 8.6.2 satisfy all of the hypotheses of Theorem 8.7.1, if the gains are properly tuned. In Figure 8.6 (top panels) the behavior is shown of the network represented in Figure 8.5, controlled by both the linear and nonlinear communication strategy. Such panels show that, as expected, all network trajectories converge towards the poli-synchronous subspace defined in (8.22). That is, at steady state, in accordance with Theorem 8.7.1 and Corollary 8.7.1, two clusters of nodes emerge, each synchronized onto a different common evolution of all its nodes.

We now assume that the two groups of agents composing the network have different computational resources. Specifically, we assume that the group of *square* agents has sampling time equal to 0.3, while the group of *circle* agents has sampling time equal to 0.5. As shown in Figure 8.6 (bottom panels), even in the asynchronous case, the same control strategies ensure cluster synchronization for the network, as predicted by Corollary 8.7.1. Finally, in Figure 8.7 the behavior is shown of the network, when the communication strategy between the *circle* nodes is chosen to be linear, while the *intra-group* strategy is chosen to be nonlinear.

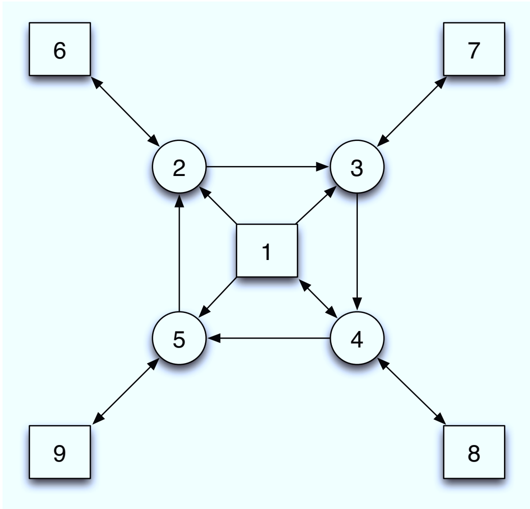

Figure 8.5: Network of heterogeneous Hopfield neurons. Notice that all the nodes belonging to the same group are input-symmetric when the coupling functions chosen as in Section 8.7.1. Indeed, each of the nodes belonging to the *square* group receives one input from one of the *circle* nodes. On the other hand, each of the *circle* nodes receives two inputs from two *square* nodes and one input from one *circle* node.

8.8 Concluding remarks

We have presented a coherent study of contraction in discrete-time and asynchronous dynamical systems. After stating the problem, a set of conditions was given guaranteeing convergence of trajectories of discrete-time and asynchronous dynamical systems of interest towards each other. Specifically, it was shown that, if the synchronous implementation of a given asynchronous system is contracting, then all trajectories of the asynchronous model converge towards each other. The results were then used to investigate consensus and synchronization of both directed and undirected networks of synchronous and asynchronous discrete time systems showing that, under appropriate conditions on the topology and on the distributed communication protocol, all nodes of such networks evolve asymptotically towards a common solution. Following our approach, we were able to design distributed control strategies ensuring consensus and (cluster) synchronization. We also gave conditions ensuring network convergence in the case where multiple protocols are used within the same network. The theoretical results were illustrated via a number of numerical examples showing the effectiveness of the methodology presented in the Chapter. We wish to emphasize that the use of nonlinear contraction theory, possibly based on the use of non-euclidean norms, is a powerful analysis and design tool in the context of consensus and synchronization of networked systems. In the next Chapter we will provide some applications to synthetic and computational biology.

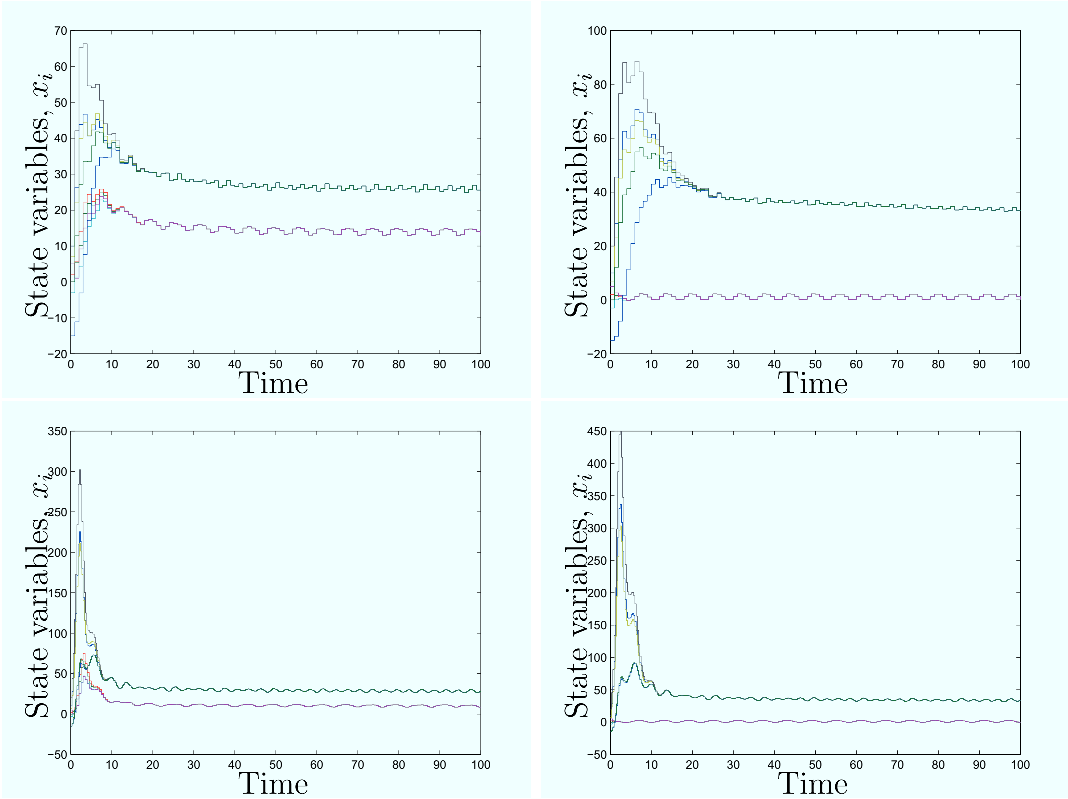

Figure 8.6: Simulation of the discrete time network in Figure 8.5, with all nodes controlled by: (top-left panel) the linear communication strategy; (top-right panel) the nonlinear communication strategy. In both panels cluster synchronization is shown, where the two groups of nodes composing the network are synchronized. A similar poli-synchronous behavior is shown by the asynchronous network with nodes controlled by the linear communication strategy (bottom-left) and the nonlinear communication strategy (bottom-right).

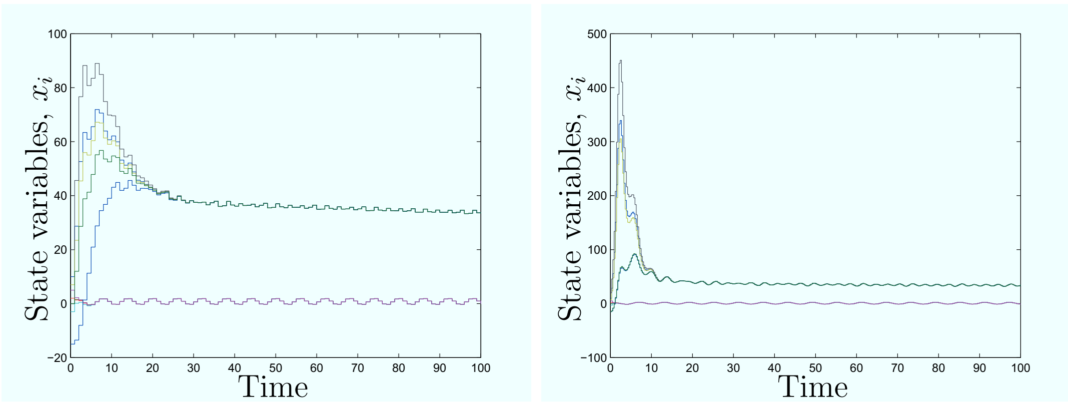

Figure 8.7: Behavior of the network in Figure 8.5, when both linear and nonlinear distributed communication strategies are used. Left panel: discrete time network; right panel: asynchronous network.

Chapter 9

Applications to synthetic and computational biology

In this Chapter, applications of contraction theory to some interesting open problems in both synthetic and computational biology are shown. Specifically, using some of the results on contracting systems of Chapter 4 we study: (i) entrainment of transcriptional modules, (ii) synchronization of quorum sensing networks, (iii) the dynamical behavior of network motifs. In particular, in this Chapter we will characterize some classes of transcriptional systems showing that they can be entrained by any exogenous input. That is, when forced by any periodic signal, such systems present an output which is periodic, with the same period of the forcing. We then turn our analysis into a design tool, showing that our methodology can be used to design novel synthetic transcriptional circuits that can be entrained. As a further application to synthetic biology, we show how to entrain a population of Repressilators. Such circuits are coupled by means of a shared variable, whose dynamics cannot be neglected. This kind of network is common in many natural instances. Motivated by this, we extend our analysis to the problem of (group, or cluster) synchronizing nodes which communicate only by means of their environment (quorum sensing). Finally, we use contraction theory and symmetries of a vector field to analyze the functionalities of network motifs. The results presented in this Chapter were partly presented in [161], [164], [163].

9.1 Introduction

In this Chapter, we apply nonlinear contraction theory to synthetic and computational biology. Specifically, the main problems addressed in the chapter are:

- finding sufficient conditions ensuring *entrainment* of transcriptional systems;
- providing guidelines for the analysis/control of synchronization in *quorum sensing* networks;

- providing a coherent theoretical framework for the analysis/control of network motifs.

Periodic, clock-like rhythms pervade nature and regulate the function of all living organisms. For instance, *circadian rhythms* are regulated by an endogenous biological clock entrained by the light signals from the environment that then acts as a pacemaker, [72]. Moreover, such an entrainment can be obtained even if daily variations are present, like e.g. temperature and light variations. Another important example of entrainment in biological systems is at the molecular level, where the synchronization of several cellular processes is regulated by the cell cycle [189].

An important question in mathematical and computational biology is that of finding conditions ensuring entrainment to occur. The objective is to identify classes of biological systems that can be entrained by an exogenous signal. To solve this problem, modelers often resort to simulations in order to show the existence of periodic solutions in the system of interest. Simulations, however, can never *prove* that solutions exist for all parameter values, and they are subject to numerical errors. Moreover, robustness of entrained solutions needs to be checked in the presence of noise and uncertainties, which cannot be avoided experimentally.

Section 9.2 answers to the above question. Some sufficient conditions are found ensuring entrainment for several classes of biochemical systems. In particular, we start by showing that a well known transcriptional module exhibits an entrained behavior for *any* value of its biochemical parameters. Motivated by such a module, we then extend our analysis to different classes of transcriptional circuits as well as to combinations of modules. The proposed methodology is then turned into a tool for designing biological systems exhibiting entrainment when forced by a periodic signal. Finally, we show an application of our results to synthetic biology. The where we design is carried out of the biochemical parameters of a Repressilator circuit (see Chapter 5) so as to guarantee entrainment of the population.

As pointed out in Section 9.2, the network of Repressilators considered can be thought of as an *all-to-all* network, with nodes coupled by means of a shared quantity (the environment), whose dynamics cannot be neglected. This modeling assumption is in contrast with networks analyzed in Chapter 6, Chapter 7 and Chapter 8, where communication between nodes was *directed* and typically present only among some node.

However, in many natural instances, network nodes do not communicate directly, but rather by means of noisy and continuously changing environments. Bacteria, for instance, produce, release and sense signaling molecules (so-called autoinducers) which can diffuse in the environment and are used for population coordination. This mechanism, known as *quorum sensing* [125], [130], [134] is believed to play a key role in bacterial infection, as well as e.g. in bioluminescence and biofilm formation [6], [129]. In a neuronal context, a mechanism similar to that of quorum sensing may involve *local field potentials*, which may play an important role in the synchronization of groups of neurons [141], [28], [181], [5], [183], [184], [60], [119], or it may occur through a different level in a cortical hierarchy [90], [27], [63], [65], [206]. Other examples of such a mechanism are the synchronization of chemical oscillations of catalyst-loaded reactants in a medium of catalyst-free solution [185], cold atoms interacting with a coherent electromagnetic field [86] and the onset of coordinated activity in a population of micro-organisms living in a shared environment [75], [147]. In this Chapter, we will use the generic term *quorum sensing* to describe the fact that interactions between nodes occur through a shared environmental variable, regardless of the dependence of this variable on the number of network nodes. Mathematical work on such quorum sensing topologies is relatively sparse (e.g., [61], [181], [156], [91], [208], [150]) compared to that on diffusive topologies, and it often neglects the dynamics of the quorum variables or the environment, as well as the global effects of nonlinearities. This sparsity of results is somewhat surprising given that, besides its biological pervasiveness, quorum sensing may also be viewed as an astute *computational* tool. Specifically, the use of a shared variable in effect significantly reduces the number of links required to achieve a given connectivity [181]. In sections 9.3 - 9.3.5 we address the problem of studying synchronization phenomena in those quorum sensing networks. In Section 9.3.6 we also show how the presented methodology can be applied to synchronize networks characterized by a quorum sensing mechanism.

We conclude this Chapter by presenting final applications of contraction analysis to the study of biological systems. We show how contraction can be used together with the symmetry properties of the vector field (see Chapter 4) to determine the behavior, and hence the functionality, of network motifs.

9.2 Entrainment of transcriptional systems

From a mathematical viewpoint, the problem of formally showing that entrainment takes place is known to be very difficult. Indeed, if a stable linear time-invariant model is used to represent the system of interest, then entrainment is usually expected, when the system is driven by an external periodic input, with the system response being a filtered, shifted version of the external driving signal. However, in general, as is often the case in biology, models are nonlinear. The response of nonlinear systems to periodic inputs is the subject of much current systems biology experimentation; for example, in [123], the case of a cell signaling system driven by a periodic square-wave input is considered. From measurements of a periodic output, the authors fit a transfer function to the system, implicitly modeling the system as linear even though (as stated in the Supplemental Materials to [123]) there are saturation effects so the true system is nonlinear. For nonlinear systems, driving the system by an external periodic signal does not guarantee the system response to also be a periodic solution, as nonlinear systems can exhibit harmonic generation or suppression and complex behavior such as chaos or quasi-periodic solutions [97]. This may happen even if the system is well-behaved with respect to constant inputs; for example, there are systems which converge to a fixed steady state no matter what is the input excitation, so long as this input signal is constant, yet respond chaotically to the simplest oscillatory input; we outline such an example in the Materials and Methods Section, see also [172]. Thus, a most interesting open problem is that of finding conditions for the entrainment to external inputs of biological systems modeled by sets of nonlinear differential equations. This problem is addressed in this Section.

For concreteness, we focus mainly on transcriptional systems, as well as related biochemical systems, which are basic building blocks for more complex biochemical systems. However, the results that we obtain are of more generality. To illustrate this generality, and to emphasize the use of our techniques in synthetic biology design, we discuss as well the entrainment of a Repressilator circuit in a parameter regime in which endogenous oscillations to not occur, as well as the synchronization of a network of Repressilators. A surprising fact is that, for these applications, and contrary to many engineering applications, norms other than Euclidean, and associated matrix measures, must be considered.

Mathematical model and problem statement

We study a general externally-driven transcriptional module. We assume that the rate of production of a transcription factor X is proportional to the value of a time dependent input function $u(t)$, and X is subject to degradation and/or dilution at a linear rate. (Later, we generalize the model to also allow nonlinear degradation as well.) The signal $u(t)$ might be an external input, or it might represent the concentration of an enzyme or of a second messenger that activates X. In turn, X drives a downstream transcriptional module by binding to a promoter (or substrate), denoted by e with concentration $e = e(t)$. The binding reaction of X with e is reversible and given by:

$$X + e \rightleftharpoons Y$$

where Y is the complex protein-promoter, and the binding and dissociation rates are k_1 and k_2 respectively. As the promoter is not subject to decay, its total concentration, e_T, is conserved, so that the following conservation relation holds:

$$e + Y = e_T \tag{9.1}$$

We wish to study the behavior of solutions of the system that couples X and e, and specifically to show that, when the input $u(t)$ is periodic with period T, this coupled system has the property that all solutions converge to some globally attracting limit cycle whose period is also T.

Such transcriptional modules are ubiquitous in both natural and synthetic biological networks, and their behavior was recently studied in [40] in the context of "retroactivity" (impedance or load) effects. If we think of $u(t)$ as the concentration of a protein Z that is a transcription factor for X, and we ignore fast mRNA dynamics, such a system can be schematically represented as in Figure 9.1, which is

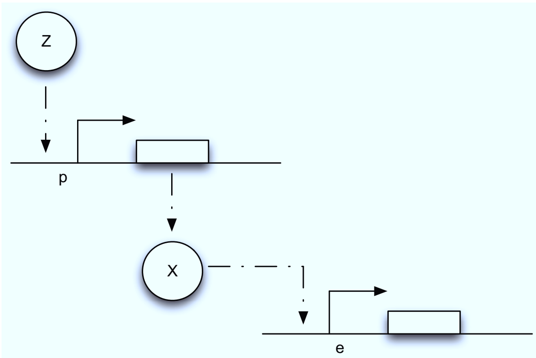

Figure 9.1: A schematic diagram of the transcriptional system modeled in (9.2). As explained in [40], the transcriptional component takes as input the concentration of protein Z and gives as output the concentration of protein X. The downstream transcriptional module takes as input the concentration of protein X.

adapted from [40]. Notice that $u(t)$ here does not need to be the concentration of a transcriptional activator of X for our results to hold. The results will be valid for any mathematical model for the concentrations, x, of X and y, of Y (the concentration of e is conserved) of the form:

$$\begin{aligned} \dot{x} &= u\left(t\right) - \delta x + k_1 y - k_2\left(e_T - y\right) x \\ \dot{y} &= -k_1 y + k_2\left(e_T - y\right) x \end{aligned} \tag{9.2}$$

An objective in this Section is, thus, to show that, when u is a periodic input, all solutions of system (9.2) converge to a (unique) limit cycle (Figure 9.2). The key tool in this analysis is to show that uniform contractivity holds, i.e. the system is contracting with respect to any (positive) input. Since in this example the input appears additively, uniform contractivity is simply the requirement that the unforced system ($u = 0$) is contractive. Thus, the main step will be to establish the following technical result:

Theorem 9.2.1. *The system*

$$\begin{aligned} \dot{x} &= -\delta x + k_1 y - k_2\left(e_T - y\right) x \\ \dot{y} &= -k_1 y + k_2\left(e_T - y\right) x \end{aligned}$$

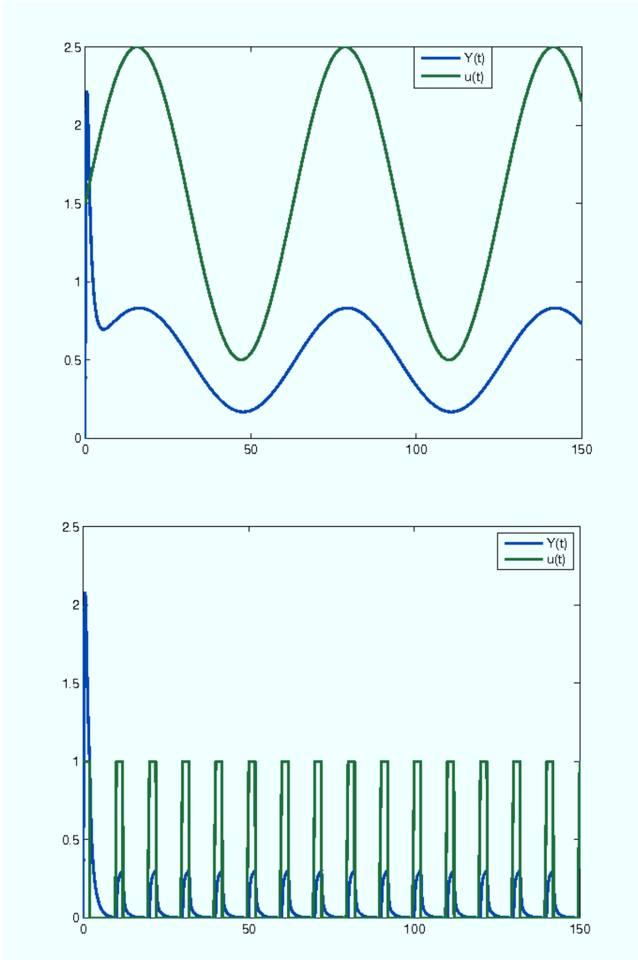

Figure 9.2: Entrainment of the transcriptional module (9.2). Time in minutes on the x-axis. The state of the system (green), y, is entrained to both $u(t) = 1.5+\sin(0.1t)$ and to a repeating $\{0, 1\}$ sequence. System parameters are set to: $\delta = 3$, k_1=1, $k_2 = 0.1$.

where

$$(x(t), y(t)) \in \mathcal{C} = [0, \infty) \times [0, e_T] \tag{9.3}$$

for all $t \geq 0$, *and* e_T, k_1, k_2, *and* δ *are arbitrary positive constants, is contracting.*

Appealing to Theorem 4.3.1, we then have the following immediate Corollary:

Theorem 9.2.2. *For any given nonnegative periodic input u of period T, all solutions of system (9.2) converge exponentially to a periodic solution of period T.*

In the following sections, we introduce a matrix measure that will help establish contractivity, and we prove Theorem 9.2.1. We will also discuss several extensions of this result, allowing the consideration of multiple driven subsystems as well as more general nonlinear systems with a similar structure. (A general graphical algorithm to prove contraction of generic networks of nonlinear systems can also be found in [159] where this transcriptional module is also studied.)

Proof of Theorem 9.2.1

We will use Theorem 4.2.1. The Jacobian matrix to be studied is:

$$J := \begin{bmatrix} -\delta - k_2 (e_T - y) & k_1 + k_2 x \\ k_2 (e_T - y) & -k_1 - k_2 x \end{bmatrix} \tag{9.4}$$

As matrix measure, we will use the measure $\mu_{P,1}$ induced by the vector norm $|Px|_1$, where P is a suitable nonsingular matrix. More specifically, we will pick P diagonal:

$$\begin{bmatrix} p_1 & 0 \\ 0 & p_2 \end{bmatrix} \tag{9.5}$$

where p_1 and p_2 are two positive numbers to be appropriately chosen depending on the parameters defining the system.

It follows from general facts about matrix measures that

$$\mu_{P,1}(J) = \mu_1\left(PJP^{-1}\right) \tag{9.6}$$

where μ_1 is the measure associated to the $|\cdot|_1$ norm and is explicitly given by the following formula:

$$\mu_1(J) = \max_j \left(J_{jj} + \sum_{i \neq j} |J_{ij}| \right) \tag{9.7}$$

Observe that, if the entries of J are negative, then asking that $\mu_1(J) < 0$ amounts to a column diagonal dominance condition. (The above formula is for real matrices. If complex matrices would be considered, then the term J_{jj} should be replaced by its real part $\Re\{J_{jj}\}$.)

Thus, the first step in computing $\mu_{P,1}(J)$ is to calculate PJP^{-1}:

$$\begin{bmatrix} -\delta - k_2 (e_T - y) & \frac{p_1}{p_2}(k_1 + k_2 x) \\ \frac{p_2}{p_1}[k_2 (e_T - y)] & -k_1 - k_2 x \end{bmatrix} \tag{9.8}$$

Using (9.7), we obtain:

$$\mu_{P,1}(J) = \max\left\{ -\delta - k_2(e_T - y) + \left| \frac{p_2}{p_1} k_2 (e_T - y) \right| ; -k_1 - k_2 x + \left| \frac{p_1}{p_2}(k_1 + k_2 x) \right| \right\} \tag{9.9}$$

Note that we are not interested in calculating the exact value for the above measure, but just in ensuring that it is negative. To guarantee that $\mu_{P,1}(J) < 0$, the following two conditions must hold:

$$-\delta - k_2(e_T - y) + \left| \frac{p_2}{p_1} k_2 (e_T - y) \right| < -c_1^2 \tag{9.10}$$

$$-k_1 - k_2 x + \left| \frac{p_1}{p_2} (k_1 + k_2 x) \right| < -c_2^2 \tag{9.11}$$

Thus, the problem becomes that of checking if there exists an appropriate range of values for p_1, p_2 that satisfy (9.10) and (9.11) simultaneously.

The left hand side of (9.11) can be written as:

$$\left(\frac{p_1}{p_2} - 1 \right) (k_1 + k_2 x) \tag{9.12}$$

which is negative if and only if $p_1 < p_2$. In particular, in this case we have:

$$\left(\frac{p_1}{p_2} - 1 \right) (k_1 + k_2 x) \leq \left(\frac{p_1}{p_2} - 1 \right) k_1 := -c_1^2$$

The idea is now to ensure negativity of (9.10) by using appropriate values for p_1 and p_2 which fulfill the above constraint. Recall that the term $e_T - y \geq 0$ represents a concentration. Thus, the left hand side of (9.10) becomes

$$-\delta + \left(\frac{p_2}{p_1} - 1 \right) k_2 (e_T - y) \tag{9.13}$$

The next step is to choose appropriately p_2 and p_1 (without violating the constraint $p_2 > p_1$). Imposing $p_2/p_1 = 1 + \varepsilon$, $\varepsilon > 0$, (9.13) becomes

$$-\delta + \varepsilon k_2 (e_T - y) \tag{9.14}$$

Then, we have to choose an appropriate value for ε in order to make the above quantity uniformly negative. In particular, (9.14) is uniformly negative if and only if

$$\varepsilon < \frac{\delta}{k_2 (e_T - y)} \leq \frac{\delta}{k_2 e_T} \tag{9.15}$$

We can now choose

$$\varepsilon = \frac{\delta}{k_2 e_T} - \xi$$

with $0 < \xi < \frac{\delta}{k_2 e_T}$. In this case, (9.14) becomes

$$-\delta + \varepsilon k_2 (e_T - y) \leq -\xi k_2 e_T := -c_2^2$$

Thus, choosing $p_1 = 1$ and $p_2 = 1 + \varepsilon = 1 + \frac{\delta}{k_2 e_T} - \xi$, with $0 < \xi < \frac{\delta}{k_2 e_T}$, we have $\mu_{1,P}(J) < -c^2$. Furthermore, the contraction rate c^2, is given by:

$$\min \left\{ c_1^2, c_2^2 \right\}$$

Notice that c^2 depends on both system parameters and on the elements p_1, p_2, i.e. it depends on the particular metric chosen to prove contraction. This completes the proof of the Theorem. □

Generalizations

In this Section, we discuss various generalizations that use the same proof technique.

Assuming X activation by enzyme kinetics

The previous model assumed that X was created in proportion to the amount of external signal $u(t)$. While this may be a natural assumption if $u(t)$ is a transcription factor that controls the expression of X, a different model applies if, instead, the "active" form X is obtained from an "inactive" form X_0, for example through a phosphorylation reaction which is catalyzed by a kinase whose abundance is represented by $u(t)$. Suppose that X can also be constitutively deactivated. Thus, the complete system of reactions consists of

$$X + e \rightleftharpoons Y$$

together with

$$X_0 \rightleftharpoons X$$

where the forward reaction depends on u. Since the concentrations of $X_0 + X + Y$ must remain constant, let us say at a value X_{tot}, we eliminate X_0 and have:

$$\begin{aligned} \dot{x} &= u(t)(X_{tot} - x - y) - \delta x + k_1 y - k_2 (e_T - y) x \\ \dot{y} &= -k_1 y + k_2 (e_T - y) x \end{aligned} \tag{9.16}$$

We will prove that if $u(t)$ is periodic and positive, i.e. $u(t) \geq u_0 > 0$, then a globally attracting limit cycle exists. Namely, it will be shown, after having performed a linear coordinate transformation, that there exists a negative matrix measure for the system of interest.

Consider, indeed, the following change of the state variables:

$$x_t = x + y. \tag{9.17}$$

The system dynamics then becomes:

$$\begin{aligned} \dot{x}_t &= u(t)(X_{tot} - x_t) - \delta x_t + \delta y \\ \dot{y} &= -k_1 y + k_2 (e_T - y)(x_t - y) \end{aligned} \tag{9.18}$$

As matrix measure, we will now use the measure μ_∞ induced by the vector norm $|\cdot|_\infty$. (Notice that this time, the matrix P is the identity matrix).

Recall that, given a real matrix J, the matrix measure $\mu_\infty(J)$ is explicitly given by the following formula (see e.g. [124]):

$$\mu_\infty(J) = \max_i \left(J_{ii} + \sum_{j \neq i} |J_{ij}| \right) \tag{9.19}$$

(Observe that this is a row-dominance condition, in contrast to the dual column-dominance condition used for μ_1.)

Differentiation of (9.18) yields the Jacobian matrix:

$$J := \begin{bmatrix} -u(t) - \delta & \delta \\ k_2(e_T - y) & -k_1 + k_2(-e_T - x_t + 2y) \end{bmatrix}$$

Thus, it immediately follows from (9.19) that $\mu_\infty(J)$ is negative if and only if:

$$-u(t) - \delta + |\delta| < -c_1^2 \tag{9.20}$$

$$-k_1 + k_2(-e_T - x_t + 2y) + |k_2(e_T - y)| < -c_2^2 \tag{9.21}$$

The first inequality is clearly satisfied since by hypotheses both system parameters and the periodic input $u(t)$ are positive. In particular, we have:

$$-u(t) - \delta + |\delta| \leq -u_0 := -c_1^2$$

By using (9.17) (recall that $e_T - y \geq 0$), the right hand side of the second inequality can be written as:

$$-k_1 + k_2(-e_T - x_t + 2y) + k_2(e_T - y) = -k_1 - k_2 x$$

Since all system parameters are positive and $x \geq 0$, the above quantity is negative and upper bounded by $-k_1 := -c_2^2$.

Thus, we have that $\mu_\infty(J) < -c^2$, where:

$$c^2 = \min\left\{c_1^2, c_2^2\right\}$$

The contraction property for the system is then proved. By means of Theorem 4.3.1, we can then conclude that the system can be entrained by any periodic input.

Simulation results are presented in Figure 9.3, where the presence of a stable limit cycle having the same period as $u(t)$ is shown.

Multiple driven systems

We may also treat the case in which the species X regulates multiple downstream transcriptional modules which act independently from each other, as shown in Fig-

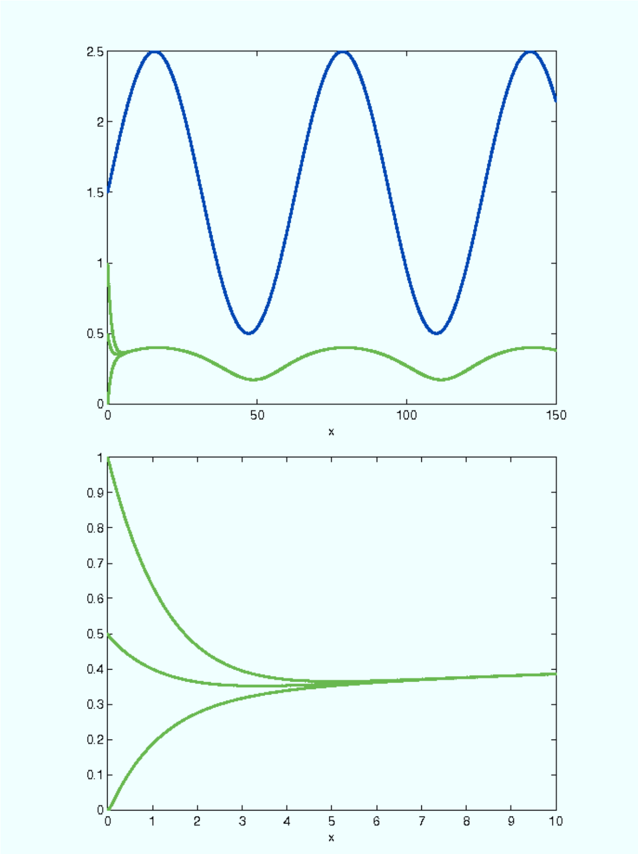

Figure 9.3: Entrainment of the transcriptional module (9.16). Time in minutes on the x-axis. The system state (green), y, is entrained to the periodic input (blue): $u(t) = 1.5 + \sin(0.1t)$. The zoom on $t \in [0, 10]$ min. points out that trajectories starting from different initial conditions converge towards the attracting limit cycle. System parameters are set to: $k_1 = 0.5$, $k_2 = 5$, $X_{tot} = 1$, $e_T = 1$, $\delta = 20$.

ure 9.4. The biochemical parameters defining the different downstream modules may be different from each other, representing a situation in which the transcription factor X regulates different species. After proving a general result on oscillations, and assuming that parameters satisfy the retroactivity estimates discussed in [40], one may in this fashion design a single input-multi output module in which e.g. the outputs are periodic functions with different mean values, settling times, and so forth.

We denote by $e_1, \ldots, e_n$ the various promoters, and use $y_1, \ldots, y_n$ to denote the concentrations of the respective promoters complexed with X. The resulting

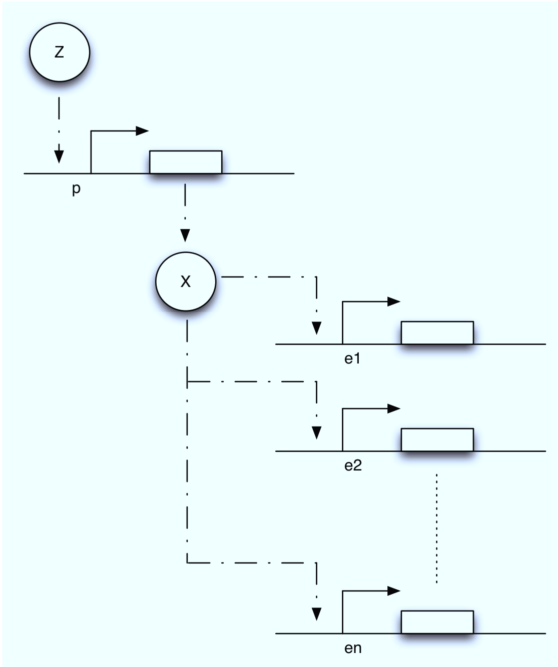

Figure 9.4: Multiple driven transcriptional modules. A schematic diagram of the transcriptional modules given in (9.2)

mathematical model becomes:

$$\begin{aligned}\dot{x} &= u(t) - \delta x + K_{11}y_1 - K_{21}(e_{T,1} - y_1)x + \\ &\quad + K_{12}y_2 - K_{22}(e_{T,2} - y_2)x + \cdots \\ &\quad + K_{1n}y_n - K_{2n}(e_{T,n} - y_n)x \\ \dot{y}_1 &= -K_{11}y_1 + K_{21}(e_{T,1} - y_1)x \\ &\vdots \\ \dot{y}_n &= -K_{1n}y_n + K_{2n}(e_{T,n} - y_n)x\end{aligned} \tag{9.22}$$

We consider the corresponding system with no input first, assuming that the states satisfy $x(t) \geq 0$ and $0 \leq y_i(t) \leq e_{T,i}$ for all t, i.

Our generalization can be stated as follows:

Theorem 9.2.3. *System (9.22) with no input (i.e. $u(t) = 0$) is contracting. Hence, if $u(t)$ is a non-zero periodic input, its solutions exponentially converge towards a periodic orbit of the same period as $u(t)$.*

Proof. We only outline the proof, since it is similar to the proof of Theorem 9.2.2. We employ the following matrix measure:

$$\mu_{P,1}(J) = \mu_1\left(PJP^{-1}\right), \tag{9.23}$$

where

$$P := \begin{bmatrix} p_1 & 0 & 0 & \dots & 0 \\ 0 & p_2 & 0 & \dots & 0 \\ \vdots & \vdots & \vdots & \vdots & \vdots \\ 0 & 0 & 0 & \dots & p_{n+1} \end{bmatrix} \tag{9.24}$$

and the scalars p_i have to be chosen appropriately ($p_i > 0, \quad \forall i = 1, \dots, n+1$).

In this case,

$$J := \begin{bmatrix} -\delta - \sum_{i=1}^{n} K_{2i}(e_{T,i} - y_i) & K_{11} + K_{21}x & K_{12} + K_{22}x & \dots & K_{1n} + K_{2n}x \\ K_{21}(e_{T,1} - y_1) & -K_{11} - K_{21}x & 0 & \dots & 0 \\ K_{22}(e_{T,2} - y_2) & 0 & -K_{12} - K_{22}x & \dots & 0 \\ \vdots & \vdots & \vdots & \ddots & \vdots \\ K_{2n}(e_{T,n} - y_n) & 0 & 0 & \dots & -K_{1n} - K_{2n}x \end{bmatrix} \tag{9.25}$$

and

$$PJP^{-1} := \begin{bmatrix} -\delta - \sum_{i=1}^{n} K_{2i}(e_{T,i} - y_i) & \frac{p_1}{p_2}(K_{11} + K_{21}x) & \frac{p_1}{p_3}(K_{12} + K_{22}x) & \dots & \frac{p_1}{p_{n+1}}(K_{1n} + K_{2n}x) \\ \frac{p_2}{p_1}K_{21}(e_{T,1} - y_1) & -K_{11} - K_{21}x & 0 & \dots & 0 \\ \frac{p_3}{p_1}K_{22}(e_{T,2} - y_2) & 0 & -K_{12} - K_{22}x & \dots & 0 \\ \vdots & \vdots & \vdots & \ddots & \vdots \\ \frac{p_{n+1}}{p_1}K_{2n}(e_{T,n} - y_n) & 0 & 0 & \dots & -K_{1n} - K_{2n}x \end{bmatrix} \tag{9.26}$$

Hence, the $n+1$ inequalities to be satisfied are:

$$-\delta - \sum_{i=1}^{n} K_{2i}(e_{T,i} - y_i) + \frac{1}{p_1}\sum_{i=1}^{n} p_{i+1}\left|K_{2i}(e_{T,i} - y_i)\right| < -c_1^2 \tag{9.27}$$

and

$$-K_{1i} - K_{2i}x + \left|\frac{p_1}{p_{i+1}}(K_{1i} + K_{2i})x\right| < -c_{i+1}^2, \qquad i = 1, 2, \dots, n \tag{9.28}$$

Clearly, the set of inequalities above admits a solution. Indeed, the left hand side of (9.28) can be recast as

$$\left(\frac{p_1}{p_{i+1}} - 1\right)(K_{1i} + K_{2i}x), \qquad i = 1, 2, \dots, n$$

which is negative definite if and only if $p_1/p_{i+1} < 1$ for all $i = 1, \dots, n$. Specifically, in this case we have

$$\left(\frac{p_1}{p_{i+1}}-1\right)(K_{1i}+K_{2i}x) \leq \left(\frac{p_1}{p_{i+1}}-1\right)K_{1i} := -c_{i+1}^2, \qquad i=1,2,\ldots,n$$

Also, from (9.27), as $e_{T,i}-y_i \geq 0$ for all i, we have that (9.27) can be rewritten as:

$$-\delta - \sum_{i=1}^{n} K_{2i}(e_{T,i}-y_i) + \sum_{i=1}^{n} \frac{p_{i+1}}{p_1}(e_{T,i}-y_i) < -c_1^2$$

Since $p_1/p_{i+1} < 1$, we can impose $p_{i+1}/p_1 = 1+\varepsilon_{1,i+1}$ (with $\varepsilon_{1,i+1} > 0$) and the above inequality becomes

$$-\delta + \sum_{i=1}^{n} \varepsilon_{1,i+1} K_{2i}(e_{T,i}-y_i) < -c_1^2$$

Clearly, such inequality is satisfied if we choose $\varepsilon_{1,i+1}$ sufficiently small; namely:

$$\varepsilon_{1,i+1} < \frac{\delta}{(n-1)\,k_2 e_{T,i}}$$

Following a similar derivation to that of the previous Section, we can choose

$$\varepsilon_{i+1} = \frac{\delta}{(n-1)\,k_2 e_{T,i}} - \xi_{i+1}$$

with $0 < \xi_{i+1} < \frac{\delta}{(n-1)k_2 e_{T,i}}$. In this case, we have:

$$c_1^2 := -\sum_{i=1}^{n} \frac{\xi_{i+1}}{n-1} K_{2i} e_{Ti}$$

Thus, $\mu\,(J) < -c^2$, where

$$c^2 = \min_i \{c_i\}\,, \quad i=1,\ldots,n+1$$

The second part of the Theorem is then proved by applying Theorem 4.3.1. □

In Figure 9.5 the behavior of two-driven downstream transcriptional modules is shown. Notice that both the downstream modules are entrained by the periodic input $u\,(t)$, but their steady state behavior is different.

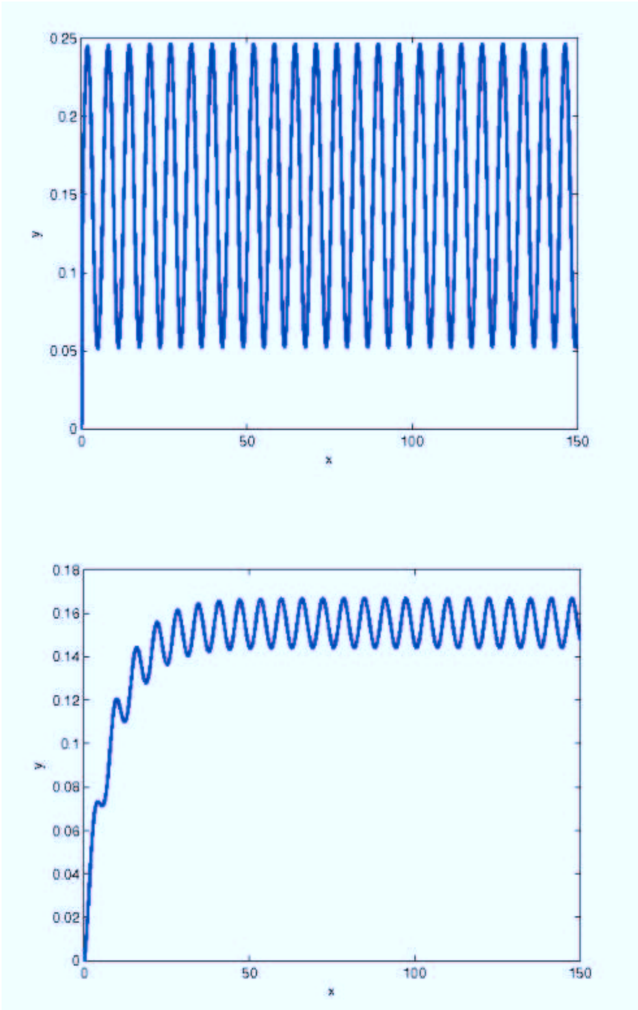

Figure 9.5: Entrainment of two-driven transcriptional modules. Time in minutes on the x-axis. Outputs Y_1 (top) and Y_2 (bottom) of two transcriptional modules driven by the external periodic input $u(t) = 1.5 + \sin(t)$. The parameters are set to: $\delta = 0.01$, $k_{11} = 10$, $k_{21} = 10$, $e_{T,1} = 1$ for module 1 and $k_{12} = 0.1$, $k_{22} = 0.1$, $e_{T,2} = 1$ for module 2.

Notice that, by the same arguments used above, it can be prover that

$$\begin{aligned}
\dot{x} \;&=\; u(t)\,(X_{TOT} - x - \textstyle\sum_{i=1}^{n} y_i) - \delta x + K_{11}y_1 - K_{21}(e_{T,1} - y_1)x + \\
&\quad + K_{12}y_2 - K_{22}(e_{T,2} - y_2)x \;+\; \cdots \\
&\quad + K_{1n}y_n - K_{2n}(e_{T,n} - y_n)x \\
\dot{y}_1 &= -K_{11}y_1 + K_{21}(e_{T,1} - y_1)x \\
&\vdots \\
\dot{y}_n &= -K_{1n}y_n + K_{2n}(e_{T,n} - y_n)x
\end{aligned} \tag{9.29}$$

is contracting.

Transcriptional cascades

A cascade of (infinitesimally) contracting systems is also (infinitesimally) contracting [111], [170] (see Section 4.4 for an alternative proof). This implies that any transcriptional cascade, will also give rise to a contracting system, and, in particular, will entrain to periodic inputs. By a transcriptional cascade we mean a system as shown in Figure 9.6. In this figure, we interpret the intermediate variables Y_i as transcription factors, making the simplifying assumption that TF concentration is proportional to active promoter for the corresponding gene. (More complex models, incorporating transcription, translation, and post-translational modifications could themselves, in turn, be modeled as cascades of contracting systems.)

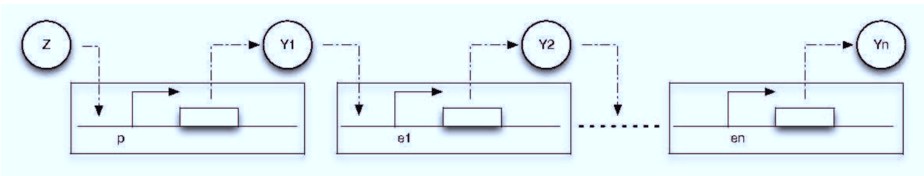

Figure 9.6: Transcriptional cascade discussed in the text. Each box contains the transcriptional module described by (9.2)

More abstract systems

We can extend our results even further, to a larger class of nonlinear systems, as long as the same general structure is present. This can be useful for example to design new synthetic transcription modules or to analyze the entrainment properties of general biological systems. We start with a discussion of a two dimensional system of the form:

$$\begin{aligned}
\dot{x} \;&=\; u\,(t) - a\,(x) + f\,(x,y) \\
\dot{y} \;&=\; -f\,(x,y)
\end{aligned} \tag{9.30}$$

In molecular biology, $a(x)$ would typically represent a nonlinear degradation, for instance in Michaelis-Menten form, while the function f represents the interaction between x and y. The aim of this Section is to find conditions on the degradation and interaction terms that allow one to show contractivity of the unforced (no input u) system, and hence existence of globally attracting limit cycles.

We assume that the state space $\mathcal{C}$ is compact (closed and bounded) as well as convex. Since the input appears additively, we must prove contractivity of the unforced system.

Theorem 9.2.4. *System (9.30), without inputs u, evolving on a convex compact subset of phase space is contracting, provided that the following conditions are all satisfied, for each $x, y \in \mathcal{C}$:*

- $\frac{\partial a}{\partial x} > 0$*;*
- $\frac{\partial f}{\partial y} > 0$*;*
- $\frac{\partial f}{\partial x}$ *does not change sign;*
- $\frac{\partial a}{\partial x} > 2\frac{\partial f}{\partial x}$*.*

Notice that the last condition is automatically satisfied if $\frac{\partial f}{\partial x} < 0$, because $\frac{\partial a}{\partial x} > 0$.

Proof. As before, we prove contraction by constructing an appropriate negative measure for the Jacobian of the vector field. In this case, the Jacobian matrix is:

$$J = \begin{bmatrix} -\frac{\partial a}{\partial x} + \frac{\partial f}{\partial x} & \frac{\partial f}{\partial y} \\ -\frac{\partial f}{\partial x} & -\frac{\partial f}{\partial y} \end{bmatrix} \tag{9.31}$$

Once again, as matrix measure we will use:

$$\mu_{P,1}(J) = \mu_1\left(PJP^{-1}\right) \tag{9.32}$$

with

$$P = \begin{bmatrix} p_1 & 0 \\ 0 & p_2 \end{bmatrix} \tag{9.33}$$

and $p_1, p_2 > 0$ appropriately chosen.

Using (9.32) we have

$$\mu_{P,1}(J) = \max\left\{-\frac{\partial a}{\partial x} + \frac{\partial f}{\partial x} + \left|\frac{p_2}{p_1}\frac{\partial f}{\partial x}\right| ; -\frac{\partial f}{\partial y} + \left|\frac{p_1}{p_2}\frac{\partial f}{\partial y}\right|\right\} \tag{9.34}$$

Following the same steps as the proof of Theorem 9.2.1, we have to show that:

$$-\frac{\partial f}{\partial y} + \left|\frac{p_1}{p_2}\frac{\partial f}{\partial y}\right| < -c_1^2 \tag{9.35}$$

$$-\frac{\partial a}{\partial x} + \frac{\partial f}{\partial x} + \left|\frac{p_2}{p_1}\frac{\partial f}{\partial x}\right| < -c_2^2 \tag{9.36}$$

Clearly, if $\partial f/\partial y > 0$ for every $x, y \in C$ and $p_1 < p_2$, the first inequality is satisfied, with

$$c_1^2 = \left(\frac{p_1}{p_2} - 1\right)\frac{\partial f}{\partial x}$$

To prove the theorem we need to show that there exists $p_1 < p_2$ and c_2^2 satisfying (9.36). For such inequality, since $\partial f/\partial x$ does not change sign in C by hypothesis, we have two possibilities:

1. $\frac{\partial f}{\partial x} < 0$, $\forall x, y \in C$;
2. $\frac{\partial f}{\partial x} > 0$, $\forall x, y \in C$.

In the first case, the right hand side of (9.36) becomes

$$-\frac{\partial a}{\partial x} + \frac{\partial f}{\partial x} - \frac{p_2}{p_1}\frac{\partial f}{\partial x} \tag{9.37}$$

Choosing $p_2/p_1 = 1 + \varepsilon$, with $\varepsilon > 0$, we have:

$$-\frac{\partial a}{\partial x} + \frac{\partial f}{\partial x} - \frac{p_2}{p_1}\frac{\partial f}{\partial x} = -\frac{\partial a}{\partial x} + \varepsilon\frac{\partial f}{\partial x}$$

Specifically, if we now pick

$$\varepsilon > \frac{A}{B}$$

where $A = \max \frac{\partial a}{\partial x}$ and $B = \min \left|\frac{\partial f}{\partial x}\right|$, we have that the above quantity is uniformly negative definite, i.e.

$$\exists c_{2,1}^2 : \quad -\frac{\partial a}{\partial x} + \varepsilon\frac{\partial f}{\partial x} < -c_{1,2}^2$$

In the second case, the right hand side of (9.36) becomes

$$-\frac{\partial a}{\partial x} + \frac{\partial f}{\partial x} + \frac{p_2}{p_1}\frac{\partial f}{\partial x} \tag{9.38}$$

Again, by choosing $p_2/p_1 = 1 + \varepsilon$, with $\varepsilon > 0$, we have the following upper bound for the expression in (9.38):

$$-\frac{\partial a}{\partial x} + 2\frac{\partial f}{\partial x} + \varepsilon\frac{\partial f}{\partial x} \tag{9.39}$$

Thus, it follows that $\mu_{P,1}(J) < -c^2$ provided that the above quantity is uniformly negative definite. Since, by hypotheses,

$$\frac{\partial a}{\partial x} > 2\frac{\partial f}{\partial x} \quad \forall x, y \in \mathcal{C} \tag{9.40}$$

then $\exists c_{2,2}^2 : \quad -\frac{\partial a}{\partial x} + \frac{\partial f}{\partial x} + \frac{p_2}{p_1}\frac{\partial f}{\partial x} \leq -c_{2,2}^2$. The proof of the Theorem is now complete.

□

From a biological viewpoint, the hardest hypothesis to satisfy in Theorem 9.2.4 might be that on the derivatives of $f(x,y)$. However, it is possible to relax the hypothesis on $\partial f/\partial x$ if the rate of change of $a(x)$ with respect to x, i.e. $\partial a/\partial x$, is sufficiently larger than $\partial f/\partial x$. In particular, the following result can be proved.

Theorem 9.2.5. *System (9.30), without inputs u, evolving on a convex compact set, is contractive provided that:*

- $\partial a/\partial x > 0$, $\forall x \in C$;
- $\partial f/\partial y > 0$, $\forall x, y \in C$;
- $\partial a/\partial x > \max_C \{2\,|\partial f/\partial x|\}$.

Proof. The proof is similar to that of Theorem 9.2.4. In particular, we can repeat the same derivation to obtain again inequality (9.36). Thence, as no hypothesis is made on the sign of $\partial f/\partial x$, choosing $p_2/p_1 = 1+\varepsilon$ we have

$$-\frac{\partial a}{\partial x}+\frac{\partial f}{\partial x}+\left|\frac{p_2}{p_1}\frac{\partial f}{\partial x}\right| = -\frac{\partial a}{\partial x}+\frac{\partial f}{\partial x}+\left|\frac{\partial f}{\partial x}\right|+\varepsilon\left|\frac{\partial f}{\partial x}\right| \tag{9.41}$$

Thus, it follows that, if $\partial a/\partial x \geq 2\,|\partial f/\partial x|$, then $\exists\ c^2$ such that $\mu_{P,1}(J) < -c^2$, implying contractivity. The above condition is satisfied by hypotheses, hence the theorem is proved. □

Remarks

Theorems 9.2.4 and 9.2.5 show the possibility of designing with high flexibility the self-degradation and interaction functions for an input-output module.

This flexibility can be further increased, for example in the following ways:

- Results similar to that of the above Theorems can be derived (and also extended) if some self degradation rate for y is present in (9.30), i.e.

$$\begin{aligned}\dot{x} &= u(t) - a(x) + f(x,y)\\ \dot{y} &= -b(y) - f(x,y)\end{aligned} \tag{9.42}$$

  with $\frac{\partial b}{\partial y} < 0$.

- Theorem 9.2.4 and Theorem 9.2.5 can also be extended to the case in which the X-module drives more than one downstream transcriptional modules.

Applications to synthetic biology

We introduced above a methodology for checking if a given transcriptional module can be entrained to some periodic input. The aim of this section is to show that our methodology can serve as an effective tool for designing synthetic biological circuits that are entrained to some desired external input.

In particular, we will consider the synthetic biological oscillator known as the Repressilator [52], for which an additional coupling module has been recently proposed in [61]. A numerical investigation of the synchronization of a network of non-identical Repressilators was independently reported in [211].

We will show that our results can be used to isolate a set of biochemical parameters for which one can guarantee the entrainment to any external periodic signal of this synthetic biological circuit. In what follows, we will use the equations presented in [61] to model the Repressilator and the additional coupling model, see Chapter 5.

Entrainment using an intra-cellular auto-inducer

Now, we study the entrainment of the Repressilator circuit (see Chapter 5). The biochemical circuit is schematically represented in Figure 9.7. Now, the concentration of the auto-inducer is labeled as S. Recall that the coupling module makes use of two proteins: (i) LuxI, which synthesizes the auto-inducer; (ii) LuxR, with which the auto-inducer synthesized by LuxI forms a complex that activates the transcription of various genes.

As in Chapter 5, the circuit is modeled with the simplified set of differential equations proposed in [61]. Specifically, the dynamics of the $mRNA$ are

$$\begin{aligned} \dot{a} &= -a + \tfrac{\alpha}{1+C^2} \\ \dot{b} &= -b + \tfrac{\alpha}{1+A^2} \\ \dot{c} &= -c + \tfrac{\alpha}{1+B^2} + \tfrac{kS}{1+S} \end{aligned} \tag{9.43}$$

Recall that the above equations are dimensionless.

The dynamics of the proteins are described by

$$\begin{aligned} \dot{A} &= \beta_A a - d_A A \\ \dot{B} &= \beta_B b - d_B B \\ \dot{C} &= \beta_C c - d_C C \end{aligned} \tag{9.44}$$

The parameters β_A, β_B, β_C represent the ratios between the $mRNA$s and the respective proteins' lifetimes and d_A, d_B, d_C represent the protein decay rate.

The last differential equation of the model from [61] keeps track of the evolution of the intra-cellular auto-inducer. It is assumed that the proteins TetR and LuxI have equal lifetimes. This in turn implies that the dynamics of such proteins are identical, and hence one uses the same variable to describe both protein concentrations. Thus, the dynamics of the auto-inducer are given by:

$$\dot{S} = -k_{s0}S + k_{s1}A$$

where k_{s0} is the rate of degradation of S.

We now model the forcing on the intracellular auto-inducer concentration by adding an external input $u(t)$ to the above dynamical equation (see Figure 9.45). The equation for S becomes (notice that this dynamics is different from the one studied in 5):

$$\dot{S} = -k_{s0}S + k_{s1}A - \eta(S - u(t)) \tag{9.45}$$

where η can be thought as a diffusion rate.

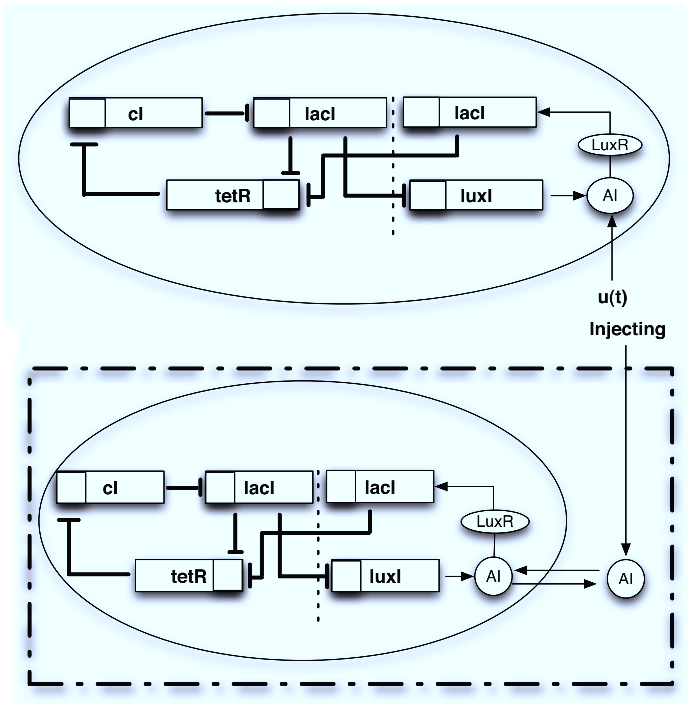

Figure 9.7: Modular addition to the Repressilator circuit. This module is used for forcing the original circuit with some external signal (represented by an extra-cellular molecule in the bottom panel).

We will now use the analytical methodology developed in the previous sections, to properly tune the biochemical parameters of the Repressilator circuit, whose mathematical model consists of the set of differential equations (9.43), (9.44), (9.45), so that it shows entrainment to the periodic input $u(t)$. That is, the measured output (e.g. cI), oscillates asymptotically with a period equal to that of $u(t)$. Of course, the periodic orbit of the output will depend on the particular choice of the parameters.

In what follows, we assume that all the system parameters can be varied except for the self-degradations that we assume to be fixed as, in practice, they are difficult to modify.

In this case, the Jacobian matrix to be studied is

$$\tilde{J} := \begin{bmatrix} -1 & 0 & 0 & 0 & 0 & \frac{-2\alpha C}{(1+C^2)^2} & 0 \\ 0 & -1 & 0 & \frac{-2\alpha A}{(1+A^2)^2} & 0 & 0 & 0 \\ 0 & 0 & -1 & 0 & \frac{-2\alpha B}{(1+B^2)^2} & 0 & \frac{k}{(1+S)^2} \\ \beta_A & 0 & 0 & -d_A & 0 & 0 & 0 \\ 0 & \beta_B & 0 & 0 & -d_B & 0 & 0 \\ 0 & 0 & \beta_C & 0 & 0 & -d_C & 0 \\ 0 & 0 & 0 & k_{s1} & 0 & 0 & -k_{s0}-\eta \end{bmatrix} \tag{9.46}$$

The matrix measure that we will use to prove contraction is

$$\mu_{P,\infty}\left(\tilde{J}\right) = \mu_\infty\left(P\tilde{J}P^{-1}\right)$$

where P is a 7×7 diagonal matrix having on the main diagonal the positive arbitrary scalars p_i. Computation of $P\tilde{J}P^{-1}$ yields

$$P\tilde{J}P^{-1} = \begin{bmatrix} -1 & 0 & 0 & 0 & 0 & \frac{p_1}{p_5}\frac{-2\alpha C}{(1+C^2)^2} & 0 \\ 0 & -1 & 0 & \frac{p_2}{p_4}\frac{-2\alpha A}{(1+A^2)^2} & 0 & 0 & 0 \\ 0 & 0 & -1 & 0 & \frac{p_3}{p_5}\frac{-2\alpha B}{(1+B^2)^2} & 0 & \frac{p_3}{p_7}\frac{k}{(1+S)^2} \\ \frac{p_4}{p_1}\beta_A & 0 & 0 & -d_A & 0 & 0 & 0 \\ 0 & \frac{p_5}{p_2}\beta_B & 0 & 0 & -d_B & 0 & 0 \\ 0 & 0 & \frac{p_6}{p_3}\beta_C & 0 & 0 & -d_C & 0 \\ 0 & 0 & 0 & \frac{p_7}{p_4}k_{s1} & 0 & 0 & -k_{s0}-\eta \end{bmatrix} \tag{9.47}$$

Thus, from the definition of μ_∞ given in (9.19), we have that there exists some $c \in \mathbb{R} - \{0\}$ such that $\mu_{P,\infty}(\tilde{J}) \leq -c^2$, $\forall t$ if and only if there exists a set of scalars $c_i, p_i \in \mathbb{R} - \{0\}$, $i = 1, \dots, 7$, such that

$$-1 + \frac{p_1}{p_5}\frac{2\alpha C}{(1+C^2)^2} \leq -c_1^2 \tag{9.48a}$$

$$-1 + \frac{p_2}{p_4}\frac{2\alpha A}{(1+A^2)^2} \leq -c_2^2 \tag{9.48b}$$

$$-1 + \frac{p_3}{p_5}\frac{2\alpha B}{(1+B^2)^2} + \frac{p_3}{p_7}\frac{k}{(1+S)^2} \leq -c_3^2 \tag{9.48c}$$

$$-d_A + \frac{p_4}{p_1}\beta_A \leq -c_4^2 \tag{9.48d}$$

$$-d_B + \frac{p_5}{p_2}\beta_B \leq -c_5^2 \tag{9.48e}$$

$$-d_C + \frac{p_6}{p_3}\beta_C \leq -c_6^2 \tag{9.48f}$$

$$-k_{s0} - \eta + \frac{p_7}{p_4}k_{s1} \leq -c_7^2 \tag{9.48g}$$

It is easy to check that the nonlinear terms in the above equations satisfy the following inequalities:

$$f(x) = \frac{2\alpha x}{(1+x^2)^2} \leq M := \frac{3\sqrt{3}\alpha}{8}$$

and

$$g(x) = \frac{k}{(1+S)^2} \leq k$$

for all $x \geq 0$. Hence, the system of inequalities (9.48a)-(9.48g) are satisfied, if the following set is fulfilled:

$$-1 + \frac{p_1}{p_5}M \leq -c_1^2 \tag{9.49a}$$

$$-1 + \frac{p_2}{p_4}M \leq -c_2^2 \tag{9.49b}$$

$$-1 + \frac{p_3}{p_5}M + \frac{p_3}{p_7}k \leq -c_3^2 \tag{9.49c}$$

$$-d_A + \frac{p_4}{p_1}\beta_A \leq -c_4^2 \tag{9.49d}$$

$$-d_B + \frac{p_5}{p_2}\beta_B \leq -c_5^2 \tag{9.49e}$$

$$-d_C + \frac{p_6}{p_3}\beta_C \leq -c_6^2 \tag{9.49f}$$

$$-k_{s0} - \eta + \frac{p_7}{p_4}k_{s1} \leq -c_7^2 \tag{9.49g}$$

The system can then be proved to be contracting for a given set of biochemical parameters, if there exists a set of scalars p_i, $i = 1\ldots7$ satisfying the above inequalities. For example, if the repressilator parameters are chosen so that

$$k + M < 1, \quad \beta_A < d_A, \quad \beta_B < d_B, \quad \beta_C < d_C, \quad k_{s1} < k_{s0} + \eta \tag{9.50}$$

then it is trivial to prove that, for any constant value $\bar{p} > 0$, the set of scalars $p_i = \bar{p}$, for $i = 1, \ldots, 7$, satisfies (9.49a)-(9.49g). Indeed, in Figure 9.8 we provide a set of biochemical parameters for which the circuit is contracting and shows entrainment to the periodic input $u(t) = 1.5 + 1.5\sin(0.5t)$. (These parameters, except for the maximal transcription rate α, are in the same ranges as those used in [52], [61]. These parameters are also close to those used in [211] and [193]. The reason for picking an α much smaller than in [61], is that we need to slow down transcription so as to eliminate intrinsic oscillations; otherwise the entrainment effect cannot be shown. This lowering of α by two orders of magnitude is also found in other works, for example in [100], where the same model is studied, with α somewhat larger but of the same order of magnitude as here.)

Note that using the set of inequalities (9.49a)-(9.49g) as a guideline, it is possible to find other parameter regions where the system is still contracting but exhibit some other desired properties. For instance, to increase the amplitude of the output oscillations shown in Figure 9.8, a possible approach can be that of increasing the biochemical parameter k so as to make stronger the effect of the auto-inducer on the dynamics of the gene *cI* (variable $c(t)$ in the model).

Again we can prove that the set of inequalities (9.49a)-(9.49g) is satisfied for k arbitrarily large, if we set $p_i = \bar{p}$, for $i = 1, \ldots, 6$ and choose p_7 such that

$$\frac{\bar{p}}{p_7} k < 1 - M$$

and

$$-k_{s0} - \eta + \frac{p_7}{\bar{p}} k_{s1} \leq -c_7^2$$

Now, due to biochemical constraints the parameter k_{s1} is considerably smaller than k_{s0} and η (in our simulations the ratio is of about two orders of magnitude). Therefore, whatever the value of k, it suffices to set $\bar{p} = 1$ and $p_7 = 10k + \varepsilon$, with ε being a positive arbitrary constant, to get a solution to (9.49a)-(9.49g) and hence guarantee the system to be contracting.

Figure 9.9 shows the behavior of the system output with the modified parameters confirming that with this choice of parameters the oscillation amplitude is indeed larger as expected.

Observe the *nonlinear character of the oscillation* depicted in Figure 9.9, which is reflected in the lack of symmetry in the behavior at minima and maxima of $cI(t)$. Our theory predicts the existence (and uniqueness) of such a nonlinear oscillations. None of the usual techniques, based on linear analysis, can explain such behavior.

Entrainment using an extra-cellular auto-inducer

We now consider the case in which the extracellular auto-inducer can change due to an external signal as well as diffusion from intracellular auto-inducer, as represented in Figure 9.7. A new variable must be introduced, to keep track of the extracellular auto-inducer concentration. The only difference in the new model with respect to the previous one is that the differential equation for S becomes:

$$\dot{S} = -k_{s0} S + k_{s1} A - \eta \left(S - S_e\right) \tag{9.51}$$

Notice that the parameter η measures the diffusion rate of the auto-inducer across the cell membrane, i.e. $\eta = \sigma \mathcal{A} / V_c$, with σ representing the membrane permeability,

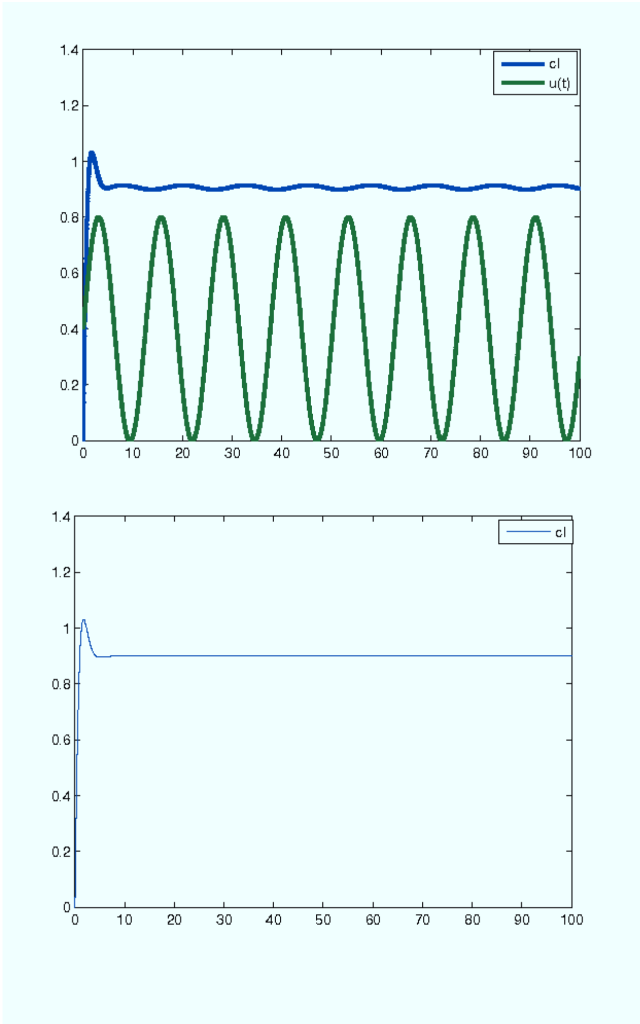

Figure 9.8: Simulation of the Repressilator model described by (9.43), (9.44), (9.45). Time (minutes) on the x-axis. Behavior of cI when the input $u(t) = 0.4{+}0.4\sin(0.5t)$ is applied. Notice that when no forcing is present cI converges to a non oscillatory regime behavior. System parameters are tuned in order to satisfy (9.50). Specifically: $\beta_A = \beta_B = \beta_C = 1$, $d_A = d_B = d_C = 1.1$, $\alpha = 1.5$, $k = 0.1$, $k_{s0} = 1$, $\eta = 1.5$, $k_{s1} = 0.01$.

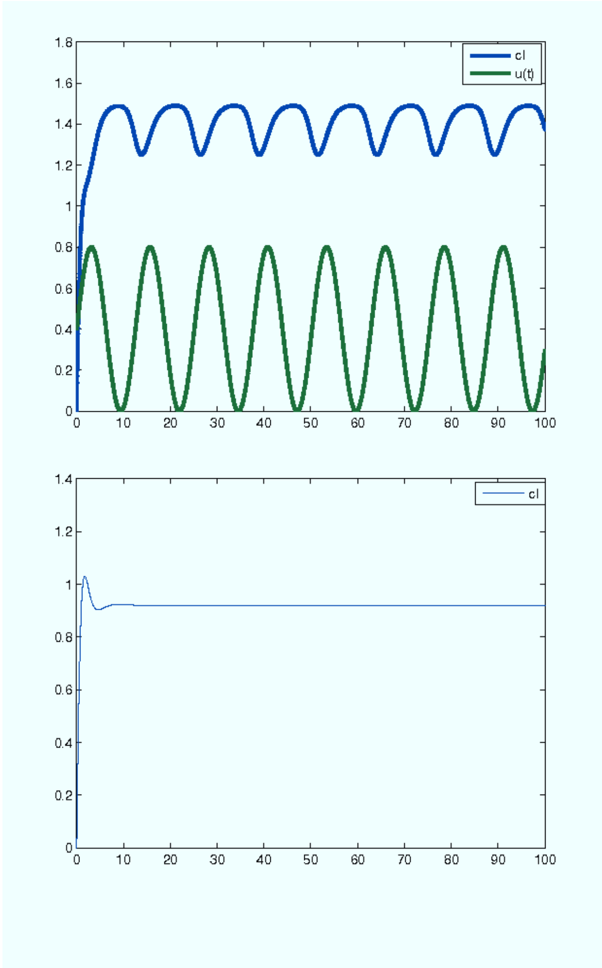

Figure 9.9: Increasing the amplitude of oscillations for the model described by (9.43), (9.44), (9.45). Time (minutes) on the x-axis. Behavior of cI when: (i) the input $u(t) = 0.4 + 0.4\sin(0.5t)$ is applied; (ii) no forcing is present. System parameters are the same as that used in Figure 9.8, except $k = 15$.

$\mathcal{A}$ its surface area and V_C the cell volume. In the above equation, S_e denotes the concentration of the extra-cellular auto-inducer, whose dynamics are given by:

$$\dot{S}_e = -k_{se}S_e + \eta_{ext}\left(S - S_e\right) + u\left(t\right) \tag{9.52}$$

where $\eta_{ext} = \sigma\mathcal{A}/V_{ext}$, with V_{ext} denoting the total extracellular volume, while k_{se} stands for the decay rate.

In analogy with the previous section, we will ensure entrainment of the dynamical system consisting of (9.43), (9.44), (9.51), (9.52), by tuning the biochemical parameters of this new circuit. Again, the guidelines for engineering the parameters will be provided by the tools developed in the previous sections.

Following the schematic of the previous section, we will prove that there exists $c \in \mathbb{R} - \{0\}$ and a 8×8 constant diagonal matrix $\bar{P}$, such that $\mu_{\bar{P},\infty}\left(J\right) \leq -c^2$, where J is the system Jacobian.

If we denote with p_i, $i = 1,\ldots,8$ the diagonal elements of $\bar{P}$, we obtain the following block-structure for the matrix $\bar{P}J\bar{P}^{-1}$:

$$\bar{P}J\bar{P}^{-1} = \begin{bmatrix} P\tilde{J}P^{-1} & v_1 \\ v_2^T & -k_{se} - \eta_{ext} \end{bmatrix} \tag{9.53}$$

where $P\tilde{J}P^{-1}$ is given in (9.47) and:

$$v_1 = \begin{bmatrix} 0 \\ 0 \\ 0 \\ 0 \\ 0 \\ 0 \\ \frac{p_7}{p_8}\eta \end{bmatrix}, \quad v_2 = \begin{bmatrix} 0 \\ 0 \\ 0 \\ 0 \\ 0 \\ 0 \\ \frac{p_8}{p_7}\eta_{ext} \end{bmatrix} \tag{9.54}$$

Thus, we have that $\mu_\infty\left(\bar{P}J\bar{P}^{-1}\right) \leq -c^2$ if and only if there exist some $c_i \in \mathbb{R} - \{0\}$, $i = 1,\ldots,8$ such that inequalities (9.48a)-(9.48f) are all satisfied and additionally:

$$-k_{s0} - \eta + \frac{p_7}{p_4}k_{s1} + \frac{p_7}{p_8}\eta \leq -c_7^2 \tag{9.55a}$$

$$-k_{se} - \eta_{ext} + \frac{p_8}{p_7}\eta_{ext} \leq -c_8^2 \tag{9.55b}$$

Again, we can find sets of biochemical parameters in order to satisfy the above inequalities and hence ensure global entrainment of the circuit to some external input. For example, if we set

$$k + M < 1, \quad \beta_A < d_A, \quad \beta_B < d_B, \quad \beta_C < d_C, \quad k_{s1} < k_{s0} \quad k_{se} > 0 \tag{9.56}$$

then, as in the previous section, it is trivial to show that setting all p_i to the same identical value satisfies the set of inequality required to prove contraction and hence guarantee entrainemnt. Notice that the last constraint in (9.56) is automatically satisfied by the physical (i.e. positivity) constraints on the system parameters.

In Figure 9.10, the behavior of the circuit is shown with the parameters chosen so as to satisfy the constraints given in (9.56).

Entraining a population of Repressilators

Consider, now, a population of N Repressilator circuits, which are coupled by means of an auto-inducer molecule. We can think of such a network as having an all-to-all topology, with the coupling given by the concentration of the extracellular auto-inducer, S_e. The aim of this section is to show that the methodology proposed here

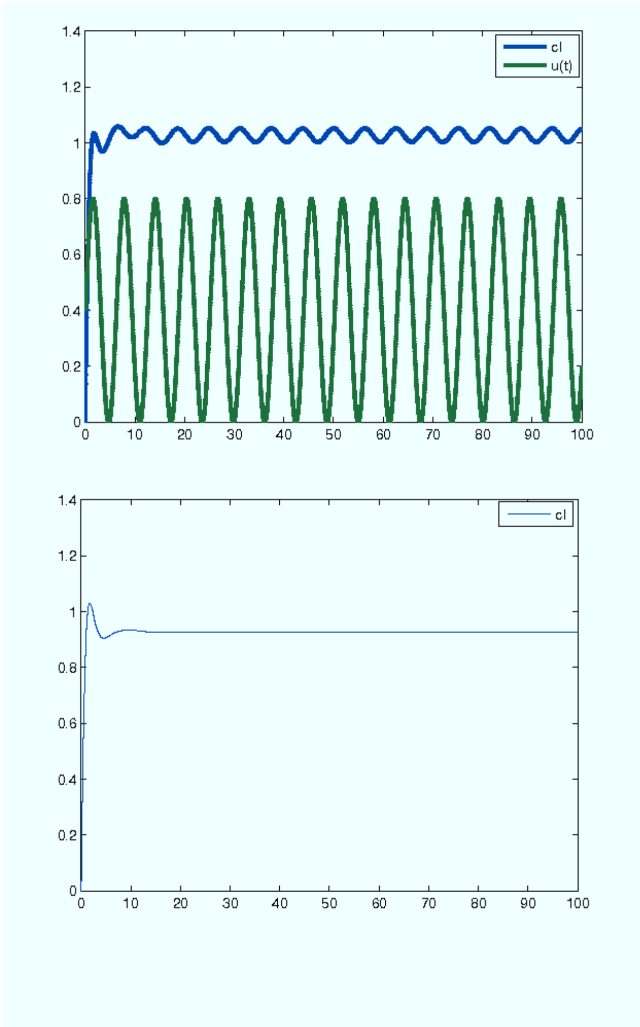

Figure 9.10: Simulation of the Repressilator forced by some extra-cellular molecule. Time (minutes) on the x-axis. Behavior of cI when the input $u(t) = 0.4+0.4\sin(0.5t)$ is applied. Notice that when no forcing is present, the steady state behavior is non-oscillatory. System parameters are: $\beta_A = \beta_B = \beta_C = 1$, $d_A = d_B = d_C = 1.1$, $\alpha = 1.5$, $k = 0.5$, $k_{s0} = 1$, $k_{s1} = 0.01$.

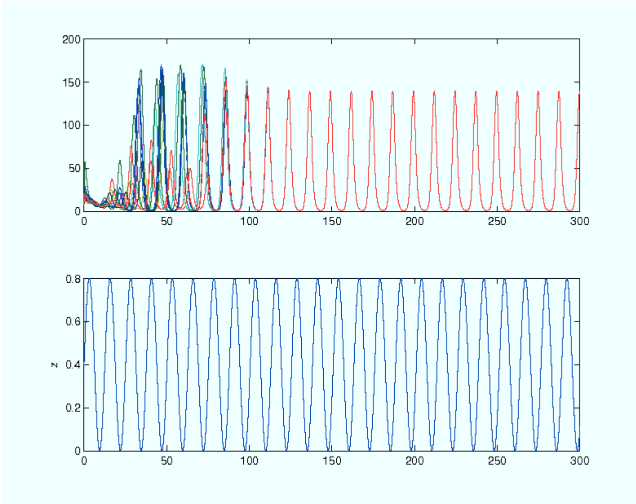

Figure 9.11: Synchronization of Repressilators. Behavior of a population of Repressilator modeled as in (9.57). Time (minutes) on x-axs. Notice that all the circuits synchronize with a steady-state evolution having the same period as $u\,(t) = 0.4 + 0.4 \sin\,(0.5t)$. System parameters are chosen as in Figure 9.9, with $\eta_{ext} = 0.1$.

can also be used as an effective tool to guarantee the synchronization of an entire population of biochemical oscillators onto some entraining external periodic input.

We denote with the subscript i the state variables of the i-th circuit in the network, which is modelled using the equations reported in [61] as:

$$\begin{aligned}
\dot{a}_i &= -a_i + \tfrac{\alpha}{1+C_i^2} \\
\dot{b}_i &= -b_i + \tfrac{\alpha}{1+A_i^2} \\
\dot{c}_i &= -c_i + \tfrac{\alpha}{1+B_i^2} + \tfrac{kS_i}{1+S_i} \\
\dot{A}_i &= \beta_A a_i - d_A A_i \\
\dot{B}_i &= \beta_B b_i - d_B B_i \\
\dot{C}_i &= \beta_C c_i - d_C C_i \\
\dot{S}_i &= -k_{s0} S_i + k_{s1} A_i - \eta\,(S_i - S_e) \\
\dot{S}_e &= -k_{se} S_e + \eta_{ext} \sum_{j=1}^{N} (S_j - S_e) + u(t)
\end{aligned} \tag{9.57}$$

Figure 9.11 shows a simulation of a population of Repressilators modeled as in (9.57), with biochemical parameters tuned so as to fulfill the constraints of the previous Section: all the circuits composing the network evolve asymptotically towards the same synchronous evolution, which has period equal to that of the input signal $u(t)$. The interested reader is referred to Appendix A for the proof, where we also show a counterexample to entrainment.

9.3 Global Convergence of Quorum sensing networks

This following sections derive sufficient conditions for the coordination of nodes communicating through dynamical quorum sensing mechanisms, based on a full nonlinear dynamic analysis. Those results can be used both to study natural networks and to guide design of communication mechanisms in synthetic or partially synthetic networks.

Recall that, from a network dynamics viewpoint, the key characteristic of quorum sensing-like mechanisms lies in the fact that communication between nodes (e.g. bacteria) occurs by means of a shared quantity (e.g. the autoinducer concentration), typically in the environment. Furthermore, the production and degradation rates of such a quantity are affected by all the nodes of the network. Therefore, a detailed model of such a mechanism needs to keep track of the temporal evolution of the shared quantity, resulting in an additional set of ordinary differential equations. Such an indirect coupling model has been recently reported in e.g. [91], [208] in the context of periodic oscillations, while in [150] synchronization of two chaotic systems coupled through the environment is investigated. In these papers it is shown that under suitable conditions oscillators can synchronize and that this kind of coupling can lead to a rich variety of synchronous behaviors.

After studying the case where the network nodes (e.g., the biological entities populating the environment) are all identical or nearly identical. We then focus, in Section 9.3.2, on networks composed of heterogeneous nodes, i.e., nodes of possibly diverse dynamics. In this case we provide sufficient conditions ensuring that all the network nodes sharing the same dynamics converge to a common behavior, a particular instance of so-called concurrent synchronization [142], [77]. In Section 9.3.3, the results are further extended to a distributed version of quorum sensing, where multiple groups of possibly heterogeneous nodes communicate by means of multiple media. In Section 9.3.4, we show that driving the shared environmental variable with an exogenous signal of a given period provides a mechanism for making the network nodes oscillate at the same period, without requiring strong stability properties of the nodes or the overall system. Finally, Section 9.3.5 studies the dependence of synchronization properties on the number of nodes, a question of interest e.g. in the context of cell proliferation. Section 9.3.6 illustrates the general approach with a set of examples.

9.3.1 The basic mathematical model and convergence analysis

We analyze the convergent behavior of networks of nodes which are globally coupled through a shared quantity (often, the environment) see Figure 9.12 (left). In such a network, the N nodes are assumed be all identical, i.e. to all share the same smooth dynamics, and to communicate by means of the same common medium, also characterized by some smooth dynamics:

$$\begin{aligned} \dot{x}_i &= f\left(x_i, z, t\right) \qquad\qquad i = 1, \ldots, N \\ \dot{z} &= g\left(z, \Psi\left(x_1, \ldots, x_N\right), t\right) \end{aligned} \tag{9.58}$$

A simplified version of the above model was recently analyzed by means of a graphical algorithm in [154]. In the above equation, the set of state variables of the nodes is x_i, while the set of the state variables of the common medium dynamics is z. Notice that the nodes dynamics and the medium dynamics can be of different dimensions (e.g. $x_i \in \mathbb{R}^n$, $z \in \mathbb{R}^d$). The dynamics of the nodes affect the dynamics of the common medium by means of some (coupling, or input) function, $\Psi : \mathbb{R}^{Nn} \to \mathbb{R}^d$. These functions may depend only on some of the components of the x_i or of z (as the example in Section 9.3.6 illustrates).

The following result is a sufficient condition for convergence of all nodes trajectories of (9.58) towards each other.

Theorem 9.3.1. *All nodes trajectories of network (9.58) globally exponentially converge towards each other if the function $f\left(x, v(t), t\right)$ is contracting for any $v(t) \in \mathbb{R}^d$.*

Proof. The proof is based on partial contraction (Section 4.5). Consider the following *reduced order* virtual system

$$\dot{y} = f\left(y, z, t\right) \tag{9.59}$$

Notice that now $z(t)$ is an exogenous input to the virtual system. Furthermore, substituting x_i to the virtual state variable y yields the dynamics of the i-th node. That is, x_i, $i = 1, \ldots, N$, are particular solutions of the virtual system. Now, if such a system is contracting, then all of its solutions will converge towards each other. Since the nodes state variables are particular solutions of (9.59), contraction of the virtual system implies that, for any $i, j = 1, \ldots, N$:

$$|x_i - x_j| \to 0 \text{ as } \; t \to +\infty$$

The Theorem is proved by noting that by hypotheses the function $f(x, v(t), t)$ is contracting for any exogenous input $v(t)$. This in particular implies that $f(y, z, t)$ is contracting, i.e. (9.59) is contracting. $\square$

Remarks

- In the case of diffusive-like coupling between nodes and the common medium, system (9.58) reduces to:

$$\begin{aligned} \dot{x}_i &= f(x_i,t) + k_z(z) - k_x(x_i) \qquad\qquad i = 1,\dots,N \\ \dot{z} &= g(z,t) + \textstyle\sum_{i=1}^N \left[u_x(x_i) - u_z(z)\right] \end{aligned} \tag{9.60}$$

  That is, the nodes and the common medium are coupled by means of the smooth functions $k_z : \mathbb{R}^d \to \mathbb{R}^n$, $k_x : \mathbb{R}^n \to \mathbb{R}^n$ and $u_x : \mathbb{R}^n \to \mathbb{R}^d$, $u_z : \mathbb{R}^d \to \mathbb{R}^d$. These functions may depend only on some of the components of the x_i or of z (as we shall illustrate in Section 9.3.6). Theorem 9.3.1 implies that synchronization is attained if $f(x,t) - k_x(x)$ is contracting. Similar results are easily derived for the generalizations of the above model presented in what follows.

- The result also applies to the case where the quorum signal is based not on the x_i's themselves, but rather on variables deriving from the x_i's through some further nonlinear dynamics. Consider for instance the system

$$\begin{aligned} \dot{x}_i &= f(x_i,z,t) \qquad\qquad i = 1,\dots,N \\ \dot{r}_i &= h(r_i,x_i,z,t) \qquad\quad i = 1,\dots,N \\ \dot{z} &= g(z,\Psi(r_1,\dots,r_N),t) \end{aligned}$$

  Theorem 9.3.1 can be applied directly by describing each network node by the augmented state (x_i, r_i), and using the property on hierarchical combinations to evaluate the contraction properties of the augmented network dynamics.

- Similarly, each network "node" may actually be composed of several subsystems, with each subsystem synchronizing with its analogs in other nodes.

- As in previous contraction work, the individual node dynamics are quite general, and could describe e.g. neuronal oscillator models as well as bio-chemical reactions. In the case that the individual node dynamics represents a system with multiple equilibria, then synchronization corresponds to a common "vote" for a particular equilibrium.

- A condition for synchronization weaker than Theorem 9.3.1 is that the function $f(x,v,t)$ be contracting only for some values of v, i.e. $v \in V \subset \mathbb{R}^d$. In this case, the medium dynamics acts as a switch which activates/deactivates synchronization according to the values of z.

9.3.2 Multiple systems communicating over a common medium

We now generalize the mathematical model analyzed in the previous Section, by allowing for $s \leq N$ groups (or clusters) of nodes characterized by different dynamics (with possibly different dimensions) to communicate over the same common medium (see Figure 9.12, right). We will prove a sufficient condition for the global exponential convergence of all nodes trajectories belonging to the same group towards each other. This regime is called concurrent synchronization [142].

The mathematical model analyzed here is

$$\begin{aligned}\dot{x}_i &= f_{\gamma(i)}\left(x_i, z, t\right)\\ \dot{z} &= g\left(z, \Psi\left(x_1, \ldots, x_N\right), t\right)\end{aligned} \tag{9.61}$$

where: i) γ is defined as in (A.6); ii) x_i denotes the state variables of the network nodes (nodes belonging to different groups may have different dimensions, say $n_{\gamma(i)}$) and z denotes the state variables for the common medium ($z \in \mathbb{R}^d$); iii) Ψ, defined analogously to the previous Section, denotes the coupling function of the group $\gamma(i)$ with the common medium dynamics ($\Psi : \mathbb{R}^{n_{\gamma(1)}} \times \ldots \times \mathbb{R}^{n_{\gamma(N)}} \to \mathbb{R}^d$).

Theorem 9.3.2. *Concurrent synchronization is achieved in network (9.61) if the functions $f_{\gamma(i)}\left(x, v(t), t\right)$ are all contracting for any $v(t) \in \mathbb{R}^d$.*

Proof. Recall that (9.61) is composed by N nodes having dynamics $f_1, \ldots, f_s$. Now, in analogy with the proof of Theorem 9.3.1, consider the following virtual system:

$$\begin{aligned}\dot{y}_1 &= f_1\left(y_1, z, t\right)\\ \dot{y}_2 &= f_2\left(y_2, z, t\right)\\ &\vdots\\ \dot{y}_s &= f_s\left(y_s, z, t\right)\end{aligned} \tag{9.62}$$

where $z(t)$ is seen as an exogenous input to the virtual system. Let $\{X_i\}$ be the set of state variables belonging to the i-th group composing the network, and denote with $X_{i,j}$ any element of $\{X_i\}$. We have that $(X_{1,j}, \ldots, X_{s,j})$ are particular solutions of the virtual system. Now, contraction of the virtual system implies that all of its particular solutions converge towards each other, which in turn implies that all the elements within the same group $\{X_i\}$ converge towards each other. Thus, contraction of the virtual system (9.62) implies concurrent synchronization of the real system (9.61).

To prove contraction of (9.62), compute its Jacobian,

$$J = \begin{bmatrix} \frac{\partial f_1(y_1,z,t)}{\partial y_1} & 0 & 0 & \dots & 0 \\ 0 & \frac{\partial f_2(y_2,z,t)}{\partial y_2} & 0 & \dots & 0 \\ \dots & \dots & \dots & \dots & \dots \\ 0 & 0 & 0 & 0 & \frac{\partial f_s(y_s,z,t)}{\partial y_s} \end{bmatrix}$$

Now, by hypotheses, we have that all the functions $f_i(x, v(t), t)$ are contracting for any exogenous input. This in turn implies that the virtual system (9.62) is contracting, since its Jacobian matrix is block diagonal with diagonal blocks being contracting. □

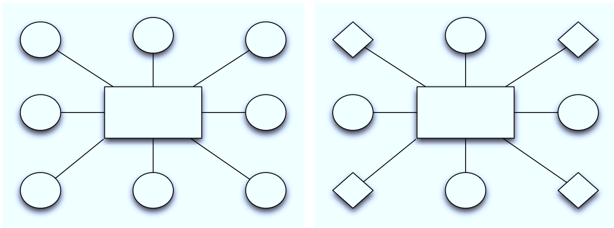

Figure 9.12: A schematic representation of networks analyzed in Section 9.3.1 (left) and Section 9.3.2 (right). The nodes denoted with circles have a different dynamics from those indicated with squares. The dynamics of the common media is denoted with a rectangle. In our models, the dynamics of the common media is affected by the nodes state variables: this implements a feedback.

9.3.3 Systems communicating over different media

In the previous Section, we considered networks where some (possibly heterogeneous) nodes communicate over a common medium. We now consider a *distributed* version of such topology, where each of the $s \leq N$ groups composing the network have a private medium. Communication between the groups is then obtained by coupling only their media (see Figure 9.13). The objective of this Section, is to provide a sufficient condition ensuring (concurrent) synchronization of such network topology.

Note that the network topology considered here presents a layer structure. In analogy with the terminology used for describing the topology of the Internet and World-Wide-Web (see e.g. [25], [132]), we term as *medium* (or private) level the layer consisting of the nodes of the network and their corresponding (private) media; we then term as *autonomous* level, the layer of the interconnections between the media. That is, the autonomous level is an *abstraction* of the network, having nodes which consist of both the network nodes and their private medium. This in turn implies that in order for two nodes of the autonomous level to be identical they have to share: i) the same dynamics and number of nodes; ii) the same medium dynamics (see Figure 9.13).

In what follows we will denote with $\mathcal{G}_p$ the set of homogeneous nodes communicating over the medium z_p. We will denote with N_p the set of media which are linked to the medium z_p. Each medium communicates with its neighboring media diffusively. The mathematical model is then:

$$\begin{array}{ll} \dot{x}_i = f_p\left(x_i, z_p, t\right) & x_i \in \mathcal{G}_p \\ \dot{z}_p = g_p\left(z_p, \Psi\left(X_p\right), t\right) + \sum_{j\in N_p}\left[\phi_p\left(z_j\right) - \phi_p\left(z_p\right)\right] & x_i \in \mathcal{G}_p \end{array} \tag{9.63}$$

where $p = 1, \ldots, s$ and X_p is the stack of all the vectors $x_i \in \mathcal{G}_p$. We assume that the dynamical equations for the media have all the same dimensions (e.g. $z_p \in R^d$), while the nodes belonging to different groups can have different dimensions (e.g. $x_i \in \mathbb{R}^p$, for any $i \in \mathcal{G}_p$). Here, the coupling functions between the media, $\phi_p : \mathbb{R}^d \to \mathbb{R}^d$, are assumed to be continuous and to have a diagonal Jacobian matrix with diagonal elements being nonnegative and bounded. All the matrices $\partial f_p/\partial z$ are assumed to be bounded.

Theorem 9.3.3. *Concurrent synchronization is attained in network (9.63) if: i) the nodes of its* autonomous *level sharing the same dynamics are input-equivalent; ii) $f_p\left(x_i, v(t), t\right)$, $g_p\left(z_p, v(t), t\right)$ are all contracting functions for any $v(t) \in \mathbb{R}^d$; iii) $\frac{\partial f_p}{\partial z_p}$ are all uniformly bounded matrices.*

Proof. Consider the following $2s$-dimensional virtual system, analogous to the one used for proving Theorem 9.3.2:

$$\begin{array}{l} \dot{y}_{1,p} = f_p\left(y_{1,p}, y_{2,p}, t\right) \\ \dot{y}_{2,p} = g_p\left(y_{2,p}, v_p(t), t\right) + \sum_{k\in N_p}\left[\phi_p\left(y_{2,k}\right) - \phi_p\left(y_{2,p}\right)\right] \end{array} \tag{9.64}$$

where $p = 1, \ldots, s$, and $v_p(t) := \Psi\left(X_p\right)$. Notice that the above system is constructed in a similar way as (9.62). In particular, solutions of (9.63) are particular solutions of the above virtual system (see the proof of Theorem 9.3.2). That is, if concurrent synchronization is attained for (9.64), then all the nodes sharing the same dynamics will converge towards each other. Now, Theorem A.2.1 implies that concurrent synchronization is attained for system (9.64) if: i) its nodes are contracting; ii) the coupling functions have a nonnegative bounded diagonal Jacobian; iii) nodes sharing the same dynamics are input equivalent. Since the last two conditions are satisfied by hypotheses, we have only to prove contraction of the virtual network nodes. Differentiation of nodes dynamics in (9.64) yields the Jacobian matrix

$$\left[\begin{array}{cc} \frac{\partial f_p(y_{1,p},y_{2,p},t)}{\partial y_{1,p}} & \frac{\partial f_p(y_{1,p},y_{2,p},t)}{\partial y_{2,p}} \\ 0 & \frac{\partial g_p(y_{1,p},v_i(t),t)}{\partial y_{2,p}} \end{array}\right]$$

The above Jacobian has the structure of a hierarchy. Thus (see Section 4.4) the virtual system is contracting if: (i) $\frac{\partial f_p(y_{1,p},y_{2,p},t)}{\partial y_{1,p}}$ and $\frac{\partial g_p(y_{2,p},v_i(t),t)}{\partial y_{2,p}}$ are both contracting; (ii) $\frac{\partial f_p(y_{1,p},y_{2,p},t)}{\partial y_{2,p}}$ is bounded.

The above two conditions are satisfied by hypotheses. Thus, the virtual network achieves concurrent synchronization (Theorem A.2.1). This proves the Theorem. □

Note that Theorems 9.3.1 and 9.3.2 do not make any hypotheses on the medium dynamics – synchronization (or concurrent synchronization) can be attained by the network nodes independently of the particular dynamics of the single medium, provided that the function f (or the f_i's) is contracting. By contrast, Theorem 9.3.3 shows that the media dynamics becomes a key element for achieving concurrent synchronization in networks where different groups communicate over different media.

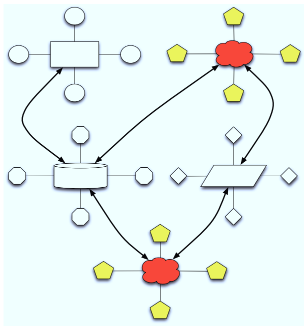

Figure 9.13: A schematic representation of the network analyzed Section 9.3.3. The connections between media (and hence the connections of the autonomous level) are pointed out. Notice that only two nodes of the autonomous level are input equivalent (also pointed out in the Figure) since: i) their media have the same dynamics; ii) both media are shared by the same number of nodes, which have the same dynamics.

Finally, note that all of the above results also allow dimensionality reduction in the analysis of the system's final behavior by treating each group as a single element, similarly to [33], a point we will further illustrate in Section 9.3.5.

9.3.4 Control of Periodicity

The objective of this section is to provide a sufficient condition to guarantee that the common node behavior, towards which all network nodes globally converge, is oscillatory and exhibits a specified *period*. This is obtained by driving the environmental dynamics with an exogenous signal of the given period. A related problem has been recently addressed in [161], where entrainment of individual contracting biological systems to periodic inputs was analyzed.

Our main result, which we shall extend later in the section, is as follows.

Theorem 9.3.4. *Consider the following network*

$$\begin{aligned} \dot{x}_i &= f\left(x_i, z, t\right) & i = 1, \ldots, N \\ \dot{z} &= g\left(z, \Psi\left(x_1, \ldots, x_N\right), t\right) + r\left(t\right) \end{aligned} \tag{9.65}$$

where $r(t)$ is a T-periodic signal. All the nodes of the network synchronize onto a periodic orbit of period T if: i) $f(x_i, v(t), t)$ and $g(z, v(t), t)$ are contracting functions for any $v(t) \in \mathbb{R}^d$; ii) $\frac{\partial f}{\partial z}$ is bounded.

Note that the dynamics f and g include the coupling terms between nodes and environment.

Proof. Consider the virtual system

$$\begin{aligned} \dot{y}_1 &= f\left(y_1, y_2, t\right) \\ \dot{y}_2 &= g\left(y_2, v(t), t\right) + r\left(t\right) \end{aligned} \tag{9.66}$$

where $v(t) := \Psi\left(x_1, \ldots, x_N\right)$. We will prove the Theorem by showing that such a system is contracting. Indeed, in this case, the trajectories of (9.66) will globally exponentially converge to a unique T-periodic solution, implying that also x_i will exhibit a T-periodic final behavior behavior. It is straightforward to check that differentiation of the virtual system yields a matrix of the form (4.15). That is, the virtual system is a hierarchy and thus (see Section 4.4) it is contracting if: (i) $\frac{\partial f(y_1,y_2,t)}{\partial y_1}$ and $\frac{\partial g(y_2,v(t),t)}{\partial y_2}$ are both contracting; (ii) $\frac{\partial f(y_1,y_2,t)}{\partial y_2}$ is bounded.

The first condition is satisfied since, by hypotheses, the functions $f(x, v(t), t)$ and $g(z, v(t), t)$ are contracting for any $v \in \mathbb{R}^d$. The second condition is also satisfied since we assumed $\partial f / \partial z$ to be bounded. The Theorem is then proved. □

System (9.65) can be thought of as a dynamical system built upon a bidirectional interaction between nodes and medium, and forced by a periodic input. In this view, the conditions of Theorem 9.3.4 guarantee global exponential synchronization of the network nodes onto a periodic orbit of the same period as the input, without requiring contraction of either the nodes or the overall dynamics. And indeed, the proof of the Theorem is based on contraction of an appropriately constructed *virtual* system, a much weaker condition.

Theorem 9.3.4 can be extended to the more general case of networks of non-homogeneous nodes communicating over non-homogeneous media.

Theorem 9.3.5. *Consider the following network*

$$\begin{aligned} \dot{x}_i &= f_p\left(x_i, z_p, t\right) & x_i \in \mathcal{G}_p \\ \dot{z}_p &= g_p\left(z_p, \Psi\left(X_p\right), t\right) + \textstyle\sum_{k \in N_p}\left[\phi\left(z_k\right) - \phi\left(z_p\right)\right] + r\left(t\right) & x_j \in \mathcal{G}_p \end{aligned} \tag{9.67}$$

where X_p is the stack of all the $x_i \in \mathcal{G}_p$ and $r(t)$ is a T-periodic signal. Concurrent synchronization is attained, with a final behavior periodic behavior of period T if:

1. *the nodes of the autonomous level sharing the same dynamics are input equivalent;*

2. *the coupling functions ϕ have bounded diagonal Jacobian with nonnegative diagonal elements;*

3. $f_p\left(x_i, v(t), t\right)$ *and* $g_p\left(z_p, v(t), t\right)$ *are contracting functions for any* $v(t) \in \mathbb{R}^d$*;*

4. $\frac{\partial f_p}{\partial z_p}$ *are all uniformly bounded matrices.*

Proof. The proof is formally the same as that of Theorem 9.3.3 and Theorem 9.3.4, and thus it is omitted. □

A simple example

Consider a simple biochemical reaction, consisting of a set of $N > 1$ enzymes sharing the same substrate. We denote with $X_1, \ldots, X_N$ the concentration of the reaction products. We also assume that the dynamics of S is affected by some T-periodic input, $r(t)$. We assume that the total concentration of X_i, i.e. $X_{i,T}$, is much less than the initial substrate concentration, S_0. In these hypotheses, a suitable mathematical model for the system is given by (see e.g. [180]):

$$\begin{aligned} \dot{X}_i &= -aX_i + \tfrac{K_1 S}{K_2 + S} \qquad\qquad i = 1, \ldots, N \\ \dot{S} &= -\textstyle\sum_{i=1}^{N} \tfrac{K_1 S}{K_2 + S} + r(t) \end{aligned} \tag{9.68}$$

with K_1 and K_2 be positive parameters. Thus, a suitable virtual system for the network is

$$\begin{aligned} \dot{y}_1 &= -ay_1 + \tfrac{K_1 y_2}{K_2 + y_2} \\ \dot{y}_2 &= -\textstyle\sum_{i=1}^{N} \tfrac{K_1 y_2}{K_2 + y_2} + r(t) \end{aligned} \tag{9.69}$$

Differentiation of the above system yields the Jacobian matrix

$$\begin{bmatrix} -a & \frac{K_2}{(K_2+y_1)^2} \\ 0 & -N\frac{K_2}{(K_2+y_1)^2} \end{bmatrix} \tag{9.70}$$

It is straightforward to check that the above matrix represents a contracting hierarchy (recall that biochemical parameters are all positive). Thus, all the trajectories of the virtual system globally exponentially converge towards a unique T-periodic solution. This, in turn, implies that X_i, $i = 1, \ldots, N$, globally exponentially converge towards each other and towards the same periodic solution.

Figure 9.14 illustrates the behavior for $N = 3$. Notice that, as expected from the above theoretical analysis, X_1, X_2 and X_3 synchronize onto a periodic orbit of the same period as $r(t)$.

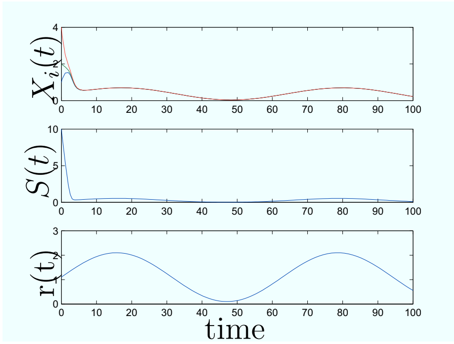

Figure 9.14: Simulation of (9.68), with $N = 3$ and $r(t) = 1.1 + \sin(0.1t)$. System parameters are set as follows: $a = 1$, $K_2 = 1$, $K_1 = 2$.

9.3.5 Emergent properties as N increases

In this Section, we analyze how the convergence properties of a given quorum sensing network vary as the number N of nodes increases. We show that for some typical quorum sensing networks, as N becomes sufficiently large, synchronization always occurs. One particular modeling context where these results have important implications is that of cell proliferation in biological systems.

A lower bound on N ensuring synchronization

It is well known [194] that for all-to-all diffusively coupled networks of the form

$$\dot{x}_i = f(x_i, t) + \sum_{i=1}^{N} k(x_j - x_i) \tag{9.71}$$

the minimum coupling gain k required for synchronization is inversely proportional to the number of nodes composing the network. That is,

$$k_{\min} \propto \frac{1}{N}$$

We now show that a similar bound holds for nodes coupled by means of quorum sensing of the form

$$\begin{aligned} \dot{x}_i &= f\left(x_i, t\right) + kN(z - x_i) \qquad i = 1, \ldots, N \\ \dot{z} &= g\left(z, \Psi(x_1, \ldots, x_N), t\right) \end{aligned} \tag{9.72}$$

To simplify notations, the above model assumes that z and all x_i have the same dimensions. In addition, the coupling strength increases with the number of nodes N, a frequent property of actual networks based on quorum sensing mechanisms, such as e.g. bacteria proliferation [134] or local field potentials.

Theorem 9.3.6. *Assume that the Jacobian* $\left(\frac{\partial f}{\partial x}\right)$ *is upper-bounded by* α *for some* *matrix measure* μ*, i.e.,*

$$\exists \alpha \in \mathbb{R}, \ \forall x, \ \forall t \geq 0, \qquad \mu\left(\frac{\partial f}{\partial x}\right) \leq \alpha$$

Then, network (9.72) synchronizes if

$$k > \frac{\alpha}{N}$$

That is, $k_{\min} \propto 1/N$ *.*

Proof. Consider the virtual system

$$\dot{y} = f(y,t) + kN(z-y) \tag{9.73}$$

Synchronization is attained if the virtual system is contracting. Now, computing the matrix measure of the Jacobian of (9.73) yields for any x and for any $t \geq 0$

$$\mu\left(\frac{\partial f}{\partial y} - kNI\right) \ \leq \ \mu\left(\frac{\partial f}{\partial y}\right) + kN\mu\left(-I\right) \ \leq \ \alpha - kN$$

Thus, the virtual system is contracting if $k > \frac{\alpha}{N}$. □

Dependence on initial conditions

We now consider the basic quorum sensing model (9.58). We derive simple conditions for the final behavior of the network to become independent of initial conditions (in the nodes and the medium) as N becomes large.

Theorem 9.3.7. *Assume that for (9.58) the following conditions hold: (i)* $\mu\left(\frac{\partial f}{\partial x}\right) \to -\infty$ *as* $N \to +\infty$*; (ii)* $g\left(z, v_2(t), t\right)$ *is contracting (for any* $v_2(t)$ *in* $\mathbb{R}^d$*); (iii)* $\left\|\frac{\partial f}{\partial z}\right\|$ *and* $\left\|\frac{\partial g}{\partial v_2}\right\|$ *are bounded for any* x*,* z*,* v_2 *(where* $\|\cdot\|$ *is the operator norm).*

Then, there exists some N^* *such that for any* $N \geq N^*$ *all trajectories of (9.58) globally exponentially converge towards a unique synchronized solution, independent of initial conditions.*

Proof. We know that contraction of $f\left(x, v_1(t), t\right)$ for any $v_1(t)$ (which the first condition implies for N large enough) ensures network synchronization. That is, there exists a unique trajectory, $x_s(t)$, such that, as $t \to +\infty$,

$$|x_i - x_s| \to 0, \quad \forall i$$

Therefore, the final behavior is described by the following lower-dimensional system:

$$\begin{aligned} \dot{x}_s &= f\left(x_s, z, t\right) \\ \dot{z} &= g\left(z, \Psi\left(x_s\right), t\right) \end{aligned} \tag{9.74}$$

If in turn this reduced-order system (9.74) is contracting, then its trajectories globally exponentially converge towards a unique solution, say $x_s^*(t)$, regardless of initial conditions. This will prove the Theorem (similar strategies are extensively discussed in [33]).

To show that (9.74) is indeed contracting, compute its Jacobian matrix,

$$\begin{bmatrix} \frac{\partial f}{\partial x_s} & \frac{\partial f}{\partial z} \\ \frac{\partial g}{\partial x_s} & \frac{\partial g}{\partial z} \end{bmatrix}$$

Lemma A.2.1 in the Appendix shows that the above matrix is contracting if there exists some strictly positive constants θ_1, θ_2 such that

$$\mu\left(\frac{\partial f}{\partial x_s}\right) + \frac{\theta_2}{\theta_1}\left\|\frac{\partial g}{\partial x_s}\right\| \qquad \text{and} \qquad \mu\left(\frac{\partial \mathrm{g}}{\partial \mathrm{z}}\right) + \frac{\theta_1}{\theta_2}\left\|\frac{\partial \mathrm{f}}{\partial \mathrm{z}}\right\| \tag{9.75}$$

are both uniformly negative definite.

Now, $\mu\left(\frac{\partial f}{\partial x_s}\right)$ and $\mu\left(\frac{\partial g}{\partial z}\right)$ are both uniformly negative by hypotheses. Furthermore, $\mu\left(\frac{\partial f}{\partial x_s}\right)$ tends to $-\infty$ as N increases: since $\left\|\frac{\partial f}{\partial z}\right\|$ and $\left\|\frac{\partial g}{\partial x_s}\right\|$ are bounded, this implies that there exists some N^* such that for any $N \geq N^*$ the two conditions in (9.75) are satisfied. □

Also, assume that actually the dynamics f and g do not depend explicitly on time. Then, under the conditions of the above Theorem, the reduced system is both contracting and autonomous, and so it tends towards a unique equilibrium point [111]. Thus, the original system converges to a unique equilibrium, where all x_i's are equal.

In addition, note that when the synchronization rate and the contraction rate of the reduced system both increase with N, this also increases robustness [142] to variability and disturbances.

9.3.6 Examples

Synchronization of FitzHugh-Nagumo oscillators

To illustrate synchronization and population effects similar to those described in Section 9.3.5, consider a network of FitzHugh-Nagumo oscillators coupled through a dynamic medium,

$$\begin{aligned} \dot{v}_i &= c\left(v_i + w_i - 1/3v_i^3 + I\right) + kN\left(z - v_i\right) \\ \dot{w} &= -1/c\left(v_i - a + bw_i\right) \\ \dot{z} &= \tfrac{D_e}{N}\textstyle\sum_{i=1}^N \left(v_i - z\right) - d_e z \end{aligned} \tag{9.76}$$

In what follows, system parameters are set as $a = 0.3$, $b = 0.2$, $c = 20$, $k = 1$,

$d_e = D_e = 1$. Similarly to the proof of Theorem 9.3.6, consider the virtual system

$$\dot{y}_1 = c\,(y_1 + y_2 - 1/3y_2^3 + I) + kN\,(z - y_1)$$
$$\dot{y}_2 = -1/c\,(y_1 - a + by_2)$$

whose Jacobian matrix is

$$J := \begin{bmatrix} c\,(1-y_1^2) - kN & c \\ -\frac{1}{c} & -\frac{b}{c} \end{bmatrix}$$

Using the matrix measure $\mu_{2,\Theta}$, with

$$\Theta = \begin{bmatrix} 1 & 0 \\ 0 & c \end{bmatrix}$$

yields $\mu_{2,\Theta}\,(J) = \mu_2\,(F)$, where

$$F \;=\; \Theta J \Theta^{-1} \;=\; \begin{bmatrix} c\,(1-y_1^2) - kN & 1 \\ -1 & -\frac{b}{c} \end{bmatrix}$$

Thus, the virtual system is contracting if the maximum eigenvalue of the symmetric part of F is uniformly negative. Similarly to Theorem 9.3.6, this is obtained if

$$N > \frac{c}{k} \tag{9.77}$$

That is, a sufficient condition for the virtual system to be contracting, and hence for network (9.76) to fulfill synchronization, is given by (9.77). Figures 9.15 and 9.16 illustrate the corresponding system behavior for values of N below and above this threshold.

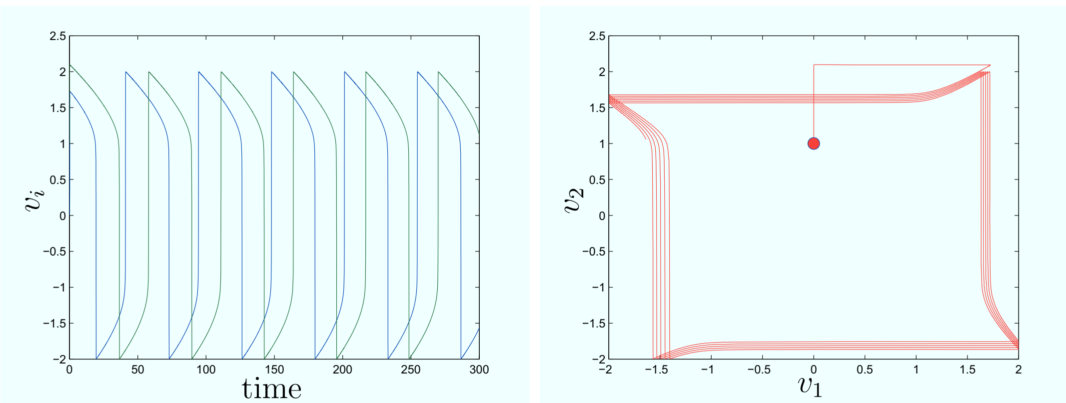

Figure 9.15: Simulation of network (9.76) for $N = 2$, showing the absence of synchronization. Left: time behavior of v_1, v_2. Right: network phase plot, with initial conditions denoted with a round marker.

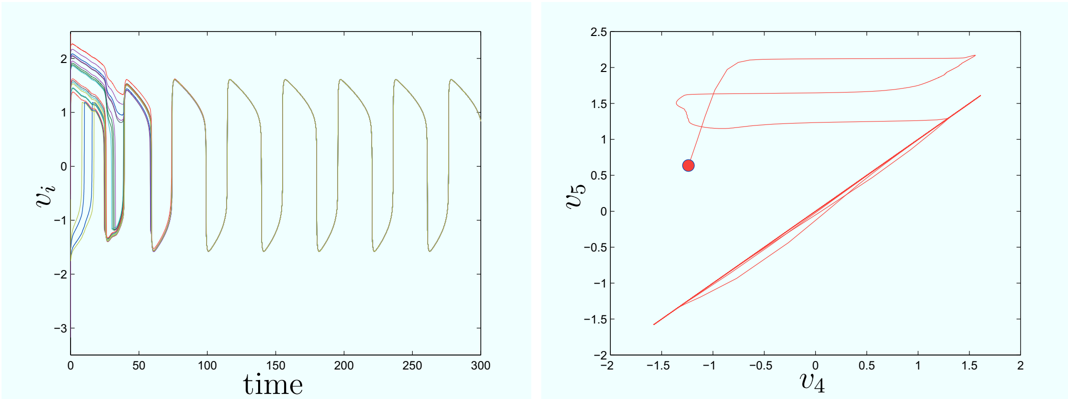

Figure 9.16: Simulation of network (9.76) for $N = 20$, showing synchronization.

9.3.7 Genetic oscillators

In Section 9.3.4 we showed that bilateral coupling with the environment also allowed the synchronized behavior of the network nodes to be of a given period, by driving the environment variable by an exogenous signal having that period. Here we illustrate this result on a model of a population of genetic oscillators coupled by means of the concentration of a protein in the environment.

Specifically, we consider the genetic circuit analyzed in [96] (a variant of [94]), and schematically represented in Figure 9.17. Such a circuit is composed of two engineered gene networks that have been experimentally implemented in *E. coli*; namely: the toggle switch [62] and an intercell communication system [205]. The toggle switch is composed of two transcription factors: the *lac* repressor, encoded by gene *lacI*, and the temperature-sensitive variant of the λcI repressor, encoded by the gene *cI857*. The expressions of *cI8547* and *lacI* are controlled by the promoters P_{trc} and P_{L^*} respectively (for further details see [96]). The intercell communication system makes use of components of the quorum-sensing system from *Vibro fischeri* (see e.g. [134] and references therein). Such a mechanism allows cells to sense population density through the transcription factor LuxR, which is an activator of the genes expressed by the P_{lux} promoter, when a small molecule AI binds to it. This small molecule, synthesized by the protein LuxI, is termed as autoinducer and it can diffuse across the cell membrane.

In [96], the following dimensionless simplified model is analyzed (see Figure 9.18):

$$\dot{u}_i = \frac{\alpha_1}{1+v_i^\beta} + \frac{\alpha_3 w_i^\eta}{1+w_i^\eta} - d_1 u_i \tag{9.78a}$$

$$\dot{v}_i = \frac{\alpha_2}{1+u_i^\gamma} - d_2 v_i \tag{9.78b}$$

$$\dot{w}_i = \varepsilon\left(\frac{\alpha_4}{1+u_i^\gamma} - d_3 w_i\right) + 2d\,(w_e - w_i) \tag{9.78c}$$

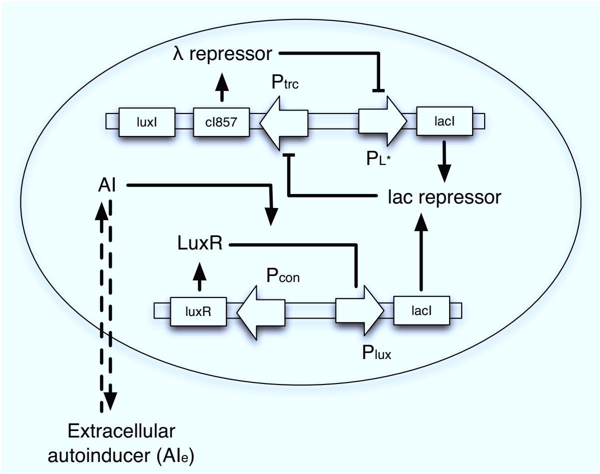

Figure 9.17: A schematic representation of the genetic circuit: detailed circuit.

$$\dot{w}_e = \frac{D_e}{N} \sum_{i=1}^{N} (w_i - w_e) - d_e w_e \tag{9.78d}$$

where u_i, v_i and w_i denotes the (dimensionless) concentrations of the *lac* repressor, λ repressor and LuxR-AI activator respectively. The state variable w_e denotes instead the (dimensionless) concentration of the extracellular autoinducer.

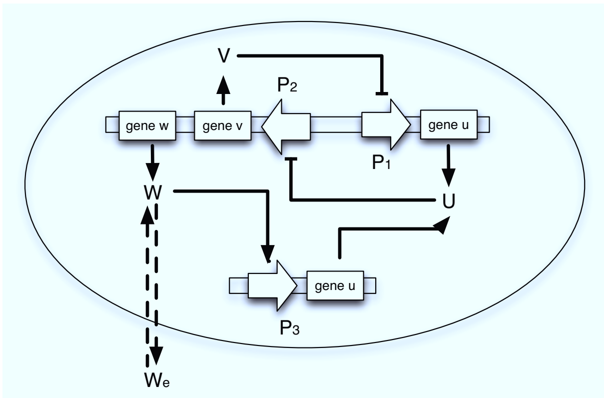

Figure 9.18: Simplified circuit using for deriving the mathematical model (9.78). Both the promoters and transcription factors are renamed.

In [96], a bifurcation analysis is performed for the above model, showing that synchronization can be attained for some range of the biochemical parameters of the circuit. However, as the objective of that paper was to analyze the onset of synchronization, the problem of guaranteeing a desired oscillatory behavior was not addressed. In what follows, using the results derived in the previous sections, we address the open problem of guaranteeing a desired period for the final oscillatory behavior of network (9.78).

The control mechanism that we use here is an exogenous signal acting on the extracellular autoinducer concentration, see also [161]. That is, the idea is to modify

(9.78d) as follows

$$\dot{w}_e = \frac{D_e}{N}\sum_{i=1}^{N}(w_i - w_e) - d_e w_e + r(t) \tag{9.79}$$

where $r(t)$ is some T-periodic signal. In the set up that we have in mind here, multiple copies of the genetic circuit of interest share the same surrounding solution, on which $r(t)$ acts. From the technological viewpoint, $r(t)$ can be implemented by controlling the temperature of the surrounding solution, and/or using e.g. the recently developed microfluidics technology (see e.g. [16] and references therein).

In what follows, we will use Theorem 9.3.1 to find a set of biochemical parameters that ensure synchronization of (9.78a)-(9.78d). This, using the results of Section 9.3.4, immediately implies that the forced network (9.78a)-(9.78c), (9.79) globally exponentially converges towards a T-periodic final behavior.

System (9.78) has the same structure as (9.60), with $x_i = [u_i, v_i, w_i]^T$, $z = w_e$, and:

$$\begin{aligned}
f(x_i,t) &= \begin{bmatrix} \frac{\alpha_1}{1+v_i^\beta} + \frac{\alpha_3 w_i^\eta}{1+w_i^\eta} - d_1 u_i \\ \frac{\alpha_2}{1+u_i^\gamma} - d_2 v_i \\ \varepsilon\left(\frac{\alpha_4}{1+u_i^\gamma} - d_3 w_i\right) \end{bmatrix} \\
k_z(z) - k_x(x_i) &= \begin{bmatrix} 0 \\ 0 \\ 2d(w_e - w_i) \end{bmatrix} \\
g(z,t) &= -d_e w_e \\
\textstyle\sum_{i=1}^{N}[u_x(x_i) - u_z(z)] &= \textstyle\frac{D_e}{N}\sum_{i=1}^{N}(w_i - w_e)
\end{aligned}$$

We know from Theorem 9.3.4 that all nodes trajectories converge towards each other if:

1. $f(x_i,t) - k_x(x_i)$ is contracting;

2. $g(z,t) - Nu_z(z)$ is contracting.

That is, contraction is ensured if there exist some matrix measures, μ_* and μ_{**}, such that

$$\mu_*((x_i,t) - k_x(x_i)) \quad \text{and} \quad \mu_{**}(g(z,t) - Nu_z(z))$$

are uniformly negative definite. We use the above two conditions in order to obtain a set of biochemical parameters ensuring node convergence. A possible choice for the above matrix measures is $\mu_* = \mu_{**} = \mu_1$ (see [160], [161]). Clearly, other choices for the matrix measures μ_* and μ_{**} can be made, leading to different algebraic conditions, and thus to (eventually) a different choice of biochemical parameters.

We assume that $\beta = \eta = \gamma = 2$, and show how to find a set of biochemical parameters satisfying the above two conditions.

Condition 1. Differentiation of $\frac{\partial f}{\partial x_i} - \frac{\partial k}{\partial x_i}$ yields the Jacobian matrix (where the subscripts have been omitted)

$$J_i := \begin{bmatrix} -d_1 & \frac{-2\alpha_1 v}{(1+v^2)^2} & \frac{2\alpha_3 w}{(1+w^2)^2} \\ \frac{-2\alpha_2 u}{(1+u^2)^2} & -d_2 & 0 \\ \frac{-2\varepsilon\alpha_4 u}{(1+u^2)^2} & 0 & -\varepsilon d_3 - 2d \end{bmatrix} \tag{9.80}$$

Now, by definition of μ_1, we have:

$$\mu_1(J_i) = \max\Big\{ -d_1 + \tfrac{2\alpha_2 u}{(1+u^2)^2} + \tfrac{2\varepsilon\alpha_4 u}{(1+u^2)^2}, \\ -d_2 + \tfrac{2\alpha_1 v}{(1+v^2)^2}, -\varepsilon d_3 - 2d + \tfrac{2\alpha_3 w}{(1+w^2)^2} \Big\}$$

Thus, J_i is contracting if $\mu_1(J_i)$ is uniformly negative definite. That is,

$$\begin{aligned} &-d_1 + \tfrac{2\alpha_2 u}{(1+u^2)^2} + \tfrac{2\varepsilon\alpha_4 u}{(1+u^2)^2} < 0 \\ &-d_2 + \tfrac{2\alpha_1 v}{(1+v^2)^2} < 0 \\ &-\varepsilon d_3 - 2d + \tfrac{2\alpha_3 w}{(1+w^2)^2} < 0 \end{aligned} \tag{9.81}$$

uniformly. Notice now that the maximum of the function $a(v) = \frac{\bar{a}v}{(1+v^2)^2}$ is $\hat{a} = \frac{3\sqrt{3}\bar{a}}{16}$. Thus, the set of inequalities (9.81) is fulfilled if:

$$\begin{aligned} &-d_1 + \tfrac{6\alpha_2\sqrt{3}}{16} + \tfrac{6\varepsilon\alpha_4\sqrt{3}}{16} < 0 \\ &-d_2 + \tfrac{6\alpha_1\sqrt{3}}{16} < 0 \\ &-\varepsilon d_3 - 2d + \tfrac{6\alpha_3\sqrt{3}}{16} < 0 \end{aligned} \tag{9.82}$$

uniformly.

Condition 2 In this case it is easy to check that the matrix $J_e := \frac{\partial g}{\partial z} - N\frac{\partial u}{\partial z}$ is contracting for any choice of the (positive) biochemical parameters D_e, d_e.

Thus, we can conclude that any choice of biochemical parameters fulfilling (9.82) ensures synchronization of the network onto a periodic orbit of period T. In [96], it was shown that a set of parameters for which synchronization is attained is: $\alpha_1 = 3$, $\alpha_2 = 4.5$, $\alpha_3 = 1$, $\alpha_4 = 4$, $\varepsilon = 0.01$, $d = 2$, $d_1 = d_2 = d_3 = 1$. We now use the guidelines provided by (9.82) to make a minimal change of the parameters values ensuring network synchronization with oscillations of period T. Specifically, such conditions can be satisfied by setting $d_1 = 6$, $d_2 = 2$. Figure 9.19 shows the behavior of the network for such a choice of the parameters. Finally, Figure 9.20 shows a simulation of the network (with $N = 2$) when the biochemical parameters are chosen so as to violate the two conditions above. In such a figure, both the time behavior of w_i and phase plot are shown, indicating that synchronization is indeed not attained.

Note again that, depending on actual parameter values, the overall system may or not be contracting, and therefore synchronization to a common period is the result of coordination through the shared variable.

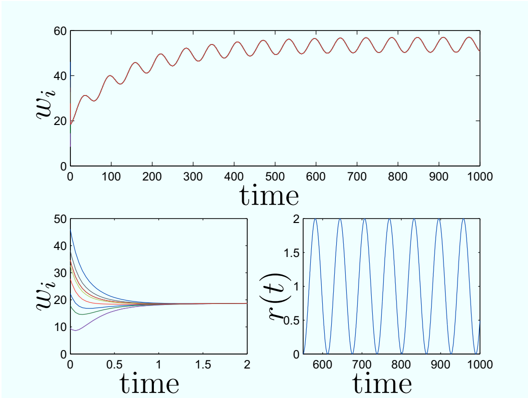

Figure 9.19: Behavior of (9.78a)-(9.78c), (9.79), when $N = 10$ and $r(t) = 1 + \sin(0.1t)$. Notice that the nodes have initial different conditions, and that they all converge (at approximatively $t = 2$) onto a common asymptotic having the same period as $r(t)$.

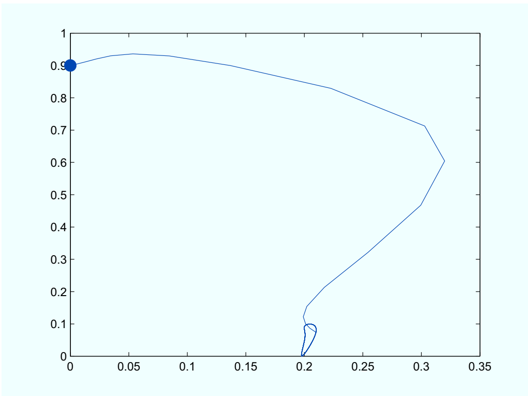

Figure 9.20: Behavior of (9.78a)-(9.78c), (9.79), when $N = 2$ and all the α's are increased, violating condition 1 and condition 2. The phase plot shows that synchronization is not attained: w_1 is on the x-axis, w_2 is on the y-axis.

Communication over different media

In the above Section, we assumed that all the genetic circuits shared the same surrounding solution. We now analyze the case where two different groups of genetic circuits are surrounded by two different media. The communication between groups is then left to some (possibly artificial) communication strategy between the two media.

We now assume that only one of the two media is forced by the exogenous T-periodic signal $r(t)$, while the two media communicate with each other in a diffusive way. The mathematical model that we analyze here is then:

$$\begin{aligned}
\dot{u}_{i1} &= \tfrac{\alpha_1}{1+v_{i1}^{\beta}} + \tfrac{\alpha_3 w_{i1}^{\eta}}{1+w_{i1}^{\eta}} - d_1 u_{i1} \\
\dot{v}_{i1} &= \tfrac{\alpha_2}{1+u_{i1}^{\gamma}} - d_2 v_{i1} \\
\dot{w}_{i1} &= \varepsilon \left(\tfrac{\alpha_4}{1+u_{i1}^{\gamma}} - d_3 w_{i1} \right) + 2d \left(w_{e1} - w_{i1} \right) \\
\dot{w}_{e1} &= \tfrac{D_e}{N} \textstyle\sum_{i=1}^{N} \left(w_{i1} - w_{e1} \right) - d_e w_{e1} + r\left(t\right) + \phi\left(w_{e2}\right) - \phi\left(w_{e1}\right) \\
\dot{u}_{i2} &= \tfrac{\bar{\alpha}_1}{1+v_{i2}^{\beta}} + \tfrac{\bar{\alpha}_3 w_{i2}^{\eta}}{1+w_{i2}^{\eta}} - \bar{d}_1 u_{i2} \\
\dot{v}_{i2} &= \tfrac{\bar{\alpha}_2}{1+u_{i2}^{\gamma}} - \bar{d}_2 v_{i2} \\
\dot{w}_{i2} &= \varepsilon \left(\tfrac{\bar{\alpha}_4}{1+u_{i2}^{\gamma}} - d_3 w_{i2} \right) + 2d \left(w_{e2} - w_{i2} \right) \\
\dot{w}_{e2} &= \tfrac{\bar{D}_e}{N} \textstyle\sum_{i=1}^{N} \left(w_{i2} - w_{e2} \right) - \bar{d}_e w_{e2} + \phi\left(w_{e1}\right) - \phi\left(w_{e2}\right)
\end{aligned} \tag{9.83}$$

where $x_{i1} = \left[u_{i1}, v_{i1}, w_{i1}\right]^T$ and $x_{i2} = \left[u_{i2}, v_{i2}, w_{i2}\right]^T$ denote the set of state variables of the i-th oscillator of the first and second group respectively. Analogously, w_{e1} and w_{e2} denote the extracellular autoinducer concentration surrounding the first and second group of genetic circuits.

Notice that the biochemical parameters of the nodes composing the two groups and of their corresponding media are not identical. Specifically, for the first group we use the same parameters as in the previous section, while for the second group we use parameters which differ from parameters of the first group by approximatively 50% (so as to still satisfy the two conditions of the previous Section). To ensure concurrent synchronization, we design the coupling function between the media ($\phi\left(\cdot\right)$) by using the guidelines provided by Theorem 9.3.3. Furthermore, using Theorem 9.3.5 we can conclude that the final behavior of the two groups is T-periodic.

It is straightforward to check that the hypotheses of Theorem 9.3.3 are all satisfied if:

- the biochemical parameters of the two groups fulfill the conditions in (9.82);
- the coupling function $\phi\left(\cdot\right)$ is increasing.

In fact, the topology of the autonomous level of the network is input equivalent by construction. Figure 9.21 shows the behavior of (9.83) when the biochemical parameters of the oscillators are tuned as in the previous Section, and $\phi\left(x\right) = Kx$, with $K = 0.1$.

Co-existence of multiple node dynamics

We now consider the case where the two groups analyzed above are identical, but connected with each other by means of a third group composed of Van der Pol oscillators. For such oscillators, the coupling between elements of the same goup is also implemented by means of a quorum-sensing mechanism. Communication

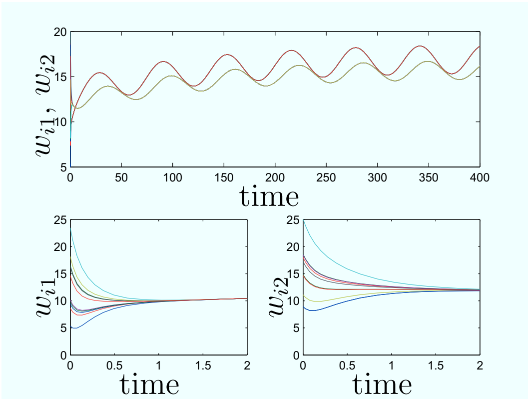

Figure 9.21: Behavior of (9.83) when $r(t) = 1 + \sin(0.1t)$. Both groups consists of $N = 10$ nodes. Concurrent synchronization is attained for the network. The time behavior of the first group of nodes is in red (upper line), while the time behavior of the second group is in yellow (lower line). Both the groups exhibit a final, synchronized, behavior having the same period as $r(t)$.

between the three groups occurs by means of some coupling between their media. The mathematical model considered here is then:

$$
\begin{aligned}
\dot{u}_{i1} &= \tfrac{\alpha_1}{1+v_{i1}^{\beta}} + \tfrac{\alpha_3 w_{i1}^{\eta}}{1+w_{i1}^{\eta}} - d_1 u_{i1} \\
\dot{v}_{i1} &= \tfrac{\alpha_2}{1+u_{i1}^{\gamma}} - d_2 v_{i1} \\
\dot{w}_{i1} &= \varepsilon\left(\tfrac{\alpha_4}{1+u_{i1}^{\gamma}} - d_3 w_{i1}\right) + 2d\left(w_{e1} - w_{i1}\right) \\
\dot{w}_{e1} &= \tfrac{D_e}{N}\sum_{i=1}^{N}\left(w_{i1} - w_{e1}\right) - d_e w_{e1} + \phi\left(w_{e3}\right) - \phi\left(w_{e1}\right) \\
\dot{u}_{i2} &= \tfrac{\alpha_1}{1+v_{i2}^{\beta}} + \tfrac{\alpha_3 w_{i2}^{\eta}}{1+w_{i2}^{\eta}} - d_1 u_{i2} \\
\dot{v}_{i2} &= \tfrac{\alpha_2}{1+u_{i2}^{\gamma}} - d_2 v_{i2} \\
\dot{w}_{i2} &= \varepsilon\left(\tfrac{\alpha_4}{1+u_{i2}^{\gamma}} - d_3 w_{i2}\right) + 2d\left(w_{e2} - w_{i2}\right) \\
\dot{w}_{e2} &= \tfrac{D_e}{N}\sum_{i=1}^{N}\left(w_{i2} - w_{e2}\right) - d_e w_{e2} + \phi\left(w_{e3}\right) - \phi\left(w_{e2}\right) \\
\dot{y}_{1i} &= y_{2i} \\
\dot{y}_{2i} &= -\alpha\left(y_{1i}^2 - \beta\right) y_{2i} - \omega^2 y_{1i} + K\left(w_{e3} - y_{1i}\right) \\
\dot{w}_{e3} &= \tfrac{K}{N_{vdp}}\sum_{i=1}^{N}\left(y_{2i} - w_{e3}\right) + g\left(w_{e3}\right) + \phi\left(w_{e1}\right) + \phi\left(w_{e2}\right) - 2\phi\left(w_{e3}\right)
\end{aligned}
\tag{9.84}
$$

with $[y_{1i}, y_{2i}]^T$ denoting the state variables of the i-th Van der Pol oscillator, and with N_{vdp} indicating the number of Van der Pol oscillators in the network. In the above model the Van der Pol oscillators are coupled by means of the medium $w_{e3} \in \mathbb{R}$. The three media, i.e. w_{e1}, w_{e2}, w_{e3}, communicate by means of the coupling function $\phi(\cdot)$, assumed to be linear. We assume that the function g governing the intrinsic dynamics of the medium w_{e3} is smooth with bounded derivative. The parameters for the Van der Pol oscillator are set as follows: $\alpha = \beta = \omega = 1$. Notice that now no external inputs is applied on the network.

Recall that Theorem 9.3.3 ensures synchronization under the following conditions:

1. contraction of each group composing the network;
2. topology of the autonomous level of the network connected and input equivalent.

Notice that the second condition is satisfied for the network of our interest. Furthermore, contraction of the two groups composed of genetic oscillators is ensured if the their biochemical parameters satisfy the inequalities in (9.82).

To guarantee the convergent behavior of the group composed of Van der Pol oscillators, we have to check that there exist two matrix measures, μ_* and μ_{**}, showing contraction of the following two matrices:

$$J_1 = \begin{bmatrix} 0 & 1 \\ -\alpha\left(y_{2i}^2 - \beta\right) - \omega^2 & -2\alpha y_{2i} y_{1i} - K \end{bmatrix} \tag{9.85a}$$

$$J_2 = \frac{\partial g}{\partial w_{e3}} - K \tag{9.85b}$$

Now in [194], using the Euclidean matrix measure μ_2, it is shown that the matrix (9.85a) is contracting if $K > \alpha$. On the other hand, to ensure contraction of J_2, we have to choose $K > \bar{G}$, where $\bar{G}$ is the maximum of $\frac{\partial g}{\partial w_{e3}}$. Thus, contraction of the group composed of Van der Pol oscillators is guaranteed if the coupling gain, K, is chosen such that:

$$K > \max\left\{\alpha, \bar{G}\right\}$$

Using $g(x) = \sin(x)$, $K = 2.5$, $N_{vdp} = 2$ and $\phi(x) = Kx$, with $K = 3$, Figure 9.22 shows that all the nodes of the two groups of genetic oscillators in (9.84) are synchronized, in agreement with the theoretical analysis. Figure 9.23 also shows that the two nodes belonging to the group of Van der Pol oscillators are synchronized with each other.

9.3.8 Analysis of a general Quorum-Sensing pathway

In the previous Section, we showed that our results (with appropriate choice of matrix measure) can be used to derive easily verifiable conditions on the biochemical parameters of the genetic oscillator ensuring contraction, and hence synchronization (onto a periodic orbit of desired period) and concurrent synchronization. We now show that our methodology can be applied to analyze a wide class of biochemical systems involved in cell-to-cell communication.

We focus on the analysis of the pathway of the quorum sensing mechanism that uses as autoinducers, molecules from the AHL (acyl homoserine lactone) family. The quorum sensing pathway implemented by AHL (see Figure 9.24) is one of the most common for bacteria and drives many transcriptional systems regulating their basic activities.

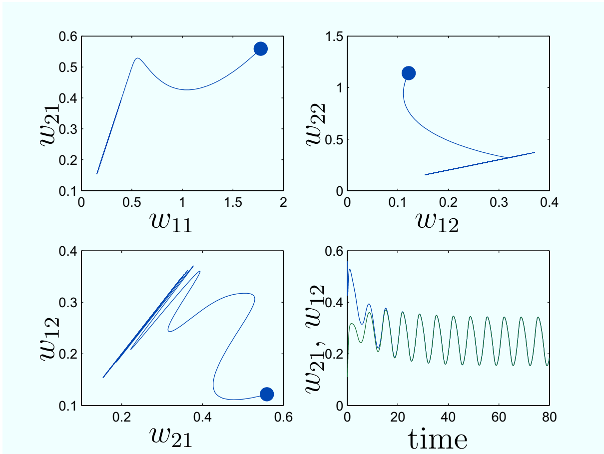

Figure 9.22: Behavior of (9.84): each of the two groups of genetic oscillators contains $N = 4$ nodes. Top: phase plot of the nodes belonging to the first group of genetic oscillators (left) and phase plot of the nodes belonging to the second group of genetic oscillators (right). Bottom: phase plot of two nodes belonging to the two different groups of genetic oscillators (left) and their time behavior. Both the phase plots and the time series show that synchronization is attained.

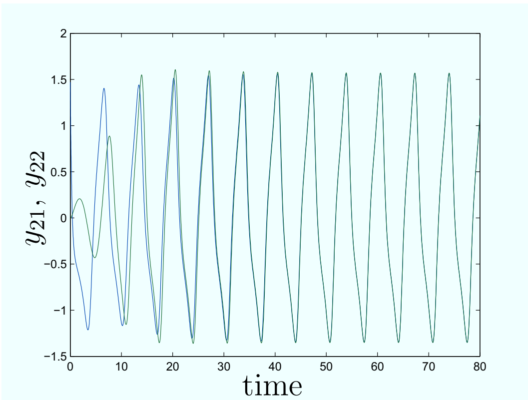

Figure 9.23: Time behavior of the two nodes composing the group of Van der Pol oscillators in (9.84).

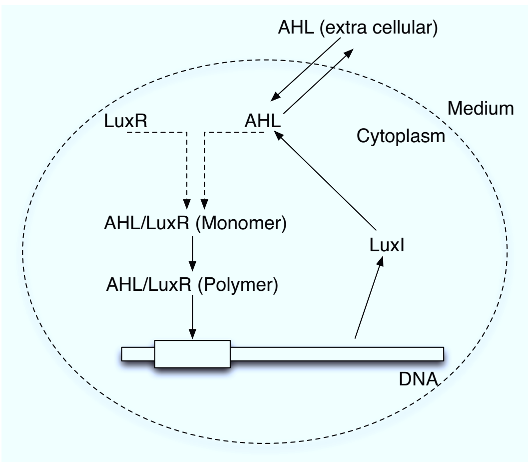

Figure 9.24: The quorum sensing pathway implemented by AHL

We now briefly describe the pathway of our interest (see [128] for further details). The enzyme LuxI produces AHL at (approximately) a constant rate. AHL in turn diffuses into and out of the cell and forms (in the cytoplasm) a complex with the receptor LuxR. Such complex polymerizes and then acts as a transcription factor, by binding the DNA. This causes the increase of the production of LuxI, generating a positive feedback loop.

The pathway can be described by a set of ordinary differential equations (using the law of mass action, see [87], [128]). Specifically, denoting with x_e the mass of AHL outside of the cell and with x_c the mass of AHL within the cell, we have the following mathematical model:

$$\begin{aligned} \dot{x}_c &= \alpha + \frac{\beta x_c^n}{x_{thresh}^n + x_c^n} - \gamma_c x_c - d_1 x_c - d_2 x_e \\ \dot{x}_e &= d_1 x_c - d_2 x_e - \gamma_e x_e \end{aligned} \tag{9.86}$$

The physical meaning of the parameters in (9.86) is given in Table 9.1.

Table 9.1: Biochemical parameters for system (9.86)

Parameter	physical meaning
α	Low production rate of AHL
β	Increase of production rate of AHL
γ_c	Degradation rate of AHL in the cytosol
γ_e	Degradation rate of AHL outside the cell
d_1	Diffusion rate of the extracellular AHL
d_2	Diffusion of the intracellular AHL
x_{thresh}	Threshold of AHL between low and increased activity
n	Degree of polymerization

Now, contraction of the above system is guaranteed if

1. $-\gamma_c + \frac{2\beta x_{thresh}^2 x_c}{\left(x_{thresh}^2 + x_c^2\right)^2}$ is uniformly negative definite;

2. $-d_2 - \gamma_e$ is uniformly negative definite.

Recall that x_c and x_e are both scalars. Now, the second condition is satisfied since system parameters are all positive. That is, to prove contraction we have only to guarantee that

$$-\gamma_c + \frac{2\beta x_{thresh}^2 x_c}{\left(x_{thresh}^2 + x_c^2\right)^2}$$

is uniformly negative. Since

$$-\gamma_c + \frac{2\beta x_{thresh}^2 x_c}{\left(x_{thresh}^2 + x_c^2\right)^2} \leq -\gamma_c + \frac{3\beta\sqrt{3}}{8 x_{thresh}}$$

contraction is ensured if the biochemical parameters β, g and x_{thresh} fulfill the following condition

$$\frac{\beta}{x_{thresh}} < \frac{8\gamma_c}{3\sqrt{3}}$$

9.4 Symmetries and contraction in network motifs

Many research efforts have been recently devoted to the study of the emerging behavior of complex networks. In particular, to uncover the design principles of many Natural networks, *network motifs*, i.e. recurring wiring patterns of nodes, have been recently defined. Interestingly, in [126] the authors show that identical motifs are shared by networks arising from different areas, like e.g. biochemistry, neuroscience, electronic, economy. In turn, this lead the authors to conclude that a possible explanation for the presence of the network motifs in such networks is the fact that they may *perform* some *functionalities* which are important for the whole network. An interesting question is then that of understanding why the same motifs perform similar functionalities in such heterogeneous networks.

To address this open problem, it is necessary to somehow *abstract* the structure and functionalities of the network motif from its actual dynamics. This can be done by using the tools developed in Chapter 4: in fact, we will show with the following examples that the *structure* of such motifs guarantees some symmetry properties. Those properties, in turn, implicitly define the possible steady state behaviors. The desired behavior (i.e. the functionality of the motif) is then guaranteed under some mild assumptions on the vector field describing the dynamics of the motif.

9.4.1 An example: invariance under input scaling

In a series of recent papers, input-output properties of some cellular signaling biochemical systems have been analyzed [68, 167, 67, 34]. Such studies point out that many sensory systems show the property of having their output invariant under input scaling, which can be formally defined as follows:

Definition 9.4.1. *Let $x_i(t)$, $x_j(t)$ be solutions of (4.28) with initial conditions $x_0 = x_i(0) = x_j(0)$, when $u(t) = \chi_i(t)$ and $u(t) = \chi_j(t)$, respectively. System (4.28) is invariant under input scaling if $x_i(t) = x_j(t)$ for any $\chi_i(t)$, $\chi_j(t)$ such that $\chi_j(t) = F(t)\chi_i(t)$, with $F(t) > 0$.*

Invariance under input scaling with *constant* $F(t) = F$ has been recently studied in transcription networks by Alon and his co-authors [68, 34, 167]. In such papers, the authors focus on the study of transcriptional networks subject to step-inputs. In this case, the invariance under input scaling is called *fold-change detection behavior*

(FCD), as the output of the system depends only on fold changes in input and not on its absolute level. For example, if the input to the system is a step function from 1 to 2, then its output is the same as if the step was increased from 2 to 4.

In [167] it is shown that FCD is necessary and sufficient to make sensory searches in which an organism moves through a spatial sensory field invariant to the amplitude of the field. This feature is of fundamental importance in e.g. vision, [167]. In fact, as shown in [92], the reflectance of an object, say $R(r)$, is multiplied by the ambient light, I, to provide the contrast filed sensed by the eye. The eyes make spatial searches by means of rapid movements (fixational eye movements) several times per second, which scan the visual field. FCD in such a system, would allow visual searches to be independent on the strength of the ambient light. Recent studies suggest that spatial visual searches, where the eyes search for a specific object, are insensitive to ambient-light levels (across several order of magnitude), see e.g. [192].

This section uses the results on symmetries presented in Chapter 4 to analyze the associated mathematical models, arising from protein signal-transduction systems and bacterial chemotaxis, and in particular it revisits the recent work [167] from this point of view. It also shows how these results could, for instance, suggest a mechanism for stable quorum sensing in bacterial chemotaxis, thus combining symmetries in cell interactions (quorum sensing) with invariance to input scaling (fold change detection).

9.4.2 Gene regulation

This first example considers a pattern (network motif) arising in gene regulation networks, the *Type* 1 *Incoherent Feed-Forward Loop* (I1-FFL) [51], [126]. The *I1-FFL* is one of the most common network motifs in gene regulation networks (see also Section 5.4). As shown in Figure 9.25, it consists of an activator, X, which controls a target gene, Z, and activate a repressor of the same gene, Y (which can be thought of as the output of the system). It has been recently shown that such a network motif can generate a temporal pulse of Z response, accelerate the response time of Z and act as a band-pass amplitude filter, see e.g. [118], [93].

In [68] it has also been shown by using a dimensionless analysis that for a certain range of biochemical parameters, the I1-FFL can exhibit invariance under step-input scaling (i.e. FCD).

A basic model

In [68], it was shown that a minimal circuit which achieves FCD is the I1-FFL, with the activator in linear regime and the repressor saturating the promoter of the

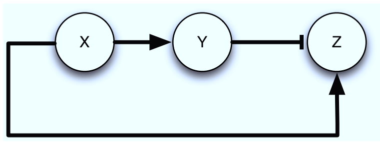

Figure 9.25: A schematic representation of the I1-FFL

target gene, Z. The model in [68] is of the form

$$\begin{aligned} \dot{Y} &= -\alpha_1 Y + \chi(t) \\ \dot{Z} &= \beta_2 \tfrac{\chi(t)}{Y} - \alpha_2 Z \end{aligned} \tag{9.87}$$

where α_1, α_2, β_2 are biochemical (positive) parameters and $\chi(t)$ is the input to the system (which can be approximated by the concentration of X). It was also shown that the dimensionless model

$$\begin{aligned} \tfrac{dy}{d\tau} &= F - y \\ r\tfrac{dz}{d\tau} &= \tfrac{F}{y} - z \end{aligned}$$

with:

$$\begin{aligned} y &= \tfrac{Y\alpha_1}{\beta_1 \chi_{\min}} & Z &= \tfrac{Z}{\beta_2\alpha_1/\beta_1\alpha_2} \\ F &= \tfrac{\chi(t)}{\chi_{\min}} & \tau &= \alpha_1 t \end{aligned}$$

exhibits invariance under input scaling. Later we will also consider more detailed mathematical models that in [68] have been analyzed numerically. In Section 5.4, we will also analyze other important network motifs under a slightly different viewpoint, i.e. by considering each of the *species* composing the motif as *nodes* of an interconnected systems.

In this Section, we show invariance under input scaling for system (9.87) for any input, $\chi_i(t)$, $\chi_j(t)$, such that

$$\frac{\chi_i(t)}{\chi_{\min,i}} = \frac{\chi_j(t)}{\chi_{\min,j}} = F(t)$$

In the above expressions $\chi_{\min,i}$ and $\chi_{\min,j}$ denote the basal level of the inputs $\chi_i(t)$ and $\chi_j(t)$ respectively. Such levels are assumed to be nonzero. Notice that the above class of inputs is wider that the one used in Definition 9.4.1.

Theorem 4.7.10 is now used to prove invariance under input scaling for (9.87). That is, we show that invariance under input scaling is a consequence of the existence of a symmetric and contracting virtual system in the spirit of Theorem 4.7.10.

In what follows, we will denote with $x_i = (Y_i, Z_i)^T$ and $x_j = (Y_j, Z_j)^T$ the solutions of (9.87), when $\chi(t) = \chi_i(t)$ and $\chi(t) = \chi_j(t)$, respectively. We assume that $Z_i(0) = Z_j(0)$. In terms of the notation introduced in Theorem 4.7.10, we have

$u(t) = \chi(t)$ and:

$$f(x, u(t)) = \begin{pmatrix} -\alpha_1 Y + \chi(t) \\ \beta_2 \frac{\chi(t)}{Y} - \alpha_2 Z \end{pmatrix}$$

Now, define the following actions:

$$\gamma_i = \begin{pmatrix} Y \\ Z \end{pmatrix} \rightarrow \begin{pmatrix} \frac{Y}{\chi_{\min,i}} \\ Z \end{pmatrix}, \quad \rho_i : \chi(t) \rightarrow \frac{\chi(t)}{\chi_{\min,i}} = F(t) \tag{9.88}$$

It is straightforward to check that:

- $f(x, u(t))$ is contracting uniformly in $u(t)$;
- $\gamma_i f(x_i, \chi_i(t)) = f(\gamma_i x_i, \rho_i \chi_i(t))$

Now, Theorem 4.7.10 implies that for any input $\chi_i(t)$, $\chi_j(t)$ such that $\rho_i \chi_i(t) = \rho_j \chi_j(t)$, $\gamma_i x_i$ and $\gamma_j x_j$ globally exponentially converge towards each other. That is:

$$|\gamma_i x_i - \gamma_j x_j| = \left| \begin{pmatrix} \frac{Y_i}{\chi_{\min,i}} - \frac{Y_j}{\chi_{\min,j}} \\ Z_i - Z_j \end{pmatrix} \right| \rightarrow 0 \tag{9.89}$$

for any χ_i, χ_j such that:

$$\frac{\chi_i(t)}{\chi_{\min,i}} = \frac{\chi_j(t)}{\chi_{\min,j}} = F(t) \tag{9.90}$$

Now, (9.89) implies that

$$|Z_i - Z_j| \rightarrow 0$$

exponentially. Since the initial conditions of Z_i and Z_j are the same we have that $Z_i(t) = Z_j(t)$ for any $t \geq 0$. That is, the system exhibits invariance under input scaling.

More detailed models

More detailed models of the I1-FFL are analyzed numerically in [68], showing that invariance under input scaling occurs for a wide range of biochemical parameters. Specifically, three different mechanisms are considered for binding the regulators X and Y to the promoter Z:

1. binding of X and Y is mutually exclusive, yielding the model

$$\begin{aligned} \dot{Y} &= \beta_1 \chi(t) - \alpha_1 Y \\ \dot{Z} &= \beta_2 \frac{\frac{\chi(t)}{K_1}}{1 + \frac{\chi(t)}{K_1} + \frac{Y}{K_2}} - \alpha_2 Z \end{aligned} \tag{9.91}$$

2. binding of X and Y is independent, yielding

$$\begin{aligned} \dot{Y} &= \beta_1 \chi(t) - \alpha_1 Y \\ \dot{Z} &= \beta_2 \frac{\frac{\chi(t)}{K_1}}{\left(1+\frac{\chi(t)}{K_1}\right)\left(1+\frac{Y}{K_2}\right)} - \alpha_2 Z \end{aligned} \tag{9.92}$$

3. binding of X and Y is cooperative, yielding

$$\begin{aligned} \dot{Y} &= \beta_1 \chi(t) - \alpha_1 Y \\ \dot{Z} &= \beta_2 \frac{\frac{\chi(t)}{K_1}}{1+\frac{\chi(t)}{K_1}+\frac{Y}{K_2}+\frac{\chi(t)Y}{K_3}} - \alpha_2 Z \end{aligned} \tag{9.93}$$

We now show that our results can be used to analyze such models, yielding conclusions in agreement with the numerical results obtained in [68]. Specifically, we show that in some region of the parameter space invariance under input scaling is determined by some symmetry of the virtual system.

Mutually exclusive binding of X and Y

Now, we show that in some region of parameter space, the model (9.91) exhibits a symmetry which causes invariance under input scaling.

In analogy with the above Section, we consider the actions, γ_i and ρ_i, defined as in (9.88). The *class* of inputs considered is that fulfilling (9.90). Notice that if

$$\frac{\chi(t)}{K_1} + \frac{Y}{K_2} \gg 1 \tag{9.94}$$

the model (9.91) is approximated by:

$$\begin{aligned} \dot{Y} &= \beta_1 \chi(t) - \alpha_1 Y \\ \dot{Z} &= \frac{\beta_2}{K_2} \frac{\chi(t)}{\chi(t)+Y} - \alpha_2 Z \end{aligned} \tag{9.95}$$

Following exactly the same outline as in previous Section, it is straightforward to check that the hypotheses of Theorem 4.7.10 are satisfied for system (9.95). This, in turn, implies that for any input such that $\chi_i/\chi_{\min,i} = \chi_j/\chi_{\min,j} = F(t)$,

$$|Z_i - Z_j| \to 0$$

exponentially, proving invariance under input scaling.

We remark here that the above result holds within the region defined by (9.94), where model (9.91) is approximated by (9.95). That is, the system exhibit invariance under input scaling only in the region of the parameter space defined by (9.94). In [68], it was shown numerically that (9.91) exhibits invariance under input scaling in the region

$$\frac{\chi_{\min}}{K_1} \gg 1 \qquad \frac{Y_{\min}}{K_2} \gg 1$$

Now, notice that the above region is a subset of (9.94).

Independent and cooperative binding of X and Y

In analogy with the previous Section, we now show that in some region of parameter space, invariance under input scaling is possible for system (9.92) and system (9.93).

Specifically, in the region defined by

$$K_2\chi(t) + K_1Y \gg K_1K_2 + \chi(t)Y \tag{9.96}$$

system (9.92) is approximated by the following model:

$$\begin{aligned} \dot{Y} &= -\alpha_1 Y + \chi(t) \\ \dot{Z} &= \tfrac{\beta_2}{K_2}\tfrac{\chi(t)}{K_1Y+K_2\chi(t)} - \alpha_2 Z \end{aligned} \tag{9.97}$$

Again, we will consider the actions, γ_i and ρ_i, defined as in (9.88). The *class* of inputs considered is that fulfilling (9.90). Now, the hypotheses of Theorem 4.7.10 are all satisfied for system (9.97). Thus, the invariance under input scaling behavior in the region (9.96) remains proved.

Notice that, the region identified by the above constraints is similar to that obtained in [68].

Following exactly the same steps as those described above, it is possible to prove that in the region defined by

$$\frac{\chi(t)}{K_1} + \frac{Y}{K_2} \gg 1 + \frac{\chi(t)Y}{K_3} \tag{9.98}$$

invariance under input scaling occurs for system (9.93). Notice that a sufficient condition for (9.98) to hold is:

$$K_2 \ \ll \ Y_{\min} \ \ll \ \tfrac{K_3}{\chi_{\min}}$$

In turn, the above constraints define a region similar to that obtained in [68].

9.4.3 A model from chemotaxis

In bacterial chemotaxis, bacteria walk through a chemo-attractant field, say $u(t, r)$ (r denotes two dimensional space vector). Along their walk, bacteria sense the concentration of u at their position and compute the tumbling rate (rate of changes of the direction) so as to move towards the direction where the gradient increases, see e.g. [30]. Typically, the input field is provided by means of a source of attractant which diffuses in the medium with bacteria accumulating in the neighborhood of the source. In this case, the information on the position of the source is encoded only in the shape of the field and not in its strength. Therefore, it is reasonable for bacteria to evolve a search pattern which is dependent only on the shape of the field and not on its strength, i.e., a search pattern which is invariant under input scaling [167]. Specifically, consider the following model [167] adapted from the chemotaxis model of [188]:

$$\begin{aligned} \dot{x} &= x f(y) \\ \epsilon \dot{y} &= \phi\left(\frac{u}{x}\right) - y \end{aligned} \tag{9.99}$$

where $u > 0$ is an increasing step-input to the system, representing the ligand concentration, and $y > 0$, the output of the system, represents the average kinase activity. The quantity $x > 0$ is an internal variable. We assume the function ϕ to be: i) a decreasing function in x with bounded partial derivative $\partial\phi/\partial x$; ii) an increasing function of u/x, with derivative $\phi' = \partial\phi/\partial(u/x) \leq b$, $b > 0$. Note that the above model becomes the one used in [167], when $\phi(u/x) = u/x$. Such a model is obtained assuming x is sufficiently large, with the term u/x actually a simplification of a term of the form $u/(x+\eta)$, with $0 < \eta \ll x$. The positive constant ϵ is typically small, so as to represent a separation of time-scales.

Assume as in [188] that $f(1) = 0$ and that $f(y)$ is strictly increasing with y. Obviously, (9.99) verifies the symmetry conditions of Theorem 4.7.10 with:

$$\gamma_i : (x_i, y_i) \rightarrow \left(\frac{x_i}{\bar{u}_i}, y_i\right) \qquad \rho_i : u_i \rightarrow \frac{u_i}{\bar{u}_i} \tag{9.100}$$

where $\bar{u}_i$ denotes the initial (lower) value, at time $t = 0$, of the step function. As in the previous Section we assume that $y_i(0) = y_j(0)$. Now, by means of Theorem 4.7.10, we can conclude that, if the system is contracting, $y_i(t) = y_j(t)$, $\forall t \geq 0$, for any input such that $\frac{u_i}{\bar{u}_i} = \frac{u_j}{\bar{u}_j} = F$.

Let us derive a condition for (9.99) to be contracting, which will give conditions on the dynamics and inputs of (9.99) ensuring invariance under input scaling. Model (9.99) can be recast as

$$\ddot{y} + \frac{1}{\epsilon}\dot{y} - \frac{1}{\epsilon}\frac{\partial\phi}{\partial x} x f(y) = 0 \tag{9.101}$$

As in [188, 167], choose $f(y) = y - 1$ for simplicity, so that (9.101) becomes

$$\ddot{y} + \frac{1}{\epsilon}\dot{y} - \frac{1}{\epsilon}\frac{\partial\phi}{\partial x} x(y-1) = 0 \tag{9.102}$$

The above dynamics is similar to a mechanical mass-spring-damper system with a time-varying spring,

$$\ddot{r} + 2\eta\omega\dot{r} + \omega^2 r = 0$$

with $2\eta\omega = \frac{1}{\epsilon}$ and $\omega^2 = -\frac{1}{\epsilon}\frac{\partial\phi}{\partial x}x$. Now, as shown in [110] such a dynamics is contracting if $\eta > \frac{1}{\sqrt{2}}$. Thus, it immediately follows that (9.102) is contracting if:

$$\frac{\partial\phi}{\partial x} x > -\frac{1}{2\epsilon} \tag{9.103}$$

Hence, contraction is attained if:

$$\phi'\left(-\frac{u}{x^2}\right)x > -\frac{1}{2\epsilon}$$

That is, a sufficient condition for (9.102) to be contracting is

$$x > 2\epsilon ub \tag{9.104}$$

Notice that, in the case where $\phi\,(u/x) = u/x$, (9.104) simply becomes:

$$x > 2\epsilon u \tag{9.105}$$

The above inequality implies that, in this case, the system is contracting (and hence exhibits invariance under input scaling) if the level of x is sufficiently high (which is true by hypotheses) and its dynamics is sufficiently slow (ϵ small) with respect to the dynamics of y. Also, given $\varepsilon < \frac{1}{2}$ and a constant u, if contraction condition (9.105) is verified at $t = 0$ with initial conditions embedded in a ball contained in the contraction region (9.105), it remains verified for any $t \geq 0$.

Finally, note that the results of this Section, and indeed of the original [68, 167], are closely related to the idea, first introduced in [142] and further studied in [64], of detecting a symmetry (here, in the environment) by using a dynamic system having the same symmetry.

Chapter 10

Conclusions

In this Thesis, we presented a coherent theoretical framework for the analysis and control of biochemical and networked systems, with applications to decentralized control and systems biology.

Chapter 2 and Chapter 3 were introductory chapters. Specifically, in Chapter 2 the notion of contracting dynamical system was briefly introduced. All the results reviewed in this Chapter were based on the use of Euclidean norms and were systematically generalized in Chapter 4. In Chapter 3, the main definitions of interconnected system used in the rest of the Thesis were introduced together with the main network coordination problems. The mathematical model introduced in this Chapter and coordination problems like e.g. consensus, synchronization and cluster synchronization were then studied in chapters 6-8.

In Chapter 4, the main results on contraction presented in Chapter 2, were revisited and extended. Specifically, we showed that: (i) contraction can be extended by using arbitrary norms; (ii) some structural properties can be used to relax the algebraic conditions for contraction.

The main result of this Chapter are then used in Chapter 5, where non-Euclidean norms were used to derive a graphical procedure for proving contraction. The key idea was to use such norms to obtain algebraic conditions that can be turned onto a graphical *algorithm*. At the core of the procedure there was the construction of a graph from system Jacobian, which was then required to be loopless. One of the main advantages of the proposed approach was that it did not require the knowledge of a metric for proving contraction.

The notions introduced in Chapter 4 were used in Chapter 6 to obtain a set of sufficient conditions ensuring stability of networked systems. In such a Chapter, a *multi-scale* approach for the study of stability of large scale systems was presented. The results of this Chapter were *robust*, in the sense that a large degree of uncertainty can be tolerated on the network nodes' dynamics. Moreover, the approach was turned into a tool for designing distributed communication protocols for network coordination ensuring, for example, set-point regulation. In the same chapter, it was also shown how symmetries and contraction can be used to design multi-purpose networks.

The study of networked systems was then continued in Chapter 7. In such a Chapter, we first presented a generic lemma that can be used to analyze the convergence of a networked system towards a linear flow invariant subspace (namely, the synchronization, or poli-synchronization subspace). We then used such a result to coordinate complex networks of both linear and nonlinear continuous time nodes. From the analysis viewpoint, we obtained novel sufficient conditions for network synchronization by deriving some explicit links between contraction analysis, Lyapunov-based techniques and the Master Stability Function.

In Chapter 8, we turned our attention to the problem of coordinating networks of discrete time and asynchronous nodes. Our main idea was that of providing conditions of the *synchronous* implementation of the network which ensured contraction of its asynchronous counterpart. Using non-Euclidean norms, we found a set of easily checkable conditions that were used for the design of distributed protocols allowing to solve consensus and cluster synchronization.

Finally, some applications of our results to the study of biochemical systems and networks were presented in Chapter 9. Specifically, sufficient conditions were obtained for the entrainment of biochemical circuits and a study on generic-quorum sensing networks was presented. Finally, a study on symmetries of some important network motif was presented which showed that this property, together with a *relaxed* contraction property, is responsible of the so-called fold change detection behavior.

Bibliography

[1] Complex networked control systems. *IEEE Control Systems Magazine*, 27(4), August 2007. Special issue.

[2] K. T. Alligod, T. Sauer, and J. Yorke. *Chaos: an introduction to dynamical systems*. Springer-Verlag, 1996.

[3] U. Alon. *An introduction to systems biology: design principles of biological circuits*. Chapman & Hall/CRC, 2006.

[4] U. Alon. Network motifs: theory and experimental approaches. *Nature*, 450:450–461, 2007.

[5] C.A. Anastassiou, S. M. Montgomery, M. Barahona, G. Buzsaki, and C. Koch. The effect of spatially inhomogeneous extracellular electric fields on neurons. *The Journal of Neuroscience*, 30:1925–1936, 2010.

[6] C. Anetzberger, T. Pirch, and K. Jung. Heterogeneity in quorum sensing-regulated bioluminescence of vibro harvey. *Molecular Microbiology*, 2:267–277, 2009.

[7] D. Angeli. A Lyapunov approach to incremental stability properties. *IEEE Transactions on Automatic Control*, 47:410–321, 2002.

[8] D. Angeli, J. E. Ferrell, and E.D. Sontag. Detection of multistability, bifurcations, and hysteresis in a large class of biological positive-feedback systems. *Proc Natl Acad Sci USA*, 101(7):1822–1827, 2004.

[9] D. Angeli and E. D. Sontag. Forward completeness, unboundedness observability, and their Lyapunov characterizations. *Systems and Control Letters*, 38:209–217, 1999.

[10] D. Angeli and E.D. Sontag. Monotone control systems. *IEEE Trans. Automat. Control*, 48(10):1684–1698, 2003.

[11] M. Arcak. On spatially uniform behavior in reaction-diffusion pde and coupled ode systems. Available at: http://arxiv.org/abs/0908.2614.

[12] M. Arcak and E.D. Sontag. A passivity-based stability criterion for a class of interconnected systems and applications to biochemical reaction networks. *Mathematical Biosciences and Engineering*, 5:1–19, 2008.

[13] V. I. Arnold. *Mathematical methods of classical mechanics.* Spriger-Verlag (New York), 1978.

[14] K. J. Astrom. *Analysis and design of nonlinear control systems: in honor of Alberto Isidori*, chapter Event Based Control, pages 127–147. Spriger-Verlag (Berlin Heidelberg), 2008.

[15] M. Barahona and L.M. Pecora. Synchronization in small-world systems. *Physical Review E*, 89:54–101, 2002.

[16] D. J. Beebe, G.A. Mensing, and G.M. Walker. Physics and applications of microfluidics in biology. *Annual Reviews of Biomedical Engineering*, 4:261–286, 2002.

[17] R. Bellman. *Introduction to matrix analysis.* McGraw-Hill (New York), 1960.

[18] V. N. Belykh, I. V. Belykh, and M. Hasler. Connection graph stability method for synchronization of coupled chaotic systems. *Physica D*, 195:159–187, 2004.

[19] Vladimir N. Belykh, Igor V. Belykh, and Erik Mosekilde. Cluster synchronization modes in an ensemble of coupled chaotic oscillators. *Physical Review E*, 63:036216, 2001.

[20] G. Beni and P. Liang. Pattern reconfiguration in swarms - convergence of a distributed asynchronous and bounded iterative algorithm. *IEEE Transactions on Robotics and Automation*, 12:485–490, 1996.

[21] M.A. Berger and Y. Wang. Bounded semigroups of matrices. *Linear Algebra and its Applications*, 166:21–27, 1992.

[22] D. S. Bernstein. *Matrix mathematics: theory, facts and formulas.* Princeton University Press (Princeton, NJ, USA), 2005.

[23] D. Bertsekas and J. Tsitsiklis. *Parallel and distributed computation: numerical methods.* Prentice-Hall (Upper Saddle River, NJ, USA), 1989.

[24] V. Blondel, J. Hendrickx, A. Olshevsky, and J. Tsitsiklis. Convergence in multiagent coordination, consensus and flocking. In *Proceedings of the IEEE Conference on Decision and Control*, pages 2996–3000, 2005.

[25] S. Boccaletti, V. Latora, Y. Moreno, M. Chavez, and D.U. Hwang. Complex networks: structure and dynamics. *Physics Report*, 424:175–308, 2006.

[26] B. Bollobas. *Modern Graph Theory.* Springer Verlag (New York), 1998.

[27] E. Borenstein and S. Ullman. Combined top-down/bottom-up segmentation. *IEEE Transactions on Pattern Analysis and Machine Intelligence*, 30:2109–2125, 2008.

[28] S. El Boustani, O. Marre, P. Behuret, P. Yger, T. Bal, A. Destexhe, and Y. Fregnac. Network- state modulation of power-law frequency-scaling in visual cortical neurons. *PLoS Computational Biolody*, 5:e1000519, 2009.

[29] C.D. Brody and J.J. Hopfield. Simple networks for spike-timing-based computation, with application to olfactory processing. *Neuron*, 37:843–852, 2003.

[30] A. Celani and M. Vergassola. Bacterial strategies for chemotaxis response. *Proceedings of the National Academy of Science*, 107:1391–1396, 2010.

[31] L. Chen, J. Lu, and C.K. Tse. Synchronization: An obstacle to identification of network topology. *IEEE Transactions on Circuits and Systems II*, 56:310–314, 2009.

[32] Tianping Chen, Xiwei Liu, and Wenlian Lu. Pinning complex networks by a single controller. *IEEE Transactions on Circuits and Systems I: Regular Papers*, 54(6):1317–1326, June 2007.

[33] S.J Chung, J.J.E. Slotine, and D.W. Miller. Nonlinear model reduction and decentralized control of tethered formation flight. *A.I.A.A. Journal of Guidance, Control and Dynamics*, 30:390–400, 2007.

[34] C. Cohen-Saidon, A.A. Cohen, A. Sigal, Y. Liron, and U. Alon. Dynamics and variability of erk2 response to egf in individual living cells. *Molecular Cell*, 36:885–893, 2009.

[35] S. Coombes. Phase locking in networks of synaptically coupled McKean relaxation oscillators. *Physica D*, 160:173–188, 2001.

[36] I.D. Couzin, J. Krause, N.R. Franks, and S.A. Levin. Effective leadership and decision making in animal groups on the move. *Nature*, 433:513–516, 2005.

[37] A. Czornik. On the generalized spectral subradius. *Linear Algebra and its Applications*, 407:242–248, 2005.

[38] G. Dahlquist. *Stability and error bounds in the numerical integration of ordinary differential equations.* Trans. Roy. Inst. Techn. (Stockholm), 1959.

[39] S. Dashkovskiy, B. Rüffer, and F. Wirth. An ISS small-gain theorem for general networks. *Mathematics of Control, Signals, and Systems*, 19:93–122, 2007.

[40] D. Del Vecchio, A. J. Ninfa, and E. D. Sontag. Modular cell biology: Retroactivity and insulation. *Nature Molecular Systems Biology*, 4:161, 2008.

[41] P. DeLellis, M. di Bernardo, and G. Russo. On quad, lipschitz and contracting vector fields for consensus and synchronization of networks. *IEEE Transcations on Circuits And Systems I*, in press, 2010.

[42] P. DeLellis, M. di Bernardo, G. Russo, and T. Gorochowski. Synchronization and control of complex networks via contraction, adaptation and evolution. *IEEE Circuits And Systems Magazine: Special Issue on Complex Networks Applications in Circuits and Systems*, 3:64–82, 2010.

[43] P. DeLellis, M. diBernardo, F. Garofalo, and M. Porfiri. Evolution of complex networks via edge snapping. *IEEE Transactions on Circuits and Systems I*, PP(99):1 –12, 2010.

[44] Pietro DeLellis, Mario diBernardo, and Francesco Garofalo. *Modelling, Estimation and Control of Networked Complex Systems*, chapter Decentralized Adaptive Control for Synchronization and Consensus of Complex Networks. Springer-Verlag, 2009.

[45] Pietro DeLellis, Mario diBernardo, and Francesco Garofalo. Novel decentralized adaptive strategies for the synchronization of complex networks. *Automatica*, 45:1312 – 1318, 2009.

[46] Pietro DeLellis, Mario diBernardo, and Franco Garofalo. Synchronization of complex networks through local adaptive coupling. *Chaos*, 18:037110, 2008.

[47] Pietro DeLellis, Mario diBernardo, Francesco Sorrentino, and Antonio Tierno. Adaptive synchronization of complex networks. *International Journal of Computer Mathematics*, 85(8):1189–1218, August 2008.

[48] Pietro DeLellis, Mario diBernardo, and Luiz Felipe Turci. Pinning control of complex networked systems via a fully adaptive decentralized strategy. Submitted to IEEE Transactions on Automatic Control.

[49] D. V. Dimarogonas and K. J. Kyriakopoulos. On the rendezvous problem for multiple nonholonomic agents. *IEEE Transactions on Automatic Control*, 52:916–922, 2007.

[50] Nonlinear Dynamics and Chaos. *Nonlinear Dynamics and Chaos*. R. Perseus, 1994.

[51] P. Eichenberger, M. Fujita, S.T. Jensen, E.M. Conlon, D.Z. Rudner, S.T. Wang, C. Ferguson, K. Haga, T. Sato, J.S. Liu, and R. Losick. The program

of gene transcription for a single differentiating cell type during sporulation in Bacillus subtilis. *PLoS Biology*, 2:e328, 2004.

[52] M. B. Elowitz and S. Leibler. A synthetic oscillatory network of transcriptional regulators. *Nature*, 403:335–338, 2000.

[53] Z. Fan. *Complex networks: From topology to dynamics*. PhD thesis, Centre for Chaos and Complex Networks, City University of Hong Kong, 2006.

[54] L. Fang and P.J. Antsaklis. Asynchronous consensus protocols using nonlinear paracontractions theory. *IEEE Transactions on Automatic Control*, 53:2351–2355, 2008.

[55] M. Fiedler. Algebraic connectivity of graphs. *Czechoslovak Mathematical Journal*, 23:298 – 305, 1973.

[56] A. F. Filippov. *Differential equations with discontinuous righthand sides.* Kluwer Academic Publishers (Dordrecht, The Netherlands), 1988.

[57] K.S. Fin. Three coupled oscillators as a universal probe of synchronization stability in coupled oscillator arrays. *Physical Review E*, 61:5080–5090, 2000.

[58] R. FitzHugh. Mathematical models of threshold phenomena in the nerve membrane. *Bulletin of Mathematical Biophysics*, 17:257–278, 1955.

[59] P.G.O. Freund. *Introduction to Supersymmetry.* Cambridge University Press (Cambridge, UK), 1988.

[60] F. Frohlich and D. A. McCormick. Endogenous electric fields may guide neocortical network activity. *Neuron*, 67:129–143, 2010.

[61] J Garcia-Ojalvo, M. B. Elowitz, and S. H. Strogatz. Modeling a synthetic multicellular clock: Repressilators coupled by quorum sensing. *Proceedings of the National Academy of Science*, 101:10955–10960, 2004.

[62] T.S. Gardner, C.R. Cantor, and J.J. Collins. Construction of a genetic toggle in Escherichia coli. *Nature*, 403:339–342, 2000.

[63] D. George and J. Hawkins. Towards a mathematical theory of cortical microcircuits. *PLoS Computational Biolody*, 5:e1000532, 2009.

[64] L. Gerard and J.J.E. Slotine. Neural networks and controlled symmetries, a generic framework. Available at: http://arxiv1.library.cornell.edu/abs/q-bio/0612049v2.

[65] G. Gigante, M. Mattia, J. Braun, and P. DelGiudice. Bistable perception modeled as competing stochastic integrations at two levels. *PLoS Computational Biology*, 5:e1000430, 2009.

[66] C. Godsil and G. Royle. *Algebraic Graph Theory*. Springer Verlag (New York), 2001.

[67] L. Goentoro and M.W. Kirschner. Evidence that fold-change, and not absolute level, of β-catenin dictates wnt signaling. *Molecular Cell*, 36:872–884, 2009.

[68] L. Goentoro, O. Shoval, M.W. Kirschner, and U. Alon. The incoherent feedforward loop can provide fold-change detection in gene regulation. *Molecular Cell*, 36:894–89, 2009.

[69] M. Golubitsky and I. Stewart. *The symmetry perspective: from equilibrium to chaos in phase space and physical space*. Birkhauser (Berlin), 2003.

[70] M. Golubitsky and I. Stewart. Nonlinear dynamics of networks: the groupoid formalism. *Bulletin of the American Journal of Mathematics*, 43:305–364, 2006.

[71] M. Golubitsky, I. Stewart, and A. Torok. Patterns of synchrony in coupled cell networks with multiple arrows. *SIAM Journal on Applied Dynamical Systems*, 4:78–100, 2005.

[72] D. Gonze, S. Bernard, C. Walterman, A. Kramer, and H. Herzerl. Spontaneous synchronization of coupled circadian oscillators. *Biophysical Journal*, 89:120–129, 2005.

[73] Bei Gou, Hui Zheng, Weibiao Wu, and Xingbin Yu. Probability distribution of blackouts in complex power networks. In *Proceedings of the 2007 IEEE International Symposium on Circuits And Systems. ISCAS2007*, pages 69–72, May 2007.

[74] A. Granas and J. Dugundji. *Fixed Point Theory*. Springer-Verlag (New York), 2003.

[75] T. Gregor, K. Fujimoto, N. Masaki, and S. Sawai. The onset of collective behavior in social Amoebe. *Science*, 328:1021–1025, 2010.

[76] R. O. Grigoriev, M. C. Cross, and H. G. Schuster. Pinning control of spatiotemporal chaos. *Phys. Rev. Lett.*, 79(15):2795–2798, Oct 1997.

[77] E. Guirey, M. Bees, A. Martin, and M. Srokosz. Persistence of cluster synchronization under the influence of advection. *Physical Review E*, 81:051902, 2010.

[78] L. Gurvits. Stability of discrete time inclusion. *Linear Algebra and its Applications*, 231:47–85, 1995.

[79] P. Hartman. On stability in the large for systems of ordinary differential equations. *Canadian Journal of Mathematics*, 13:480–492, 1961.

[80] D.J. Hill and Guanrong Chen. Power systems as dynamic networks. In *Proceedings of the 2006 IEEE International Symposium on Circuits and Systems. ISCAS2006*, pages 722–725, 2006.

[81] .J. Hopfield. Neural networks and physical systems with emergent collective computational abilities. *Proc Natl Acad Sci USA*, 79:2554–2558, 1982.

[82] R. A. Horn and C. R. Johnson. *Matrix Analysis*. Cambridge University Press (Cambridge, UK), 1999.

[83] Q. Hui and W. H. Haddad. Distributed nonlinear control algorithms for network consensus. *Automatica*, 44:2375–2381, 2008.

[84] E. M. Izhikevich. *Dynamical Systems in Neuroscience: The Geometry of Excitability and Bursting*. MIT Press (Cambridge, MA, USA), 2006.

[85] A. Jadbabaie, J. Lin, and A. S. Morse. Coordination of groups of mobile autonomous agents using nearest neighbor rules. *IEEE Transactions on Automatic Control*, 48:988–1001, 2003.

[86] J. Javaloyes, M. Perrin, and A. Politi. Collective atomic recoil laser as a synchronization transient. *Physical Review E*, 78:011108, 2008.

[87] J.Dockery and J. Keener. A mathematical model for quorum sensing in Pseudomonas aeruginosa. *Bulletin of Mathematical Biology*, 63:95–116, 2004.

[88] G.-P. Jiang, W. K.-S. Tang, and G. Chen. A state-observer-based approach for synchronization in complex dynamical networks. *IEEE Transactions on Circuits and Systems I*, 53(12):2739–2745, Dec. 2006.

[89] J. Jouffroy. Some ancestors of contraction analysis. In *Proceedings of the International Conference on Decision and Control*, pages 5450– 5455, 2005.

[90] E. Kandel, J. Schwartz, and T. Jessel. *Principles of Neural Science (4th Edition)*. Oxforn University Press, 2000.

[91] G. Katriel. Synchronization of oscillators coupled through an environment. *Physica D*, 237:2933–2944, 2008.

[92] J. Keener and J. Sneyd. *Mathematical Physiology*. Springer (Berlin), 2nd edition, 2009.

[93] D. Kim, Y.K. Kwon, and K.H. Cho. The biphasic behavior of incoherent feed-forward loops in biomolecular regulatory networks. *Bioessays*, 30:1204–1211, 2008.

[94] H. Kobayashi, M. Kaern, M. Araki, K. Chung, T.S. Gardner, C.R. Cantor, and J.J. Collins. Programmable cells: interfacing natural and engineered gene networks. *Proceedings of the National Academy of Science*, 101:8414–8419, 2004.

[95] M. A. Krasnosel'skii and S. G. Krein. Nonlocal existence and uniqueness of solutions of ordinary differential equations (in russian). *Dokl. Akad. Nauk. SSSR*, 102:13–16, 1955.

[96] A. Kuznetsov, M. Kaern, and N. Kopell. Synchrony in a population of hysteresis-based genetic oscillators. *SIAM Journal of Applied Mathematics*, 65:392–425, 2004.

[97] Y. A. Kuznetsov. *Elements of applied bifurcation theory.* Spriger-Verlag (New York), 2004.

[98] N. E. Leonard and E. Fiorelli. Virtual leaders, artificial potentials and coordinated control of groups. In *40th Conf. on Decision and Control*, 2001.

[99] D. C. Lewis. Metric properties of differential equations. *American Journal of Mathematics*, 71:294–312, 1949.

[100] C. Li, L. Chen, and K. Aihara. Stochastic synchronization of genetic oscillator networks. *BMC Systems Biology*, 1:6, 2007.

[101] Xiang Li, Xiaofan Wang, and Guanrong Chen. Pinning a complex dynamical network to its equilibrium. *IEEE Transactions on Circuits and Systems I: Regular Papers*, 51(10):2074–2087, Oct. 2004.

[102] Z. Li, Z. Duan, G. Chen, and L. Huang. Consensus of multi-agent systems and synchronization of complex networks: A unified viewpoint. *IEEE Transcactions on Circuits and Systems I*, Forthcoming:–, 2009.

[103] Zhi Li and Guanrong Chen. Global synchronization and asymptotic stability of complex dynamical networks. *IEEE Transactions on Circuits and Systems II*, 53(1):28–33, Jan. 2006.

[104] J. Lin, A. S. Morse, and B. D. O. Andersosn. The multi-agent rendezvous problem. In *Proceedings of the 42nd Conf. on Decision and Control*, pages 1508–1513, 2003.

[105] Z. Lin, M. Broucke, and B. Francis. Local control strategies for groups of mobile autonomous agents. *IEEE Transactions on Automatic Control*, 49:622–629, 2004.

[106] Xiwei Liu and Tianping Chen. Network synchronization with an adaptive coupling strength. *arXiv:math/0610580*, October 2006.

[107] Xiwei Liu and Tianping Chen. Exponential synchronization of nonlinear coupled dynamical networks with a delayed coupling. *Physica A*, 381:82–92, 2007.

[108] Xiwei Liu and Tianping Chen. Boundedness and synchronization of y-coupled lorenz systems with or without controller. *Physica D*, 237:630–639, 2008.

[109] Xiwei Liu and Tianping Chen. Synchronization analysis for nonlinearly-coupled complex networks with an asymmetrical coupling matrix. *Physica A*, 387:4429–4439, 2008.

[110] W. Lohmiller and J.J.E. Slotine. Higher order contraction. Available at http://arxiv.org/abs/nlin/0510025.

[111] W. Lohmiller and J.J.E. Slotine. On contraction analysis for non-linear systems. *Automatica*, 34:683–696, 1998.

[112] W. Lohmiller and J.J.E. Slotine. Nonlinear process control using contraction theory. *AIChe Journal*, 46:588–596, 2000.

[113] W. Lohmiller and J.J.E. Slotine. Contraction analysis of non-linear distributed systems. *International Journal of Control*, 78:678–688, 2005.

[114] S. M. Lozinskii. Error estimate for numerical integration of ordinary differential equations. I. *Izv. Vtssh. Uchebn. Zaved. Mat.*, 5:222–222, 1959.

[115] Jianquan Lu and Daniel W.C. Ho. Local and global synchronization in general complex dynamical networks with delay coupling. *Chaos, Solitons and Fractals*, 37:1497–1510, 2008.

[116] Jinhu Lu, Xinghuo Yu, Guanrong Chen, and Daizhan Cheng. Characterizing the synchronizability of small-world dynamical networks. *IEEE Transactions on Circuits and Systems I*, 51(4):787–796, April 2004.

[117] N.A. Lynch. *Distributed Algorithms*. Morgan Kaufman, Inc., 1997.

[118] S. Mangan, S. Itzkovitz, N. Kashtan, D. Chklovskii, and U. Alon. The incoherent feed-forward loop accelerates the response-time of the gal system of Eschericha coli. *Journal Molecular Biology*, 356:1073–1081, 2006.

[119] E.O. Mann and O. Paulsen. Local field potential oscillations as a cortical soliloquy. *Neuron*, 67:3–5, 2010.

[120] G. Martinelli. Hopfield-like neural nets and sensor networks. *Neural processing letters*, 27:277–283, 2008.

[121] S. Mascolo. Smith's principle for congestion control in high-speed data networks. *IEEE Transactions on Automatic Control*, 45:358–364, 2000.

[122] D. McMillen, N. Kopell, J. Hasty, and J.J. Collins. Synchronization of genetic relaxation oscillators by intercell signaling. *Proceedings of the National Academy of Science*, 99:679–684, 2002.

[123] J. T. Mettetal, D. Muzzey, C. Gomez-Uribe, and A. van Oudenaarden. The frequency dependence of osmo-adaptation in Saccharomyces Cerevisiae. *Science*, 319:482–484, 2008.

[124] A. N. Michel, D. Liu, and L. Hou. *Stability of Dynamical Systems: Continuous, Discontinuous, and Discrete Systems*. Springer-Verlag (New-York), 2007.

[125] M.B. Miller and B. Bassler. Quorum sensing in bacteria. *Annual Review of Microbiology*, 55:165–199, 2001.

[126] R. Milo, S. Shen-Orr, S. Itzkovitz, N. Kashtan, D. Chklovskii, and U. Alon. Network motifs: simple building blocks of complex network. *Science*, 298:824–827, 2002.

[127] P.J. Moylan and D.J. Hill. Stability criteria for large-scale systems. *IEEE Trans. Autom. Control*, 23(2):143–149, 1978.

[128] J. Muller, C. Kuttler, B.A. Hense, M. Rothballer, and A. Hartmann. Cell-cell communication by quorum sensing and dimension reduction. *Journal of Mathematical Biology*, 53:672–702, 2006.

[129] C. D. Nadell, J.B. Xavier, S. A. Levin, and K. R. Foster. The evolution of quorum sensing in bacteria biofilms. *PLoS Computational Biolody*, 6:e14, 2008.

[130] C.D. Nardelli, B. Bassler, and S.A. Levin. Observing bacteria through the lens of social evolution. *Journal of Biology*, 7:27, 2008.

[131] A. Nedic and A. Ozdaglar. Convergence rate for consensus with delays. *Journal of Global Optimization*, 47:437–456, 2008.

[132] M. E. Newman. The structure and function of complex networks. *SIAM Review*, 45:167–256, 2003.

[133] M. E. J. Newman, A. L. Barabàsi, and D. J. Watts. *The structure and dynamics of complex networks*. Princeton University Press, 2006.

[134] W.L. Ng and B. Bassler. Bacterial suorum-sensing network architectures. *Annual Review of Genetics*, 43:197–222, 2009.

[135] R. Olfati-Saber and R. Murray. Consensus problems in networks of agents with switching topology and time-delays. *IEEE Transactions on Automatic Control*, 49(9), September 2004.

[136] E. Ott. *Chaos in dynamical systems*. Cambridge University Press (Canada), 1993.

[137] P. Parrilo and A. Jadbabaie. Approximation of the joint spectral radius using sum of squares. *Linear Algebra and its Applications*, 428:2385–2402, 2008.

[138] A. Pavlov, A. Pogromvsky, N. van de Wouv, and H. Nijmeijer. Convergent dynamics, a tribute to Boris Pavlovich Demidovich. *Systems and Control Letters*, 52:257–261, 2004.

[139] L. M. Pecora and T. L. Carroll. Synchronization in chaotic systems. *Physical Review Letters*, 64:821–824, February 1990.

[140] L.M. Pecora and T.L. Carroll. Master stability function for synchronized coupled systems. *Physical Review E*, 80:2019–2112, 1998.

[141] B. Pesaran, J.S. Pezaris, M. Sahani, P.P. Mitra, and R.A. Andersen. Temporal structure in neuronal activity during working memory in macaque parietal cortex. *Nature*, 5:805–811, 2002.

[142] Q. C. Pham and J.J.E. Slotine. Stable concurrent synchronization in dynamic system networks. *Neural Networks*, 20:62–77, 2007.

[143] A. Pikovsky, M. Rosenblum, and J Kurths. *Synchronization: A Universal Concept in Nonlinear Science*. Cambridge University Press, 2001.

[144] A. Pitsillides, P. Ioannou, G. Hadjipollas, and M. Lestas. Adaptive congestion protocol: a congestion control protocol with learning capability. *Computer Networks*, 51:3773–3798, 2007.

[145] M. Porfiri and M. di Bernardo. Criteria for global pinning-controllability of complex networks. *Automatica*, 44(12):3100 – 3106, 2008.

[146] M. Porfiri, D. J. Stilwell, and E. M. Bollt. Synchronization in random weighted directed networks. *IEEE Transactions on Circuits and Systems I*, 55(10):3170–3177, Nov. 2008.

[147] A. Prindle and J. Hasty. Stochastic emergence of groupthink. *Science*, 328:987–988, 2010.

[148] V.Y. Protasov. The generalized joint spectral radius. a geometric approach. *Izvestiya: Mathematics*, 61:995–1030, 1997.

[149] W. Ren and R. Beard. Consensus seeking in multiagent systems under dynamically changing interaction topologies. *IEEE Transactions on Automatic Control*, 50:655–665 655–661, 2005.

[150] V. Resmi, G. Ambika, and R. E. Amritkar. Synchronized states in chaotic systems coupled indirectly through a dynamic environment. *Physical Review E*, 81:046216, 2010.

[151] C. Rocsoreanu, A. Georgescu, and N. Giurgiteanu. *The FitzHugh-Nagumo Model: Bifurcation and Dynamics*. Kluwer Academic Publishers (Boston), 2000.

[152] G. C. Rota and G. Strang. A note on the joint spectral radius. *Inag. Math.*, 22:379–381, 1960.

[153] Jonathan E. Rubin. Bursting induced by excitatory synaptic coupling in nonidentical conditional relaxation oscillators or square-wave bursters. *Phys. Rev. E*, 74:021917, 2006.

[154] G. Russo and M. di Bernardo. An algorithm for the construction of synthetic self synchronizing biological circuits. In *International Symposium on Circuits and Systems*, pages 305–308, 2009.

[155] G. Russo and M. di Bernardo. Contraction theory and the master stability function: linking two approaches to study synchronization in complex networks. *IEEE Transactions on Circuit and Systems II*, 56:177–181, 2009.

[156] G. Russo and M. di Bernardo. How to synchronize biological clocks. *Journal of Computational Biology*, 16:379–393, 2009.

[157] G. Russo and M. di Bernardo. Solving the rendezvous problem for multiagent systems using contraction theory. In *Proceedings of the International Conference on Decision and Control*, pages 5821 – 5826, 2009.

[158] G. Russo, M. di Bernardo, and J.J.E. Slotine. Convergence of discrete-time and asynchronous systems and networks. Submitted to IEEE Transactions on Automatic Control.

[159] G. Russo, M. di Bernardo, and J.J.E. Slotine. An algorithm to prove contraction, consensus, and network synchronization. In *Proceedings of the International Workshop NecSys*, 2009.

[160] G. Russo, M. di Bernardo, and J.J.E. Slotine. A graphical algorithm to prove contraction of nonlinear circuits and systems. *IEEE Transactions on Circuits and Systems I*, in press, 2010.

[161] G. Russo, M. di Bernardo, and E. D. Sontag. Global entrainment of transcriptional systems to periodic inputs. *PLoS Computational Biology*, 6:e1000739, 2010. PLoS Computational Biology: accepted for publication.

[162] G. Russo, M. di Bernardo, and E.D. Sontag. Stability of networked systems: a multi-scale approach using contraction. In *Proceedings of the 49th International Conference on Decision and Control*, 2010.

[163] G. Russo and J.J.E. Slotine. Symmetries, stability, and control in nonlinear systems and networks. Submitted to Physical Review E, available on arxiv at http://arxiv.org/abs/1011.0188.

[164] G. Russo and J.J.E. Slotine. Global convergence of quorum-sensing networks. *Physical Review E*, 82:041919, 2010.

[165] L. H. Ryder. *Quantum Field Theory (2nd Edition)*. Cambridge University Press (Cambridge, UK), 1996.

[166] M. H. Shih. Simultaneous Schur stability. *Linear Algebra and its Applications*, 287:323–336, 1999.

[167] O. Shoval, L. Goentoro, Y. Hart, A. Mayo, E.D. Sontag, and U. Alon. Fold-change detection and scalar symmetry of sensory inputs. *Proceedings of the National Academy of Science*, 107:15995–16000, 2010.

[168] H. Simon. *Neural networks: a comprehensive foundation (2nd Ed.)*. Prentice Hall, 1998.

[169] J. J.E. Slotine and W. Li. *Applied nonlinear control*. Prentice Hall (Englewood Cliffs, NJ, USA), 1990.

[170] J.J.E. Slotine. Modular stability tools for distributed computation and control. *International Journal of Adaptive Control and Signal Processing*, 17(6):397—416, 2003.

[171] Q. Song and J. Cao. On pinning synchronization of directed and undirected complex dynamical networks. *IEEE Transactions on Circuits and Systems I*, 57:672 – 680, 2010.

[172] E. D. Sontag. An observation regarding systems which converge to steady states for all constant inputs, yet become chaotic with periodic inputs. Technical report, Dept. of Mathematics, Rutgers University, 2009. http://arxiv.org/abs/0906.2166.

[173] E.D. Sontag. Input to state stability: Basic concepts and results. In P. Nistri and G. Stefani, editors, *Nonlinear and Optimal Control Theory*, pages 163–220. Springer-Verlag, Berlin, 2007.

[174] E.D. Sontag. Monotone and near-monotone biochemical networks. *Systems and Synthetic Biology*, 1:59–87, 2007.

[175] Eduardo D. Sontag. *Mathematical Control Theory. Deterministic Finite-Dimensional Systems*. Springer-Verlag (New York), 1998.

[176] M.W. Spong and F. Bullo. Controlled symmetries and passive walking. *IEEE Transactions on Automatic Control*, 2005:1025–1031, 50.

[177] K. A. Stokkan, S. Yamazaki, H. Tei, Y. Sakaki, and M. Menaker. Entrainment of the circadian clock in the liver by feeding. *Science*, 19:2001, 2001.

[178] S.H. Strogatz. *Sync: the emerging science of spontaneous order*. Hyperion (New York, USA), 2003.

[179] T. Strom. On logarithmic norms. *SIAM J. Numer. Anal.*, 12:741–753, 1975.

[180] Z. Szallasi, J. Stelling, and V. Periwal. *System Modeling in Cellular Biology: From Concepts to Nuts and Bolts*. The MIT Press, 2006.

[181] N. Tabareau, J.J.E. Slotine, and Q.C. Pham. How synchronization protects from noise. *PLoS Computational Biology*, 6:e1000637, 2010.

[182] H. G. Tanner, A. Jadbabaie, and G. J. Pappas. Stale flocking of mobile agents, part ii: dynamic topology. In *42nd Conf. on Decision and Control*, 2003.

[183] M. Toiya, H.O. Gonzalez-Ochoa, V. K. Vanag, S. Fraden, and I. R. Epstein. Synchronization of chemical micro-oscillators. *The Journal of Physical Chemistry Letters*, 1:1241–1246, 2010.

[184] M. Toiya, V. K. Vanag, and I. R. Epstein. Diffusively coupled chemical oscillators in a microfluidic assembly. *Angew. Chem. Int. Ed.*, 47:7753–7755, 2008.

[185] R. Toth, A. F. Taylor, and M. R. Tinsley. Collective behavior of a population of chemically coupled oscillators. *The Journal of Physical Chemistry*, 110:10170–10176, 2006.

[186] J. Tsitsiklis. *Problems in decentralized decision making and computation.* PhD thesis, Dept. of Electrical Engineering and Computer Science of the Massachusetts Institute of Technology, 1984.

[187] J. Tsitsiklis, D. Bertsekas, and M. Athans. Distributed asynchronous deterministic and stochastic gradient optimization algorithms. *IEEE Transactions on Automatic Control*, 31:803–812, 1986.

[188] Y. Tu, T.S. Shimizu, and H.C. Berg. Modeling the chemotactic response of Escherichia coli of time-varying stimuli. *Proc. of the Natl. Acad. of Sci.*, 105:14855–14860, 2008.

[189] J. J. Tyson, A. Csikasz-Nagy, and B. Novak. The dynamics of cell cycle regulation. *Bioessays*, 24:1095–1109, 2002.

[190] M. Vidyasagar. *Input-Output Analysis of Large Scale Interconnected Systems.* Springer-Verlag, Berlin, 1981.

[191] M. Vidyasagar. *Nonlinear systems analysis (2nd Ed.).* Pretice-Hall (Englewood Cliffs, NJ), 1993.

[192] H.C. Walkey, J.A. Harlow, and J.L. Barbur. Changes in reaction time and search time with background luminance in the mesopic range. *Ophthalmic Physiology*, 26:288–299, 2006.

[193] R. Wang, L. Chen, and K. Aihara. Synchronizing a multicellular system by external input: an artificial control strategy. *Bioinformatics*, 22:1775–1781, 2006.

[194] W. Wang and J.J. E. Slotine. On partial contraction analysis for coupled nonlinear oscillators. *Biological Cybernetics*, 92:38–53, 2005.

[195] Xiao Fan Wang and Guanrong Chen. Synchronization in scale-free dynamical networks: robustness and fragility. *IEEE Transactions on Circuits and Systems I: Fundamental Theory and Applications*, 49(1):54–62, Jan 2002.

[196] D.B. West. *Introduction to Graph Theory.* Prentice Hall (Englewook Cliffs, NJ), 1995.

[197] A. Winfree. Biological rhythms and the behavior of populations of coupled oscillators. *Journal of Theoretical Biology*, 16:15–42, 1967.

[198] A.T. Winfree. *The geometry of biological time.* Springer Verlag (New York), 2000.

[199] Chai Wah Wu. Localization of effective pinning control in complex networks of dynamical systems. In *ISCAS 2008. IEEE International Symposium on Circuits and Systems*, pages 2530–2533, May 2008.

[200] Wei Wu, Wenjuan Zhou, and Tianping Chen. Cluster synchronization of linearly coupled complex networks under pinning control. *IEEE Transactions on Circuits and Systems I: Regular Papers*, 56(4):829–839, April 2009.

[201] Yongxiang Xia and D.J. Hill. Attack vulnerability of complex communication networks. *IEEE Transactions on Circuits and Systems II*, 55(1):65–69, Jan. 2008.

[202] F. Xiao and L. Wang. Asynchronous consensus in continuous-time multi-agent systems with switching topology and time-varying delays. *IEEE Transactions on Automatic Control*, 53:1804–1816, 2008.

[203] L. Xiao and S. Boyd. Fast linear iterations for distributed averaging. *Systems and Control Letters*, 53:65–78, 2004.

[204] M. Yarvis, N. Kushalnagar, H. Singh, A. Rangarajan, Y. Liu, and S. Singh. Exploiting heterogeneity in sensor networks. In *IEEE InfoCom*, 2005.

[205] L. You, R.S. Cox 3rd, R. Weiss, and F.H. Arnold. Programmed population control by cell-cell communication and regulated killing. *Nature*, 428:868–871, 2004.

[206] G. Yu and J.J.E. Slotine. Visual grouping by oscillator networks. *IEEE Transactions on Neural Networks*, 20:1871–1884, 2009.

[207] L. Yuan, Z. Yuan, and Y. He. Convergence of non-autonomous discrete-time hopfield model with delays. *Neurocomputing*, 72:3802–3808, 2009.

[208] J. Zhang, Z. Yuan, and T. Zhou. Synchronization and clustering of synthetic genetic networks: a role for cis-regulatory modules. *Physical Review E*, 79:041903, 2009.

[209] Qunjiao Zhang, Junan Lu, Jinhu Lu, and C.K. Tse. Adaptive feedback synchronization of a general complex dynamical network with delayed nodes. *IEEE Transactions on Circuits and Systems II*, 55(2):183–187, Feb. 2008.

[210] Jin Zhou and Tianping Chen. Synchronization in general complex delayed dynamical networks. *IEEE Transactions on Circuits and Systems I*, 53(3):733–744, March 2006.

[211] T. Zhou, J. Zhang, Z. Yuan, and A. Xu. External stimuli mediate collective rhythms: artificial control strategies. *PLoS ONE*, 3:e231, 2007.

Appendix A

Auxiliary results for Chapter 9

A.1 Entraining a population of Repressilators: proof

The general principle that we apply to prove entrainment of a population of Repressilators is as follows.

Assume that the cascade system

$$\begin{aligned} \dot{x} &= f(x, y), \\ \dot{y} &= g(y, v(t)), \end{aligned} \tag{A.1}$$

with $v(t)$ being an exogenous input, satisfies the contractivity assumptions of the above Section. Then, consider the interconnection of N identical systems which interact through the variable y as follows:

$$\begin{aligned} \dot{x}_i &= f(x_i, y), \qquad\qquad i = 1, \ldots, N, \\ \dot{y} &= g(y, \textstyle\sum_{i=1}^{N} x_i + u). \end{aligned} \tag{A.2}$$

Suppose that $[x_1(t), \ldots, x_N(t), y(t)]$ is a solution of (A.2) defined for all $t \geq 0$, for some input $u(t)$. Then, we have the synchronization condition: $x_i(t) - x_j(t) \to 0$, as $t \to +\infty$.

Indeed, we only need to observe that every pair $[x_i(t), y(t)]$ is a solution of (A.1) with the same input

$$v(t) = \sum_{i=1}^{N} x_i(t) + u(t).$$

Furthermore, if $u(t)$ is a T-periodic function, the N interconnected dynamical systems synchronize onto a T-periodic trajectory.

The above principle can be immediately applied to prove that synchronization onto a T-periodic orbit is attained for the Repressilator circuits composing network (9.57) (see also [156], [154]).

Specifically, let $x_i := [a_i, b_i, c_i, A_i, B_i, C_i, S_i]$ and $y = S_e$; we have that $[x_1, \ldots, x_N, y]$

is a solution of (9.57). We notice that any pair $[x_i, y]$ is a solution of the following cascade system

$$\begin{aligned}
\dot{a} &= -a + \alpha / \left(1 + C^2\right) \\
\dot{b} &= -b + \alpha / \left(1 + A^2\right) \\
\dot{c} &= -c + \alpha / \left(1 + B^2\right) + (kS) / (1 + S) \\
\dot{A} &= \beta_A a - d_A A \\
\dot{B} &= \beta_B b - d_B B \\
\dot{C} &= \beta_C c - d_C C \\
\dot{S} &= -k_{s0} S + k_{s1} A - \eta \left(S - S_e\right) \\
\dot{S}_e &= -k_{se} S_e - \eta_{ext} N S_e + u(t) + \eta_{ext} \left(S_1 + ... + S_N\right).
\end{aligned} \tag{A.3}$$

Thus, as shown above, contraction of (A.3) implies synchronization of (9.57). Differentiation of (A.3) yields the Jacobian matrix

$$J = \begin{bmatrix}
-1 & 0 & 0 & 0 & 0 & f_1\left(C_v\right) & 0 & 0 \\
0 & -1 & 0 & f_1\left(A_v\right) & 0 & 0 & 0 & 0 \\
0 & 0 & -1 & 0 & f_1\left(B_v\right) & 0 & f_2\left(S_v\right) & 0 \\
\beta_A & 0 & 0 & -d_A & 0 & 0 & 0 & 0 \\
0 & \beta_B & 0 & 0 & -d_B & 0 & 0 & 0 \\
0 & 0 & \beta_C & 0 & 0 & -d_C & 0 & 0 \\
0 & 0 & 0 & k_{s1} & 0 & 0 & -k_{s0} - \eta & \eta \\
0 & 0 & 0 & 0 & 0 & 0 & 0 & -k_q
\end{bmatrix} \tag{A.4}$$

where f_1 and f_2 denote the partial derivatives of decreasing and increasing Hill functions with respect to the state variable of interest and $k_q = k_{se} + k_{diff}$, $k_{diff} = \eta_{ext} N$.

Note that the Jacobian matrix J has the structure of a cascade, i.e.

$$J = \begin{bmatrix} A & B \\ 0 & C \end{bmatrix},$$

with:

$$A = \begin{bmatrix}
-1 & 0 & 0 & 0 & 0 & f_1(C) & 0 \\
0 & -1 & 0 & f_1(A) & 0 & 0 & 0 \\
0 & 0 & -1 & 0 & f_1(B) & 0 & f_2(S) \\
\beta_A & 0 & 0 & -d_A & 0 & 0 & 0 \\
0 & \beta_B & 0 & 0 & -d_B & 0 & 0 \\
0 & 0 & \beta_C & 0 & 0 & -d_C & 0 \\
0 & 0 & 0 & k_{s1} & 0 & 0 & -k_{s0} - \eta
\end{bmatrix},$$

$B = \begin{bmatrix} 0 & 0 & 0 & 0 & 0 & 0 & \eta \end{bmatrix}^T$, $C = -k_q$. Thus, to prove contraction of the virtual system (A.3) it suffices to prove that there exist two matrix measures, μ_* and μ_{**} such that:

1. $\mu_* (A) \leq -c_*^2$;
2. $\mu_{**} (C) \leq -c_{**}^2$;

where $c_*, c_{**} \in \mathbb{R} - \{0\}$. Clearly, since k_q is a positive real parameter, the second condition above is satisfied (with μ_{**} being any matrix measure). Now, notice that matrix A has the same form as the Jacobian matrix of the Repressilator circuit (9.46). Hence, if the parameters of the Repressilator are chosen so that they satisfy (9.56), then there exist a set of positive real parameters p_i, $i = 1, \ldots, 7$, such that $\mu_{P,\infty} (A) \leq -c_*^2$ (that is, the first condition above is also satisfied with $\mu_* = \mu_{P,\infty}$).

Thus, we can conclude that (A.3) is contracting. Furthermore, all the trajectories of the virtual system converge towards a T-periodic solution (see Theorem 4.3.2). This in turn implies that all the trajectories of network (9.57) converge towards the same T-periodic solution. That is, all the nodes of (9.57) synchronize onto a periodic orbit of period T.

A.2 A counterexample to entrainment

In [172] there is given an example of a system with the following property: when the external signal $u(t)$ is constant, all solutions converge to a steady state; however, when $u(t) = \sin t$, solutions become chaotic. (Obviously, this system is not contracting.) The equations are as follows:

$$
\begin{aligned}
\dot{x} &= -x - u \\
\dot{p} &= -p + \alpha(x + u) \\
\dot{\xi} &= 10(\psi - \xi) \\
\dot{\psi} &= 28p\xi - \psi - p\xi\zeta \\
\dot{\zeta} &= p\xi\psi - (8/3)\zeta
\end{aligned}
$$

where $\alpha(y) = y^2/(K + y^2)$ and $K = 0.0001$. Figure A.1 shows typical solutions of this system with a periodic and constant input respectively. The function "rand" was used in MATLAB to produce random values in the range $[-10, 10]$.

A.2.1 Networks of contracting nodes

We consider a network where its $N > 1$ nodes may have different dynamics:

$$
\dot{x}_i = f_{\gamma(i)} (x_i, t) + \sum_{j \in N_i} \left[h_{\gamma(i)} (x_j) - h_{\gamma(i)} (x_i) \right] \tag{A.5}
$$

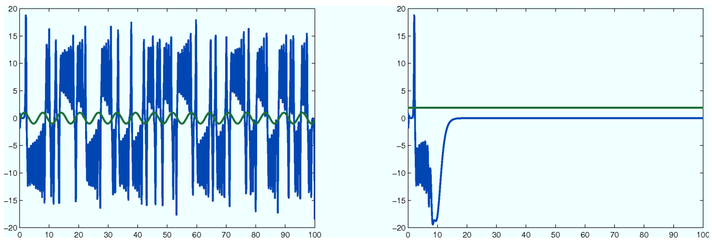

Figure A.1: **Simulation of counter-example.** The following randomly-chosen input and initial conditions are used: $u(t) = 1.89$, $x(0) = 2.95$ $p(0) = -0.98$, $\xi(0) = 0.94$, $\psi(0) = -4.07$, $\zeta(0) = 4.89$. Green: inputs are $u(t) = \sin t$ (left panel) and $u(t) = 5.13$ (randomly picked, right panel). Blue: $\xi(t)$. Note chaotic-like behavior in response to periodic input, but steady state in response to constant input.

where N_i denotes the set of neighbors of node i and γ is a function defined between two set of indices (not necessarily a permutation), i.e.

$$\gamma : \{1, \dots, N\} \to \{1, \dots, s\} \quad s \leq N \tag{A.6}$$

Thus, two nodes of (A.5), e.g. x_i and x_j, share the same dynamics and belong to the p-th group (denoted with $\mathcal{G}_p$), i.e. $x_i, x_j \in \mathcal{G}_p$, if and only if $\gamma(i) = \gamma(j) = p$. The dimension of the nodes' state variables belonging to group p is $n_{\gamma(i)}$, i.e. $x_i \in \mathbb{R}^{n_{\gamma(i)}}$ for any $x_i \in \mathcal{G}_p$. In what follows we assume that the Jacobian of the coupling functions $h_{\gamma(i)}$ are diagonal matrices with nonnegative diagonal elements. We will derive conditions ensuring *concurrent synchronization* of (A.5), i.e. all nodes belonging to the same group exhibit the same regime behavior.

Theorem A.2.1. *Assume that in (A.5) the nodes belonging to the same group are all input-equivalent and that the nodes dynamics are all contracting. Then, all node trajectories sharing the same dynamics converge towards each other, i.e. for any x_i, $x_j \in \mathcal{G}_p$, $p = 1, \dots, s$,*

$$|x_j(t) - x_i(t)| \to 0 \quad \text{as} \quad t \to +\infty$$

In the case of networks of identical nodes dynamics, the above result amounts to only requiring contraction for each node.

To prove Theorem A.2.1 we need the following Lemma, which is a generalization of a result proven in [161]:

Lemma A.2.1. *Consider the block- partition for a square matrix J:*

$$J = \begin{bmatrix} A(x) & B(x,y) \\ C(x,y) & D(y) \end{bmatrix}$$

where A and D are square matrices of dimensions $n_A \times n_A$ and $n_D \times n_D$ respectively. Assume that A and B are contracting with respect to μ_A and μ_D (induced by the vector norm $|\bullet|_A$ and $|\bullet|_D$). Then, J is contracting if there exists two positive real numbers θ_1, θ_2 such that

$$\begin{array}{l} \mu_A(A) + \frac{\theta_2}{\theta_1} \|C(x,y)\|_{A,D} \leq -c_A^2 \\ \mu_D(D) + \frac{\theta_1}{\theta_2} \|B(x,y)\|_{D,A} \leq -c_B^2 \end{array}$$

where $\|\bullet\|_{A,D}$ and $\|\bullet\|_{D,A}$ are the operator norms induced by $|\bullet|_A$ and $|\bullet|_D$ on the linear operators C and B. Furthermore, the contraction rate is $c^2 = \max\{c_A^2, c_B^2\}$.

Proof. Let $z := (x,y)^T$. We will show that, with the above hypotheses, J is contracting with respect to the matrix measure induced by the following vector norm:

$$|z| := \theta_1 |x|_A + \theta_2 |y|_D$$

with $\theta_1, \theta_2 > 0$. In this norm, we have

$$|(I+hJ)z| = \theta_1 |(I+hA)x + hBy|_A + \theta_2 |(I+hD)y + hCx|_D$$

Thus,

$$\begin{array}{l} |(I+hJ)z| \leq \theta_1 |(I+hA)x|_A + h\theta_1 |By|_{D,A} + \\ +\theta_2 |(I+hD)y|_D + h\theta_2 |Cx|_{A,D} \end{array}$$

Pick now $h > 0$ and a unit vector z (depending on h) such that $\|(I+hJ)z\| = |(I+hJ)z|$. We have, dropping the subscripts for the norms:

$$\begin{array}{l} \frac{1}{h}(\|I+hJ\|-1) \leq \frac{1}{h}\left(\|I+hA\| - 1 + \frac{\theta_2}{\theta_1} h \|C\|\right) |x| \theta_1 + \\ +\frac{1}{h}\left(\|I+hD\| - 1 + \frac{\theta_1}{\theta_2} h \|B\|\right) |y| \theta_2 \end{array}$$

Since $1 = |z| = \theta_1 |x|_A + \theta_2 |y|_B$, we finally have

$$\begin{array}{l} \frac{1}{h}(\|I+hJ\|-1) \leq \max\left\{\frac{1}{h}\left(\|I+hA\| - 1 + \frac{\theta_2}{\theta_1} h \|C\|\right), \right. \\ \left. \frac{1}{h}\left(\|I+hD\| - 1 + \frac{\theta_1}{\theta_2} h \|B\|\right)\right\} \end{array}$$

Taking now the limit for $h \to 0^+$:

$$\mu(J) \leq \max\left\{\mu(A)_A + \frac{\theta_2}{\theta_1}\|C\|, \mu(D)_D + \frac{\theta_1}{\theta_2}\|B\|\right\}$$

thus proving the result. □

Following the same arguments, Lemma A.2.1 can be straightforwardly extended to the case of a real matrix J partitioned as

$$J = \begin{bmatrix} J_{11} & J_{12} & \dots & J_{1N} \\ \dots & \dots & \dots & \dots \\ J_{N1} & J_{N2} & \dots & J_{NN} \end{bmatrix}$$

where the diagonal blocks of J are all square matrices. Then J is contracting if

$$\begin{aligned} &\mu(J_{11}) + \tfrac{\theta_2}{\theta_1}\|J_{12}\| + \ldots + \tfrac{\theta_N}{\theta_1}\|J_{1N}\| \leq -c_{11}^2 \\ &\dots \\ &\mu(J_{NN}) + \tfrac{\theta_1}{\theta_N}\|J_{N1}\| + \ldots + \tfrac{\theta_{N-1}}{\theta_N}\|J_{1N}\| \leq -c_{NN}^2 \end{aligned} \tag{A.7}$$

(where subscripts for matrix measures and norms have been neglected).

Proof of Theorem A.2.1

The assumption of input equivalence for the nodes implies the existence of a linear invariant subspace associated to the concurrent synchronization final behavior. We will prove convergence towards such a subspace, by proving that the network dynamics is contracting. Let μ_f be the matrix measure where the nodes dynamics is contracting and define: $X := (x_1^T, \ldots, x_N^T)^T$, $F(X)$ as the stack of all intrinsic nodes dynamics, $H(X)$ the stack of nodes coupling functions. We want to prove that there exist a matrix measure, μ, (which is in general different from μ_f) where the whole network dynamics is contracting. Denote with $L := \{l_{ij}\}$ the Laplacian matrix [66] of the network and define the matrix $\tilde{L}(X)$, whose ij-th block, $\tilde{L}_{ij}(X)$, is defined as follows:

$$\tilde{L}_{ij}(X) := l_{ij}\frac{\partial h_{\gamma(i)}}{\partial x_j}$$

(Notice that if all the nodes are identical and have the same dynamics and the same coupling functions, then $\tilde{L}$ can be written in terms of the Kronecker product, $\otimes$, as $(L \otimes I_n)\frac{\partial H}{\partial X}$, with n denoting the dimension of the nodes and I_n the $n \times n$ identity matrix.)

The Jacobian of (A.5) is then:

$$J := \left[\frac{\partial F}{\partial X} - \tilde{L}(X)\right] \tag{A.8}$$

The system is contracting if

$$\mu\left(\frac{\partial F}{\partial X} - \tilde{L}(X)\right)$$

is uniformly negative definite. Now:

$$\mu\left(\frac{\partial F}{\partial X} - \tilde{L}(X)\right) \leq \mu\left(\frac{\partial F}{\partial X}\right) + \mu\left(-\tilde{L}(X)\right)$$

Notice that, by hypotheses, the matrix $-\tilde{L}(X)$ has negative diagonal blocks and zero column sum. Thus, using (A.7) with $\theta_i = \theta_j$ for all $i, j = 1, \ldots, N$, $i \neq j$ yields

$$\mu\left(-\tilde{L}(X)\right) = 0$$

Thus:

$$\mu\left(\frac{\partial F}{\partial X} - \tilde{L}(X)\right) \leq \mu\left(\frac{\partial F}{\partial X}\right)$$

Since the matrix $\frac{\partial F}{\partial X}$ is block diagonal, i.e. all of its off-diagonal elements are zero, (A.7) yields:

$$\mu\left(\frac{\partial F}{\partial X}\right) = \max_{x,t,i}\left\{\mu_f\left(\frac{\partial f_{\gamma(i)}}{\partial x}\right)\right\}$$

The theorem is then proved by noticing that by hypothesis the right hand side of the above expression is uniformly negative.